19ª RAU

REUNIÃO ANUAL DE USUÁRIOS DO LNLS

09 E 10 FEV 2009

RESUMOS
DE TRABALHOS CIENTÍFICOS

LNLS
Laboratório Nacional de Luz Síncrotron

Ministério da Ciência e Tecnologia

BRASIL UM PAÍS DE TODOS
GOVERNO FEDERAL

RESUMOS
DE TRABALHOS CIENTÍFICOS

COORDENAÇÃO
Chairmen

Flávio Garcia (LNLS)
Pedro Augusto de Paula Nascente (UFSCar)

COMITÊ CIENTÍFICO
Scientific Comittee

Arnaldo Naves de Brito (LNLS)

Altair Soria (UFRGS)

Jean Guillaume Eon (UFRJ)

Rodrigo Gribel Lacerda (UFMG)

Shaker Chuck Farah (USP / SP)

Sérgio Teixeira Ribeiro (UFRGS)

Valmor Roberto Mastelaro (USP / São Carlos)

Watson Loh (Unicamp)

COMITÊ LOCAL
Local Organizing Comittee

Cleonice Ywamoto
Dennis Massaroto Campos
Guilherme Tavares de Oliveira

SECRETÁRIA
Secretary

Ana Lucia Ferreira

19ª REUNIÃO ANUAL DE USUÁRIOS

Laboratório Nacional de Luz Síncrotron
09 e 10 de fevereiro de 2009 – Campinas – SP, Brasil

19th ANNUAL USERS' MEETING

Brazilian Synchrotron Ligth Laboratory
February 09-10, 2009 – Campinas – SP, Brazil

Laboratório Nacional de Luz Síncrotron

PREFÁCIO

O Laboratório Nacional de Luz Síncrotron (LNLS) completará doze anos de pleno funcionamento em 2009. Durante este período, a cada Reunião Anual de Usuários (RAU), foram apresentados trabalhos científicos de impacto cada vez maior, assim como novidades técnicas, tanto por parte da equipe do LNLS quanto pelos usuários, deixando claro o amadurecimento gradual de ambos, ou seja, uma equipe preparada para novos desafios e uma comunidade de usuários cada vez mais exigente. Neste contexto, já há algumas edições da RAU, é sistematicamente levantada a preocupação, por parte dos usuários, com a eminente saturação do nosso anel de armazenamento e com o seu futuro, sobretudo, quando percebemos e comparamos o LNLS com as novas máquinas de terceira geração que vêm sendo construídas mundo afora, para citar algumas, Swiss Light Source – Suíça, SOLEIL – França, Diamond – Inglaterra, Boomerang – Austrália, entre outras. Esta preocupação sempre teve repercussão dentro do LNLS, que, por sua vez, vem realizando grandes esforços para tornar nossa máquina cada vez mais competitiva. Porém, sabemos que essa competitividade fica a cada ano mais difícil. Posto isso, passa a ser importante discutirmos uma nova máquina, sendo esta pensada para ser atual quando for inaugurada, daqui a 10 ou 15 anos. Em 2008, foi lançado o projeto desta nova máquina, LNLS-2, cujos parâmetros e características precisam ser amplamente debatidos com a comunidade científica.

Sendo assim, além de desempenhar seu papel primordial, que é congregar a comunidade de usuários do LNLS, esta reunião terá como diferencial a preocupação de suscitar discussões sobre esse tema. Neste sentido, teremos duas plenárias sobre assuntos relacionados à coerência, resolução temporal e alto brilho, características que esperamos ser contemplados no projeto da nova máquina. Também neste contexto, será realizado um Workshop Satélite, na seqüência da RAU, sobre o projeto do LNLS-2, organizado pelo diretor científico do LNLS, Caio Lewenkopf.

Outra novidade desta edição da RAU, e que também é um marco do LNLS, foi disponibilizado aos usuários externos o novo centro de microscopia no Prédio Cesar Lattes. Por isso, a terceira plenária será sobre microscopia eletrônica. Ainda no sentido de apresentarmos esta nova instalação aberta, a sessão de pôsteres e o coquetel de confraternização serão realizados neste prédio.

No mais, a 19ª RAU segue o modelo das anteriores, com apresentações orais e uma grande sessão de pôsteres, além das já estabelecidas sessões temáticas.

Terminamos por desejar a todos uma excelente reunião.

Flávio Garcia e Pedro Augusto de Paula Nascente

Coordenadores da 19ª RAU

ORIENTAÇÕES AOS PARTICIPANTES
Guidelines to Participants

Prezado Participante, */ Dear Participant*,

Seja bem-vindo ao Laboratório Nacional de Luz Síncrotron (LNLS). A equipe envolvida na organização da 19ª Reunião Anual de Usuários fez o melhor possível para recebê-lo. Para sua orientação, pedimos atenção para as informações abaixo.
Welcome to the Brazilian Synchrontron Light Laboratory (LNLS). The organizing of the 19th Annual User's Meeting has done its best to make sure everything will run smoothly. Please, read carefully the following instructions.

1. TRASLADOS / *Transfer*

Traslados entre HOTEL / LNLS / HOTEL serão feitos em ônibus especial:
A shuttle will be provided for the transportation from HOTEL / LNLS / HOTEL:

Dia 09/02, segunda-feira / *Monday 09th*	
Saída do Hotel às 07h15	Saída do LNLS às 21h30
Departure from hotel at 07:15 am	*Departure from LNLS at 09:30 pm*

Dia 10/02, terça-feira / *Tuesday 10th*	
Saída do Hotel às 07h15	Saída do LNLS às 14h00 e 17h00
Departure from hotel at 07:15 am	*Departure from LNLS at 2:00 and 5:00 pm*

2. SESSÕES / *Sessions*

As Comunicações Orais e Sessões Temáticas ocorrerão em diferentes locais no LNLS:
Oral presentations and technical sessions will be held at four different locations at LNLS campus:

(A) Prédio do Anel – Auditório (Mezanino I)
(B) Prédio Amarelo – Sala de Leitura (Biblioteca)
(C) Prédio da Biologia – Sala 69 (Mezanino)
(D) Prédio Amarelo – Sala 50 (Mezanino)

3. LOCALIZAÇÃO DOS PAINÉIS / *Posters Location*

Os painéis deverão ser afixados no primeiro dia da reunião (09/02), logo após a recepção do crachá. A localização dos painéis estará sinalizada por etiquetas com numeração correspondente à indicada no Sumário deste Livro de Resumos.
The posters must be in its designated place in the first day of the meeting (Feb 18th), just after registration. The poster location will be indicated by tags corresponding to the same numbers present in the Abstract Book.

4. PREMIAÇÃO / *Prizes*

Os autores das três melhores apresentações de painéis receberão uma assinatura anual da revista Scientific American. O anúncio dos vencedores acontecerá durante a sessão de encerramento do evento.
Authors of the three best posters will be awarded a subscription of Scientific American Magazine. Winners will be announced in the closing ceremony.

5. CRACHÁ DE IDENTIFICAÇÃO / *Identification Badge*

O crachá de identificação deve ser usado durante a sua permanência no LNLS.
The identification badge must be used at all times during your stay at LNLS.

6. GUARDA-VOLUME / *Lockers*

Para sua comodidade, guarda-volumes estão disponíveis na entrada do Prédio do Anel.
For your convenience, lockers are available at the entrance of the Storage Ring Building.

7. ALMOÇO / *Lunch*

Os almoços serão servidos no refeitório do LNLS, a partir do horário indicado no programa.
Lunch will be served at the LNLS canteen, following the schedule in the program.

8. CÓPIAS XEROX / *Photocopies*

Cópias xerográficas devem ser solicitadas à Biblioteca do LNLS e custam R$ 0,10 (dez centavos) cada. Dependendo da quantidade de cópias, elas serão enviadas posteriormente pelo correio, mediante pagamento antecipado.
Photocopies must be requested at LNLS Library, at a cost of R$ 0,10 (tem cents) each. Depending on quantity, they may be sent after the meeting by mail, after pre-payment.

9. TELEFONE / *Pay-phones*

Há um telefone público disponível no campus do LNLS, na entrada do prédio amarelo. Cartões magnéticos podem ser adquiridos na lanchonete.
One pay-phone is available at LNLS, at the entrance of administration building. Phone cards can be purchased at LNLS canteen.

10. E-MAIL

Computadores de uso coletivo estarão disponíveis na entrada do Prédio do Anel (Sala 04). Siga as instruções afixadas no local para acesso aos e-mails.
Computers will be available at the entrance of the Storage Ring Building (Room 04). In order to access your e-mail, please follow instructions posted at the room.

MAPA DO LNLS
LNLS CAMPUS MAP

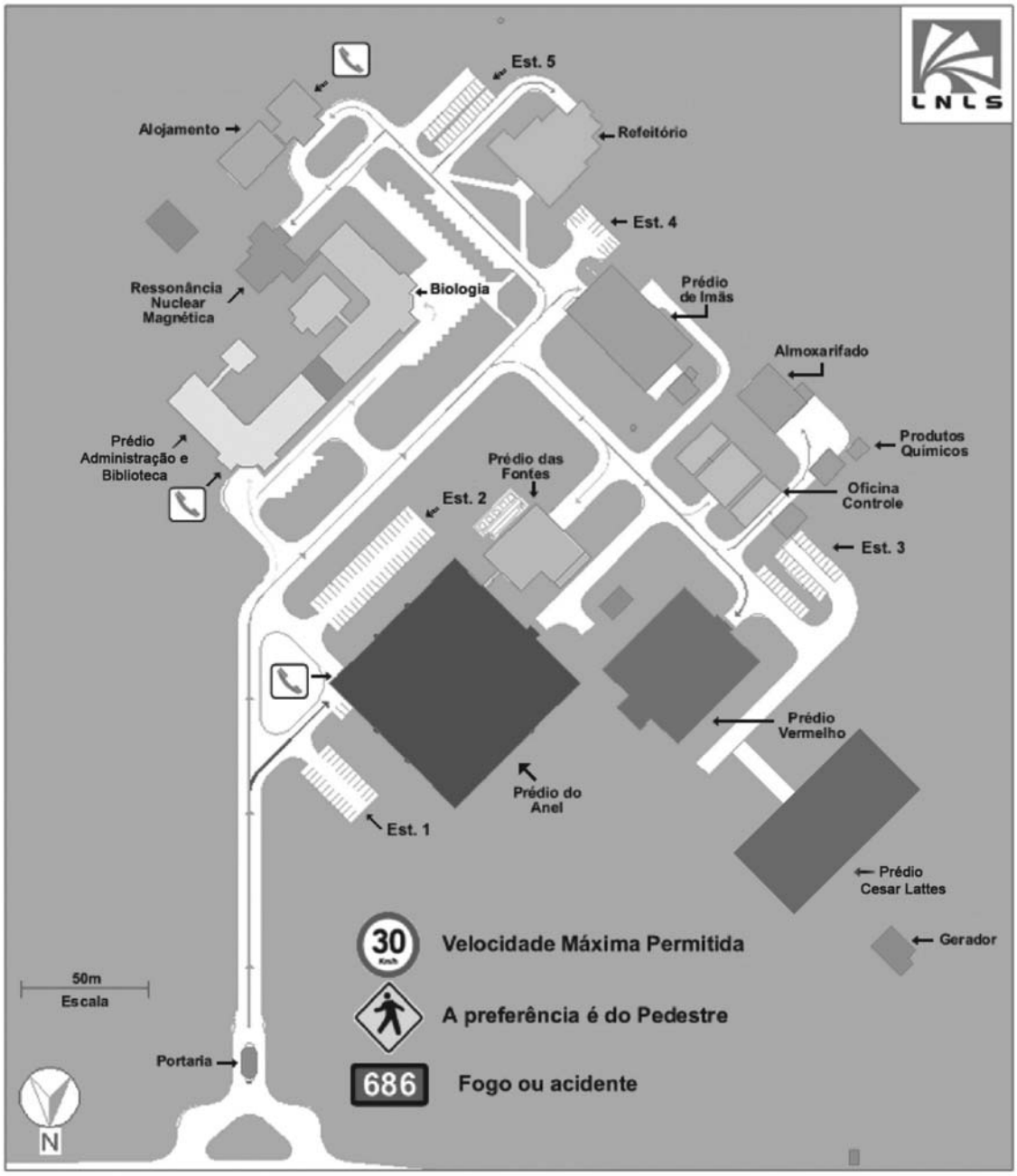

PROGRAMACÃO

09 DE FEVEREIRO, SEGUNDA-FEIRA

Comunicações Orais

Sessão 1 **Prédio do Anel, Auditório**
Chairperson: **Márcia Fantini - USP/SP**

12h00 Characterization of a new material based on polyaniline doped with [Cs][In(dmit)2], (cesium) [bis(1,3-dithiole-2-thione-4,5-dithiolato)indium (III)] by X-Ray Photoelectron Spectroscopy
Paulo Henrique de Souza Picciani (pág. 135)

12h20 Short and long range order study of Bi(4-x)LaxTi3O12 ferroelectric System
Mirta Mir (pág. 132)

12h40 Local structure study of multiferroic RMn2O5 with EXAFS
Gilberto Fabbris (pág. 166)

13h00 XANES of (Hg,Re)-1223 superconctor under pressure up to 6 GPa
Marcos Tadeu d'Azeredo Orlando (pág. 142)

Sessão 2 **Prédio Amarelo, Sala de Leitura (Biblioteca)**
Chairperson: **Abner de Siervo - LNLS**

12h00 Direct strain and elastic energy evaluation in rolled-up semicon ductor tubes by x-ray micro-diffraction
Angelo Malachias (pág. 211)

12h20 III-V Semiconductor Nonowires VLS Growth: Does Arsenic Diffuse Through the Metal Nanoparticle Catalyst?
Luiz Henrique Tizei (pág. 222)

12h40 Study of Nanostructured ZnO thin films prepared by Sol-Gel Spin-Coating by Synchrotron Techniques
Jorge Ramon Casanova (pág. 183)

13h00 STM and TEM Investigation of Reactive EPITAXY: HFSIX
Vinicius Lago Pimentel (pág. 219)

Sessão 3 **Prédio Amarelo, Sala 50**
Chairperson: **Maria Luiza Rocco - UFRJ**

12h00 HeI Photoelectron and Valence Syncrothron Photoionization Studies of CClH2SCN
Maurício F. Erben (pág. 52)

12h20 Estudos teórico-experimentais da produção parcial de íons do ácido fórmico
Manuela Souza Arruda (pág. 57)

12h40 Rock art paintings at Maqui shelter, Valle Encantado, Patagônia, Argentina: charcterization through SRXRD
Cristina Vásquez (pág. 71)

13h00 Analysis of trace elements in normal, benign and malignant breast tissues measured by total reflection x-ray fluorescence
Martin Eduardo Poletti (pág. 73)

Sessão 4 **Prédio da Biologia, Sala 69**
Chairperson: **Maria Cristina Nonato – USP / Ribeirão Preto**

12h00 A hypothetical protein coded by the Type IV Secretion System of a bacterial phytopathogen combines a VirB7 motif with a C-terminal signaling domain
Diorge P. Souza (pág. 29)

12h20 Estudos estruturais por RMN da proteína SBDS humana
Ana Carolina Zeri (pág. 26)

12h40 Crystal structure of Dioclea rostratalectin: insights into understanding the pH-dependent dimmer-tetramer equilibrium and the structural basis for carbohydrate recognition in Diocleinae lectins
Plinio Delatorre (pág. 21)

13h00 Interleukin-22 forms dimmers that are recognized by two interleukin-22R1 receptor chains
Mario Oliveira Neto (pág. 12)

10 DE FEVEREIRO, TERÇA-FEIRA

Comunicações Orais

Sessão 1 **Prédio do Anel, Auditório**
Chairperson: **Félix Requejo**

08h30 Lattice distotions in oxygen deficient SrMnOy coumponds
Leopoldo Suescun (pág. 161)

08h50 Modeling the atomic structure of na Amorphous Se90S10 Alloy Produced by Mechanical Alloying
Dario Sanches (pág. 120)

09h10 ZnO2-CeO2 solid solutions synthesized by different chemical routes: crystal structure and local order
Leandro Marcelo Acuña (pág. 134)

09h30 Caracterização de cristais de KDP dopados com L-arginina através de difração múltipla de raios-X utilizando radiação síncrotron
Paulo Tarso Cavalcante Freire (pág. 133)

Sessão 2 **Prédio Amarelo, Sala de Leitura (Biblioteca)**
Chairperson: **Ângelo Malachias - LNLS**

08h30 Chitosan influence on the phospholipid organization
Maria Ismênia Lionzo (pág. 178)

08h50 Zr and Ag L-edge XANES studies of Ag nanoparticles in nanoporuos Zr-Si-O thin films
Leandro Ruben Andrini (pág. 122)

09h10 An angle-scanned photoelectron diffraction study on the surface structure of Pd growth on Nb(100)
Fernando Cesar Lussani (pág. 218)

09h30 Study of structural deformation and Mn segregation in CdMnTe quantum dots
Sukarno O. Ferreira (pág. 199)

Sessão 3 **Prédio Amarelo, Sala 50**
Chairperson: **Luis Gallego Martinez – IPEN / CCTM**

08h30 Characterization of TiO2 nanoparticles synthesised in ionic liquids
Giovanna Machado (pág. 92)

08h50 Poly (methyl methacrylate)- Clay nanocomposites prepared by in situ intercalative polymerization the effect of the acrylic acid
Adriana dos Anjos Silva (pág. 96)

09h10 Study of 1s3p resonant inelastic x-ray scattering processes in transition metals
Guillermo Eduardo Stutz (pág. 125)

09h30 New superconducting wiggler beamline (SCW)
Bernd Christian Meyer (pág. 112)

Sessão 4 **Prédio da Biologia, Sala 69**
Chairperson: **Ricardo Aparício - UNICAMP**

08h30 Crystallographic studies of Cys-based proteins
Eduardo Hiroshi Nakamatsu (pág. 11)

08h50 Análise estrutural do complexo SPCI-quimotripsina por fluorescência dinâmica
Adelson Joel Silva (pág. 17)

09h10 Características estruturais e macanismo de ação do inativador iodoacetamida em complexo com a enzima Gliceraldeído-3-Fosfato Desidrogenase de Trypanosoma cruzi
Tatiane Balliano (pág. 46)

09h30 Crystal structure of Batroxase, a hemorrhagic zinc-dependent metalloproteinase from Bothrops atrox venom
Mario Tyago Murakami (pág. 24)

09 DE FEVEREIRO, TERÇA-FEIRA

Sessões Temáticas I

Sessão A1 **Prédio do Anel, Auditório**
Chairperson: **Jean Guillaume Eon**

14h30 Status e perspectivas das Linhas XAS / XAFS I e XAFS II / DXAS
Gustavo Azevedo e Flávio Garcia

Sessão B1 **Prédio Amarelo, Sala de Leitura (Biblioteca)**
Chairperson: **Altair Sória**

14h30 Status e perspectivas das Linhas XRD I e XRD II / XPD
Daniela Zanchet, Ângelo Malachias e Eduardo Granado

Sessão C1 **Prédio Amarelo, Sala 50**
Chairperson: **Pedro Nascente**

14h30 Status e perspectivas das Linhas Soft X-Rays / SGM / TGM / PGM / SXS
Arnaldo Naves de Brito, Richard Landers e Abner de Siervo

Sessão D1 **Prédio da Biologia, Sala 69**
Chairperson: **Chuck Farah**

14h30 Status e perspectivas das Linhas MX I e MX II / MAS / RMN / VUVF
João Alexandre, Mário Murakami, Ana Carolina Zeri e Fábio Gozzo

10 DE FEVEREIRO, TERÇA-FEIRA

Sessões Temáticas II

Sessão A2 **Prédio do Anel, Auditório**
Chairperson: **Watson Loh**

17h00 Status e perspectivas das Linhas SAXS I e SAXS II
Harry Westfahal Jr. e Íris Torriani

Sessão B2 **Prédio Amarelo, Sala de Leitura (Biblioteca)**
Chairperson: Marcelino José dos Anjos

17h00 Status e perspectivas das Linhas XRF
Carlos Perez

Sessão C2 **Prédio Amarelo, Sala 50**
Chairperson: Rodrigo Lacerda

17h00 Status e perspectivas da Microscopia Eletrônica
Antonio Ramirez

Sessão D2 **Prédio da Biologia, Sala 69**
Chairperson: **Mônica Cotta**

17h00 Status e perspectivas das Linhas STM / AFM e Micrifabricação
Gilberto Medeiros e Ângelo Gobbi

Sumário

Parte I Plenárias

IN-SITU OBSERVATIONS OF CATALYTIC SILICON NANOWIRE AND CARBON NANOTUBE CVD
Hofmann, S. 3

Magnetic soft X-ray microscopy - imaging nanoscale magnetic structures and their fast spin dynamics
Fischer, P. 4

Forma geométrica e função dielétrica de nanocristais individuais: determinação experimental por espalhamento de um único pulso curto de luz
Castro, A. R. B. 5

Parte II Biologia Estrutural

Análise da distribuição de chumbo e cálcio em dentes decíduos por fluorescência de raios X induzida por radiação síncrotron
de Souza Guerra, C, Pinto, N.G.V, Moreira, S., Barroso, R.C., Gerlach, R.F. 9

Structural analysis of BTCI in ternary complex with β-trypsin and α-chymotrypsin
Esteves, G. F., Silva, A. J., Barbosa, J.A.R.G., Freitas, S. M. 10

Crystallographic studies of Cys-based proteins.
Monteiro, G., Horta, B. B., Nakamatsu, E. H., Discola, K. F., Netto, L.E.S. 11

Interleukin-22 forms dimers that are recognized by two interleukin-22R1 receptor chains
Mario de Oliveira Neto, Ferreira Júnior, J. R., Fischer, H., Craievich AF, Polikarpov, I. 12

Crystal structure of cytosolic thioredoxin peroxidase I (cTPxI), C47S mutant, from *Saccharomyces cerevisiae*
Bataghin, F. A., Oliveira, M.A., Genu, V, Discola, K. F., Alves, S.V., Guimarães, B.G., Netto, L.E.S. 13

Crystallization and X-ray diffraction data collection of BthTX-I in different temperatures.
Marchi-Salvador, D. P., Silva,M.C.O, Salvador, G. H. M., Soares, A. M., Fontes, M. R. M. 14

Kinetic and structural stability studies of Oligopeptidase B from *Trypanosoma cruzi*
Motta, F. S. N., Bastos, I.M.D., Barbosa, J.A.R.G., Freitas, S. M., Santana, J. M. 15

Oligomerização e análise conformacional de uma Leucil aminopeptidase de *Leptospira interrrogans*
Álvares, A.C.M., Silva, A. J., Silva, H. A., Slovic, A.M., Barbosa, J.A.R.G., Santana, J. M., Freitas, S. M. 16

Análise estrutural do complexo SPCI-quimotripsina por fluorescência dinâmica
Silva, A. J., Teles, R. C. L., Schaberle, F. A., Barbosa, J.A.R.G., Freitas, S. M. 17

Cristalização e estudos cristalográficos preliminares do complexo SPCI-quimotripsina a 2,8 de resolução
Silva, A. J., Teles, R. C. L., Esteves, G. F., Santos, C. R., Barbosa, J.A.R.G., Freitas, S. M. 18

IDENTIFICAÇÃO E AVALIAÇÃO DA EXPRESSÃO DE MARCADORES MOLECULARES ENVOLVIDOS NA TUMORIGÊNESE DE PULMÃO
Henrique, T, Polachini, G.M., Vidotto, A., Cury, P.M., Zanelato, P., Nietmann, H., FARIA, Celso Murilo Nálio Matias de, Cury, F.A., Tajara, E.H. 19

Crystal structures of two lectins from *Cymbosema roseum*
Rocha, B.A.M., Delatorre, P., Benevides, R. G., Naganao, C.S., Sampaio, A.H., Azevedo Jr., W. F., Cavada, B.S. 20

Crystal structure of *Dioclea rostrata* **lectin: insights into understanding the pH-dependent dimmer-tetramer equilibrium and the structural basis for carbohydrate recognition in Diocleinae lectins**
Delatorre, P., Oliveira, T.M., Rocha, B.A.M., Bezerra, G.A., Moura TR, Benevides, R. G., Bezerra, E.H.S., Azevedo Jr., W. F., Sampaio, A.H., Cavada, B.S. 21

Structure determination of PilZ from Xanthomonas axonopodis pv. citri
Guzzo, C.R., Kopke Salinas, R., Farah, C.S. 22

CHARACTERIZATION OF RECOMBINANT PROCATHEPSIN L 3 FROM *TENEBRIO MOLITOR* **MIDGUT**
Beton, D., Guzzo, C.R., Farah, C.S., Terra, W.R. 23

Crystal structure of Batroxase, a hemorrhagic zinc-dependent metalloproteinase from *Bothrops atrox* venom
Murakami, M. T., Vilela, S. S., Arni, R.K., Cintra, A. O. 24

Structural analysis of the ModABC transporter from the pathogenic bacteria *Xanthomonas axonopodis* pv. *citri* by homology modeling and molecular dynamics
Santacruz-Perez, C., Balan, A., Pegos, V.R., Barbosa, J.A.R.G. 25

Estudos estruturais por RMN da proteína SBDS humana
Oliveira, J. F., Sforça, ML, Zanchin, N. I. T, Zeri, AC; 26

Crystallization and Preliminary X-ray diffraction analysis of the leptospiral protein LIC12922
Giuseppe, P. O., Atzingen, M. V., Nascimento, ALTO, Zanchin, N. I. T, Guimarães, B.G. 27

Crystallization of TIPRL: a novel regulator of type 2A phosphatases
Smetana, J. H. C., Alves, A. C., Teixeira, E. C., Zanchin, N. I. T 28

A hypothetical protein coded by the Type IV Secretion System of a bacterial phytopathogen combines a VirB7 motif with a C-terminal signaling domain
Souza, D. P., Farah, C.S., Kopke Salinas, R. 29

Parte III Biologia Molecular e Química de Proteínas

Efeitos do tratamento PUVA (Psoralenos mais Ultravioleta A) no DNA: Variedade de lesões e implicações em nível biológico
de Paula-Pereira Jr., M. V., Soares, M., C. Lage, Leitão, A.C. 33

DIFFERENTIALLY EXPRESSED PROTEINS IN LYMPH NODE AND IN BODY FLUIDS OF PATIENTS WITH HEAD NECK CANCER
Vidotto, A, Polachini, G. M., Cury, P.M., Maniglia, J.V, GENCAPO, P., Tajara, E.H. 34

SAXS studies on the temperature stability of extracellular hemoglobin of Glossoscolex paulistus in the oxy- form.
Santiago, P.S., Barbosa, L.R.S., Itri, R., Tabak, M. 35

Determination of human breast tissue structures between 0.15 and 8.50nm^{-1} using Small Angle X-ray Scattering
Conceição, A. L. C., Poletti, M. E. 36

Amplification and cloning of nahB gene and expression of NahB dehydrogenase for structural and functional studies
COSTA, D. M.A, Corrêa, N. C. R., Salas, C.E., Nagem, R. A. P. 37

A human protein involved in PKR protein kinase activation interacts with the 3´SL region of Dengue virus RNA
Alves, B.S.C., Figueiredo, L. T. M., Zanchin, N. I. T 38

Identification of a putative o-linked glycosylated subpopulation of the PP2A regulator α4 in the nuclear compartment of HEK293 cells
Smetana, J. H. C., Zanchin, N. I. T 39

Differentially expressed genes and their functional relationships in a blast-mesenchymal cell co-culture model.
Vaz, T. H., Vasconcellos, J.F., Alves, A. C., Melo, J.O., Yunes, J. A., Zanchin, N. I. T 40

Expression Systems for the Human Protein Kinase S6K1 and its Phosphorylation Substrate, the C-terminal Region of RPS6
Paier, C. R. K., Zanchin, N. I. T 41

Characterization of interactions between PthA protein from *Xanthomonas axonopodis pv citri* **and citrus proteins involved in transcription and translation**
Soprano, S. A., Souza, T. A., Cernadas, R. A., Benedetti C.E. 42

Análise de chaperones hipotéticas da Xanthomonas axonopodis pv. citri
Martins, A. M., Tasic, L., Arruda, M. A. Z. 43

Expression, purification and preliminary structural studies of human Nek1 and Nek6
Meirelles, G. V., Lanza, D.C.F, Lenz, G., Silva, J.C., Torriani, I., Kobarg, J. 44

Padronização da Ressonância Magnética Nuclear para determinação precoce da resistência à quimioterapia na leucemia linfóide aguda pediátrica
Melo,CPS, Yunes, J. A., Zeri, AC; 45

Características estruturais e mecanismo de ação do inativador iodoacetamida em complexo com a enzima Gliceraldeído-3-Fosfato Desidrogenase de *Trypanosoma cruzi*
BALLIANO, T. L., Guido R.V.C., Andricopulo, A. D., G.OLIVA 46

Cloning and expression of FtsJ3, a putative human ribosomal RNA methyltransferase.
MORELLO, L.G., Zanchin, N. I. T 47

Parte IV Ciência Atômica e Molecular

Fragmentação da Molécula da Vanilina Utilizando Feixes de Elétrons e a Luz Síncrotron
Silva,L.B., Bernini, R.B., Gomes, T. S., de Souza, G.G.B., Coutinho, L. H. 51

HeI Photoelectron and Valence Synchrotron Photoionization Studies of $CClH_2SCN$
Erben, Mauricio F., Rodriguez Pirani, Lucas, Romano, Rosana M., Geronés, Mariana, Cavasso Filho, R. L., Della Védova, Carlos O. 52

Dissociative Photoionization of $ClC(O)SCH_2CH_3$ following sulfur 2p and chlorine 2p.
Rodriguez Pirani, Lucas, Erben, Mauricio F., Geronés, Mariana, Romano, Rosana M., Cavasso Filho, R. L., Della Védova, Carlos O...... 53

Fragmentation Dynamic of Benzene, Aniline and Nitrobenzene Induced by Synchrotron Radiation
Flora, D., Paschoal, R. C., Ferreira, G. B., Turci, C. C., Guerra, A. C. O. . 54

Dynamical correlation in the double ionization of methane and ammonia molecules
ACF Santos, Boechat-Roberty , H.M., MONTENEGRO, E.C., Pilling, S., W. Wolff, de Jesus, V. L. B., Sigaud, L...... 55

Experimental evidence of the oxidation state through resonant Raman sacttering
Valentinuzzi, M. C., H. J. Sánchez, Abraham, J. A., Pérez, C. A...... 56

Estudos Teórico-Experimentais da Produção Parcial de Íons do Ácido Fórmico
M.S. Arruda, PRUDENTE, F. V., Marinho, R. R. T., Naves de Brito, A., Mundim, M. S. P., MANIERO, A. M...... 57

DEPENDÊNCIA ANGULAR DA FOTOFRAGMENTAÇÃO DA MOLÉCULA DE TIOFENO
Vieira, C.C.O., Mundim, M.S. P., Correia, N., Attie, M.R.P., Marinho, R. R. T., Naves de Brito, A., Mocellin,A. 58

Parte V Geociência, Meio-ambiente e Aplicações em Materiais Biológicos

---

EFECTO DEL CONSUMO DE ANTIOXIDANTES SOBRE LA DISTRIBUCION Y CONCENTRACION DE ELEMENTOS EN CORTEZA RENAL DE RATAS EXPUESTAS A ARSENICO
Rubatto Birri, P.N., R.D. Pérez, Pérez, C. A., Rubio, M., Bongiovanni, G.A. 61

Bone Imaging Investigation by X-Ray Microfluorescence Technique with Capillary Optics
LIMA, I., Anjos, M. J., Assis, J. T., Lopes, R.T...... 62

Determinación de la presencia de drogas de tipo bifosfonatos o raloxifeno en huesos humanos, de pacientes con osteoporosis que han sido tratados clínicamente con estos compuestos.
Fernández de Rapp, M. E., Fábregas, I. O., Lamas, D. G...... 63

INFLUENCE OF THE CONTENT OF PRAZIQUANTEL ON STRUCTURAL FEATURES OF THE LIPOSOMES
Souza, A. L. R., Sarmento, V.H.V, Terruggi, C.H.B., Chiavacci, L.A., Allegretti, S. M., Gremião, M. P. D. 64

Phase transitions in ZrO_2-Sc_2O_3 solid solutions: crystallite size effect
Abdala, P. M., Lamas, D. G., Craievich AF, Fantini, M. C. A. 65

CHARACTERIZATION OF THE CRAB TISSUES AND SEDIMENT BY SR-TXRF
Salvador, M. J., Sawazaki, D.T.A., Hattori, G.Y., Zucchi, O. L. A. D 66

MICROELEMENT ANALYSIS BY ED-XRF IN CEREBRAL SLICES OF RATS SUSCEPTIBLE TO AUDIOGENIC SEIZURES
Salvador, M. J., Arantes, F.C., Rodrigues, MCA, Rossetti F., Arisi, G. M., Garcia-Cairasco, N., Zucchi, O. L. A. D 67

ESTUDO DO PROCESSO DE MORTE CELULAR EM CÉLULAS EMBRIONÁRIAS SOB AÇÃO DE CANABINÓIDES
Cardoso, S.C., Magalhães, S.D. 68

ESTUDO FRACAO ASFALTENICA DE AMOSTRAS DE ROCHAS GERADORAS DA BACIA DO PARANA POR ESPECTROMETRIA DE MASSAS POR TEMPO DE VOO COM DESORCAO A LASER E IONIZACAO ASSISTIDA POR MATRIZ (MALDI-TOF-MS)
Silva,C.G.A., Peralba, M.C.R., Dos Santos, J. H. Z., Kern, L. M., Franco, R. N., Kalkreudt,W. 69

Oxalato de Cálcio monohidratado encontrado em pedras de rins
Corrêa, H. P. S., Orlando, M. T. D., Martinez, L. G. 70

Rock art paintings at Maqui shelter, Valle Encantado, Patagonia, Argentina: characterization through SRXRD
Vázquez, C, Maury, A. M., Adan Hajduk, Alnornoz, Ana, Boeykens, S. 71

Hexavalent chromium detoxification by living aquatic macrophytes root-based biosorption using high resolution x-ray fluorescence
Espinoza Quiñones, F.R., Stutz, G., Tirao G., Palacio, S.M., M.A. Rizzutto, Módenes, A. N., Silva Jr, F. G., Szymanski, N. 72

Analysis of Trace Elements in Normal, Benign and Malignant Breast Tissues measured by Total Reflection X-Ray Fluorescence
Silva, M.P., Zucchi, O. L. A. D, Costa, J. J. G., Poletti, M. E. 73

X-ray diffraction induced by synchrotron radiation in archaeology: compositional study of prehistoric pigments (Carriqueo rock shelter, Argentina)
Palacios, O.M., Maury, A. M., Boeykens, S., Vázquez, C 74

Formação de imagens por Contraste de Fase: Imagens Realçadas por Difração
Mardegan, J. R. L., Giles, C., Rocha, H. S., Pereira, G.R., Mazzaro I., Freitas, M. B. 75

Parte VI Matéria Mole e Fluídos Complexos

Room Temperature Humidity XRD Investigations for Li-FH and Ni-FH in Synthetic Clay.
da Silva, G. J., Ribeiro, L., Mundim, M.S. P., Sousa, M. H., Fossum J. O. . 79

Estudo de estrutura supramolecular do poliestirenossulfonato de sódio
Batista, T, MACHADO, D. S., Neumann, M. G., Polikarpov, I., Mario de Oliveira Neto, A.F. Craievich, Schmitt, C.C. ou Cavalheiro, C.C.S 80

STUDY OF BPP7A PEPTIDE AND ITS β-CYCLODEXTRIN INCLUSION COMPLEXES: COMPLETE SEQUENCE SPECIFIC NMR ASSIGNMENTS
Lula, I., Sinisterra R. D., Santos, R.A.S., Camargo, A.C.M. 81

Structural characterization of systems formed by an anionic copolymer and a cationic surfactant
Percebom, A. M., W. Loh 82

Caracterização de frações de Asfaltenos de petróleos Brasileiros
Seidl, P.R. 83

The Structure of Monoolein:Oleic acid containing Photosensitizers
Rossetti, F. C., Moreira, B.J., Fantini, M. C. A., Bentley, M.V.L.B. 84

Efeito de grupos retiradores de elétrons na síntese de nanofibras por gelificação a partir de moléculas orgânicas derivadas da glicose.
Vitorazi, L., Abreu, M. F., Giacomini, R. A., Cardoso, S.L., Gatts, C., dos Santos, D. R., Miranda, P. C. M. L. 85

Parte VII Materiais Estruturais e Aplicações na Indústria

MICROSTRUCTURE OF NANOTEFLON/POLYURETHANE FILMS
Anbinder, P. S., Peruzzo, P. J., Amalvy, J. I. 89

Expansão térmica do $Y_2Mo_3O_{12}$ em baixas temperaturas
Ari M., Marinkovic, B. A., Jardim, P. M., Rizzo, F. 90

Template removal process in mesoporous $Zr - Ce$ oxides
Bacani, R., Martins, T. S., Matos, J. R., Lamas, D. G., Fantini, M. C. A. . 91

Characterization of TiO2 nanoparticles synthesised in ionic liquids
Teixeira, S.R., Dupont, J., Migowski, P, Weibel, D. E. or Weibel, D., Machado, G, Feil, A. F. 92

Effect of the curing agent on the nanostructure of polybutadiene-modified epoxy resin
Soares, B.G., DAHMOUCHE, K, Lima, V.D. 93

A XANES and EXAFS study on Ti doped low silica calcium aluminosilicate glasses
Filadelpho, M. C., Andrade, A. A., Rohling, J.H., Medina, A.N., Baesso, M.L., Sampaio, J. A. 94

Desenvolvimento de um dispositivo para determinação de constantes elásticas cristalográficas por medidas de difração síncrotron
Martinez, L. G., Orlando, M. T. D., Corrêa, H. P. S., J.L.Passamai Jr, Rossi, J. L. 95

Poly(methyl methacrylate)- Clay nanocomposites prepared by in situ intercalative polymerization the effect of the acrylic acid
Silva, A.A. 96

Structural and optical properties of Tb^{3+} and Er^{3+} doped BaY_2F_8
de Mello, A.C.S., Baldochi, S. L., Valerio, M.E.G. 97

Crystalline and amorphous mixed basic carbonates as a source of nanometric: $Ce_{1-x}La_xO_{2-y}$ and $Ce_{1-x}Cu_xO_{2-z}$: PXRD and XAS characterization
E. E. Sileo, Jobbagy, M. 98

Experimentos XANES in situ em Catalisadores Ni/MCM-41
Brandão, S. T., Oliveira, O.B., Mundim, M.S. P., da Silva, G. J. 99

Análise de catalisador comercial HTS por difração de raios X *in situ* **na reação de deslocamento água-gás**
Braga, A. H., Rodella, C. B., Olivira Junior N.G.O., Zanchet, D. 100

Study of RF Magnetron sputtering TiOx and TiOxNy films
Albertin, K.F., I. Pereyra 101

The structural dynamics of FDU-1 ordered mesoporous silica calcination process
Mariano-Neto, F., Silva, L.C.C., Martins, T. S., Matos, J. R., Fantini, M. C. A. 102

Parte VIII Métodos e Instrumentação

Prototipagem rápida de microchips em vidro para separações eletroforéticas
Segato, T. P., Coltro, W. K. T., Mazo L H, Carrilho, E. 105

Current Status of the Wavelenght Dispersive System of the XRF Beamline
Pérez, C. A., H. J. Sánchez 106

Characterization of standard reference materials for powder diffraction
Martinez, L. G., Orlando, M. T. D., Corrêa, H. P. S., Rocha, C. J., Paiva-Santos,C.O., Ferreira, F. F. 107

Implementation of confocal setup in the LNLS using polycapillary optics.
R.D. Pérez, H. J. Sánchez, Pérez, C. A., Rubio, M. 108

Experimental study of the elliptical polarization in monochromatic synchrotron X-ray beams
Droppa Jr., R., Morelhão, S.L. 109

Medição de tensões residuais em filmes finos por difração de raios X com ângulo de incidência rasante
Gómez, A. G., Recco, A.A.C., Martinez, L. G. 110

Future developments of the X-ray powder diffraction (D10B-XPD) beamline
Ferreira, F. F., Granado, E. 111

New superconducting wiggler beamline (SCW)
Meyer, B.C., Granado, E., Neueschwander, R. T., Rodrigues, F 112

Scientific Opportunites with the New Superconducting Wiggler Beamline for Materials Science
Granado, E. 113

Parte IX Propriedades Estruturais, Eletrônicas e Magnéticas de Sólidos

New In-Situ Blends of Polyaniline and Polycardanol Characterized by SAXS/WAXS
Souza Jr, F. G., Richa, P. R. F., Cosme, T. A., Pinto, J.C. 117

Electronic and structural evolution of pentacyanonitrosylmetallates during thermal decomposition
Soria,B., Taylor, M.A., Ceolin M. 118

Kinetics of crystallization in $Cu_{1-x}TM_xO$ (TM=Fe or Ni) by X-ray Absorption and Diffraction
Meneses, C. T., Duque J.G.S., Knobel, M. 119

Modeling the atomic structure of an Amorphous $Se_{90}S_{10}$ Alloy Produced by Mechanical Alloying
Sanchez, D. F., K. D. Machado, Maciel, G.A., Jóvári, P., Brunatto, S. F., Stolf, S. F. 120

Estructura atómica, dinámica local, anharmonicidad y expansión térmica en nanoaleaciones FexCu100-x: determinación del potencial interatómico mediante EXAFS empleando teoría de perturbaciones estadístico-cuántica.
Lede, E. J., Socolovsky, L. M. 121

Zr and Ag L-edge XANES studies of Ag nanoparticles in nanoporous Zr-Si-O thin films
Andrini, L., Wolosiuk, A., Angelomé, P. C., Soler-Illia, G.J.A.A., Requejo, F. G. 122

A pre-edge analysis of Ti K-edge XANES spectra of photoluminescent PZT powder
de Figueiredo, A. T., Mastelaro, V.R., Varela, J.A., Longo, E. 123

Study of the changes in Ti coordination in $CaTiO :_3 Sm$ by Ti K-edge XANES
R. Oliveira da Silva, de Figueiredo, A. T., Mastelaro, V.R., Longo, E. 124

Study of 1s3p resonant inelastic x-ray scattering processes in transition metals
Stutz, G., Tirao G. 125

IRON DOPING IN TIN DIOXIDE NANOPARTICLES
Barrero, C.A. 126

Fe-doping and strain effects on structural and magnetotransport properties in La2/3Ca1/3Mn1-yFeyO3 thin films
Arnache, O., Girata, D, Hoffmann, A 127

DIFRAÇÃO DE RAIOS-X USANDO RADIAÇÃO SÍNCROTRON NO CRISTAL ORGÂNICO DE MBANP SUBMETIDO A CAMPO ELETRICO
C. M. R. Remedios, dos Santos, A. O., de Menezes, A. S., Cardoso, L.P. ... 128

Structural characterization of ZrO_2-CeO_2 nanotubes
Acuña, L. M., Lamas, D. G., Fuentes, R. O. 129

XAS study of nanostructured $SrTi_{1-x}Fe_xO_3$ compounds
da Silva, L. F., Maia, L. J. Q., M.I.B.Bernardi, Mastelaro, V.R. 130

Difração Múltipla de raios-X em co-cristais de L-Asparagina e L-Alanina
Pinheiro, G. S., Melo, F. E. A., Freire, P. T. C., C. M. R. Remedios, Menezas, A. S., dos Santos, A. O. 131

Short and long range order study of $Bi_{(4-x)}La_xTi_3O_{12}$ ferroelectric System
Santos, V. B., Mastelaro, V.R., Mir, M., Neves P.P, Doriguetto, A.C., Mascarenhas, Y.P. 132

Caracterizacao de cristais de KDP dopados com L-arginina através de difracao múltipla de raios-X utilizando radiacao síncrotron
Freire, P. T. C., Pinheiro, G. S., Melo, F. E. A., C. M. R. Remedios, Moreira, S. G. C., dos Santos, A. O. 133

ZrO_2-CeO_2 solid solutions synthesized by different chemical routes: crystal structure and local order
Acuña, L. M., Zimicz, M. G., Lamas, D. G., Fuentes, R. O., S.A. Larrondo, Fantini, M. C. A., Craievich AF 134

Characterization of a new material based on polyaniline doped with [Cs][$In(dmit)_2$], (cesium) [bis(1,3-dithiole-2-thione-4,5-dithiolato)indium (III)] by X-Ray Photoelectron Spectroscopy
Picciani, P.H.S, Comerlato, N.M., Soares, B.G., Souza Jr, F. G. 135

XANES Study of Si and Zr in Composite Hollow Spheres
Andrini, L., Arnal, P. M., Requejo, F. G. 136

Microstructural Evaluation of Rapidly Solidified Ti-Si-B Alloys via High Resolution TEM
Candioto, K.C.G., Nunes, C. A., Coelho, G. C. 137

Structural features on corrosion inhibiting properties of siloxane-PMMA hybrid coatings by SAXS and XPS
Sarmento, V.H.V, Hammer, P., Pulcinelli, S.H., Santilli, C.V. 138

Estudo das transformações estruturais de compósitos de ferro nanoestruturados em materiais carbonosos porosos em função da temperatura utilizando a linha D10B-XPD
Miguel A. Schettino Jr., Freitas, JCC, Morigaki, M. K., E. Nunes, Cunha, A. G., Passamani, E. C., Francisco G. Emmerich 139

TERMODINÂMICA DE FORMAÇÃO E ESTRUTURA DE MICELAS REVERSAS DE $(EO)_{13}$ $(PO)_{30}$ $(EO)_{13}$ EM P-XILENO
Gomes, D. S. B., Teixeira, A. V., Da Silva, L. H. M., Rocha, J.C. 140

Thermal expansion of Ta_5Si_3 and Cr_5Si_3
Ribeiro, L.S., Suzuki, P. A., Renosto, S. T., Nunes, C. A., Coelho, G. C. . . . 141

XANES of (Hg,Re)-1223 superconductor under pressure up to 6 GPa
Orlando, M. T. D., J.L.Passamai Jr, Martinez, L. G., E. J. Carvalho, Garcia, F., Corrêa, H. P. S. 142

RADIATION DAMAGE AND RADIATION INDUCED OXI - REDUCTION OF Eu IONS IN RARE EARTHS DOPED $SrAl_2O_4$
Montes, PJR, Valerio, M.E.G. 143

Alterações estruturais em $Fe[Co(CN)_6]$ sob altas pressões
Catafesta, J., Zorzi, J. E., Garcia, F., Haines, J., Pereira, A. S., Perottoni, C. A. 144

XAFS study of $Zn_{0.85}Co_{0.15}O$ powders prepared by ball milling
A.M. Mudarra Navarro, L.C.Damonte, Rodríguez Torres, C. E. 145

Molecular Structure and Dynamics of Polyfluorene Derivative Films
Faria, G. C., Plivelic, T.S., Souza,A.A., R. F. Cossiello, Atvars, T.D.Z., Torriani, I., deAzevedo, ER 146

ELECTRONIC PROPERTIES OF COORDINATION COMPOUNDS OF THE DMIT, DMIO AND DMT LIGANDS
Lopes, L. J. S., Guerra, A. C. O., Ferreira, G. B., Turci, C. C. 147

Síntese, Caracterização e Fotoatividade de Fotossensibilizadores Derivados de Protoporfirina IX
Uchoa AF, BAPTISTA, MS 148

Caracterização estrutural de formas polimórficas de insumos farmacêuticos
Neves P.P, Doriguetto, A.C., Mir, M., Camps, I., Pereira, S. V., Martins, F. T., Ellena J. 149

Ordem química local em nanocristais de GaSb em função da temperatura
Campos, C. E. M., De Lima, J.C. 150

Chemical enviroment of europium in low silica calcium aluminosilicate glasses
Sampaio, J. A., Filadelpho, M. C., Rohling, J.H., Medina, A.N., Baesso, M.L., Andrade, A. A. 151

Long-range ordering in $Pb_{1-0.5x}La_xTiO_3$ relaxor ferroelectric ceramics
Doriguetto, A.C., Neves P.P, Mir, M., Mastelaro, V.R., Mascarenhas, Y.P., Landre, I. M. R. 152

EFFECT OF THE STATE OF METALS OXIDATION ON POLYSULFUR LIGANDS
Turci, C. C., Guerra, A. C. O., Comerlato, N.M., Lopes, L. J. S., Ferreira, G. B. 153

Synthesis and Properties of Titanate nanotubes modified.
Viana, B. C., Ferreira, O.P., SOUZA FILHO, A. G., Alves. O. L. 154

ESTUDO DA ESTRUTURA LOCAL DO $Ba_{0,77}Ca_{0,23}TiO_3$:Nd^{3+} POR ESPECTROSCOPIA DE ABSORÇÃO RAIOS-X.
Moraes, A. P. A., SOUZA FILHO, A. G., Azevedo, G. de M., Antonelli, E., MPeko, J.-C. 155

Structural characterization of $La_{0.80}Sr_{0.30}Mn_{0.90}Cr_{0.10}O_3$
Cavalcante, I. P., Corrêa, H. P. S., Dorotéia F. Bozano ou D. F. Bozano, Orlando, M. T. D., Martinez, L. G. 156

Electronic structure, stability and surface tension of ZrO_2 nanoparticles
Casali, R.A., Ponce, C.A., Caravaca, M.A. 157

ESTRUTURA MAGNETICA DO INTERMETALICO TbCo2B2C
R. M. Briones, ElMassalami,M; El Massalami, M; Massalami, M 158

Ternary Ni-based boro-aluminides (Al-Ni-B): their synthesis, structure, and physical characterization.
M. M. Elhadi, ElMassalami,M; El Massalami, M; Massalami, M 159

Insights on growth mechanism of Carbon Nanofibers: Catalyst particle studied by Transmission Electron Microscopy and additional techniques
Roa, D. B, S de Oliveira, Ferlauto, A. S., Ladeira L.O., Magalhaes-Paniago, R., Lacerda, R. G. 160

Lattice distortions in oxygen deficient $SrMnO_y$ compounds.
Suescun, L., Dabrowski B., Faccio, R., Mombrú, A.W. 161

Analysis of Prostate Tissues using SRTXRF
Leitão,R.G, Canellas,C.G.L, Palumbo, A.J, Souza, P.A.V.R, Nasciutti, L.E, Anjos, M. J., Lopes, R.T. 162

Structural and Magnetic Characterization of $Cu_{1-x}TM_xO$ (MT = Co, Fe, Ni)
Duque J.G.S., Meneses, C. T., Knobel, M. 163

HRTEM and XAS study of V_2O_5 nanoparticles prepared through the hydrothermal method
Avansi, W., Ribeiro, C., Leite,E.R., Mastelaro, V.R. 164

Crystallographic Changes Accompanying the Verwey Transition in a Magnetite from Steatite
Silva, F. D. da, FABRIS, J. D., COUCEIRO, P.R.C., Goulart, A.T. 165

Local structure study of multiferroic RMn_2O_5 with EXAFS
Fabbris, G. F. L., Maciel, G.A., Granado, E., Massa, N. E., souza, J. A., Alonso, J.A., Azevedo, G. de M., Lope-Martinez, M.J. 166

Evaluation of the amorphous to crystalline phase transition temperature in Ti-Si-B alloys by Synchrotron Radiation XRD.
Candioto, K.C.G., Nunes, C. A., Suzuki, P. A. 167

Low resolution structure of synthetic melanin aggregates in aqueous solutions and organic solvents
Torriani, I.L., Silva, J.C., Autreto, P. A. S., D. S. Galvao, Caldas, M. J., Graeff, C. F. O. 168

MORPHOLOGICAL AND STRUCTURAL PROPERTIES OF EXPANDED AUSTENITE
C. A. Figueroa, Basso, R. L. O., Pimentel, V. L. 169

Caracterização de sub-frações de asfaltenos usando SAXS
Navarro, L. C., Seidl, P.R., Tasic, L., W. Loh 170

The origin of multiferroicity at $DyMn_2O_5$
Azimonte, C., Granado, E., Terashita, H 171

Parte X Superfícies, Interfaces e Nanossistemas

Nanocrystalline diamond formation in porous silicon obtained by Chemical Vapor Deposition/Infiltration (CVD/CVI) process
Miranda, C.R.B., Baldan, M.R., Beloto, A.F., Ferreira, N.G. 175

Surface anisotropy, exchange bias and particle size effects in magnetite nanoparticles: a Monte Carlo simulation study
J. Restrepo 176

Structure and electronic properties of magnetite clusters: A first-principles study
J. Restrepo 177

CHITOSAN INFLUENCE ON THE PHOSPHOLIPID ORGANIZATION
Lionzo, M. I. Z., Silveira, N. P. 178

Nonaqueous Synthesis of Antimony Tin Oxide Nanocrystals
R. Oliveira da Silva, Conti T. G., Stroppa, D. G., Longo, E., Leite,E.R. 179

Structural studies of biocompatible iron oxide nanoparticles for biological applications
Socolovsky, L. M. 180

Relation between structural properties and in vitro release of amphotericin B from delivery system based on soya phosphatidylcholine
Pestana. K.C., FRANZINI, C.M., Sarmento, V.H.V, Chiavacci, L.A., OLIVEIRA, A.G. 181

Interação entre átomos de ouro e cobre com superfícies Si (111): Um estudo combinado de GIXRF e DFT.
*Batista, A. P. L., Carvalho, H.W.P, Ramalho, TC, Gobbi, A. L., Pérez, C. A.*182

STUDY OF NANOSTRUCTURED ZnO THIN FILMS PREPARED BY SOL-GEL SPIN-COATING BY SYNCHROTRON TECHNIQUES
Bojorge, C. D., Cánepa, H. R., Casanova, J. R., A.F. Craievich, Heredia, E., Kellermann, G. 183

Effects of organophilic clay on nanostructure of epoxy networks
Zaioncz, S., Soares, B.G., DAHMOUCHE, K 184

Local structure of nanocrystalline ZrO_2-Sc_2O_3 powders
Abdala, P. M., Lamas, D. G., Fantini, M. C. A., Craievich AF 185

Photocatalytic decomposition of H_2O_2 by silicon wafer doped with Au and Cu: theoretical and experimental study
Carvalho, H.W.P, Batista, A. P. L., Ramalho, TC, Gobbi, A. L., Pérez, C. A. 186

Growth of Indium Tin Oxide Nanobelts with controlled In:Sn ratio by Carbothermal Reduction Process
Orlandi, M.O., Leite,E.R., Longo, E. 187

SMALL-ANGLE X-RAY SCATTERING STUDIES IN POLYMER COLLOIDS
Peruzzo, P. J., Anbinder, P. S., Plivelic, T.S., Amalvy, J. I. 188

Estudio XAFS de la estructura de nanopartículas Pd_xAu_{1-x} encapsuladas en tioles
Giovanetti, L. J., Ramallo-López, J. M., Requejo, F. G., Grumelli, D., Salvarezza R C, Shon, Y. S. 189

GISAXS study of CoMo nanoparticles on Si(111) used for catalytic synthesis of single wall carbon nanotubes.
Giovanetti, L. J., Kellermann, G., dos Santos Claro, P. C., A.F. Craievich, Requejo, F. G. 190

Study of silver nanoparticles inclusion in single and multilayered mesoporous oxide films using XRR and 2D-SAXS
Fuertes, M.C., Marchena M. H., Wolosiuk, A., Soler-Illia, G.J.A.A. 191

Estudos XANES e EXAFS de catalisadores de gálio suportados em zeólita H-ZSM5
Faro Jr., A. C., Eon J-G., Rodrigues, V. O., Silva, R. F., Nogueira, L. 192

EXAFS characterization of PdIr/USY catalysts
Faro Jr., A. C., Eon J-G., Rodrigues, V. O., FRANÇA, M. C. K. 193

EXAFS characterization of the local disorder in Y2O3 nanoparticles produced via a coconut water-assisted sol-gel method
Gomes, M.A., Valerio, M.E.G., Macedo, Z.S. 194

Correlations between magnetic phases and structural properties in Co/Ru superlattices
Alayo, W., V. P. Nascimento, Miguel Tafur, F. Pelegrini, Y.T.Xing, Baggio-Saitovitch, E. 195

Induced Magnetism in the NiO/Cu/NiFe and NiO/Cr/NiFe trilayers systems
Miguel Tafur, Alayo, W., Y.T.Xing, Nascimento, V. P., Baggio-Saitovitch, E. 196

Photoabsorption and desorption studies on poly(3-hexylthiophene) at the S K-edge
Araujo,G.S, Arantes, C., Roman, L. S., Rocco, M.L.M. 197

Core-shell atomic structure formation in Pt-X (X = Co, Cu or Pd) nanoparticles
Bernardi, F., Silva, D. O., Ribeiro, D.C.A., Alves, M.C.M., A. Traverse, Dupont, J., Morais, J. 198

Study of structural deformation and Mn segregation in CdMnTe quantum dots
Scudeller, L. A., Malachias, A., Ferreira, S. O. 199

Scintillation Properties and Dopant Location in Rare Earths Doped $Ca_{12}Al_{14}O_{33}$ via XAFS and XEOL
Valerio, M.E.G., Montes, PJR 200

Characterization of Au nanparticles immobilized in alumina nanoporous membranes
da Costa, M. V., Feil, A. F., Migowski, P, Machado, G, Dupont, J., AMARAL L., Teixeira, S.R. 201

Water splitting using Gold nanoparticles embedded in TiO_2 nanotubes
Feil, A. F., da Costa, M. V., Weibel, D. E. or Weibel, D., Migowski, P, Machado, G, Dupont, J., AMARAL L., Teixeira, S.R. 202

Estudo da Dessorção Iônica Induzida por Fótons em Filmes de HMDSO Polimerizados por Plasma
Veiga, A.G., Rocco, M.L.M. 203

Micellar Solutions and Microemulsions formed with Ionic Surfactants applied as Corrosion Inhibitors: Characterization by Small-Angle X-Ray Scattering
Wanderley Neto, A. O., Gurgel, A., Dantas, T.N.C., Moura, E.F., Dantas Neto, A.A. 204

SRSAXS to study the limits of different concentration regimes in polysacharide aqueous solutions
Caracciolo, N., Boeykens, S., Vázquez, C 205

Simultaneous XAFS and XRD Studies of Water Intercalation in Synthetic Ni-Fluorohectorite
Ribeiro, L., Mundim, M. S. P., Fossum J. O., da Silva, G. J. 206

Au-Pd bilayred films grown by dc magnetron sputtering: structural, morphological, and chemical characterization
Machado, A.C., Silva, P.J.M., Gobbi, A. L., Fantini, M. C. A., Gheno, S. M., Paulin Filho, P.I., Nascente, P. A. P. 207

Formação e Caracterização de Fases Micelares e Líquido-Cristalinas Constituídas por Óleos e Surfatantes Siliconados
Ferreira, M.S., Westfahl Jr., H., W. Loh 208

Influence of interface and confinement phenomena in silicon based systems photoluminescence.
M. Ribeiro, I. Pereyra 209

Influência dos efeitos de tamanho de cristalito e de textura na reação de oxidação eletroquímica de monóxido de carbono sobre platina não suportada
Ciapina, E. G., Santos, S.F., Gonzalez, E. R. 210

Direct strain and elastic energy evaluation in rolled-up semiconductor tubes by x-ray micro-diffraction
Malachias, A. 211

Propriedades estruturais de nanopartículas de Ge encapsuladas em sílica
Gasperini, A. A., Avendano, E., Gobbi, A. L., Azevedo, G. de M. 212

Applying the LOC concepts to improve an *"electronic tongue"* **system**
Dantas, C.A.R., Almeida, A.L.J., Piazzetta,O.M.H, Gobbi, A. L., Riul Jr, A. 213

Surface properties influence on electrochemical behavior of boron doped diamond produced at different doping levels
Ferreira, N.G., Azevedo, A.F., Baldan, M.R., Matsushima, J.T. 214

Dinâmica do Crescimento de Nanofios Semicondutores Auto-Sustentados de InP
Th. Chiaramonte, Tizei, L. H. G., Ugarte, D., Cotta, M.A. 215

Nanodiamond grown on porous silicon using reticulated vitreous carbon as a solid carbon source
Miranda, C.R.B., Azevedo, A.F., Baldan, M.R., Beloto, A.F., Ferreira, N.G. 216

Caracterização de Fases Líquido-Cristalinas por SAXS
Campos, DDP, Bertran, C. A. 217

An angle-scanned photoelectron diffraction study on the surface structure of Pd growth on Nb(100)
Lussani, F.C., Pancotti A., Landers R, Carazzolle M.F., de Siervo A. 218

STM AND TEM INVESTIGATION OF REACTIVE EPITAXY: HFSIX
Leite, M. S., G.A. Fiorentini, Pimentel, V. L., Montoro, L. A., Ramirez, A.J., Medeiros-Ribeiro, G. 219

Eletrocatálise de oxidação de etanol em monocamadas mistas de Pt, Ru e Rh depositadas em nanopartículas de Au/C
Lima, F. H. B., Profeti, D., Ticianelli, E. A., Gonzalez, E. R. 220

Catalisadores de Co suportados aplicados nos processos de reforma a vapor e reforma autotérmica do etanol
Liberatori, J. W. de C., Ribeiro, R.U., Zanchet, D., Bueno, J.M.C. 221

III-V Semiconductor Nanowires VLS Growth: Does Arsenic Diffuse Through the Metal Nanoparticle Catalyst?
Tizei, L. H. G., Th. Chiaramonte, Cotta, M.A., Ugarte, D. 222

Síntese e caracterização de nanopartículas de Platina
Meira, D. M., Ribeiro, R.U., Prieto, P. J. S., Zanchet, D., Bueno, J.M.C. . . 223

Parte I

Plenárias

IN-SITU OBSERVATIONS OF CATALYTIC SILICON NANOWIRE AND CARBON NANOTUBE CVD

Hofmann, S.[1]

University of Cambridge - Cambridge United Kingdom

Self assembled nanowires and nanotubes offer the prospect of accurate and scalable device engineering at an atomistic scale. Limited control of their growth is one of the largest bottlenecks towards the numerous potential applications in electronics, photonics and biology. We study the catalytic chemical vapour deposition of these one dimensional nanostructures and investigate nanometrology that allows a monitoring of the contributing atomistic processes under high temperatures and reactive gas atmospheres. We present environmental transmission electron microscopy (ETEM), in-situ X-ray photoelectron spectroscopy (XPS) and in-situ X-ray diffraction (XRD) experiments analysing catalyst dynamics during the growth of silicon nanowires [1] and carbon nanotubes [2,3,4]. Our results aim to establish a framework for a detailed growth model and an understanding of the materials and chemistry on the nano-scale.

[1] Hofmann et al., Nature Materials 7, 372 (2008) [2] Hofmann et al., Nano Lett. 7, 602 (2007) [3] Mattevi et al., J. Phys. Chem. C 112, 12207 (2008) [4] Hofmann et al., J. Phys. Chem. C, in press

Acknowledgements:

Magnetic soft X-ray microscopy - imaging nanoscale magnetic structures and their fast spin dynamics

Fischer, P.[1]

Lawrence Berkeley National Laboratory - Berkeley CA United States of America

The scientific desire and technological demand to manipulate spins on the nanoscale can only be met by advanced analytical tools. The ultimate goal for modern magnetic microscopies is to combine spatial resolution in the nanometer regime, a time resolution on a ps to fs scale and elemental specificity which allows to study novel multicomponent and multifunctional magnetic nanostructures and their ultrafast spin dynamics down to fundamental magnetic length and time scales. Magnetic soft X-ray microscopy is a very promising candidate since it combines X-ray magnetic circular dichroism (X-MCD) as element specific magnetic contrast mechanism with high spatial and temporal resolution. Fresnel zone plates used as X-ray optical elements provide a spatial resolution down to currently ¡15nm [1] thus approaching fundamental magnetic length scales such as the grain size in media with perpendicular magnetic anisotropy [2]. Utilizing the inherent time structure of current synchrotron sources fast magnetization dynamics with 70ps time resolution, limited by the lengths of the electron bunches, can be performed with a stroboscopic pump-probe scheme [3]. Focus of research activities with magnetic soft X-ray microscopy are time resolved current induced vortex [4] and domain wall phenomena [5]. Current developments in X-ray optics will soon provide less than 10nm spatial resolution and with the availability of upcoming high brilliant fsec X-ray sources X-ray microscopy taking snapshot images of fsec spin dynamics is within reach. In this talk I will review the achievements, the potential and the future directions of using soft X-rays for advanced magnetic microscopies.

[1] W. Chao, et al., Nature 435, 1210, (2005); D.-H. Kim, et al., J. Appl. Phys. 99, 08H303, (2006) [2] M.-Y. Im, D.-H. Kim, K.-D. Lee, S.H. Lee, P. Fischer, and S.-C. Shin, Adv. Mater 20 (2008) 1750 [3] P. Fischer, et al., JMMM 310(2) pt 3 (2007) 2689 [4] S. Kasai, P. Fischer, M-Y. Im, K. Yamada, Y. Nakatani, K. Kobayashi, H. Kohno, and T. Ono, Phys Rev Lett 101, 237203 (2008) [5] L. Bocklage, B. Krueger, R. Eiselt, M. Bolte, P. Fischer, and G. Meier, Phys Rev B 78 180405(R) (2008)

This work was supported by the Director, Office of Science, Office of Basic Energy Sciences, Materials Sciences and Engineering Division, of the U.S. Department of Energy.

Acknowledgements:

Forma geométrica e função dielétrica de nanocristais individuais: determinação experimental por espalhamento de um único pulso curto de luz

Castro, A. R. B.[1]

Laboratório Nacional de Luz Síncrotron - Campinas SP Brazil

A Rubens B de Castro, em colaboração com o grupo de TU Berlin

Um nanocristal iluminado com um pulso curto de ultra-alta intensidade na região espectral de raios-X moles se fragmenta completamente. Antes entretanto que a fragmentação se inicie, o padrão angular de luz espalhada elasticamente dá informação sobre a estrutura geométrica e eletrônica. Os padrões angulares de espalhamento elástico de luz por clusters de Ar e Xe em vôo livre, registrados em experimentos recentes com o laser de elétrons livres de Hamburg (FLASH, com λ_{FLASH} 13 nm, EFLASH$_{FLASH}$40 μJ, TFLASH$_{FLASH}$ 10 fsec, ϕ_{FLASH} 20 μm) mostram que a forma geométrica da nanoparticula pouco se altera durante o pulso; as constantes óticas, ao contrário, sofrem modificações significativas durante o pulso, indicando que os processos eletrônicos tem uma dinâmica muito rápida. A instrumentação usada será descrita. Resultados e simulações teóricas representativas para espalhamento de luz por nanoparticulas e dinâmica de superfícies óticas altamente excitadas serão apresentados e discutidos. Decorrem desses resultados que tanto a dinâmica de um nanocristal altamente excitado como a instrumentação para tais experimentos apresentam questões e desafios , cuja solução é essencial para o objetivo último de determinação estrutural com resolução atômica de uma biomolécula individual.

Acknowledgements:

Parte II

Biologia Estrutural

Análise da distribuição de chumbo e cálcio em dentes decíduos por fluorescência de raios X induzida por radiação síncrotron

de Souza Guerra, C[1], Pinto, N.G.V[2], Moreira, S.[3], Barroso, R.C.[4], and Gerlach, R.F.[5]

[1] Faculdade de Odontologia de Piracicaba - UNICAMP - Piracicaba SP Brazil
[2] Universidade Federal do Rio de Janeiro - Rio de Janeiro RJ Brazil
[3] Universidade Estadual de Campinas - Campinas SP Brazil
[4] Universidade do Estado do Rio de Janeiro - Rio de Janeiro RJ Brazil
[5] Universidade de São Paulo - Ribeirão Preto - Ribeirão Preto SP Brazil

Introdução e Objetivos: A exposição ao chumbo nos primeiros meses e anos de vida afeta de forma irreversível o desenvolvimento neuropsicológico infantil, levando a perdas cognitivas, agressividade e hiperatividade. Na década de 70 os dentes de leite (decíduos) foram fundamentais para comprovar os efeitos nocivos dos dentes a crianças, uma vez que eles são marcadores da história passada de exposição. Entretanto, nesses trabalhos os dentes decííduos exfoliados eram coletados e as medidas de chumbo eram feitas na dentina, o tecido interno dos dentes. O objetivo deste trabalho é determinar as concentrações de chumbo e cálcio com resolução especial em dentes decíduos coletados de uma região altamente contaminada por chumbo.

Material e Métodos: Foram utilizados 5 incisivos inferiores decíduos esfoliados de diferentes crianças, residentes em Santo Amaro da Purificação, BA. Os dentes foram imersos em peróxido de hidrogênio por 15 minutos e lavados no ultrassom por 15 minutos com água Ultrapura, cortado e polido com lixas de água de diferentes granulações até obtermos a espessura de 100 μum. A coroa de cada dente foi analisada por scaning bidimensional (x,y), sendo que o padrão de *scaning* foi similar para todas as amostras: da superfíície do esmalte até a dentina circumpulpar no eixo y e da incisal para cervical no eixo x.

Resultados e discussão: Os resultados mostraram que a distribuição de chumbo é heterogênea nos dentes decíduos, com maiores concentrações no esmalte superfical, vindo a seguir a região da dentina próxima à câmera pulpar, depois a dentina interna e o esmalte interno. Porém, quando o dente apresenta áreas de hipomineralização e/ou lesões de cárie, a distribuição do cálcio e do chumbo não acontece da mesma forma.

Acknowledgements: Os autores agradecem à Fapesp e CNPq. Pesquisa parcialmente financiada pelo LNLS (Projeto XRF 7092).

Structural analysis of BTCI in ternary complex with β-trypsin and α-chymotrypsin

Esteves, G. F.[1], Silva, A. J.[1], Barbosa, J.A.R.G.[2], and Freitas, S. M.[1]

[1] Universidade de Brasília - Brasília DF Brazil
[2] Laboratório Nacional de Luz Síncrotron - Campinas SP Brazil

The black-eyed pea trypsin/chymotrypsin inhibitor (BTCI) is a Bowman-Birk inhibitor presenting two different and independent reactive sites for trypsin and chymotrypsin (Barbosa et al., 2007). In this work, we present the resolution of crystallographic structure of BTCI in ternary complex with β-trypsin and α-chymotrypsin and structural analysis of BTCI in free form and in binary/ternary complex by dynamic fluorescence. The complex was crystallized by the vapor-difusion sitting-drop technique using several screening kits. The best crystals grew in 0.5 .M ammonium sulfate pH 7.5, 0.1 M Na HEPES and 30 % MPD and diffracted to a resolution of 1.7 . The X-ray diffraction datasets were collected at the MX1-D03B beamline of the Brazilian Synchrotron Light Laboratory (LNLS) at a wavelength of 1.431 with an oscillation of 1 ° on a MAR CCD detector with a circular X-ray-sensitive surface of 165 mm in diameter combined with a MAR DTB goniostat (Esteves et al, 2007). Indexing showed an orthorhombic crystal lattice and space group P1 with cell parameters a = 49.48, b = 54.57 and c = 69.29 and alpha = 67.28 , beta = 71.04 and gamma = 73.55 °. A molecular-replacement solution was found using two search models independently; the first was the structure of the trypsin BTCI complex (PDB code 2g81) and the second was that of chymotrypsin (PDB code 4cha). The structure was refined with R and Rfree factor of 0.218 and 0.171, respectively. The final quality of the model was checked by PROCHECK. The conformational changes of the BTCI complex were analyzed in free form and in association with chymotrypsin and/or trypsin using fluorescence lifetime technique (frequency domain). Fluorescence lifetime values indicated the presence of different substates for tryptofan residues and suggest the conformational changes occurring during the association of the molecules.

Acknowledgements: We thank the Brazilian Synchrotron Light Laboratory (LNLS) and CAPES.

Crystallographic studies of Cys-based proteins.

Monteiro, G.[1], Horta, B. B.[1], Nakamatsu, E. H.[1], Discola, K. F.[1], and Netto, L.E.S.[1]

Universidade de São Paulo - São Paulo - São Paolo SP Brazil

Many proteins with reactive cysteines (Cys-based) are involved in controlling thiol/disulfide exchange reactions, a central aim in cellular redox homeostasis. AhpE is a 1-Cys Peroxiredoxin with only one cysteine residue involved in catalysis. Peroxiredoxin enzymes (1 and 2-Cys) have been described as strictly dependent on thiols, but we have shown that 1-Cys peroxiredoxin can also receive electrons from ascorbate (Monteiro et al., 2007, Proc Natl Acad Sci USA 104:4886). Crystals from AhpE have been obtained (0.1M AcNa pH5.0; 150mM NaCl; 1.26M (NH_4) Sulfate) and they have been soaked with ascorbate before data collection. Soaked crystals have diffracted X-ray with a resolution of 1.7, however, through molecular replacement (PDB: 1xxu) we have not seen electron density compatible with an ascorbate molecule in the active site cavity. Interestingly, in one condition, the reactive cysteine was overoxidized to sulfonic acid (SO_3) as observed in the refined structure at 2.2 resolution. Another protein analyzed was Peroxiredoxin Q from *Xylella fastidiosa* (xfPrxQ). Typical PrxQ proteins are monomers with two Cys separated by four amino acids. XfPrxQ does not contain one of the two conserved Cys, but it shares 34% of amino acid similarity with *E. coli* PrxQ. Recombinant xfPrxQ has been obtained and it has thiol-peroxidase activity against several hydroperoxides which depended of thioredoxin. Non-reducing SDS-PAGE has shown that the oxidized xfPrxQ behaves as a monomeric enzyme and mutagenesis studies have indicated that an intramolecular disulfide bond has been formed between two of the four cysteines residues. We have conducted an initial screening using the LNLS automated crystal screening facility with C47S PrxQ which resulted crystals from several conditions. We have chosen the buffer consisting of 100mM Hepes-NaOH pH 7.5 and 20% PEG8000 as the initial condition for optimization. Data collected using synchrotron radiation at the LNLS MX-2 beamline have revealed significant diffraction at 1.55 resolution. Eventually, we have obtained protein crystals from the mitochondrial thioredoxin system of *Saccharomyces cerevisiae*, but so far the crystals have not diffracted with good resolution. We hope the data obtained from these studies may assist us in the comprehension of mechanisms involved in antioxidant defense, protein-protein interaction and cell signaling among others.

Acknowledgements: This work was supported by FAPESP.

Interleukin-22 forms dimers that are recognized by two interleukin-22R1 receptor chains

Mario de Oliveira Neto[1], Ferreira Júnior, J. R.[1], Fischer, H.[2], Craievich AF[2], and Polikarpov, I.[1]

[1] Universidade de São Paulo - São Carlos - São Carlos SP Brazil
[2] Universidade de São Paulo - São Paulo - São Paulo SP Brazil

Interleukin-22 (IL-22) is a class 2 cytokine whose primary structure is similar to that of interleukin 10 (IL-10) and interferon-γ (IFN-γ). IL-22 induction during acute phase immune response indicates its involvement in mechanisms of inflammation. Structurally different from IL-10 and a number of other members of IL-10 family, which form intertwined inseparable V-shaped dimers of two identical polypeptide chains, a single polypeptide chain of IL-22 folds on itself in a relatively globular structure. Measures of IL-22 and of complex IL-22/IL-22R1 were made on LNLS SAXS beamline using one-dimensional detector. Low-resolution molecular shape of IL-22 dimers is strikingly similar to that of IL-10 and other intertwined cytokine dimeric forms and *ab initio* molecular shape of the IL-22/IL-22R1 complex which reveals the V-shaped IL-22 dimer interacting with two cognate IL-22R1 molecules. Based on this collective evidence, we argue that dimerization might be a common mechanism of all class 2 cytokines for the molecular recognition with their respective membrane receptor.

Acknowledgements: This work was supported by FAPESP - CBME

Crystal structure of cytosolic thioredoxin peroxidase I (cTPxI), C47S mutant, from *Saccharomyces cerevisiae*

Bataghin, F. A.[1], Oliveira, M.A.[2], Genu, V[2], Discola, K. F.[2], Alves, S.V.[2], Guimarães, B.G.[3], and Netto, L.E.S.[2]

[1] Universidade Estadual Paulista Julio de Mesquita Fillho - Assis SP Brazil
[2] Universidade de São Paulo - São Paulo - São Paolo SP Brazil
[3] Laboratório Nacional de Luz Síncrotron - Campinas SP Brazil

Thioredoxin peroxidases (TPx) are able to reduce H_2O_2 and a wide range of organic peroxides using a very reactive cysteinyl residue present in their active sites, nominated peroxidatic cysteine (Cys_P). In *Saccharomyces cerevisiae*, two cytosolic isoforms, cTPxI and cTPxII, are obligate dimers but exposition of yeast cells to heat shock or oxidative stress triggers an intense oligomerization of cTPxI and cTPxII dimers, resulting in formation of $[\alpha(_2)_5]$ and higher molecular weight protein complexes. This structural change is correlated with a transition of the protein function from thiol peroxidase to molecular chaperone. cTPxI and cTPxII, shares high primary sequence homology, (86% of identity and 96% of similarity), and exhibits the oligomerization and chaperone activities, but recently was demonstrated that the pKa of the peroxidatic cysteine differs considerably among the two thioredoxins peroxidases (5.4 and 6.3 respectively). The difference in the peroxidatic reactivity probably relies in slightly differences in the active site environment of Cys_P and may be relevant in the peroxidatic and chaperone activities of these proteins. In order to investigate the structural differences among yeast cTPxI and cTPxII the we determinated the crystal structure of cTPxI, carrying a serine substitution of the peroxidatic cysteine. Structure refinement is in progress (Rfactor = 0.24; Rfree = 0.35) and preliminary analysis of *S. cerevisiae* $TPxI_{C47S}$ structure reveals a decameric quaternary organization. We expect that the knowledge of the tertiary and quaternary structures of yeast cTPxI will contribute to the understanding of the molecular mechanisms concerning peroxide decomposition and the process involved in the switch from peroxidase to chaperone activities, which may be involved in fundamental processes of cellular homeostasis. Additionally, the cTPxI refined structure may be helpful in construction of high-quality theoretical model of cTPxII. It can shed light on the differences between the pKa of the peroxidatic cysteines from the two TPs cytosolic isoforms, and contribute to the understanding of the molecular basis of the functional switch among thioredoxin peroxidases from different organisms.

Acknowledgements: This work was supported by FAPESP and CNPq.

Crystallization and X-ray diffraction data collection of BthTX-I in different temperatures.

Marchi-Salvador, D. P.[1], Silva,M.C.O[1], Salvador, G. H. M.[1], Soares, A. M.[2], and Fontes, M. R. M.[1]

[1] Universidade Estadual Paulista - Botucatu - Botucatu SP Brazil
[2] Universidade de São Paulo - Ribeirão Preto - Ribeirão Preto SP Brazil

Botropstoxin-I or BthTX-I is the main protein of *Bothrops jararacussu* venom. BthTX-I is a basic myotoxic Lys49-PLA_2, which is catalytically inactive on artificial substrates, but promotes blockade of neuromuscular transmission. Here, we report the crystallization experiments in five different temperatures and preliminary X-ray diffraction results of these crystals. All crystals were obtained by hanging-drop vapour-diffusion method using similar crystallization conditions but with different temperatures (277K to 308K). X-ray diffraction data were collected at a wavelength of 1.425 (at 100K) using a Synchrotron Radiation Source (Laboratório Nacional de Luz Síncrotron, LNLS, station MX1, Campinas, Brazil). Data were processed using the denzo/scalepack program at 1.8 - 2.8 resolution. The crystals belong to different space group and have several oligomeric conformations: monomer, dimer and tetramer. The crystal structures were determined using molecular replacement techniques implemented by AMoRe program. Currently, these structures are in final stage of refinement using CNS or REFMAC programs.

Acknowledgements: This work has received financial support from FAPESP, FUNDUNESP, CNPq and LNLS.

Kinetic and structural stability studies of Oligopeptidase B from *Trypanosoma cruzi*

Motta, F. S. N.[1], Bastos, I.M.D.[1], Barbosa, J.A.R.G.[2], Freitas, S. M.[1], and Santana, J. M.[3]

[1] Universidade de Brasília - Brasília DF Brazil
[2] Laboratório Nacional de Luz Síncrotron - Campinas SP Brazil
[3] Universidade de Brasília - Brasília DF

Prolyl Oligopeptidases of *Trypanosoma cruzi* are potential drug targets for Chagas disease chemotherapy. Oligopeptidase B of *T. cruzi* (OligoBTc), a member of proly oligopeptidase family, seems to trigger the lysosome recruitment that is crucial to parasite entry into mammalian cells by a Ca^{2+}-dependent process. Structural studies and physicochemical characterization of OligoBTc can help establish a better condition to perform biological assays and are fundamental to understand its interactions with the environment and host cells. In this work, we present OligoBTc kinetic and structural stability studies under different conditions of pH and temperature. The OligoBTc gene was amplified by PCR and cloned into pET-19b. The recombinant protein was expressed in *E. coli* BL21 (DE3) and purified by affinity in nickel-Agarose resin. The OligoBTc exhibits a maximal activity at pH 8, which is totally preserved up to 45^{o}C, but is sensitive to ionic strength. The mainly secondary structure of this protein is β-sheet as predicted from circular dichroism spectra. Its structural stability was investigated through thermal and chemical unfolding processes by circular dichroism and fluorescence spectroscopy. The thermal unfolding processes revealed that OligoBTc is a highly stable protein at different pHs and less stable at moderate ionic strength conditions.

Acknowledgements: This work was supported by CNPq, FINEP and ABTLuS (LNLS).

Oligomerização e análise conformacional de uma Leucil aminopeptidase de *Leptospira interrrogans*

Álvares, A.C.M.[1], Silva, A. J.[2], Silva, H. A.[2], Slovic, A.M.[3], Barbosa, J.A.R.G.[3], Santana, J. M.[1], and Freitas, S. M.[2]

[1] Universidade de Brasília - Brasília DF
[2] Universidade de Brasília - Brasília DF Brazil
[3] Laboratório Nacional de Luz Síncrotron - Campinas SP Brazil

Leucil aminopeptidases (LAP) são exopeptidases hexaméricas que clivam, preferencialmente, substratos de leucil na porção amino-terminal de proteínas. Essas enzimas estão relacionadas à patogenicidade de bactérias como a *Leptospira interrogans*, uma espiroqueta aeróbica causadora da leptospirose. O gene da L. interrogans foi isolado, clonado e expressado em *E. coli* BL21-DE3. A proteína recombinante, LAP-Li, foi purificada em coluna de níquel para estudos estruturais. Essa enzima apresenta estabilidade e atividade máxima em pH 8,5 e temperatura ótima de 50-60C. Mudanças conformacionais da LAP-Li, dependentes do pH, foram monitoras por atenuação de fluorescência, utilizando acrilamida e iodeto de potássio. A tendência de formação de oligômeros da LAP-Li foi analisada por espalhamento de luz dinâmico (ELD). Os resultados obtidos mostram que os resíduos de triptofano da LAP-Li estão parcialmente expostos e de fácil acesso aos atenuadores. Adicionalmente, mudanças conformacionais no microambiente estrutural desses resíduos ocorreram em decorrência do acesso dos atenuadores, por processos estático e dinâmico, indicados pelo gráfico de Stern-Volmer. Monômeros da LAP-Li tendem a formar oligômeros, predominante na forma de hexâmeros, com aumento da concentração, da temperatura e sob efeito de diferentes pHs, indicando que a proteína recombinante apresenta um padrão de dobramento esperado para as LAP.

Acknowledgements: CNPq, ABTLuS (LNLS) e FINEP.

Análise estrutural do complexo SPCI-quimotripsina por fluorescência dinâmica

Silva, A. J.[1], Teles, R. C. L.[1], Schaberle, F. A.[2], Barbosa, J.A.R.G.[2], and Freitas, S. M.[1]

[1] Universidade de Brasília - Brasília DF Brazil
[2] Laboratório Nacional de Luz Síncrotron - Campinas SP Brazil

O inibidor de quimotripsina de *Schizolobium parahyba* (SPCI) pertence à família Kunitz e inibi especificamente essa enzima na proporção molar de 1:1. Esse inibidor foi purificado a partir do extrato bruto das sementes de *S. parahyba*, precipitado com ácido tricloacético, e por cromatografia de troca iônica. O complexo binário foi purificado por cromatografia de exclusão molecular. As medidas do tempo de vida (τ) das moléculas foram realizadas em um espectrofluorímetro K-2, utilizando a fonte de radiação síncrotron do LNLS. Essas medidas foram feitas no domínio da freqüência, de 8 a 200 MHz com número de freqüência de 20 MHz. O equipamento foi calibrado com *p*-terfenil ($\tau = 1{,}05$ ns), com excitação em 295 nm. Para os ajustes dos dados foi considerado o valor mínimo do χ^2, desvios padrões de $0{,}2^o$ para ângulo de fase e 0,004 para a modulação. O melhor ajuste foi o modelo *Discreto* para dois τ resultando nos valores: SPCI ($\tau_1 = 0{,}68$ ns e $f_1 = 0{,}53$, $\tau_2 = 4{,}98$ ns e $f_2 = 0.47$, $\chi^2 = 25$); α-quimotripsina ($\tau_1 = 0{,}91$ ns e $f_1 = 0{,}36$, $\tau_2 = 4{,}15$ ns e $f_2 = 0{,}63$, $\chi^2 = 2{,}46$); complexo ($\tau_1 = 0{,}88$ ns e $f_1 = 0{,}35$, $\tau_2 = 4{,}16$ ns e $f_2 = 0{,}65$, $\chi^2 = 2{,}20$). Para a α-quimotripsina e o complexo, os valores dos τ indicam que existem duas populações distintas de triptofanos: enterrada (τ_1) e exposta (τ_2). Considerando que o SPCI tem apenas um único triptofano, esse decaimento bi-exponencial caracteriza a presença de subestados conformacionais do triptofano no estado excitado. A análise da interação SPCI-quimotripsina foi baseada na equação de Stern-Volmer. Os resultados sugerem a ocorrência de modificações conformacionais nas vizinhanças dos triptofanos, provavelmente em decorrência de alterações na hidrofobicidade.

Acknowledgements: Este trabalho recebeu suporte financeiro do CAPES, FINATEC e ABTLuS (LN LS).

Cristalização e estudos cristalográficos preliminares do complexo SPCI-quimotripsina a 2,8 de resolução

Silva, A. J.[1], Teles, R. C. L.[1], Esteves, G. F.[1], Santos, C. R.[2], Barbosa, J.A.R.G.[2], and Freitas, S. M.[1]

[1] Universidade de Brasília - Brasília DF Brazil
[2] Laboratório Nacional de Luz Síncrotron - Campinas SP Brazil

Os inibidores de serinoproteinases são amplamente distribuídos na natureza e podem inibir a ação de enzimas em diferentes organismos. Esses inibidores participam da regulação de diversos processos que envolvem proteinases, tais como transcrição, ciclo celular, invasão celular e apoptose. O inibidor de quimotripsina de *Schizolobium parahyba* (SPCI), membro da família Kunitz, apresenta uma única cadeia polipeptídica com duas ligações dissulfeto e inibi especificamente a quimotripsina na proporção molar de 1:1. Neste trabalho, apresentamos a purificação, a cristalização e a resolução da estrutura cristalográfica do complexo binário SPCI-quimotripsina. O SPCI foi purificado em duas etapas: precipitação com ácido tricloroacético a 1,2% e cromatografia de troca iônica. O complexo binário foi purificado por cromatografia de exclusão molecular. Os cristais foram obtidos em placas de gota sentada, por difusão de vapor, na condição MES-NaOH 100 mM pH 5,5, PEG 6000 20% (w/v) e LiCl 200 mM, na presença do aditivo sulfobetaína não-detergente de massa molecular 201 (NDSB-201). Os dados de difração de raios-X foram obtidos de um único cristal do complexo binário sob condições criogênicas a 2,8 de resolução. O cristal pertence ao grupo espacial $P2_1P2_1P2_1$, com os seguintes parâmetros da célula unitária: a = 45.28, b = 64.57, c = 169.23 e R_{merge} = 0.122 para 11254 reflexões. A estrutura tridimensional desse complexo foi resolvida por substituição molecular, utilizando a estrutura cristalográfica do SPCI e da quimotripsina (pdb 4cha). Atualmente, as condições iniciais de cristalização estão sendo refinadas para obtenção de cristais que difratem em melhor resolução.

Acknowledgements: Este trabalho recebeu apoio financeiro da FAPESP, CAPES, CNPq e ABTLuS (LNLS).

IDENTIFICAÇÃO E AVALIAÇÃO DA EXPRESSÃO DE MARCADORES MOLECULARES ENVOLVIDOS NA TUMORIGÊNESE DE PULMÃO

Henrique, T[1], Polachini, G.M.[1], Vidotto, A.[1], Cury, P.M.[1], Zanelato, P.[1], Nietmann, H.[1], FARIA, Celso Murilo Nálio Matias de[1], Cury, F.A.[1], and Tajara, E.H.[1]

Faculdade de Medicina de São José do Rio Preto - São José do Rio Preto SP Brazil

câncer de pulmão é um dos tumores malignos mais freqüentes na população mundial. No Brasil, o número de casos novos estimados para 2008 é de aproximadamente 18 mil entre os homens e 9 mil entre as mulheres e a maioria está associada ao consumo de derivados do tabaco. Os tumores restritos ao pulmão possuem chances elevadas de cura, mas a avaliação desses casos não é simples em função das dificuldades de acesso à lesão e dos limites de sensibilidade das técnicas de imagem. Por esse motivo, a maioria dos pacientes exibe tumores em estágios avançados ao diagnóstico. Essas características tornam a investigação das alterações moleculares relacionadas ao processo neoplásico muito importante para a identificação de marcadores de rastreamento de grupos de risco, de diagnóstico e de prognóstico. O presente projeto tem como objetivo geral investigar, por técnicas de proteômica, o perfil molecular de tumores de pulmão. Os objetivos específicos do projeto incluem avaliar e validar a expressão de marcadores potenciais identificados nesses tumores. Após utilização de eletroforese bidimensional e espectrometria de massa, foram identificadas diferenças qualitativas e quantitativas entre amostras de adenocarcinomas de pulmão e tecidos normais correspondentes, incluindo expressão alterada de peroxirredoxina, galectina 1, alfa-enolase 1, superóxido dismutase, peptidil-prolil cis-trans isomerase A e polipeptídeo ativador de adenilato ciclase. Essas proteínas estão relacionadas com resposta a estímulos externos, apoptose, proliferação celular, transcrição e sinalização celular. O estudo dessas proteínas pode auxiliar no entendimento da tumorigênese de pulmão e na identificação de biomarcadores de diagnóstico de câncer de pulmão.

Acknowledgements: Financiamento: FAPESP, FINEP, CAPESP, CNPq.

Crystal structures of two lectins from *Cymbosema roseum*

Rocha, B.A.M.[1], Delatorre, P.[2], Benevides, R. G.[3], Naganao, C.S.[3], Sampaio, A.H.[3], Azevedo Jr., W. F.[4], and Cavada, B.S.[3]

[1] Universidade Federal de Alagoas - Maceió AL Brazil
[2] Universidade Regional do Cariri - Crato CE Brazil
[3] Universidade Federal do Ceará - Fortaleza CE Brazil
[4] PUC - Rio Grande do Sul - Porto Alegre RS Brazil

Although lectins from Leguminosae family were so well studied, sequences of Diocleinae lectins have been shown that the circular permutation of peptide chains do not occur in some legume lectins. Amino acid sequences and tridimensional structure determinations of some legume lectins can help to understand the carbohydrate affinity differences in lectins from the same subfamily and also can help to obtain information about the evolutive origin of lectins. In these studies, can be observed the binding properties of lectins, interacting with non-protein amino acids and the existence of lectins with chitinase activity, both of them related to plant defense mechanisms against pathogens. This work shows structural features of two lectins purified from seeds of *Cymbosema roseum*. The mannose- (CRLI) and lactose- (CRLII) specific lectins present distinct primary, tertiary and quaternary structures. The overall structures of native CRLI and CRLII have been refined at 1.7 and 2.5 resolution, respectively. The different binding properties of these lectins reveals that even being isolated from the same plant source they developed different responses against pathogens. CRLI also can interact with a non-protein amino acid related to this response and the CRLII assemble suggests a possible new type of quaternary structure in this group of proteins.

Acknowledgements: This work was supported by CNPq, CAPES and FUNCAP. We also thanks LNLS.

Crystal structure of *Dioclea rostrata* lectin: insights into understanding the pH-dependent dimmer-tetramer equilibrium and the structural basis for carbohydrate recognition in Diocleinae lectins

Delatorre, P.[1], Oliveira, T.M.[2], Rocha, B.A.M.[3], Bezerra, G.A.[2], Moura TR[2], Benevides, R. G.[2], Bezerra, E.H.S.[2], Azevedo Jr., W. F.[4], Sampaio, A.H.[2], and Cavada, B.S.[2]

[1] Universidade Regional do Cariri - Crato CE Brazil
[2] Universidade Federal do Ceará - Fortaleza CE Brazil
[3] Universidade Federal de Alagoas - Maceió AL Brazil
[4] PUC - Rio Grande do Sul - Porto Alegre RS Brazil

The legume lectins from the Diocleinae sub tribe, often referred as concanavalin A-like lectins, are a typical example of highly similar proteins that show distinct biological activities. The pH-dependent oligomerization, that some of these lectins undergo, and the relative position of amino acids within the carbohydrate-binding site are factors that have been reported by their contribution to these differences in the biological activities of Diocleinae lectins. In the present work, we determined the amino acid sequence and the crystal structure of *D. rostrata* seed lectin (DRL), with the aim of investigating the structural bases of the different behavior displayed by this lectin in comparison to other Diocleinae lectins and determining the reason for the distinct pH-dependent dimmer-tetramer equilibrium. Thus, we report that the orientation undertaken by His 51 has an important influence on how this equilibrium is displayed by a particular lectin. In addition, we discovered a novel multimeric arrangement for this lectin and local modifications that seem to justify the DRLs recognition pattern regarding some complex carbohydrates.

Acknowledgements: This work was supported by CNPq, CAPES, FUNCAP.

Structure determination of PilZ from Xanthomonas axonopodis pv. citri

Guzzo, C.R.[1], Kopke Salinas, R.[1], and Farah, C.S.[1]

Universidade de São Paulo - São Paulo - São Paulo SP Brazil

PilZ domains have been recently been shown to bind the important bacterial second messenger bis-(3',5')-cyclic diguanylic acid (c-diGMP). C-diGMP controls a number complex behaviors gram negative bacteria, including quorum sensing, biofilm formation, motility and the production of exopolysaccharides and virulence factors. PilZ domains form an extremely large (¿1500 members identified so far) and divergent superfamily and most bacterial genomes code for several proteins with a PilZ domain. The original PilZ protein from P. aeruginosa (PA2960) was shown to be involved in the production type IV pili an extracellular surface structure required for twitching and swarming motility. Recently the structures of PilZ domains of PA4608 from Pseudomonas aeruginosa and VCA0042/PlzD from Vibrio cholerae were determined. The citrus pathogen Xanthomonas axonopodis pv. citri (Xac) genome codes for four proteins with PilZ domains: XAC1133, XAC3402, XAC1971 and BcsA a subunit of cellulose synthase. In this study we describe the expression, purification, crystallization and structure determination of Xac PilZ (XAC1133), an ortholog of PA2960. Crystals of PilZ containing selenomethionine diffracted up to 1.9A resolution and belong to the P61 hexagonal space group. The unit cell parameters are a = 62.13, b = 62.13, c = 83.54 A. Two PilZ molecules are present per asymmetric unit. Multiwavelength anomalous dispersion phasing calculations were carried out with SHELXD and autoSHARP and an interpretable electron density map was obtained. The structure has been refined (Rwork = 0.19 and Rfree = 0.24) and the final model deposited in the PDB (code 3CNR). Analysis of the PilZ structure has provided leads through which may be gained information regarding its function. An analysis of PilZ secondary structure in solution by NMR was compared to the structure observed in the crystalline state. Furthermore, the results of preliminary functional experiments will be presented including the phenotypes of Xac PilZ knockouts and the identification of proteins with which Xac PilZ interacts.

Acknowledgements: This work was supported by FAPESP and CNPq, Brazil.

CHARACTERIZATION OF RECOMBINANT PROCATHEPSIN L 3 FROM *TENEBRIO MOLITOR* MIDGUT

Beton, D.[1], Guzzo, C.R.[1], Farah, C.S.[1], and Terra, W.R.[1]

Universidade de São Paulo - São Paulo - São Paulo SP Brazil

Cathepsin L corresponds to the major digestive proteinase in the midgut of *Tenebrio molitor* larvae. In our laboratory, three procathepsin L-like proteinases (pCALs) were cloned and sequenced from a *T. molitor* midgut cDNA library: pCAL1 (lysosomal CAL), pCAL2 and pCAL3 (digestive enzymes). The cDNA coding pCAL3 was cloned in the vector pAE fused to a His tag in its N-terminus. The construct pAE/pCAL3 was used to transform OrigamiB(DE3) *E. coli* and high recovery of soluble recombinant protein was observed by induction at 20°C. The recombinant proenzyme was purified by Ni^{+2} affinity chromatography. The activation of the zymogen pCAL3 to the active CAL3 occurs under acidic conditions and CAL3 was able to hydrolyse typical cathepsin substrates, such Z-FR-MCA and Z-RR-MCA. To crystallographic studies we expressed an inactive form of the pCAL3 by replacing the active site cysteine at position 26 with a serine to prevent autocatalytic processing of the zymogen. pCAL3Cys26Ser was concentrated to 9.7mg/mL and crystallized by vapor diffusion in sitting drops against 0.1-1.6 M mono-ammonium dihydrogen phosphate. The crystals are monoclinic, space group C2, with cell parameters: a = 59.425 , b = 91.894 , c = 72.084 , $\alpha = \gamma = 90°$, $\beta = 91.86°$ and contain one molecule in the asymmetric unit. The structure has been determined by molecular replacement with the structure of *Fasciola hepatica* procathepsin L (42.5% identity) and refined at 2.0 resolution to an R factor of 0.18 ($R_{free} = 0.22$).

Acknowledgements: FAPESP, CNPq and LNLS

Crystal structure of Batroxase, a hemorrhagic zinc-dependent metalloproteinase from *Bothrops atrox* venom

Murakami, M. T.[1], Vilela, S. S.[2], Arni, R.K.[3], and Cintra, A. O.[2]

[1] Laboratório Nacional de Luz Síncrotron - Campinas SP Brazil
[2] Universidade de São Paulo - Ribeirão Preto - Ribeirão Preto SP Brazil
[3] Universidade Estadual Paulista - São José do Rio Preto - São José do Rio Preto SP Brazil

Snake venom metalloproteinases (SVMPs) are multimodular proteins that comprise a metalloprotease domain (class PI), a disintegrin-like domain (class PII), a cysteine-rich domain (class PIII) and a C-type lectin-like domain (class PIV). These hemostatically-active toxins exhibit both anti- and coagulant activities due to the ability either to degrade fibrinogen and fibrin or to activate prothrombin and factor Xa. Based on these activities, the fibrino(geno)lytic non-hemorrhagic SVMPs can be used as thrombolytic agents, and prothrombinase and factor X-activating enzymes are already applied in coagulation research and diagnosis. Beyond clinical applications, the SVMPs can be explored as biochemical tools for molecular studies, biotechnology industry applications, studies of the action mechanism of venoms, design of MP inhibitors and comprehension of other MP features. In this work, we have determined at 1.75 resolution the crystal structure of Batroxase, a PI-class zinc-dependent metalloproteinase from *Bothrops atrox* venom. Our structural results dealing with its pharmacological activities could bring new insights into the molecular mechanims and regulation of SVMPs.

Acknowledgements: This work was funded by FAPESP and CNPq.

Structural analysis of the ModABC transporter from the pathogenic bacteria *Xanthomonas axonopodis* pv. *citri* by homology modeling and molecular dynamics

Santacruz-Perez, C.[1], Balan, A.[2], Pegos, V.R.[2], and Barbosa, J.A.R.G.[2]

[1] Universidade de São Paulo - São Paulo - São Paulo SP Brazil
[2] Laboratório Nacional de Luz Síncrotron - Campinas SP Brazil

The *modABC* operon of *Xanthomonas axonopodis* pv. *citri* (*Xac*) encodes for the proteins ModA, ModB and ModC, which couple ATP hydrolysis to the transport of molybdate to the interior of the cell. The *Xac* periplasmic molybdate-binding protein (ModA) determines the affinity of the system and its crystallographic structure was recently solved by our group. Focusing on the analysis of the binding-pocket residues that interact with the molybdate, we have obtained and expressed two ModA mutant proteins. Spectroscopic analyses by circular dichroism and structural characterization showed a different behavior of the mutants when compared to the native protein. Moreover, molecular dynamics simulations of the ModA protein were performed in the presence and absence of molybdate and showed that the binding and release mechanism of this ion-binding protein is coincident with data already described for other type of binding proteins. Additionally, with the aim of studying the interactions between ModB and ModA or ModC, we have explored the tridimensional structure of the membrane protein (ModB) in complex with the ATPase-binding protein (ModC), both models obtained by homology modeling. The model for *Xac* transporter showed conservation of the interacting regions when compared with other orthologs including *Archaeoglobus fulgidus*, which was used as the template. The comparison of the *Xac* molybdate transporter with other ABC transporters will be of great interest for identification of similarities and differences among them regarding the interactions between: i) periplasmic protein and ligand and ii) periplasmic or citoplasmic proteins and trans-membrane domains.

Key Words: molybdate, ModA, ModB, ModC, *Xanthomonas axonopodis* pv. *citri*, homology modeling, molecular dynamics.

Acknowledgements: FAPESP, CNPq and ABTLuS.

Estudos estruturais por RMN da proteína SBDS humana

Oliveira, J. F.[1], Sforça, ML[1], Zanchin, N. I. T[1], and Zeri, AC;[1]

Laboratório Nacional de Luz Síncrotron - Campinas SP Brazil

Um dos projetos desenvolvidos pelo grupo de RMN do CeBiME/LNLS envolve a proteína SBDS humana (Shwachman-Bondian-Diamond Syndrome), de 250 resíduos, implicada no processamento de RNA ribossomal. Os dados foram obtidos para a proteína produzida com marcação isotópica de 13C, 15N e 2H, e os experimentos foram realizados no equipamento de 600MHz com sonda criogênica do LNLS. Os dados coletados no LNLS permitiram o assinalamento da maioria dos resíduos da cadeia principal e cadeias laterais da proteína, e ensaios de interação com RNA, ainda em fase inicial, já permitem uma análise da interação entre essas moléculas. Cálculos estruturais estão sendo finalizados.

Acknowledgements: FAPESP, ABTLuS

Crystallization and Preliminary X-ray diffraction analysis of the leptospiral protein LIC12922

Giuseppe, P. O.[1], Atzingen, M. V.[2], Nascimento, ALTO[2], Zanchin, N. I. T[1], and Guimarães, B.G.[1]

[1] Laboratório Nacional de Luz Síncrotron - Campinas SP Brazil
[2] Instituto Butantan - São Paulo SP Brazil

Leptospira interrogans is the etiological agent of leptospirosis, the most widespread zoonosis in the world. Recently, the complete genome sequence of *Leptospira interrogans* serovar Copenhageni was reported, revealing a substantial number of hypothetical proteins such as LIC12922. Sequence analyses predict that LIC12922 is a periplasmic protein distantly related to the periplasmic chaperone SurA and the extracytoplasmic folding factor PrsA. However, reliable experimental evidence is required in order to confirm this hypothesis. Therefore, we have started a project on the functional and structural characterization of LIC12922. Recombinant LIC12922 was produced in *Escherichia coli*, purified and submitted to crystallization. Crystals suitable for data collection were obtained following removal of the N-terminal His_6-tag by limited proteolysis. X-ray diffraction data were collected at the LNLS protein crystallography MX2 beam line. LIC12922 crystals diffract up to 3.4 resolution and belong to the space group P23, with unit-cell parameters a=b=c=137. For structure determination using anomalous methods (SAD, MAD), we intend to produce and to crystallize seleno-methionine-labeled LIC12922. In addition, several plasmids were constructed to produce N- and C-terminal deletion mutants of LIC12922 hoping to improve crystal diffraction pattern.

Acknowledgements: Financial Support: LNLS, FAPESP

Crystallization of TIPRL: a novel regulator of type 2A phosphatases

Smetana, J. H. C.[1], Alves, A. C.[1], Teixeira, E. C.[1], and Zanchin, N. I. T[1]

Laboratório Nacional de Luz Síncrotron - Campinas SP Brazil

Type 2A phosphatases are part of the PPP subfamily that is formed by PP2A, PP4 and PP6, and participate in a variety of cellular processes including transcription, translation, regulation of the cell cycle, signal transduction and apoptosis. Each one of these phosphatases has its own specific regulatory subunits, but they also share two common regulators, TIPRL (target of rapamycin signaling pathway regulator-like) and α4. The function of TIPRL is still poorly understood and it presents no sequence similarity to any other family of proteins. The objective of this study is to crystallize TIPRL and determine its three dimensional structure. Initial attempts to crystallize full length TIPRL were unsuccessful, which led us to produce deletion mutants lacking short unstructured regions from the C-terminus (TIPRLΔC) and N-terminus (TIPRLΔN). TIPRLΔC was expressed exclusively as inclusion bodies, but TIPRLΔN was abundantly expressed in the soluble fraction of *E. coli* BL21(DE3). Purification was carried by using Ni-Affinity chromatography followed by size exclusion chromatography. Subsequently, TIPRL samples were dialyzed against 20 mM Tris-HCl pH 8.0, 20 mM NaCl and 5 mM βME buffer for 16 hours. Initial TIPRLΔN crystallization screens were performed at 12 mg/mL (Crystal Screen-Hampton, PACT- Qiagen, Wizard Emerald Biosystems, JCSG-Qiagen, SaltRx-Qiagen and Precipitant Synergy Emerald Biosystems). Some crystals and crystalline structures were observed after 15 days. Optimization of the crystallization conditions are in progress.

Acknowledgements: This work was supported by CNPQ, FAPESP and LNLS.

A hypothetical protein coded by the Type IV Secretion System of a bacterial phytopathogen combines a VirB7 motif with a C-terminal signaling domain

Souza, D. P.[1], Farah, C.S.[1], and Kopke Salinas, R.[1]

Universidade de São Paulo - São Paulo - São Paulo SP Brazil

Xanthomonas axonopodis pv. citri (Xac) is a gram-negative bacterial phytopathogen that infects citrus. One possible virulence determinant is a chromosomally encoded Type IV Secretion System (T4SS), a multiprotein complex that spans the bacterial periplasm and both inner and outer membranes, and is used by some bacteria to secrete proteins and/or DNA to the extracellular milieu or the host interior. VirB7 is a periplasmic lipoprotein of the T4SS but it is not found in the Xanthomonadaceae family based on sequence similarity. We predicted that the hypothetical lipoprotein Xac2622 is a VirB7 equivalent, however it is significantly larger (139 residues) than typical VirB7 proteins (∼50 amino acids). With the aim of understanding if Xac2622 is a member of the VirB7 family and if it has an extra domain, we solved its three dimensional structure by solution NMR (residues 24-139), and studied its interaction with VirB9. Xac2622 has an unfolded N-terminal segment of ∼30 residues followed by a folded and compact domain. We observed changes in the ^{15}N-HSQC spectra acquired with different protein concentrations, indicating that Xac2622 oligomerizes in fast exchange at the NMR time scale. Affected residues mapped predominantly in a surface of the folded domain. The Xac2622 interaction with VirB9 (residues 34-255) was assayed by fluorescence titration, indicating a Kd of $4x10^{-8}$M. The formation of a tight complex was also observed by NMR, as the VirB9 C-terminus (residues 154-255) recognizes the Xac2622 unfolded N-terminus forming a complex in slow exchange at the NMR time scale. Relaxation data (^{15}N T1, T2 and NOE) indicate that the flexible N-terminus of Xac2622 becomes rigid upon interaction with the VirB9Ct. These results showed that Xac2622 like other VirB7 proteins interacts with VirB9 via an N-terminal peptide after a lipobox sequence. Surprisingly, unlike other VirB7 proteins, Xac2622 has an extra C-terminal folded domain whose topology is strikingly similar to that of the periplasmic signaling domain of bacterial TonB-dependent receptors though they lack significant sequence similarity. This observation may imply a signal transduction function for VirB7 in the T4SS of the Xanthomonadaceae family.

Acknowledgements: We thank Dr. Ana C. Zeri, Dr. Maurício L. Sforça (LNLS) and Dr. Miriam Uemi (Central Analítica-IQ/USP). This work was supported by CNPq and Fapesp.

Parte III

Biologia Molecular e Química de Proteínas

Efeitos do tratamento PUVA (Psoralenos mais Ultravioleta A) no DNA: Variedade de lesões e implicações em nível biológico

de Paula-Pereira Jr., M. V.[1], Soares, M.[1], C. Lage[1], and Leitão, A.C.[1]

Universidade Federal do Rio de Janeiro - Rio de Janeiro RJ Brazil

A terapia PUVA consiste da ação combinada entre psoralenos e a radiação UV-A (320 a 400nm)(Viola et al., 2006), sendo utilizada no tratamento de desordens dermatológicas (psoríase e vitiligo) e em patologias mais graves como o linfoma cutâneo de células T (Roelandts, 2003). Os psoralenos possuem ligações importantes fotobiologicamente que, se ativadas, interagem com as bases pirimidínicas do DNA (Hearst et al., 1984). O efeito da fotoquimioterapia consiste da fotoativação destes psoralenos, que resulta na formação de adutos com o DNA das células (DallAcqua et al., 2004). Estas ligações podem ser formadas com apenas uma das fitas de DNA (monoadutos) ou, havendo uma base pirimidínica na fita oposta do DNA, formar uma segunda ligação (crosslink)(Hearst et al., 1984). Diferentes ferramentas têm sido utilizadas para se estudar os efeitos do tratamento PUVA em ácidos nucléicos, dentre as quais a utilização da Espectrometria de Massas. Relatos anteriores (de Paula-Pereira Jr., 2008) demonstram que diversos tipos de lesões podem ser formadas como um produto da interação de diferentes quimioterápicos e os ácidos nucléicos. Procura-se então investigar até que ponto estes tratamentos possuem relevância terapêutica e quais os prováveis riscos em nível biológico. Este trabalho tem como objetivo o estudo dos efeitos da terapia PUVA na formação de lesões em DNA, correlacionando com dados biológicos já existentes. Metodologia: Amostras de DNA purificado tratadas com diferentes tipos de furocumarinas (PSO - Psoraleno; 8MOP - 8-Metoxipsoraleno; ANG - Angelicina; DMC - Dimetoxicumarina; 3-CPs - 3-Carbetoxipsoraleno e TMP - Trimetilpsoraleno) e uma dose única de UV-A foram injetadas no espectrômetro de massas (ESI-QTOF) e analisadas. Os resultados revelam uma variada quantidade de lesões nas diferentes condições testadas, sugerindo uma considerável interação entre o DNA e PUVA. Tais resultados confirmam o potencial genotóxico do tratamento, abrindo a possibilidade de a terapia ser revista em termos de quais são as suas conseqüências biológicas.

Acknowledgements: Agradecemos pela utilização das instalações do Laboratório de Espectrometria de Massas (MAS), do Centro de Biologia Molecular e Estrutural (CeBiME), Laboratório Nacional de Luz Síncrotron (LNLS). Esta utilização ocorreu devido à aprovação de propostas de pesquisa (MAS 3914, MAS 4553 e MAS 6348), para utilização do MAS. Apoio Financeiro: CNPq, CAPES, FAPERJ e LNLS

DIFFERENTIALLY EXPRESSED PROTEINS IN LYMPH NODE AND IN BODY FLUIDS OF PATIENTS WITH HEAD NECK CANCER

Vidotto, A[1], Polachini, G. M.[1], Cury, P.M.[1], Maniglia, J.V[1], GENCAPO, P.[2], and Tajara, E.H.[1]

[1] Faculdade de Medicina de São José do Rio Preto - São José do Rio Preto SP Brazil
[2] Fundação de Amparo à Pesquisa do Estado de São Paulo - São Paulo SP Brazil

The regional lymph nodes play a pivotal role in diagnosis, staging and management of head and neck squamous cell carcinomas (HNSCC). Despite their importance, detailed understanding of the probable mechanisms of lymphatic metastases has not been completely achieved. Differently of lymph nodes but potentially valuable in HNSCC study, saliva and serum have not been used to screen or to diagnose cancer. In order to investigate potential markers for diagnosis and prognostic of HNSCC, we analyzed metastatic and normal lymph node tissues, from thirty-two patients with HNSCC using two-dimensional electrophoresis and MALDI-Q-TOF. In addition, we evaluated the protein profile of saliva and serum from thirteen patients and twenty-nine controls. A number of proteins were found to be over-expressed (heat shock proteins, glutathione S-transferases, stratifin, S100s family, apolipoprotein A-I, alpha-1-microglobulin and galectins) or underexpressed (cal-reticulin, tropomyosin, triosephosphate isomerase, pyruvate kinase isozymes and cystatins) in metastatic lymph nodes, serum and saliva from patients. These proteins are involved in epidermis development, cell proliferation, cell communication, apoptosis, cell migration, metabolic process and transport, indicating their potential role in cancer. The data may help to understand the molecular mechanisms governing head and neck tumorigenesis and may reveal novel biomarkers with diagnostic and prognostic value for HNSCC, as well as potential molecular targets for therapeutic strategies against this disease. The present findings demonstrated the rich protein information that can be produced by means of proteomic analysis which may be the basis for rational designs of diagnostic and therapeutic methods in cancer.

Acknowledgements: FINEP, FAPESP, CAPES, CNPq and LNLS.

SAXS studies on the temperature stability of extracellular hemoglobin of Glossoscolex paulistus in the oxy- form.

Santiago, P.S.[1], Barbosa, L.R.S.[2], Itri, R.[2], and Tabak, M.[1]

[1] Universidade de São Paulo - São Carlos - São Carlos SP Brazil
[2] Universidade de São Paulo - São Paulo - São Paulo SP Brazil

Extracellular hemoglobin of Glossoscolex paulistus (HbGp) is an oligomeric protein constituted by subunits containing heme groups, monomers and trimers, and non-heme structures, linkers. The whole protein has a molecular mass near $3.6x10^6$ Da. Due to their extracellular nature, large size and resistance to oxidation, erythrocruorins have been proposed as useful model systems for developing therapeutic blood substitutes and preliminary animal experiments have been encouraging. HbGp has been previously studied by small angle X-ray scattering (SAXS) both in the absence and in the presence of surfactants. These studies have allowed to differentiate the effects of opposite surfactant headgroup charges on the HbGp oligomeric structure dissociation and autoxidation. In our previous work, the structural conformation of the HbGp in the oxy- and met- forms in the absence and presence of SDS, at pH 7.0 and 9.0, has been studied by SAXS. Changes produced in the protein structure upon both, alkaline dissociation and interaction with the surfactants, were investigated. In the present work, the dissociation and denaturation of HbGp in the oxy-form, at pH 7.0, as a function of temperature were studied by SAXS. SAXS studies of oxy-HbGp at pH 7.0 as a function of temperature in the range 20-65^0C shows a great stability up to 45^0C. Above this temperature the structure of the scattering curve is lost suggesting that significant changes occur in the oligomeric structure associated to its dissociation into smaller subunits. On the other hand, the experimental curves also suggest significant protein aggregation: the particle dimensions can be only estimated here as the minimum values due to the shift of the curve to the low q region, which is not accessible experimentally in our measurements. SAXS data are consistent with results from other techniques.

Acknowledgements: Thanks are due to FAPESP and CNPq for partial financial support. P.S.S. is a recipient of a pos-doctoral grant from FAPESP. Research fellowship to M.T. from CNPq is appreciated. The authors are also grateful to the SAXS beam line staff at LNLS, Campinas, Brazil, for support in the experiments.

Determination of human breast tissue structures between 0.15 and 8.50nm^{-1} using Small Angle X-ray Scattering

Conceição, A. L. C.[1] and Poletti, M. E.[1]

Universidade de São Paulo - Ribeirão Preto - Ribeirão Preto SP Brazil

Human breast tissues are formed mainly by four basics component: water, lipids, proteins and ash (minerals), building the molecular structure of human breast tissues. However, it is known that pathological process provide changes in this molecular structure . Small angle x-ray scattering (SAXS) is a powerful tool that allow determinate molecular structures larger than 10. Therefore, SAXS experiments can provide the identification of the molecular systems presents in normal and pathological human breast tissues. In this work, SAXS technique was used to identify the molecular structures of normal and pathological human breast tissues at native and lyophilized state.

SAXS experiment was implemented at the synchrotron radiation source of Campinas in Brazil. A focused monochromator of Si (111) was used in order to provide an X-ray beam of wavelength 1.488 and to reduce the irradiation area on the sample. The sample to detector distance was fixed in two distances, 381mm and 1600mm, allowing to record the range 0.150nm^{-1} $\leq$q(=$4\pi.\sin(\theta/2)/\lambda$)$\leq$8.500nm^{-1} and this space was evacuated in order to minimize air scattering and absorption losses. The detector was a two-dimensional MarCCD. Standard sample of Silver Behenate, was used as a calibrant, in order to establish the correct reciprocal space scale of each scattering profile.

From analysis of angular distribution of photons scattered (scattering profile), it is possible identify the presence of several peaks between q=0.29nm^{-1} and q=1.17nm^{-1} in all tissues, corresponding a collagen-rich regions, related to protein component. Moreover, a peak arise at q=1.50nm^{-1} in all normal tissues, corresponding to packing of triacylglycerols molecules, which are the main component of lipids. Another peak arise in all pathological samples native at q= 4.16nm^{-1}, but do not is present in lyophilized tissues, indicating to be related to water component. While the peak positions are the same independently of tissues condition, the intensity of these peaks corresponding to basic components (lipids and protein) changed as the normal and pathological condition.

Although in beginning stage this study indicate the possibility of build a diagnosis model of breast cancer based on concentration of basic components of the breast tissues.

Acknowledgements: The authors would like to thank LNLS - Brazilian Synchrotron Light Laboratory. This work was supported by FAPESP.

Amplification and cloning of nahB gene and expression of NahB dehydrogenase for structural and functional studies

COSTA, D. M.A[1], Corrêa, N. C. R.[1], Salas, C.E.[1], and Nagem, R. A. P.[1]

Universidade Federal de Minas Gerais - Belo Horizonte MG Brazil

Polycyclic aromatic hydrocarbons (PAHs) are compounds that consist of two or more fused aromatic rings and most of them are mutagenic and carcinogenic to humans and animals. PAHs are released through the environment by anthropogenic activities related to the extraction, transport, refine, transformation and use of petroleum and its derivatives. Bioremediation is a strategy for PAHs elimination from the environment which uses enzymes or microorganisms displaying the capacity to metabolize these compounds and transform them into inert substances. Naphthalene is one of the most commonly found PAHs in the environment. The degradation of naphthalene by *Pseudomonas sp.* is an alternative procedure for the decontamination of the environment with this contaminant. nahB is a gene responsible for codification of the protein cis-1,2-dihydro-1,2-dihydroxynaphthalene-1,2-dehydrogenase (NahB), which is one of the enzymes involved in the conversion of naphthalene to salicylate. In this work we have amplified and cloned the nahB gene from *Pseudomonas putida G7* and expressed the NahB protein. The bacteria *Pseudomonas putida G7* was cultivated in minimum media with naphthalene and its DNA was extracted. Specific primers for the nahB gene were constructed and a protocol for the amplification of the gene by PCR (Polymerase Chain Reaction) was standardized. Cloning of the fragment was performed in pCR 2.1-TOPO vector. The recombinant plasmid was transformed in competent cells E. coli TOP10 and the clones were analyzed by colony PCR. The plasmidial DNA was extracted for sequencing and the gene of interest was, later, sub-cloned in prokaryote expression vectors pET28a-TEV and pET28a-GST-TEV (Carneiro et al., 2006[1]). These were later transformed in BL21 pRARE competent cells for protein expression. Initial purification attempts are under way.

[1] Carneiro, F. R. G., Silva, T. C. L., Alves, A. C., Haline-Vaz, T., Gozzo, F. C. Zanchin, N. I. T. *Biochemical and Biophysical Research Communications*, **343**, 260-268, 2006.

Acknowledgements: This work was supported by FAPEMIG and CAPES.

A human protein involved in PKR protein kinase activation interacts with the 3´SL region of Dengue virus RNA

Alves, B.S.C.[1], Figueiredo, L. T. M.[2], and Zanchin, N. I. T[1]

[1] Laboratório Nacional de Luz Síncrotron - Campinas SP Brazil
[2] Universidade de São Paulo - Ribeirão Preto - Ribeirão Preto SP Brazil

The Dengue virus genome is composed by a single stranded RNA of positive polarity. The viral 5´ untranslated region (UTR) is similar to the 5´UTR of eukaryotic mRNAs, containing about 100 bases and a cap structure. The 3´UTR is long, without a poly (A) tail, containing stable secondary structures which are conserved among the different Flaviviruses. Deletion studies have demonstrated that 3´ UTR secondary structures and the 3´ Stem-Loop (3´SL) are essential both for synthesis of the viral proteins and for virus viability. The 3´SL mediates anchoring of viral proteins responsible by viral replication and also some human proteins whose function on the Dengue virus biology is unknown. In this work, we have used the yeast three-hybrid (Y3H) system to screen for novel proteins that interact with the dengue virus 3´SL. This screen identified PACT as a putative 3´SL interacting protein. This protein was able to interact with 3´SL, but not with the control RNA used in the assay, unlike other proteins which were isolated in the screen but did not distinguish the 3´SL RNA from the IRE control RNA. PACT is the PKR cellular activator protein. PKR is an interferon-inducible double-stranded RNA activated protein kinase, which is activated by most viral infections and plays a key role in viral infection resistance mechanisms. PACT possesses RNA-binding motifs and in vitro assays indicated that it shows higher affinity to the 3´SL RNA than to unrelated RNAs. This finding led us to characterize further this interaction to determine the role of PACT in the mechanism of dengue virus infection. For this purpose, we will study DV infection in cell lines knock down for PACT. This cell line was already constructed and PACT was knocked down by using the pMaleficent system [Heggestad AD *et al.* 2004. Biochem Biophys Res Commun, 316:643] to generate a shRNA against PACT. The DV proliferation rate in cells knock down for PACT relative to DV proliferation in cells expressing PACT should answer the question whereas PACT interaction with DV 3´SL is important for PKR activation and cell protection on DV infection.

Acknowledgements: This work was supported by FAPESP and LNLS.

Identification of a putative o-linked glycosylated subpopulation of the PP2A regulator α4 in the nuclear compartment of HEK293 cells

Smetana, J. H. C.[1] and Zanchin, N. I. T[1]

Laboratório Nacional de Luz Síncrotron - Campinas SP Brazil

Type 2A phosphatases (PP2A, PP4 and PP6) are the major soluble serine/threonine phosphatases in animal cells and regulate most cellular processes, such as signal transduction, cell cycle progression and apoptosis. These phosphatases are found in complexes with specific regulatory subunits and also share two common regulators, TIPRL and α4 (IGBP1), the orthologues of yeast Tip41 and Tap42. Endogenous α4 shows cytoplasmic and nuclear distribution in HEK293 cells, with a predominantly nuclear staining as shown by immunocytochemistry. Using a standard subcellular fractionation approach and immunoblot with an α4 specific antibody, we identified a band of higher apparent molecular weight in the nuclear compartment of HEK293 cells which is absent in cytoplasmic fractions. This band is enriched in insoluble nuclear preparations, suggesting an association with chromatin. Primary structure analysis using the Expasy proteomics server identified a short serine-rich motif within the α4 sequence which concentrates potential "YinOYang"phosphorylation/glycosylation sites, which correspond to serine or threonine residues that can be either phosphorylated or glycosylated. O-linked glycoslation is a reversible regulatory modification found in many nuclear and cytoplasmic proteins, specially transcription factors and chromatin associated proteins. This finding suggests a direct role for α4 in the regulation of gene expression, which will be explored using deletion mutants that allow us to map the site of this modification and understand its functional significance.

Acknowledgements: We thank Adriana C. Alves, Elaine C. Teixeira and Tereza C. Lima Silva for technical assistance. This work was supported by CNPq, FAPESP and LNLS.

Differentially expressed genes and their functional relationships in a blast-mesenchymal cell co-culture model.

Vaz, T. H.[1], Vasconcellos, J.F.[2], Alves, A. C.[1], Melo, J.O.[1], Yunes, J. A.[3], and Zanchin, N. I. T[1]

[1] Laboratório Nacional de Luz Síncrotron - Campinas SP Brazil
[2] Centro Infantil Boldrini - Campinas SP Brazil
[3] Universidade Estadual de Campinas - Campinas SP Brazil

Acute Lymphoblastic Leukemia (LLA) results from a defect in the differentiation of blood cells: there is an overproduction of immature B lymphocytes that overtakes the normal development of blood cells in the bone marrow. Most cases of LLA develop in early childhood. The central role played by the bone marrow microenvironment for the disease onset and maintenance is illustrated by the fact that it is the primary site where residual leukemic cells survive during cancer treatment, and additionally, the observation that the leukemic blasts die faster without its support *in vitro*. It is clinically important to understand the survival signals provided by stroma cells, as the genes differentially expressed by blasts in situations where they receive support from stroma cells can be used as targets for cancer therapy. In order to identify the genes expressed in response to the survival signals received by the leukemic blasts, we performed global gene expression analysis of leukemic blasts co-cultured with mesenchymal stem cells and of leukemic blasts alone. The global gene expression analysis was performed using DNA Microarray (GeneChip Affymetrix, Inc.). The microarray data were analyzed with GeneSpringGX (Agilent Technologies) using the RMA algorithm and a filter on five present probes. Differentially expressed genes were defined as those with a fold change greater than 2 and with a p value smaller than 0.05. The gene list was subsequently submitted to gene ontology analysis, where only genes belonging to a biological process enriched in the differentially expressed list, compared to the original list of genes included on the microarray chip, using a p value cutoff of 0.1, were further considered in the analysis. The resulting list contains 199 differentially expressed genes, and these will be analyzed with the Pathway Architect software (Agilent Technologies) for the identification of importantly regulated biological pathways. Genes candidates to play important roles as mediators of survival signals will be selected to confirm differential expression by quantitative PCR.

Acknowledgements: This work was supported by CNPq

Expression Systems for the Human Protein Kinase S6K1 and its Phosphorylation Substrate, the C-terminal Region of RPS6

Paier, C. R. K.[1] and Zanchin, N. I. T[1]

Laboratório Nacional de Luz Síncrotron - Campinas SP Brazil

In mammals, S6K1 has been described as an effector of the target of rapamycin (mTOR), which is implicated in cancer and metabolic diseases. Its best characterized substrate is the ribosomal S6 protein (RPS6), a component of the 40S ribosomal subunit. Activation of S6K1 and phosphorylation of RPS6 triggers selective recruitment of the 5`-TOP mRNAs by the ribosome. This class of mRNAs includes most genes encoding translation factors. In this work, we constructed vectors to express a truncated form of S6K1 (S6K1α2T389EΔCT) in insect cells and the C-terminal region of RPS6 (CTRPS6) in *E. coli*. Truncation of S6K1 removes the partially unfolded carboxyterminal region of the protein, which contains the auto-inhibitory domain. In addition, the site of phosphorylation by mTOR (Thr_{389}) was mutated to a Glu residue to mimic a phosphorylated form of S6K1. The objective of these modifications is the production of a partially active kinase. The pFastBac Dual-GFP-S6K1α2T389EΔCT bicistronic vector was constructed, with the E-GFP cDNA under the p10 and the S6K1α2T389EΔCT cDNA under the polyhedrin baculovirus promoters. The *E. coli* DH10Bac strain was transformed with this vector for the production of the bacmid with the bicistronic expression cassette, employed in the transfection of *Sf*9 cells, as described by the protocol of the Bac-to-Bac System from Invitrogen. The success of transfection was followed by visual inspection of GFP fluorescence on a microscope. The virus was titrated by using quantitative PCR, based on the E-GFP cDNA target detection and SyBR Green as fluorophore. Expression of S6K1 was performed in *HighFive* insect cells. In addition to producing active S6K1, we plan to develop an assay to test S6K1 activity using the CTRPS6 as a substrate for S6K1 phosphorylation *in vitro*. For this purpose, two expression vectors derived from pBUF were constructed, which express CTRPS6 with or without a cystein residue at the N-terminus. This cystein residue will facilitate immobilization of CTRPS6 in subsequent S6K1 activity assays. The C-terminal construct was expressed mainly in inclusion bodies, and it was refolded by step dialysis against buffers with decreasing urea concentrations, starting with 6 $mol.L^{-1}$.

Acknowledgements: FAPESP, CBME/CEPID/FAPESP, LNLS

Characterization of interactions between PthA protein from *Xanthomonas axonopodis pv citri* and citrus proteins involved in transcription and translation

Soprano, S. A.[1], Souza, T. A.[2], Cernadas, R. A.[2], and Benedetti C.E.[3]

[1] Universidade Estadual de Campinas - Campinas SP Brazil
[2] Centro de Biologia Molecular e Estrutural - Campinas SP Brazil
[3] Laboratório Nacional de Luz Síncrotron - Campinas SP Brazil

Citriculture is the second most important agricultural activity in the State of São Paulo (Brazil), the largest sweet orange production area in the world. Citrus canker disease, caused by the bacterium *Xanthomonas axonopodis pv. citri* (*Xac*), is a devastating disease responsible for large losses to the agroindustry every year. *Xac* affects various citrus species and the canker symptoms induced on sweet oranges, lemons and limes are characterized by pustule-like lesions that develop on both surfaces of the leaf and which later become corky and surrounded by a water-soaked margin. Canker lesions can also develop on stems and fruits and are thought to be the result of intense cell division (hyperplasia) and expansion (hypertrophy) of the host tissues after pathogen infection. The molecular mechanism by *Xac* causes canker is not entirely known; however, the efector protein PthA, delivered by the type III secretion system, is sufficient to induce the cell hypertrophy and hyperplasia. Recent studies have suggested that members of the PthA/AvrBs3 family act as transcription factors. Therefore, elucidating how PthA activates transcription is important to understanding the development of canker lesions. In this context, we describe here the characterization of new interactions between PthA and sweet orange (*Citrus sinensis*) proteins involved in transcription and translation processes in eukaryotes and which have been associated with mammalian and plant cell proliferation.

Acknowledgements: This work is supported by FAPESP

Análise de chaperones hipotéticas da Xanthomonas axonopodis pv. citri

Martins, A. M.[1], Tasic, L.[1], and Arruda, M. A. Z.[1]

Universidade Estadual de Campinas - Campinas SP Brazil

Este projeto tem por objetivo estudar a expressão protéica da bactéria *Xanthomonas axonopodis pv. citri* (*Xac*), causadora do cancro cítrico nos laranjais, em contato com seu hospedeiro. Pretendemos definir e comparar a expressão de 40 proteínas classificadas como possíveis chaperones de secreção dos sistemas secretórios tipo III e IV na bactéria *Xac* nas condições que mimetizam a presença da planta hospedeira por conter nutrientes provenientes da laranja, em extrato de folha, de casca e em suco de laranja. A separação das proteínas da *Xac* será realizada por géis bidimensionais (SDS-PAGE) com intenção de definir a presença de proteínas alvo do tamanho de 8-23 kDa e com pI na faixa 3-7. As proteínas de interesse serão seqüenciadas após lise tríptica por técnicas de espectrometria de massas (EM), utilizando, principalmente a técnica de ionização mole (*Matrix assisted laser desorption/ionization* MALDI). Acredita-se que as proteínas alvo participem no processo de translocação de fatores de virulência da *Xac*, proporcionando-lhes uma estrutura específica e compatível ao tamanho dos sistemas de secreção e, também, tendo um papel importantíssimo em seu encaminhamento para a secreção. Adicionalmente, pretende-se avaliar consumo preferencial da *Xac* em relação a extratos e suco aplicando técnicas de cromatografia gasosa acoplada à espectrometria de massas (CG-EM) e cromatografia líquida de alta eficiência (CLAE), respectivamente, e, também, possíveis metais ligados às proteínas alvo, aumentando o grau de informação sobre o papel que co-fatores podem desempenhar na interação planta-patógeno.

Acknowledgements: Este trabalho tem o suporte do Instituto de Química - UNICAMP e das agências de fomento CAPES e FAPESP.

Expression, purification and preliminary structural studies of human Nek1 and Nek6

Meirelles, G. V.[1], Lanza, D.C.F[2], Lenz, G.[3], Silva, J.C.[2], Torriani, I.[1], and Kobarg, J.[1]

[1] Laboratório Nacional de Luz Síncrotron - Campinas SP Brazil
[2] Universidade Estadual de Campinas - Campinas SP Brazil
[3] Universidade Federal do Rio Grande do Sul - Porto Alegre RS Brazil

The vertebrate *N*IMA-r*e*lated *k*inases (Neks) represent an evolutionarily conserved family of 11 serine/threonine kinases, containing 40-45% identity to the *Aspergillus nidulans* mitotic regulator NIMA within their N-terminal catalytic domain. Among the mammalian Nek proteins, Nek1 and Nek6 are described as related to pathologies. Nek1 was implicated in cilia function and associated with polycystic kidney disease (PKD) in mouse models. Indeed, in previous two-hybrid studies our group identified hNek1 interacting proteins involved in PKD, neural cell development and G2/M DNA damage checkpoint. Human Nek6 was recently found to be linked to carcinogenesis. It is over-expressed in gastric cancer and up-regulation of Nek6 mRNA correlates with Pin1 up-regulation in 70% of hepatic cell carcinomas, while the over-expression of a catalytically-inactive Nek6 reduces the growth rate of human breast cancer cells. These facts highlight Neks as potential chemotherapeutic targets. In this work, we present the expression and purification of recombinant hNek6, both mutant (S206A) and wild type, and the mutant hNek1 kinase domain (T162A) in *E. coli*, for structural and functional studies. Initial structural analysis involving Dynamic Light Scattering, Far-UV Circular Dichroism, Analytical Gel Filtration Chromatography and Small Angle X-ray Scattering demonstrated that Nek6 (S206A) is a monomeric, mostly globular protein with a secondary structure constituted predominantly by alpha-helix. Crystallization assays are also currently being optimized and we hope that these studies may provide useful information for the development of new chemotherapeutic strategies.

Acknowledgements: We would like to thank FAPESP, LNLS and CNPq for the financial support.

Padronização da Ressonância Magnética Nuclear para determinação precoce da resistência à quimioterapia na leucemia linfóide aguda pediátrica

Melo,CPS[1], Yunes, J. A.[1], and Zeri, AC;[2]

[1] Universidade Estadual de Campinas - Campinas SP Brazil
[2] Laboratório Nacional de Luz Síncrotron - Campinas SP Brazil

O uso intensivo e combinado de diferentes quimioterápicos tem permitido a cura de 70-80% das leucemias linfóides agudas (LLA) da infância. A intensidade e o uso das drogas são adaptados ao risco de recaída dos pacientes, aferido ao diagnóstico e nas primeiras semanas do tratamento. Embora existam diferenças, os critérios básicos para estratificação dos pacientes nos grupos de risco são idade e contagem leucocitária. Além disso, a resposta inicial ao tratamento, mensurada pela citoredução na medula óssea e/ou sangue periférico, é um fator prognóstico poderoso, independente, que permite identificar pacientes com maior ou menor risco de recaída. Ao mensurar a citoredução, faz-se, indiretamente, uma avaliação in loco da sensibilidade intrínseca da leucemia à quimioterapia. A proposta deste projeto é implementar a metodologia de Ressonância Magnética Nuclear (RMN) para uso futuro na identificação de pacientes de LLA com resistência aos quimioterápicos usados na fase de indução. A implementação do método de RMN será feita com células (linhagens celulares e células primárias de LLA) em cultura e doses crescentes de quimioterápicos usados individualmente ou combinados. O perfil de RMN dos quimioterápicos e seus metabólitos serão obtidos tanto do meio de cultura quanto de extratos celulares. Buscamos associações entre os perfis dos espectros de RMN e a resistência das células aos quimioterápicos. O método poderá ser futuramente usado para análise de plasma ou células de pacientes em tratamento, subsidiando, com maior precisão do que os métodos atuais, a alocação dos pacientes nos grupos de risco. Além disso, espera-se que a análise do perfil metabólico permita formular alguma hipótese sobre as vias metabólicas implicadas na resistência às drogas. Para prova de conceito iniciamos o estudo com a L-asparaginase, e linhagens celulares resistentes e sensíveis ao medicamento.

Acknowledgements: FAPESP (2007/00952-0), ABTLuS, Centro Infantil Boldrini

Características estruturais e mecanismo de ação do inativador iodoacetamida em complexo com a enzima Gliceraldeído-3-Fosfato Desidrogenase de *Trypanosoma cruzi*

BALLIANO, T. L.[1], Guido R.V.C.[1], Andricopulo, A. D.[1], and G.OLIVA[1]

Universidade de São Paulo - São Carlos - São Carlos SP Brazil

A doença de Chagas, causada pelo protozoário parasita *Trypanosoma cruzi*, é um dos problemas médico-sanitários mais importantes na América Latina. A doença atinge cerca de 20 milhões de indivíduos causando 50 mil mortes ao ano. Os fármacos disponíveis para o tratamento quimioterápico (benznidazol e o nifurtimox) são limitados e tem seu uso restrito devido à elevada toxidez, baixa eficácia e sérios efeitos colaterais. Dessa forma, o desenvolvimento de novos fármacos, seguros e eficazes, é de fundamental importância no controle da doença. Um alvo macromolecular muito investigado em nosso grupo de pesquisa é a enzima gliceraldeído-3-fosfato desidrogenase (GAPDH) de T. cruzi, essencial no controle do fluxo glicolítico em tripanosomatídeos. Triagens biológicas realizadas com sucesso em nossos laboratórios resultaram na identificação de vários inibidores de diversidade química elevada. Um aspecto de extrema importância no contexto do planejamento de inibidores é a investigação do modo de ligação e mecanismo de ação. Nesse sentido foram realizados estudos cinéticos e cristalográficos com o inativador iodoacetamida (ACM), que interage com resíduos de cisteína presentes no sítio catalítico de várias enzimas inclusive as GAPDHs. Entretanto, os determinantes estruturais subjacentes ao mecanismo de inibição permanecem desconhecidos. Ensaios de cristalização foram desenvolvidos utilizando o método hanging drop com solução de proteína purificada a 11 mg/mL. Os cristais cresceram após 2 semanas a 18 ^{o}C. A coleta de dados foi realizada no LNLS. A análise do modo de ligação do ACM revelou que a fixação covalente à cisteína catalítica é estabilizada por interações pi entre a cadeia lateral do resíduo Tyr339 e o grupo amida do ACM. O modo de interação também indica impedimento estérico na região do grupo nicotinamida do NAD^{+} evitando assim a formação do complexo GAPDH- NAD^{+}. Nesse trabalho os determinantes químicos e estruturais envolvidos no processo de reconhecimento molecular e no mecanismo de reação entre GAPDH e ACM foram estudados. A análise desse complexo mostrou características estruturais relevantes para o estudo da atividade biológica que serão úteis no planejamento de novos inibidores mais potentes e seletivos.

Acknowledgements: CNPq, FAPESP e LNLS

Cloning and expression of FtsJ3, a putative human ribosomal RNA methyltransferase.

MORELLO, L.G.[1] and Zanchin, N. I. T[2]

[1] Universidade Estadual de Campinas - Campinas SP Brazil
[2] Laboratório Nacional de Luz Síncrotron - Campinas SP Brazil

Eukaryotic ribosomal RNA (rRNA) molecules are transcribed as a primary transcript that undergoes extensive processing and posttranscriptional modifications to give rise to mature rRNAs. The human protein FtsJ3 is the putative ortholog 3 of *E. coli* FtsJ, which is involved in rRNA 2-*0*-ribose methylation. In prokaryotes, this protein methylates U_{2552} in the rRNA 23S, while the yeast ortholog Spb1p methylates G_{2922} in the rRNA 25S. The equivalent position in bacteria is the docking site for aminoacyl-tRNA, and it is critical for translation. This position is located within the A-loop region in the ribosome large subunit (LSU). The A-loop region is found in the peptidyl transfer center (PTC) and is potentially involved in the peptidyl transfer reaction. The human FtsJ3 ortholog has not been characterized yet, but it was found to interact with HsNip7 and based on the conservation of the pre-ribosomal biosynthesis machinery it may be involved in methylation of G_{4469} of the 28S rRNA, equivalent to G_{2922} of the yeast 25S rRNA. In order to determine FtsJ3 biochemical function, we describe in this work a baculovirus expression system to produce recombinant FtsJ3 in insect cells. For this purpose, we have employed a bicistronic vector co-expressing GFP along with target genes. This system is used to monitor the infection of insect cells and gives preliminary information to optimize expression conditions. Quantitative PCR (QPCR) was used to titer recombinant baculoviruses in the supernatant of infected cultures by amplifying the target gene. By combining these techniques, we have obtained heterologous expression of FtsJ3 in insect cells.

Acknowledgements: FAPESP, LNLS

Parte IV

Ciência Atômica e Molecular

Fragmentação da Molécula da Vanilina Utilizando Feixes de Elétrons e a Luz Síncrotron

Silva,L.B.[1], Bernini, R.B.[1], Gomes, T. S.[1], de Souza, G.G.B.[1], and Coutinho, L. H.[2]

[1] Universidade Federal do Rio de Janeiro - Rio de Janeiro RJ Brazil
[2] Centro Universitário da Zona Oeste - Rio de Janeiro RJ Brazil

A vanilina ($C_8H_8O_3$), um dos componentes da baunilha, é um dos compostos aromáticos mais apreciados no mundo e um importante flavorizante para alimentos e bebidas. Em sistemas biológicos, a vanilina atua no combate a radicais livres, sendo considerada um potente antioxidante[1]. Apresentamos um estudo da fragmentação iônica desta molécula, empregando a espectrometria de massas de tempo-de-vôo[2] e feixes de elétrons ou a luz síncrotron como agentes ionizantes. No primeiro caso, as medidas foram efetuadas no Laboratório de Impacto de Feixe e ElétronsLIFE, UFRJ. As medidas com luz foram por sua vez realizadas na linha de luz TGM do Laboratório Nacional de Luz Síncrotron LNLS, em Campinas. Tratando-se de um sólido cristalino, um forno foi utilizado na volatilização da amostra. A metodologia experimental permite o estudo de processos de ionização tanto simples quanto dupla, e a obtenção de parâmetros importantes como o Rendimento Iônico parcial (RIP). Embora fundamentalmente os mesmos fragmentos sejam observados nos espectros obtidos com elétrons de 800 eV e fótons de 310 eV, o íon molecular $C_8H_8O_3^+$, apresenta maior intensidade relativa (rendimento parcial) na interação com feixe de elétrons. Na ionização com a luz síncrotron, observa-se um maior grau de fragmentação. Os íons de maior intensidade passam a corresponder às relações m/z = 1 e 29. Embora tanto elétrons quanto a luz síncrotron possam induzir a fragmentação da molécula da vanilina, podemos considerar o primeiro processo como mais suave no sentido de maior preservação do íon molecular. A dupla ionização da molécula estudada a 310 eV, utilizando Luz Síncrotron como agente ionizante e a técnica de coincidência elétron-íon-íon. A maior parte das coincidências (44,38

Referência Bibliográfica 1. Daugsch, A., Pastore, G., Obtenção de Vanilina: Oportunidade Biotecnológica, Química Nova, 2005, 28, 642-645. 2. Souza,G.G.B, Lago, A.F. Mass Spectrometry Study of the Fragmentation of Valence and Core-shell (Cl 2p) Excited CHCl3 and CDCl3 Molecules, Journal of chemical physics, 2004, 120, 9547-9555.

Acknowledgements: Os autores agradecem ao CNPq, FAPERJ e LNLS pelo apoio financeiro.

HeI Photoelectron and Valence Synchrotron Photoionization Studies of $CClH_2SCN$

Erben, Mauricio F.[1], Rodriguez Pirani, Lucas[1], Romano, Rosana M.[1], Geronés, Mariana[1], Cavasso Filho, R. L.[2], and Della Védova, Carlos O.[1]

[1] Universidad Nacional de La Plata - La PLata B.A. Argentina
[2] Universidade Federal do ABC - Santo André SP Brazil

Organosulfur compounds have attracted much attention and several outstanding reviews covering the chemistry of thiocyanates (RSCN) and isothiocyanates (RNCS) can be found in the chemical literature [1-4]. Recently, we became interested in the CH_3SCN molecule, in particular the inner shell electronic properties and the ionic fragmentation of photon excited CH_3SCN following S 2p excitation were studied by using synchrotron radiation [5]. The recent development of a neon gas filter in the TGM line at the Brazilian Synchrotron National Laboratory (LNLS) now affords pure synchrotron radiation in the 12-21.5 eV range, and this has permitted us to enlarge the study of photoionization processes into the valence region. The coalition of PES and multicoincidence Time-Of-Flight (TOF)-based techniques seems to offer a most promising approach to a deeper understanding of the electronic structure and the ionic dissociation induced by photon absorption in the valence region. Following this methodology, relatively simple species such as XC(O)SCl (X= F and Cl) and $CH_3C(O)SCH_3$ have been studied [6,7]. Here we report a study of the photon impact excitation and ionization dissociation dynamics of $CClH_2SCN$, in a combined approach that includes the use of HeI PES and of photoionization under the action of synchrotron radiation in the valence region. TIY and PIY spectra have been measured, together with the PEPICO spectra at selected photon energies, thereby allowing the study of the dissociation dynamics of excited $CClH_2SCN$ molecules.

[1] Mukerjee, A. K.; Ashare, R. Chem. Rev. 1991, 91, 1. [2] Erian, A. W.; Sherif, S. M. Tetrahedron 1999, 55, 7957. [3] Sharma, S. J. Sulfur Chem. 1989, 8, 327. [4] Moore, C. B.; Álvarez, R. A. Science 1994, 263, 205. [5] Cortés, E. et al. J. Phys. Chem. A 2008, subbmited. [6] Geronés, M. et. al J. Phys. Chem. A 2008, 112, 2228. [7] Geronés, M. et al. J. Phys. Chem. A 2008, 112, 5947.

Acknowledgements: The authors wish to thank Arnaldo Naves de Brito and his research group for fruitful discussions and generous collaboration during their several stays in Campinas and the TGM beamline staffs for their assistance throughout the experiments. This work has been largely supported by LNLS, CONICET, CIC, DAAD, ANPCyT and UNLP.

Dissociative Photoionization of $ClC(O)SCH_2CH_3$ following sulfur 2p and chlorine 2p.

Rodriguez Pirani, Lucas[1], Erben, Mauricio F.[1], Geronés, Mariana[1], Romano, Rosana M.[1], Cavasso Filho, R. L.[2], and Della Védova, Carlos O.[1]

[1] Universidad Nacional de La Plata - La PLata B.A. Argentina
[2] Universidade Federal do ABC - Santo André SP Brazil

Thioesters of the type XC(O)SY occur naturally in a variety of environments. In vivo, thioesters result from the association of a methanethiol moiety and acyl CoA via spontaneous or enzymatically promoted reactions [1]. This, allied to the biochemical importance of coenzyme A and its acyl derivatives, has ensured the maintenance of a lively interest in thioesters [2]. We have started recently a general project aimed at elucidating the shallow and innershell core electronic properties of thioesters, and hence gaining a fuller understanding of the photodissociation channels open to these compounds. Thus, photoionization studies have been carried out on species such as FC(O)SCl [3], ClC(O)SCl [4] thioacetic acid [5] and $CH_3OC(O)SCl$ [6] using synchrotron radiation in the range 1001000 eV. Following these studies, we became interested in other simple thioester compound. Here we report a study of the photon impact excitation and dissociation dynamics of $ClC(O)SCH_2CH_3$ exited at the S 2p and Cl 2p levels by using synchrotron radiation. The TIY spectra of $ClC(O)SCH_2CH_3$ following S 2p excitations is dominated by a group of four signals centered at 164.6, 165.9, 167.2 and 168.4 eV, while the ionization edge is located at approximately 170.9 eV. In the Cl 2p region only one signal can be observed at 201.0 eV. PEPICO and PEPIPICO spectra for this molecule were recorded on each resonance, and also below and above resonance bands. Possible fragmentations mechanisms are deduced from the interpretation of the PEPIPICO spectra.

[1] Helinck, S. et al.. FEMS Microbiol. Lett. 2000, 193, 237. [2] Yang, W.; Drueckhammer, D. G. J. Am. Chem. Soc. 2001, 123, 11004. [3] Erben, M. F. et al. J. Phys. Chem. A 2004, 108, 3938. [4] Erben, M. F.et al. ibid. 2005, 109, 304. [5] Erben, M. F. et al. ibid. 2006, 110, 875. [6] Erben, M. F. et al. ibid. 2007, 111, 8062.

Acknowledgements: The authors wish to thank Arnaldo Naves de Brito and his research group for fruitful discussions and generous collaboration during their several stays in Campinas and the TGM beamline staff for their assistance throughout the experiments. This work has been largely supported by LNLS, CONICET, CIC, DAAD, ANPCyT and UNLP.

Fragmentation Dynamic of Benzene, Aniline and Nitrobenzene Induced by Synchrotron Radiation

Flora, D.[1], Paschoal, R. C.[1], Ferreira, G. B.[2], Turci, C. C.[2], and Guerra, A. C. O.[1]

[1] Centro Federal de Educação Tecnológica - Rio de Janeiro RJ Brazil
[2] Universidade Federal do Rio de Janeiro - Rio de Janeiro RJ Brazil

Inner-shell excitation, and associated spectroscopies of the ionic fragmentation of inner shell states, are site specific probes of electronic and geometrical structure and photoionization dynamics [1]. Here we present recent results of coincidence studies in the K-edge of gaseous benzene, aniline and nitrobenzene. The ionic fragmentation has been measured with tuned synchrotron light and time-of-flight mass spectrometry apparatus [2]. Benzene, aniline and nitrobenzene are the simplest aromatic molecules and may be used as a model system for other aromatic molecules with more complicated chemical structures. Our goal is to investigate the fragmentation dynamic of those aromatic molecules following core excitation in K-edge region. How the both donor $-NH_2$ and acceptor $-NO_2$ groups influencing the charge transfer into the aromatic ring? [3]. The experiments have been performed using the Spherical Grating Monochromator (SGM) beamline at the Laboratório Nacional de Luz Síncrotron (LNLS), Campinas-SP (D08A-SGM-7250). High purity samples were obtained commercially and used without any further purification. They were introduced into the apparatus from the vapours of the room temperature liquids after removing air and volatile impurities by a series of freeze-pump-thaw cycles. The work pressure was maintained at 1.0×10^{-6} mbar during data acquisition. The base pressure was 1×10^{-8} mbar.

[1]A.P. Hitchcock and J.J. Neville, in Chemical Applications of Synchrotron Radiation (T.K. Sham, ed.) (World Scientific, 2002) 154.
[2]F. Burmeister , et al., *J. Electron Spectrosc. Relat. Phenom.* (2007) in press; Lago, A.F., et al., *J. Chem. Phys.* 120 (2005) 9547.
[3]A.C.O. Guerra, et al., *Inter. J. Quant. Chem.* 108 (2008) 2340.

Acknowledgements: LNLS, FAPERJ, CEFET/RJ.

Dynamical correlation in the double ionization of methane and ammonia molecules

ACF Santos[1], Boechat-Roberty , H.M.[1], MONTENEGRO, E.C.[1], Pilling, S.[2], W. Wolff[1], de Jesus, V. L. B.[3], and Sigaud, L.[2]

[1] Universidade Federal do Rio de Janeiro - Rio de Janeiro RJ Brazil
[2] PUC - Rio de Janeiro - Rio de Janeiro RJ Brazil
[3] Centro Federal de Educação Tecnológica - Nilópolis RJ Brazil

We report an unexpected, appreciable and broad resonance-like structure observed for the first time in the fragmentation of some polyatomic molecules. This structure is characterized by a strong inhibition for producing stable single ionized parent molecule and by a strong enhancement of explosive fragmentation of light products. Qualitative reasonings for this new resonance are also presented. The partial ion yields for photofragmentation of methane and ammonia molecules have been measured in the Xray region, for 100-400 eV photon impact, using time-of-flight spectrometry. A new, strong and unexpected resonant-like structure is observed in the measured ionic products at photon energies around 230 eV, where the de Broglie wavelength of the photoelectron is of the same order of the molecular dimensions. It is proposed that the observed fragmentation pattern is a combination of interference effects due to internuclei scattering of the photoelectron together with dynamically correlated re-scattering by the non-bonding molecular orbital electrons.

Acknowledgements: CNPq, FAPERJ and LNLS for support.

Experimental evidence of the oxidation state through resonant Raman sacttering

Valentinuzzi, M. C.[1], H. J. Sánchez[1], Abraham, J. A.[2], and Pérez, C. A.[3]

[1] Universidad Nacional de Cordoba - Córdoba Cba Argentina
[2] Universidad Nacional de Cordoba - Cordoba Argentina
[3] Laboratório Nacional de Luz Síncrotron - Campinas SP Brazil

When atoms are irradiated by x-ray photons different kinds of interactions take place: the photon can be absorbed by the photoelectric effect or can suffer a Rayleigh or Compton scattering. However, under resonant conditions other low probability interactions can occur. One of these interactions is the resonant Raman scattering: when the energy of the incident photon approaches from below to the absorption edge of the target element, a strong resonant behavior takes place contributing to the attenuation of x rays in matter. The resonant character of the process and the existence of an onset energy in the Raman spectrum enable the probing of the edge structure characteristics by tunning the incident energy towards the edge. In the case of oxide compounds, the Raman peak changes the maximum energy, the peak shifts to energies lower by a few electron volts due to a change in the absorption edge energy. By employing a low resolution detecting system, changes in the Raman structure can be observed, providing the possibility of identifying the elements of a sample and their oxidation state. The analyzed samples consisted on pure foils (99.99%) of Cu and oxide foils (99%) of CuO and Cu_2O. Samples were irradiated with monochromatic syncrotron radiation below the K absorption edge of Cu to inspect the Raman emissions. As it should be expected, the Raman scattering process is resonantly enhaced as the energy of the incident photons is closer to the K absorption threshold and the Raman peak dominates the background. In the case of oxides, the Raman peak shifts to lower energies a few electron volts due to the change of the absorption edge energy. However peak areas of pure elements were quite similar to those of oxides and no signicant changes were observed. After fitting, the residuals were calculated. A clear difference was observed among the oxidations states of Cu. The results suggest the possibility of structural characterization by means of resonant Raman scattering using an energy dispersive system combined with synchrotron radiation.

Acknowledgements: This work has been supported by the Brazilian Synchrotron Light Laboratory (LNLS) under proposal D09B-XRF 5749

Estudos Teórico-Experimentais da Produção Parcial de Íons do Ácido Fórmico

M.S. Arruda[1], PRUDENTE, F. V.[1], Marinho, R. R. T.[2], Naves de Brito, A.[3], Mundim, M. S. P.[4], and MANIERO, A. M.[1]

[1] Universidade Federal da Bahia - Salvador BA Brazil
[2] Universidade Federal da Bahia - Barreiras BA Brazil
[3] Laboratório Nacional de Luz Síncrotron - Campinas SP Brazil
[4] Universidade de Brasília - Brasília DF Brazil

Estudos envolvendo biomoléculas, tais como os aminoácidos e as nucleobases do DNA, sempre atraíram considerável interesse devido a sua intrínseca relação com a vida. Entre os vários questionamentos acerca dessas moléculas, um bastante intrigante é relacionado a origem da homoquiralidade molecular. Alguns modelos propostos sugerem que biomoléculas mais complexas, como os amino ácidos, seriam formados pela recombinação de moléculas mais simples após interação com radiação circularmente polarizada no espaço. Assim, diversas experiências foram conduzidas para tentar observar a presença de biomoléculas complexas e também de suas precursoras (ácidos carboxílicos, amônia, entre outras substâncias) no espaço. Para se obter maiores informações do comportamento de amino ácidos maiores e mais complexos, ou ainda proteínas, durante exposição à radiação podemos utilizar ácidos carboxílicos e grupos aminas como sistemas modelos. Do ponto de vista experimental, podemos obter informações de processos de fotoionização que levam a um maior conhecimento da fotoestabilidade, assim como da fotodegradação, destes compostos quando expostos a radiação com comprimentos de onda na região do ultravioleta de vácuo e raios X moles que são de grande interesse em áreas tais como a astrofísica e fotoquímica. Por outro lado, o estudo teórico de tais processos se baseia no emprego de métodos rigorosos (ab initio e DFT) de estrutura eletrônica que levem em conta efeitos eletrônicos como reatividade e correlação eletrônica, permitindo o estudo de moléculas ionizadas e de estados eletrônicos excitados, entre outros.Nesse trabalho, serão apresentados dados da produção parcial de íons do ácido fórmico, que foram medidos por um espectrômetro de massa por tempo vôo que é montado numa câmara rotativa, em função de fótons de baixa energia (12 à 21 eV). A linha de luz utilizada foi a D05A TGM do LNLS que possui um filtro gasoso de Neônio que permite suprimir harmônicos de ordens superiores. Na análise dos resultados experimentais serão utilizados cálculos teóricos da estrutura molecular do estado fundamental da molécula neutra e dos estados eletrônicos do sistema ionizado, bem como dos seus níveis vibracionais.

Acknowledgements: LNLS, CAPES

DEPENDÊNCIA ANGULAR DA FOTOFRAGMENTAÇÃO DA MOLÉCULA DE TIOFENO

Vieira, C.C.O.[1], Mundim, M.S. P.[2], Correia, N.[3], Attie, M.R.P.[3], Marinho, R. R. T.[4], Naves de Brito, A.[5], and Mocellin,A.[1]

[1] Universidade de Brasília - Brasília DF Brazil
[2] Universidade de Brasília - Brasilia DF Brazil
[3] Universidade Estadual de Santa Cruz - Ilhéus BA Brazil
[4] Universidade Federal da Bahia - Barreiras BA Brazil
[5] Laboratório Nacional de Luz Síncrotron - Campinas SP Brazil

A molécula de tiofeno (C_4H_4S) corresponde a um dos possíveis precursores dos polímeros politiofenos, cujas propriedades eletrônicas e interações fundamentais têm sido amplamente estudadas, em virtude de seu aproveitamento tecnológico. Os politiofenos podem ser usados em dispositivos óticos - eletrônicos como diodos emissores de luz (LED), células fotovoltaicas e em transistores. No presente trabalho investigamos a dependência angular na dissociação do tiofeno, induzidas pela luz síncrotron na borda de absorção do S 2p. Utilizamos um espectrômetro de massas por tempo vôo montado em uma câmara rotativa, o que possibilitou realizar medidas nos ângulos de detecção de 0 e 90 graus, com relação ao vetor de polarização da luz. Para determinar os fragmentos e como estes foram gerados, utilizamos as técnicas de coincidências múltiplas, designadas por PEPICO (PhotonElectron - PhotonIon - COincidence Coincidência entre um elétron e um íon) e PEPIPICO (Coincidência entre um elétron e dois íons). Os efeitos de dependência angular foram observados a partir das análises dos espectros de PEPIPICO. Medimos também espectros de produção total de íons, o que possibilitou atribuir as transições eletrônicas, tendo como referência os dados de literatura. Analisamos as duas primeiras ressonâncias. A primeira corresponde àtransição S $2p_{3/2}$ para σ^* (163,5 eV) e a segunda, S $2p_{1/2}$ para σ^* + S $2p_{3/2}$ para π^* (166,9 eV). Observamos que o efeito de dependência angular ocorre apenas para a primeira ressonância devido ao seu caráter sigma (163,5 eV), enquanto que na segunda este efeito é mascarado pois ocorre uma superposição de distribuições eletrônicas de diferentes simetrias. Observamos também que o efeito de dependência angular é melhor resolvido para os pares de íons que possuam maiores diferenças em massa, fato este corroborado pela conservação do momento linear dos fragmentos. Os experimentos foram realizados na linha de luz D05A-TGM (Thoroidal Grating Monochromator) do Laboratório Nacional de Luz Síncrotron (LNLS) Campinas - SP.

Acknowledgements: Este trabalho foi parcialmente financiado pela Universidade de Brasília, Universidade Estadual de Santa Cruz e Laboratório Nacional de Luz Síncrotron.

Parte V

Geociência, Meio-ambiente e Aplicações em Materiais Biológicos

EFECTO DEL CONSUMO DE ANTIOXIDANTES SOBRE LA DISTRIBUCION Y CONCENTRACION DE ELEMENTOS EN CORTEZA RENAL DE RATAS EXPUESTAS A ARSENICO

Rubatto Birri, P.N.[1], R.D. Pérez[2], Pérez, C. A.[3], Rubio, M.[2], and Bongiovanni, G.A.[4]

[1] Universidad Nacional de Cordoba - Cordoba Argentina
[2] Centro de Excelencia de Productos y Procesos de Córdoba - Cordoba Argentina
[3] Laboratório Nacional de Luz Síncrotron - Campinas SP Brazil
[4] Universidad Nacional de Cordoba - Córdoba CO Argentina

El arsénico (As) es un contaminante natural de muchos acuíferos subterráneos y cauces fluviales de Argentina, donde se ha observado HACRE (hidroarsenicismo crónico regional endémico) y una mayor incidencia de cáncer. La metodología Sincrotrón nos ha permitido elaborar mapas de la distribución de elementos en órganos de ratas expuestas a As y un posterior seguimiento durante el ensayo de terapias preventivas. Hemos determinado que el As se acumula en glomérulos renales y zona peri-glomerular de ratas que bebieron 50 ppm As durante 60 días (Pérez et al., 2006) y un aumento en la concentración de Cu que co-localiza con As. Debido a que su principal efecto tóxico es estrés oxidativo (Bongiovanni et al., 2007), se agregó un antioxidante vegetal al agua de bebida lográndose una disminución de hasta 30 % de la retención de As y Cu (Pérez et al., 2008). En el presente reporte se comparan resultados de la administración del antioxidante después de 60 días de exposición o co-administrado con As durante 120 días. Se observó que el antioxidante previene la retención de As y Cu, sin importantes modificaciones de la concentración de otros elementos, únicamente cuando es co-administrado con As sugiriendo un potencial preventivo pero no curativo. La espectroscopía de Fluorescencia de Rayos-X utilizando radiación sincrotrón (SR-XRF) es sin dudas una valiosa herramienta durante la bioprospección de agentes antioxidantes con capacidad de reducir los daños producidos por As.

-Bongiovanni G., et al., (2007). Food Chem. Toxicol 45(6): 971-976. -Pérez R.D., et al. (2008). LNLS Activity Report 2007 (enviado). -Pérez RD., et al. (2006). X Ray Spectrom, 35(6): 352-358. -Soria E.A., Goleniowski M.E., Cantero J.J., Bongiovanni G.A. (2008) Human Exp. Toxicol. 27: 341-346

Acknowledgements: The authors would like to thank LNLS - Brazilian Synchrotron Light Source, Campinas, Brazil, under proposal D09B-XRF-7587 /2008. This work was supported by the CONICET and the Ministry of Science and Technology of Córdoba, Argentina.

Bone Imaging Investigation by X-Ray Microfluorescence Technique with Capillary Optics

LIMA, I.[1], Anjos, M. J.[1], Assis, J. T.[1], and Lopes, R.T.[2]

[1] Universidade do Estado do Rio de Janeiro - Rio de Janeiro RJ Brazil
[2] Universidade Federal do Rio de Janeiro - Rio de Janeiro RJ Brazil

Bone structures consist essentially of a protein and hydroxyapatite. These components can be distributed in different patterns in several types of bones. Minerals contents are correlated with mechanical properties contributing to bone strength. Trace elements are found in both mineral and organic phases, although their role in normal bone function and in bone pathology is not fully established. The most famous and common bone innless is osteoporosis. It is a condition characterized by the loss of bone density. In this disease, bones become more fragile and susceptible to fractures. The participation of trace minerals in the normal development and maintenance of the skeleton is related to their catalytic functions in organic bone matrix. It is known that the deficiency of ovarian hormone in menopause stimulates bone loss. Animal ovariectomization process (OVX) also causes osteoporosis due to lack of estrogen. Nevertheless, alterations in bone the morphology are not exclusive to osteoporosis process. In hyperthyroidism diseases, for example, the thyroid gland produces excess of thyroid hormone, which increases the metabolic activity. Besides iodine, zinc is another mineral that is related with the thyroid hormones. In recent years, it is a consensus that the bone mineral density alone does not explain the whole aspects of bone health. We have to looking for other parameters, such as its mineral compositions. In this context, we used X-Ray microfluorescence by synchrotron radiation (SRXRF) with optical capillary in order to imaging bone sites and evaluate its degree of osteoporosis. For that purpose bones (femur and spine) of more than 20 animals were studied. The results show that quantitative SRXRF analysis is a powerful and alternative technique to characterize topologically bone structures. It was possible to observe the osteoporotic modifications on the bone structures with respect to the morphology and the chemical elements. This is particularly important in bone innless which is related to bone fractures and strengths. The results show that T4 and OVX process influence in trace elements distribution all over the bone sites (femur and spine)and bone locations (trabecular and cortical).

Acknowledgements: This work was partially supported by CNPq, FAPERJ and LNLS Projects 4307, 4822, 5375, 5737 and 7079.

Determinación de la presencia de drogas de tipo bifosfonatos o raloxifeno en huesos humanos, de pacientes con osteoporosis que han sido tratados clínicamente con estos compuestos.

Fernández de Rapp, M. E.[1], Fábregas, I. O.[1], and Lamas, D. G.[1]

Consejo Nacional de Investigaciones Científicas y Técnicas - Buenos Aires Argentina

Como e el trabajo anterior, en éste también se analizaron huesos humanos de pacientes de osteoporosis. En este caso se realizó una impregnación in vitro del material óseo con el bisfosfonato (P-C-P) alendronato monosódico puro, en distintas dosis. Los P-C-Ps son las drogas mas utilizadas en la actualidad como agentes antirresorptivos de los tejidos duros. Los integrantes de esta familia de bisfosfonatos, de los cuales hay mas de vinte reconocidos por su actividad biológica, actúa con gran especificidad en los diferentes tipos de osteogenias imperfectas que se presentan en el organismo humano, desde las más benignas hasta las más graves como cáncer de huesos. Su acción consiste en inhibir el mecanismo acidificante de los osteoclastos sobre la superficie del hueso. Los P-C-P se fijan como tal en el tejido vivo y se van acumulando a través de un prolongado tratamiento de ingesta. Al cabo de un periodo de tiempo que puede ir de 5 a 10 años de consumo de P-C-P por el paciente de OI, el depósito en el tejido óseo puede ser suficiente como para continuar su acción antiresorptiva aunque haya sido suspendido el tratamiento. En el caso de suministrarse solamente raloxiphene luego de ese período de tratamiento, se produce un efecto sinérgico sobre los osteoclastos, con gran aumento de la masa ósea del paciente. El trabajo consistió en detectar, por difracción de rayos X, la presencia de P-C-P en las muestras tratadas con dos dosis en distintos períodos de tiempo. También se estudiaron los cambios en los parámetros de la red cristalina de la hidroxiapatita y las relaciones Ca/P. Con la radiación Síncrotron sólo una muestra tratada con la dosis máxima y mayor tiempo de contacto mostró la insinuación del pico máximo del alendronato monosódico. Efecto que no había sido detectado con difracción de rayos x común. Asociado con esta presencia podría también haber una modificación en los parámetros de la red cristalina que esta siendo estudiada por el método de refinamiento de Rietveldt. Con esta información se replanteará otro ensayo con mayores dosis para establecer el momento límite en que comienza la acumulación del P-C-P que permita el tratamiento con el raloxiphene en el momento adecuado.

Acknowledgements: Agradecimiento: Agradecemos al LNLS y en particular a la línea D12A - XRD1 por permitirnos realizar nuestros estudios.

INFLUENCE OF THE CONTENT OF PRAZIQUANTEL ON STRUCTURAL FEATURES OF THE LIPOSOMES

Souza, A. L. R.[1], Sarmento, V.H.V[1], Terruggi, C.H.B.[1], Chiavacci, L.A.[1], Allegretti, S. M.[2], and Gremião, M. P. D.[1]

[1] Universidade Estadual Paulista - Araraquara - Araraquara SP Brazil
[2] Universidade Estadual de Campinas - Campinas SP Brazil

Schistosomiasis is a parasitic infection caused by trematodes of the genus Schistosoma, which affects approximately 200 million people, killing as many as 280,000 people per annum. Praziquantel (PZQ) is active against all species of Schistosoma and is considered the drug of choice for the treatment of this disease. Because of its low water solubility and the risk of parasite resistance or tolerance to PZQ, it would be very useful to develop novel techniques to produce a pharmaceutical product that could increase the therapeutic efficacy and improve the bioavailability of this drug. Some clinical studies have demonstrated capacity of liposomes to compartmentalize the drug and modify its behavior. In this study, the structural evolution of phosphatidylcholine (PC) liposomes as a function of the incorporation of high concentrations of PZQ has been investigated. The experimental results demonstrated a correlation between the composition and the structural features. SAXS measurements indicated that both higher concentrations of PC and the presence of PZQ induce multilamellar system formation. The variations in the rheological behavior of the samples were directly related to the concentration of PZQ and PC.

Acknowledgements: We acknowledge the LNLS (Campinas, SP, Brazil) staff for SAXS facilities and CNPq, CAPES and FAPESP for financial support.

Phase transitions in ZrO_2-Sc_2O_3 solid solutions: crystallite size effect

Abdala, P. M.[1], Lamas, D. G.[1], Craievich AF[2], and Fantini, M. C. A.[2]

[1] Consejo Nacional de Investigaciones Científicas y Técnicas - Buenos Aires Argentina
[2] Universidade de São Paulo - São Paulo - São Paulo SP Brazil

In the recent development of intermediate-temperature solid-oxide fuel cells, ZrO_2-Sc_2O_3 ceramics had attracted a lot of attention. Due to their high ionic conductivity, these materials are considered as promising candidates as solid electrolytes in these devices. The polymorphs observed in this system have monoclinic, tetragonal, cubic or rhombohedral symmetries. Only the tetragonal and cubic phases exhibit excellent electrical properties. There are three forms of the tetragonal phase: t, t′ and t" [1]. The t form is the equilibrium tetragonal phase. The t′ and t" forms are metastable and have been observed in compositionally homogeneous materials. The further has similar atom position to the t form and the later has an axial ratio, c/a, of unity with the oxygen atoms displaced from their sites of the cubic phase. Three rhombohedral phases have been reported, designed as: β, γ and δ [2].

In a previous work carried at the LNLS, we found that the metastable t"-form of the tetragonal phase or the cubic one (depending on the composition) can be retained in nanocrystalline powders. Materials with crystallite sizes larger than 35nm exhibited a mixture of cubic or t" and β or γ phases.

In this work, we have investigated the phase transitions in ZrO_2-Sc_2O_3 nanopowders with crystallite sizes between 30 and 100nm and compositions between 10 and 14 mol% Sc_2O_3 by in-situ high temperature X-ray powder diffraction. These experiments were carried out at the D10B - XPD beamline of the LNLS, operated in the high-intensity mode. All the powders exhibited phase transitions in the temperature range considered in this study (25 to 900°C) amd we established that the transition temperature depend on the crystallite size and dopant content. The measurements were performed on cooling and on heating, observing an hysteretic behavior.

1. M. Yashima et al., Solid State Ionics 86-88 (1996) 1131
2. J. Le Fèvre, Ann. Chim. 8 (1963) 117

Acknowledgements: This work has been supported by the Brazilian Synchrotron Light Laboratory (LNLS, Brazil), the scientific collaboration agreements CNPq-CONICET and CAPES-SECyT (Brazil-Argentina), CNPq (Brazil, PROSUL program 490289/2005-3), ANPCyT (Argentina, PICT No. 14268 and PICT No. 38309), CONICET (Argentina, PIP No. 6559) and CLAF.

CHARACTERIZATION OF THE CRAB TISSUES AND SEDIMENT BY SR-TXRF

Salvador, M. J.[1], Sawazaki, D.T.A.[2], Hattori, G.Y.[3], and Zucchi, O. L. A. D[4]

[1] Universidade Estadual de Campinas - Campinas SP Brazil
[2] Faculdade de Ciencias Farmaceuticas de Ribeirão Preto/USP - Ribeirão Preto SP Brazil
[3] Universidade Federal do Amazonas - Manaus AM Brazil
[4] Universidade de São Paulo - Ribeirão Preto - Ribeirão Preto SP Brazil

In this work is reported the use of Synchrotron Radiation Total Reflection X-Ray Fluorescence analysis (SR-TXRF) as a technique for macro, micro and trace elements determination in the tissues of the crab *Ulcides cordatus* and in the sediments from Iguape estuary (São Paulo, Brazil) for environmental pollution control and toxicological evaluation. This crab, which is used as food for the population of the coast of the São Paulo, is a potential bio-indicator of environmental pollution because metals can be monitored in its tissues. The analyses were performed in the *U. cordatus* tissues (muscle and hepatopancreas) and sediments from 24 sites of the Iguape estuary (São Paulo, Brazil). The samples of the tissues and sediments, after digestion in open system, were analyzed by SR-TXRF. Standard solutions with Ga as internal standard were prepared. The elements K, Ca, Ti, V, Cr, Mn, Fe, Ni, Cu, Zn, Sr, and Ba were detected in hepatopancreas samples with concentration raging from 0.516 (Mn) to 2061 (K) μg/g, while in the muscle were detected the elements K, Ca, Ti, V, Cr, Fe, Ni, Cu, Zn, Br and Sr with concentration varying from 0.043 (Ni) to 1917 (K) μg/g. The results indicate that some elements such as K, Ca, Ti, V, Cr, Mn, Fe, Co, Ni, Cu, Zn, Rb, Sr, Sn, Ce, and Pb have principal content in the sediment samples with concentration between 3.8 (Cu) and 14628 (Fe) μg/g.

Acknowledgements: Research partially performed at National Synchrotron Light Laboratory (LNLS), Brazil. Fellowship given to second author (FAPESP n. 06 51967-5).

MICROELEMENT ANALYSIS BY ED-XRF IN CEREBRAL SLICES OF RATS SUSCEPTIBLE TO AUDIOGENIC SEIZURES

Salvador, M. J.[1], Arantes, F.C.[2], Rodrigues, MCA[3], Rossetti F.[3], Arisi, G. M.[3], Garcia-Cairasco, N.[3], and Zucchi, O. L. A. D[3]

[1] Universidade Estadual de Campinas - Campinas SP Brazil
[2] Faculdade de Ciencias Farmaceuticas de Ribeirão Preto/USP - Ribeirão Preto SP Brazil
[3] Universidade de São Paulo - Ribeirão Preto - Ribeirão Preto SP Brazil

The inorganic elements have not only a crucial rule for physiology of central nervous system, but they are also important for pathologic situations. Among these elements, zinc has a prominent role in epilepsy. Ionic zinc is enriched in synaptic vesicles of specialized glutamatergic neurons and released in the synaptic cleft along with the neurotransmitter where it modulates post-synaptic neuron excitability. Zinc also is related to Alzheimers plaque deposition, neuron excitotoxic injuries and hippocampal mossy fiber sprouting. Our objective is to standardize a protocol which allows the use of ED-XRF in the quantification of microelements in cerebral slices from of Wistar audiogenic rats (WAR strain) and control rats (Wistar strain) slices. MicroMatter standard samples were employed in calibration curves fitting. Hippocampal slices including dentate gyrus and CA1, CA3 areas were made at bregma 3.14 mm and mounted on pure silicon adhesive tape. Four 100s analyses were made in each region. The following elements were detected in all samples: P, S, Cl, K, Ca, Ni, Cu and Zinc with concentrations ranging from 0.001 μg.cm^2 (Cu Wistar) to 116 μg.cm^2 (P WAR).

Acknowledgements: Research partially performed at National Synchrotron Light Laboratory (LNLS n.4676), Brazil. Fellowship given to second author (FAPESP n. 07/54144-2)

ESTUDO DO PROCESSO DE MORTE CELULAR EM CÉLULAS EMBRIONÁRIAS SOB AÇÃO DE CANABINÓIDES

Cardoso, S.C.[1] and Magalhães, S.D.[1]

Universidade Federal do Rio de Janeiro - Rio de Janeiro RJ Brazil

Canabinóides são substâncias presentes na planta *Cannabis sativa*. Apesar dos canabinóides endógenos, conhecidos como endocanabinóides, estarem presentes desde estágios iniciais do desenvolvimento, os efeitos de sua ativação são desconhecidos em células embrionárias. O objetivo deste trabalho foi fazer a análise multi-elementar (K, Ca, Cl, Fe, Zn), através da técnica de micro-fluorescência de Raios-X, das células de camundongos sob ação de receptores canabinóides e avaliar os efeitos de um agonista canabinóide (WIN 55212-2) sobre essas células. Para tal, células embrionárias de camundongo foram cultivadas e, em seguida, transferidas para placas não aderentes até ocorrer à formação de estruturas esféricas denominadas corpos embrióides (EBs). Após tal procedimento, os EBs foram pré-tratados de três maneiras diferentes: com ácido retinóico, LiF e WIN 55212-2. Nossos resultados preliminares indicam que o tratamento com WIN 55212-2 aumentou significativamente a concentração de Ca e, consequentemente, diminuiu a taxa de morte celular. Nossos dados sugerem que endocanabinóides podem estar envolvidos em mecanismos associados ao controle da sobrevivência de células embrionárias.

Acknowledgements: Agradecemos o apoio financeiro do LNLS e da FAPERJ.

ESTUDO FRACAO ASFALTENICA DE AMOSTRAS DE ROCHAS GERADORAS DA BACIA DO PARANA POR ESPECTROMETRIA DE MASSAS POR TEMPO DE VOO COM DESORCAO A LASER E IONIZACAO ASSISTIDA POR MATRIZ (MALDI-TOF-MS)

Silva,C.G.A.[1], Peralba, M.C.R.[1], Dos Santos, J. H. Z.[1], Kern, L. M.[1], Franco, R. N.[1], and Kalkreudt,W.[1]

Universidade Federal do Rio Grande do Sul - Porto Alegre RS Brazil

A caracterizacao geoquimica organica de rochas geradoras de petroleo atraves da determinacao de parametros fisico-quimicos dos asfaltenos, pode revelar importantes informacoes em relacao ao grau de maturacao da materia organica. A determinacao desses parametros pode utilizar tecnicas convencionais como a cromatografia de permeacao em gel (GPC) ou tecnicas menos corriqueiras como a espectrometria de massas por tempo de voo com desorcao a laser e ionizacao assistida por matriz (MALDI-TOF-MS). A proposta deste estudo foi realizar a determinacao do perfil das razoes massa/carga (m/z) da fracao asfaltenica atraves da espectrometria de massas por tempo de voo com desorcao a laser e ionizacao assistida por matriz (MALDI-TOF-MS) de 17 amostras de rochas geradoras da Bacia do Parana (Formacao Irati). Para avaliar o efeito de matriz na analise dos asfaltenos, foram empregados tras distintas substancias: acido 3,5 dimetoxi-4-hidroxicinamico (acido sinapico), acido 2,5 dihidroxibenzoico (DHB ou acido genticico) e acido α-ciano-4-hidroxicinamico (CNCA). Considerando que processos de ionizacao nao eficientes conduzem a resultados de distribuicao m/z mais baixos, optou-se por analisar as amostras sem a utilizacao de matriz (Artok et al, 1999). No caso das amostras de betume e oleo expulso, verifica-se uma tendencia de aumento, seguido de decrescimo da razao m/z com tempo de hidropirolise. Tal fato pode ser provavelmente atribuido ao processo de craqueamento que ocorre com o aumento de tempo de hidropirolise, o que foi confirmado atraves da caracterizacao por Ressonancia Magnetica Nuclear (RMN) de 1H. Para as amostras de betume dos Folhelhos da Formacao Irati, o maximo de abundancia m/z se apresentou em torno de m/z 500, resultado semelhante aqueles encontrados na literatura para amostras de oleos Venezuelanos (Acevedo et al, 2005) .

Acknowledgements: Ao Laboratorio Nacional de Luz Sincotron (LNLS) A Universidade Federal do Rio Grande do Sul Ao CTPetro

Oxalato de Cálcio monohidratado encontrado em pedras de rins

Corrêa, H. P. S.[1], Orlando, M. T. D.[2], and Martinez, L. G.[3]

[1] Universidade Federal do Mato Grosso do Sul - Campo Grande MS Brazil
[2] Universidade Federal do Espírito Santo - Vitória ES Brazil
[3] Instituto de Pesquisas Energéticas e Nucleares - São Paulo SP Brazil

Neste trabalho, apresentamos os resultados de caracterização por difração de luz síncrotron de uma única amostra escolhida entre 100 amostras, obtidas entre os habitantes da cidade de Vitória no Estado do Espírito Santo, que apresentou o oxalato de cálcio monohidratado monoclínico em uma única fase. As análises dos padrões de difração de raios X convencional das 100 amostras revelaram que existem traços de hidroxiapatita em 60% delas, sendo esses traços associados a uma patologia específica de crescimento de pedra de rins, pedras não papilares formadas em cavidades fechadas. A amostra aqui estudada não apresenta traços de hidroxiapatita e foi medida na linha D10B XPD à temperatura ambiente na energia de 8,900 keV, em alta resolução com o uso de cristal analisador e posterior análise por Rietveld. Foi estudada também a evolução do perfil de difração desta amostra em diferentes temperaturas (250°C, 300°C, 400°C, 450°C e 500°C) e foi realizada comparação com os resultados obtidos por TGA, realizados na mesma amostra (trabalho em convênio com a Universidade de La Plata). A partir dessas medidas, avaliamos a energia de ligação da molécula de água com a rede cristalina, comparando esse resultado com os resultados obtidos por TGA. A avaliação desta energia permite sugerir valores energéticos adequados para serem adotados nos procedimentos de Litotripsia Extra Corpórea.

Acknowledgements: Agradecemos ao LNLS pela disponibilização de suas instalações, bem como pelo apoio técnico.

Rock art paintings at Maqui shelter, Valle Encantado, Patagonia, Argentina: characterization through SRXRD

Vázquez, C[1], Maury, A. M.[2], Adan Hajduk[3], Alnornoz, Ana[4], and Boeykens, S.[5]

[1] Comisión Nacional de Energia Atómica - Buenos Aires B.A. Argentina
[2] Universidad de Buenos Aires - Buenos Aires CapFe Argentina
[3] Consejo Nacional de Investigaciones Científicas y Técnicas - Bariloche Rio N Argentina
[4] Consejo Nacional de Investigaciones Científicas y Técnicas - Buenos Aires Argentina
[5] Universidad de Buenos Aires - Buenos Aires Argentina

One of the main characteristics of the manifestations of rock art are in their high archaeological visibility what implies the immediacy of the finding with no need to practice excavations as it happens with most of the archaeological vestiges. Studies made by investigators of our country could settle down as hypothesis that as much by stylistic variants of the rock art in the zone of study and by references of first written chronicles of centuries XVII and XVIII would be the possibility of the existence of two ethnic groups of inhabitants in that region The knowledge of the chemical composition of the inorganic fraction present in rock painting samples is indispensable in order to identify the type and modality of preparation of pigments, to carry out correlations with rest of pigments found in coherent archaeological layers and to identify potential provenance sources. This work shows the results obtained from the analysis of inorganic compounds presents in rock painting samples coming from the rock shelter El Maqui, locatedat the right side of Limay river in Río Negro province , Argentina. The techniques used for this study were total reflection X ray fluorescence and X ray diffraction. The evaluation of the collected data will allow to detect possible cultural variants and temporary behavior.

Acknowledgements: This work was partially supported by UBACYT I809 and IAEA 13824 and LNLS XRD 7029

Hexavalent chromium detoxification by living aquatic macrophytes root-based biosorption using high resolution x-ray fluorescence

Espinoza Quiñones, F.R.[1], Stutz, G.[2], Tirao G.[2], Palacio, S.M.[1], M.A. Rizzutto[3], Módenes, A. N.[1], Silva Jr, F. G.[1], and Szymanski, N.[1]

[1] Universidade Estadual do Oeste do Paraná - Toledo PR Brazil
[2] Universidad Nacional de Cordoba - Cordoba Argentina
[3] Universidade de São Paulo - São Paulo - São Paulo SP Brazil

Three species of floating aquatic macrophytes Salvinia auriculata, Pistia stratiotes and Eicchornia crassipes have been chosen to investigate the hexavalent chromium reduced by root-based biosorption at chromium uptake experiment using a high resolution X-ray fluorescence technique. These plants were grown in hydroponics medium supplied with non-toxic chromium ion concentrations during 27-days metal uptake experiment in greenhouse. From a speciation chemical technique, it was not observed in nutrient media to occur the reduction from Cr^{6+} to Cr^{3+} due to the changes in the solution pH. The high-resolution Cr-Kβ fluorescence spectra for dried roots were measured using an inelastic X-ray scattering spectrometer. X-ray Kβ fluorescence spectrum of metallic chromium was used as reference one. From the comparison between Cr_2O_3 and CrO_3 compounds and Cr^{6+} treated-plant spectra, the energy of Cr-K$\beta_{2,5}$ line resemble not to those for Cr^{6}+ spectra. For all studied plants, the feature of Cr-K$\beta_{2,5}$ line at Cr^{6+} treated-plant spectra are almost identical in both energy and width to the Cr^{3+} treated-plant one, indicating that there is the occurrence of a Cr^{6+} reduction process during the metal biosorption by plants.

Acknowledgements: We would like to thank CNPq (Brazilian research supporting council, project 476724/2007-4) and SeCyT (Universidad Nacional de Córdoba, Argentina) for financial support. This work was partially supported by LNLS (proposal D12A-XRD1 6510).

Analysis of Trace Elements in Normal, Benign and Malignant Breast Tissues measured by Total Reflection X-Ray Fluorescence

Silva, M.P.[1], Zucchi, O. L. A. D[1], Costa, J. J. G.[1], and Poletti, M. E.[1]

Universidade de São Paulo - Ribeirão Preto - Ribeirão Preto SP Brazil

In this work the Total Reflection X-ray Fluorescence (TRXRF) technique has been employed to determine trace element concentrations in different human breast tissues (normal, normal adjacent, benign and malignant). A multivariate discriminant analysis of observed levels was performed in order to build a predictive model and perform tissue-type classifications. A total of 83 breast tissues samples were studied. Results showed the presence of Ca, Ti, Fe, Cu and Zn trace elements in all samples analysed. All trace elements, except for Ti, were found in higher concentrations in neoplastic tissues, both malignant and benign, when compared to normal tissues and normal adjacent tissues. In addition, the concentration of Fe was higher in malignant tissues than in benign neoplastic tissues. An opposite behaviour was observed for Ca, Cu and Zn. Results have shown that discriminant analysis was able to successfully identify differences between trace element distributions from normal and malignant tissues with an overall accuracy of 73% and 53% respectively for independent and paired breast samples, and of 80% for benign and malignant tissues. This study shows that the combination of trace element distributions patterns of breast tissues with an appropriated statistical technique can be used as a useful tool for distinguishing normal tissues from various types of cancer, including differentiating benign and malignant tumours. It is clear that further studies with a larger number of tissue samples must be performed in order to consolidate the present conclusions.

Acknowledgements: We would like to acknowledge the support by the Brazilian agencies Fundação de Amparo à Pesquisa do Estado de São Paulo (FAPESP) and Coordenação de Aperfeiçoamento de Pessoal de Nível Superior (CAPES).

X-ray diffraction induced by synchrotron radiation in archaeology: compositional study of prehistoric pigments (Carriqueo rock shelter, Argentina)

Palacios, O.M.[1], Maury, A. M.[2], Boeykens, S.[3], and Vázquez, C[4]

[1] Universidad de Buenos Aires - Buenos Aires DF Argentina
[2] Universidad de Buenos Aires - Buenos Aires CapFe Argentina
[3] Universidad de Buenos Aires - Buenos Aires Argentina
[4] Comisión Nacional de Energia Atómica - Buenos Aires B.A. Argentina

The application of Synchrotron Radiation in archaeological and cultural heritage work is a growing field. Applications now cover a variety of material and techniques in several SR facilities and publications rapidly increase. The main advantages of SR excitation are the high brightness, small beam footprint and wavelength tunability. In this project the use of Synchrotron X Ray Powder Diffraction (SRXRD) is proposed for characterize the mineralogical composition of the pigments, essential to identify the original material employed for past societies as well as the rock composition present in the site. This technique is specially adapted for this purpose considering the enormous advantages of the synchrotron beam over the conventional x ray tube excitation. In this work, the D12A-XRD1 beam line at the LNLS facility was successfully used. In this line, the Huber diffractometer permits the rotation of the sample in three axes conducting the polarization of the incident beam in relation to the sample. The task of our investigation was to determine and to compare the composition of prehistoric pigments from excavating layers. The pigment samples were collected in the Carriqueo rock shelter archaeological site. The Carriqueo rock shelter is located on the west side of La Oficina canyon, a tributary of the Limay river, Pilcaniyeu area, in the Río Negro province. Usually the natural yellow, orange or red pigments, composed of yellow and red ochres are frequently detected in rock paintings. The main components of ochre are iron (hydro)oxide (haematite or goethite), clay and silica. The knowledge of the inorganic chemical fraction is essential to identify the possible sources of provenance and the modality of preparation of the pigments. These can be made not only of the substance that produces the coloration, but also for other chemical additions which facilitate the adhesion and fixation of the paintings.

Acknowledgements: This work was partialy supported by LNLS, I809 UBACYT and 13824 IAEA

Formação de imagens por Contraste de Fase: Imagens Realçadas por Difração

Mardegan, J. R. L.[1], Giles, C.[1], Rocha, H. S.[2], Pereira, G.R.[2], Mazzaro I.[3], and Freitas, M. B.[1]

[1] Universidade Estadual de Campinas - Campinas SP Brazil
[2] Universidade Federal do Rio de Janeiro - Rio de Janeiro RJ Brazil
[3] Universidade Federal do Paraná - Curitiba PR Brazil

Dentre os métodos de obtenção de imagens que exploram o contraste de fase, a técnica de Imagens Realçadas por Difração (*Diffraction Enhanced Imaging*), que utiliza um arranjo cristalino em condição de difração dinâmica, tem sido a principal metodologia em estudos na visualização de patogenias em tecidos de mama. Neste trabalho, apresentaremos resultados de imagens obtidas na linha XRD2 tanto em pequenos corpos de prova quanto em tecidos de mama *in vitro* mostrando que por este método as imagens possuem resolução de contraste muito superior às imagens obtidas pelos métodos convencionais de radiografia. Nas imagens obtidas dos corpos de prova a técnica consegue distinguir claramente regiões de bordas onde há uma maior variação do índice de refração e conseqüentemente mudança de fase, mesmo para sistemas onde a absorção é praticamente a mesma. Fica claro também as mudanças de contraste nas imagens ao obtê-las em diferentes posições da *rocking curve* do cristal analisador. É possível obter nestas imagens uma certa noção de relevo do objeto, que fornece notável contraste. Já para as imagens de mama onde tem-se a presença de anomalias (carcinomas), a região patogênica mostrou-se bem distinguível da região sadia da amostra. Isto faz com que haja uma melhor delimitação da interface entre tecidos tornando assim o diagnóstico mais preciso. A técnica também é capaz de distinguir e avaliar regiões da mama como os Ligamentos de Cooper, que permitem um diagnóstico da malignidade da doença dependendo do seu estado físico, já que ligamentos destruídos indicam tumores malignos e ligamentos somente destorcidos indicam tumores benignos. Além de obter as imagens por realce de difração, nosso grupo de pesquisa aprofundou-se na metodologia proposta por Chapman *et. al.* (1997) de produzir imagens de absorção aparente e refração, não só a meia altura da *rocking*, mas também em regiões como um quarto, um terço, entre outras. Com a correção, nas equações propostas por Chapman, para produzir as imagens de refração e absorção aparente em regiões distantes do topo e com métodos de processamento de imagens pudemos reproduzir imagens com alta resolução, mostrando que a técnica tem um futuro promissor na área diagnóstica.

Acknowledgements: À FAPESP e ao CNPq pelo apoio financeiro e ao Laboratório Nacional de Luz Síncrotron pelo apoio técnico.

Parte VI

Matéria Mole e Fluídos Complexos

Room Temperature Humidity XRD Investigations for Li-FH and Ni-FH in Synthetic Clay.

da Silva, G. J.[1], Ribeiro, L.[2], Mundim, M.S. P.[3], Sousa, M. H.[1], and Fossum J. O.[4]

[1] Universidade de Brasília - Brasília DF Brazil
[2] Universidade Estadual de Goiás - Anápolis GO Brazil
[3] Universidade de Brasília - Brasilia DF Brazil
[4] Norwegian University of Science and Technology - Trondheim Norway

The XRD room temperature measurements (LNLS Research Proposal D12A-XRD1 7118/08) were done as a function of the relative humidity for the Li and Ni as intercalated ions in a synthetic clay sample of Fluorohectorite (FH). Fluorohectorite has the chemical formula per half unit cell M_x-$(Mg_{3-x}Li_x)Si_4O_{10}F_2$ were M refers to Ni or Li as the intercalated ion. Hectorite is a 2:1 phyllosilicate, meaning that the platelets are formed by two inverted silicate tetrahedral sheets, sharing their apical oxygens with one octahedral sheet sandwiched in between. It is classified as a trioctahedral smectite since Li^{+1} substitutes for Mg^{+2} in the octahedral sheet sites, which are fully occupied. Fluorohectorites differs from natural hectorites in that the OH groups have been replaced by F. The proportion x of the Li^{+1} ions determines the surface charge of the platelets, which are held together in the stacked structure by an interlayer cation. Among the smectites polydisperse Fluorohectorite has one of the largest values for particle diameter, up to more than 1 mm. Water can be intercalated in between each platelet causing the clay to swell. The parameters utilized to control the swelling behavior are the temperature and the relative humidity. In this work, a fine scan of the relative humidity under room temperature was done for both Ni-FH and Li-FH samples and the result shows that the intercalation process is completely dependent of the type of the intercalated ion yielding consequently different stable and Hendrix-Teller [1, 2] hydration states.

[1] da Silva, G. J., Fossum, J. O., Di Mais, E., Maloy, K. J., Lutnaes, S. B., *Phys. Rev. E* **66**, 011303 (2002).

[2] Y. Meheust, B. Sandnes, G. Lovol, K. J. Maloy, J. O. Fossum, D. M. Fonseca, G. J. da Silva, M. S. P. Mundim and R. Droppa Jr., *Clay Science* **12**, 66(2006).

Acknowledgements: This work was supported by LNLS under research proposal D12A-XRD1 no. 7118/08.

Estudo de estrutura supramolecular do poliestirenossulfonato de sódio

Batista, T[1], MACHADO, D. S.[2], Neumann, M. G.[2], Polikarpov, I.[2], Mario de Oliveira Neto[2], A.F. Craievich[3], and Schmitt, C.C. ou Cavalheiro, C.C.S[2]

[1] Instituto de Quimica de Sao Carlos - São Carlos SP Brazil
[2] Universidade de São Paulo - São Carlos - São Carlos SP Brazil
[3] Universidade de São Paulo - São Paulo - São Paulo SP Brazil

Polietrólitos são sistemas poliméricos consistindo de macro-íons, positivos ou negativos, acompanhados de contra-íons assegurando a eletroneutralidade do sistema. Destacam-se ainda devido a sua estrutura supramolecular, que proporciona uma forte dependência de suas propriedades em solução com meio (pH, solvente, temperatura, força iônica) [1-2]. No presente trabalho Poliestirenossulfonato de sódio (NaPSS) e seus compósitos com Laponita RD foram obtidos por via fotoquímica utilizando-se o corante *Safranina O* como iniciador, em uma dispersão do monômero estirenossulfonato de sódio em suspensão de argila. Os compósitos e polímero obtidos foram analisados em solução por SAXS (Small angle x-ray scattering) utilizando-se a linha de luz D02A- SAXS 2. Foi utilizado um detector bidimensional (MarCCD), comprimento de onda λ = 0,1488 nm e duas distâncias amostra-detector (1796,4 e 383, 86 mm) de forma a cobrir o intervalo de transferência de momento entre 0.10 - 2,5 nm^{-1} e 0,4 - 8 nm^{-1} ($q = 4\ \pi\ sen\ \theta\ /\ \lambda$) sendo 2 θ o ângulo de espalhamento. Foi observado um pico de correlação correspondente a distância $D=2\ \pi/q_{max}$, apresentando dependência com a concentração (medida entre 1 e 30 g L^{-1}), sendo atribuído a formação de lamelas pelo sistema polieletrólito / água, no regime semi-diluído / concentrado [3]. Os resultados obtidos para os compósitos indicam que a presença da argila no material desloca o pico apresentado pelo polímero, indicando que a argila interfere na distância de correlação do polímero.

[1] Dautzemberg, H., et al. Poly-electrolytes: Formation, Characterization and Application, Carl Hanser Verlag, Munich Vienna New York, 1994. [2] Carvajal-Tinoco, M. D., Willians, C. E. Static properties of hydrophobic polyectrolytes in the thermodynamic limit, Europysics letters, v. 52, p. 284 290, 2000. [3] Nishida, K., Kaji, K., Kanaya, K., High cocentration crossovers of polyectrolytes solution, Journal of chemical physics, v. 114, p. 8671 8677, 2001

Acknowledgements: Os autores agradecem à Fapesp, CNPq, Capes e LNLS.

STUDY OF BPP7A PEPTIDE AND ITS β-CYCLODEXTRIN INCLUSION COMPLEXES: COMPLETE SEQUENCE SPECIFIC NMR ASSIGNMENTS

Lula, I.[1], Sinisterra R. D.[2], Santos, R.A.S.[3], and Camargo, A.C.M.[4]

[1] UNIVERSIDADE FEDERAL DE MINAS GERAIS - Belo Horizonte MG Brazil
[2] Universidade Federal de Minas Gerais - Belo Horizonte MG Brazil
[3] UNIVERSIDADE FEDERAL DE MINAS GERAIS - MG Brazil
[4] Instituto Butantan - São Paulo SP Brazil

The heptapeptide BPP7a with the amino acid sequence p-GluAspGlyProIleProPro forms a complex with β-cyclodextrin with the association of the proline residues with the hydrogens external to the β-cyclodextrin cavity. NMR experiment at 400 MHz and 600 MHz with BPP7a and its β-cyclodextrin complex allowed assigning all hydrogen resonance signals of the peptide chains amino acid residues. Nuclear Overhauser effects (NOE) results showed that BPP7a presents a random structure with a totally extended conformation in aqueous solution. NMR measurements also confirmed the formation of the association complex BPP7a/β-cyclodextrin with the interaction between proline residues and hydrogens H2 and H4 external to β-cyclodextrin cavity. The distance restrictions obtained in this experiment showed that the formation of the association compound did not change the random conformational tendency of the peptide chain of BPP7a, which continued to exhibit a flexible structure in aqueous solution with a totally extended conformation. HR-DOSY experiments were used to establish the self-aggregation state of BPP7a molecule and it also showed that the β-cyclodextrin breaks the molecular clusters leading to the complex formation

Acknowledgements: This work was supportesd by CNPq, FAPEMIG. NMR facilities at 600 MHz were supported by LNLS - Brazilian Synchrotron Light Laboratory/MCT.

Structural characterization of systems formed by an anionic copolymer and a cationic surfactant

Percebom, A. M.[1] and W. Loh[1]

Universidade Estadual de Campinas - Campinas SP Brazil

Systems formed by oppositely charged polymers and surfactants are very interesting due to the strong tendency to precipitate and form a complex salt. In solution, the complex molecules are capable of forming micelles with several geometrical forms, and these micelles can be periodically organized, leading to the development of liquid crystalline mesophases. In this project, a complex salt, CTAP(SS-AM), formed by the anionic copolymer poly(4-styrenesulfonic acid-co-maleic acid), P(SS-AM), and the cationic surfactant hexadecyltrimethylammonium bromide, CTAB, was investigated in systems with water and the alcohols 1-butanol and 1-decanol. SAXS measurements provided structural and dimensional information about the formed micelles and the liquid crystalline mesophases in this system.

The complex salt was prepared using the method developed by Piculell[1]. As the copolymer has three different acidic groups, the titration was stopped at the second equivalence point (pH=3). So, there are CTA^+ molecules bound only to two acidic sites. In the following stages, we will be able to compare these results with those from the complex salts with CTA^+ bound to all acidic groups.

In binary systems (CTAP(SS-AM) + Water) with complex salt concentrations below 30 % (wt.), occurs segregation of two micellar phases. In concentrations between 30 and 60%, the system displays only one micellar phase (the more viscous one), which is formed by elongated micelles. And in concentrations above 60% there is a formation of a hexagonal mesophase.

Ternary systems were prepared by the addition of an alcohol: 1-butanol or 1-decanol. The complex salt is very soluble in 1-butanol because it displays a very large region of reversed micellar phase. But in 1-decanol, this region is very small. On the other hand, this alcohol acts as a co-surfactant, leading to the formation of a lamellar phase.

The SAXS method was essentially important to identify the structures formed and to provide information about their dimensions, such as the radius of the aggregate cylinder in hexagonal phases, the lamellae thickness and the area per surfactant headgroup.

[1] L. Picullel; A. Svensson; J. Norman; J.S. Bernardes; L. Karlsson; W. Loh *Pure Appl. Chem.* 2002, *79*, 1419.

Acknowledgements: The authors gratefully acknowledge FAPESP and CNPq for financial support and the LNLS for the use of the SAXS beamline and the support of the line staff.

Caracterização de frações de Asfaltenos de petróleos Brasileiros

Seidl, P.R.[1]

Universidade Federal do Rio de Janeiro - Rio de Janeiro RJ Brazil

A combinação de modelagem molecular com dados analíticos leva a geração de estruturas tridimensionais que refletem as moléculas que tenderiam a se associar entre si, e não as médias comumente empregadas. Utilizando um dímero formado por estruturas que tendem a se associar como modelo para um agregado, pode-se investigar a influência de diferentes fatores, como o tipo e posição de substituintes ou heteroátomos sobre a associação e simular suas propriedades sob diferentes condições. Tomando o aumento da distância entre os planos dos anéis aromáticos como um indicador da tendência à desagregação, pode-se verificar o comportamento do agregado sob diferentes condições. A técnica de espalhamento a baixo ângulo será utilizada,em conjunção com outras técnicas, para caracterizar os agregados formados por diferentes tipos de asfaltenos. Servirá para verificar se o dímero que é utilizado como modelo para o agregado é adequado para refletir a ação de solventes e de temperatura.

Acknowledgements:

The Structure of Monoolein:Oleic acid containing Photosensitizers

Rossetti, F. C.[1], Moreira, B.J.[1], Fantini, M. C. A.[2], and Bentley, M.V.L.B.[1]

[1] Universidade de São Paulo - Ribeirão Preto - Ribeirão Preto SP Brazil
[2] Universidade de São Paulo - São Paulo - São Paulo SP Brazil

This work aimed to investigate the internal structure of nanoparticles with cubic and hexagonal symmetry (CPN and HPN, respectively) formed by momolein and oleic acid, MO:OA, both containing N-methylpyrrolidinone (NMP), before and after the addition of amphiphilic photosensitizers (PSs): ZnPc, ClAlPc and PpIX. The influence of addition of the thickening polymer Hydroxyethyl Cellulose (HEC) was also investigated. Nanoparticles of MO:OA 100:0; 80:20 w/w in excess of water (90 percent, w/w), containing 6.7 percent (MO:OA 100:0 w/w) and 5.3 percent (MO:OA 80:20 w/w) of NMP were analyzed. HEC was added at 1.0 percent in both CPN and HPN. All studied CPN, MO:OA (100:0), present cubic structure. Comparing the lattice parameters (a) for unloaded and ZnPc and PpIX loaded CPN without thickening, they are the same before and after the PSs addition. Differently, ClAlPc loaded CPN presented two values for a. The addition of HEC in the CPN revealed the presence of two values for a. The addition of ZnPc and ClAlPc in the thickened CPN also revealed the presence of two values for a. On the other hand, PpIX does not alter a in the thickened CPN. All studied the HPN, MO:OA (80:20), present hexagonal structure (HII). Comparing the lattice parameter a for unloaded and PSs loaded HPN without thickening, they are similar for unloaded and PpIX loaded, but presented two values for ZnPc loaded and a higher value for ClAlPc loaded. The addition of HEC in the HPN increased a. The addition of ZnPc and PpIX in the thickened HPN presented similar a. Differently, ClAlPc altered a value. The results revealed that the amphiphilic PpIX is not localized inside the lipid bilayers, while the hydrophobic ZnPc and ClAlPc are localized between the lipid bilayers in the hexagonal phase. The presence of HEC permitted ZnPc and ClAlPc entrapment in the lipid domains of the cubic phase. The internal structure of the phases is differently influenced by the presence of the PSs and thickening agent. ZnPc is not entrapped in the lipid domain of the CPN, but the presence of HEC promotes its entrapment. The opposite occurs for HPN. ClAlPc is entrapped in the lipid domain of the CPN and HPN, and the presence of HEC does not alter its localization in both phases. PpIX is not entrapped in the lipid domain of the CPN and HPN, but promotes structural disorder in all the analyzed phases, except thickened CPN.

Acknowledgements: Thanks are due to CNPq and FAPESP for supporting this research.

Efeito de grupos retiradores de elétrons na síntese de nanofibras por gelificação a partir de moléculas orgânicas derivadas da glicose.

Vitorazi, L.[1], Abreu, M. F.[1], Giacomini, R. A.[1], Cardoso, S.L.[1], Gatts, C.[1], dos Santos, D. R.[1], and Miranda, P. C. M. L.[1]

Universidade Estadual Norte Fluminense - Campos dos Goytacazes RJ Brazil

Neste trabalho foram sintetizados quatro novos agentes gelificantes de baixo peso molecular derivados do 4,6-O-benzilideno-α-d-glicopiranosídeo de metila pela adição de diferentes grupos alcoxicarbonil na posição *para* do anel aromático. As moléculas sintetizadas, contendo no grupo alcoxicarbonil cadeias alifáticas lineares com 3, 4, 8 e 16 átomos de carbono, foram avaliadas quanto à habilidade de formação de gel em determinados solventes por meio de uma triagem qualitativa, e desta forma foram escolhidos os géis que seriam estudados mais especificamente. No intervalo de concentrações estudado a molécula com 16 átomos de carbono na cadeia lateral foi a que apresentou o melhor desempenho quanto à diversidade de solventes enrijecidos, sendo estes, tanto solventes apolares como polares próticos e apróticos. Alguns géis foram estudados por meio da técnica de microscopia eletrônica de varredura com intuito de caracterizar a morfologia das fibras, sendo que foi possível verificar diferentes formas nas fibras, sendo estas, cilindros ou cilindros compactados. Com a técnica de espalhamento de raios X a baixos ângulos foi possível determinar o diâmetro das nanofibras formadas nos géis. A partir da técnica de espectroscopia no infravermelho foi possível evidenciar que a ligação hidrogênio intermolecular atua como força de agregação entre os monômeros durante a gelificação dos compostos no solvente tetracloroetileno.

Acknowledgements: Os autores agradecem o suporte financeiro da FAPERJ e do LNLS.

Parte VII

Materiais Estruturais e Aplicações na Indústria

MICROSTRUCTURE OF NANOTEFLON/POLYURETHANE FILMS

Anbinder, P. S.[1], Peruzzo, P. J.[1], and Amalvy, J. I.[1]

Universidad Nacional de La Plata - La PLata B.A. Argentina

The incorporation of Teflon nanoparticles to a polymeric matrix can provide films with improved barrier and surface properties. In this work was studied the effect of the addition of different concentrations of a PTFE nanoparticles dispersion (45 nm) to a polyurethane (IPDI-PPG1000) matrix. Besides the changes in the superficial properties of the films, other properties were studied by means of XPS, SAXS, ATR/FTIR, TEM and mechanical properties. SAXS measurements on films samples were performed at the SAXS2 beam line at the LNLS (Campinas, Brazil) using a monochromatic beam of wavelength 1.608 and exposure time of 300 sec, and a sampledetector distance of 728.32 *mm*. Pure PU shows in the SAXS curve a typical shoulder at about 0.1 $^{-1}$ due to the hard segments/soft segments segregation and the interdomain spacing. All samples containing nano-PTFE show SAXS curves with weak oscillations at q around 0.015 and 0.028 $^{-1}$. Scattering intensity increases as nano-PTFE content of sample increases. This behavior is related partly to particle interaction but also to the morphology of the samples. Porod's plots have an asymptotic linear regime for all the samples indicating the presence of abrupt and well-defined interfaces. This observation is consistent with TEM results, as well as nano-PTFE particles size (42 nm). The contact angle values confirm the surface hydrophobicity of the nano-PTFE/PU films with the major value for 20 % wt of nano-PTFE. XPS shows that even though the nanoparticles are present in the bulk, major concentration appears at the surface. This effect could be associated to the migration of the nano-particles towards the surface (at low concentrations) and the aggregates formation (at high concentrations) that limit the above-mentioned migration towards the surface, which also affect negatively the mechanical properties. For instance the tensile strength and elongation were highly diminished up to 70% and 62% for 40 wt. % of nanoparticles incorporation.

Acknowledgements: The authors would like to acknowledge Brazilian Synchrotron Light Laboratory (LNLS), Campinas, Brazil; CICPBA and ANPCYT are thanked by financial assistance and Solvay Solexis (Italy) for donating the Nanoteflon. PSA is member of ANPCyT, PJP is member of CONICET, JIA is member of CIC.O.R. Pardini is thanked for technical assistance.

Expansão térmica do $Y_2Mo_3O_{12}$ em baixas temperaturas

Ari M.[1], Marinkovic, B. A.[1], Jardim, P. M.[1], and Rizzo, F.[1]

PUC - Rio de Janeiro - Rio de Janeiro RJ Brazil

Materiais de expansão térmica baixa, zero e negativa são requeridos para diversas aplicações tecnológicas. Óxidos cerâmicos representados pela fórmula $A_2M_3O_{12}$, onde A = metal de transição trivalente e M = Mo^{+6} ou W^{+6}, apresentam expansão térmica baixa ou negativa após a transição de fase da estrutura monoclínica à ortorrômbica. A estrutura consiste de octaedros AO_6 e MO_4 interconectados pelos vértices através do átomo de oxigênio. No caso, o movimento térmico transversal do oxigênio na ligação A-O-M seria responsável pelo fenômeno de expansão térmica negativa. Foi reportado na literatura que o $Y_2Mo_3O_{12}$ a temperatura ambiente apresenta estrutura ortorrômbica e expansão térmica negativa (ETN) na faixa de temperatura de 273 a 1073K. Mas, este composto é higroscópico devido ao tamanho do cátion Y^{3+} que forma octaedros grandes criando espaços vazios maiores, capazes de alojar moléculas de água. Assim a ETN é observada somente após a remoção destas. Para complementar a informação sobre o $Y_2Mo_3O_{12}$, realizaram-se análises de difração de raios-X utilizando luz síncrotron (LNLS) na faixa de temperatura de 20 a 450K, utilizando criostato. Calculou-se o coeficiente de expansão térmica intrínseco, resultando o valor de α_l = -9,08 x 10^{-6}/K e observou-se que este composto não apresenta transição de fase.

Acknowledgements: Ao Laboratório Nacional de Luz Síncrotron (LNLS) pelo projeto D10B-XPD 7756. Ao Departamento de Ciência de Materiais e Metalurgia, DCMM, da PUC-Rio. M. S. Ari agradece à FAPERJ pela bolsa de pós-doutorado concedida.

Template removal process in mesoporous $Zr - Ce$ oxides

Bacani, R.[1], Martins, T. S.[1], Matos, J. R.[2], Lamas, D. G.[3], and Fantini, M. C. A.[1]

[1] Universidade de São Paulo - São Paulo - São Paulo SP Brazil
[2] Universidade de São Paulo - São Paulo - Sao Paulo SP Brazil
[3] Consejo Nacional de Investigaciones Científicas y Técnicas - Buenos Aires Argentina

There are few works dealt with $ZrO_2 - CeO_2$ ordered mesoporous structures for catalytic applications. These systems, as anodes in solid oxide fuel cells may lead to better performance, due to an enhancement on surface area, aiming to achieve a lower operation temperature limit. In this work, the synthesis of the Zr-Ce oxides was performed with anhydrous $CeCl_2$ and $ZrCl_3$ precursors, using the triblock copolymer Pluronic P-123. The Ce/Zr atomic content was 0.5 and 0.9. Ex-situ experiments (heating rate of 2^oC/min) showed that the total polymer removal by calcination happens at 540^oC on 4 hours in N_2 atmosphere and 2 hours in air, but the ordered mesostructure is destroyed during this process. The samples were also calcined under vacuum, but some carbonaceous material remained inside the structure and the destruction of the ordered mesoporous network was also observed.

In-situ SAXS experiments were carried out (D11A/SAXS1-7124) in order to analyze the process of template removal. A Si-(111) crystal was used as monochromator, with $\lambda = 1.608$. The sample to detector distance was 800mm and the detector was a bi-dimensional CCD. The oven was programmed for a heating rate of 2^oC/min, with an isotherm at 540^oC. The sample was set under vacuum (around 10^{-2}Torr). The tested template removal procedures showed that these systems have a very low mechanical stability, related to the preservation of the ordered mesoporous structure. Nowadays that is the most difficult task in this research area. The synchrotron experiment revealed that the ordered mesopores are destroyed at temperatures below 300^oC, that is not enough to remove the polymer.

The diffraction measurements (D10B/XPD-2960) were used to analyze the mesopore walls. High-intensity configuration, without crystal analyzer, was chosen, with $\lambda = 1.5498$, 2θ from 18^o to 102^o with a 0.05^o step, and counting times between 2.5-3.0s/step. The single cubic phase (90% CeO_2) is structurally more stable than the tetragonal phase (50% CeO_2), which is not a single crystalline phase material. After calcination, gas adsorption measurements showed that the 90% CeO_2 templated sample presents a higher surface area than that of a similar one prepared by a gel-combustion process.

Acknowledgements: Supported by CNPq.

Characterization of TiO2 nanoparticles synthesised in ionic liquids

Teixeira, S.R.[1], Dupont, J.[1], Migowski, P[1], Weibel, D. E. or Weibel, D.[1], Machado, G[1], and Feil, A. F.[1]

Universidade Federal do Rio Grande do Sul - Porto Alegre RS Brazil

Titanium powders are widely used in industrial applications as pigments, opacifiers, photocatalists and fillers. Because of their properties as UV light absorbers they are used also in the cosmetic industries as solar protectors. In the past decade considerable research and industry attention has been paid to both dye-sensitized solar cells (DSCs) with a nanostructured TiO_2 film and energy production by water splitting, using TiO_2 powders or nanotubes as photocatalists to generate H_2. At present, they have become a potential low-cost, efficient alternative to conventional inorganic photovoltaic devices; and have been obtained either directly from titanium-bearing minerals or by precipitation from solutions of titanium salts. Here in we describe the synthesis and characterization of TiO_2 nanopowders by two different routes, using Ionic Liquids as templates for TiO_2 precipitation. Structural characterization was accede by XRD, SAXS and EXAFS. Results in water splitting using these TiO_2 as photocatalists are also presented.

Acknowledgements: We acknowledge the LNLS staff for the technical support, CNPq, FINEP and FAPERGS Brazilian financial support agencies

Effect of the curing agent on the nanostructure of polybutadiene-modified epoxy resin

Soares, B.G.[1], DAHMOUCHE, K[2], and Lima, V.D.[1]

[1] Universidade Federal do Rio de Janeiro - Rio de Janeiro RJ Brazil
[2] Centro Universitário da Zona Oeste - Rio de Janeiro RJ Brazil

Epoxy modified with polybutadiene presented a transparent characteristic by using functionalized hydroxyl terminated polybutadiene with isocyanate groups. The goal of the present study is to confirm the nano-scale rubber domain size in this sytem by using small X-ray scattering (SAXS) combined with atomic force microscopy and to investigate the influence of different curing systems, based on aliphatic amine (which cures at room temperature) and anhydride (which requires higher temperatures for curing). Before and after the curing process, all mixtures of epoxy precursors (epoxy, curing system and the functionalized PBD) were transparent, indicating that no phase separation has occurred. In spite of the homogeneous system, the values of the glass transition temperature (obtained from DMA) were similar to that found in neat epoxy network. All these results suggest that both rubber-modified epoxy thermosets presented phase separated structure in nao-scale. The SAXS profiles for the thermosets containing different amount of functionalized PBD presented no well-defined scattering peaks in both cured systems, indicating no great phase-separated morphology. The TETA cured system containing 10 phr of the functionalized PBD presented a Guinier plateau indicating a diluted system. The average distance between the neighboring domains increased as the amount of the rubber increased, as expected. In TETA cured systems, it is also possible to observe a small scattering peak at around q = 1nm -1, indicating microphase separated structure and the formation of micelle structure. This feature is explained because epoxy system behaves as a selective solvent for the triblock copolymer formed by the reaction between the epoxy resin and the isocyanate functionalized PBD. In the case of anhydride-cured system, there is no scattering peak in this region, indicating no discernible phase separation structure, even at nanometric scale. this behavior is in agreemento with the AFM data.

Acknowledgements: This work has been support by D11A-SAXS1 6529; CNPq and FAPERJ

A XANES and EXAFS study on Ti doped low silica calcium aluminosilicate glasses

Filadelpho, M. C.[1], Andrade, A. A.[1], Rohling, J.H.[2], Medina, A.N.[2], Baesso, M.L.[2], and Sampaio, J. A.[1]

[1] Universidade Estadual Norte Fluminense - Campos dos Goytacazes RJ Brazil
[2] Universidade Estadual de Maringá - Maringá PR Brazil

Low silica calcium aluminosilicate (LSCAS) glass is an interesting material to be used as the host for the doping ions because they combine superior properties of an oxide glass with a relatively low phonon energy, of the order of 800 cm^{-1}, and a high transmitance in the UV-VIS-IR region when melted under vacuum atmosphere, thus high emission rates can be achieved. It was observed recently that Ti^{3+} in OH- free aluminosilicate glass, present a very long lifetime (170 μs) and broad emission band shifted towards the visible region. This lifetime value was attributed to the trapping of the excited electrons by the glass defects and detrapping by thermal energy, and it is 2 orders of magnitude higher than those published for Ti^{3+} doped materials, suggesting that glasses of this system are promissing to overcome the challenge of extending the spectral range of traditional tunable solid state lasers towards the visible region. However, up to date there is no investigation on the chemical environment of transition metal ions in this glass system, which are important to provide information for development of these materials to be used in photonics. Information regarding coordination number, interatomic distances, Debye-Waller factors can be obtained in very diluted amorphous systems only by EXAFS spectrocopy. On the other hand, XANES provides information on the valence state of the doping ions. In this work we present the results regarding the chemical environment of Ti in LSCAS glasses, doped with various concentrations of TiO_2, obtained using both spectroscopies. In addition we have investigated the effect of heat treatment on the valence state of Ti in LSCAS glasses, since we have observed a change on the fluorescence spectra, that is probably due to the conversion of Ti^{3+} into Ti^{2+}.

Acknowledgements: This work has been supported by the Brazilian Synchrotron Light Laboratory (LNLS) under proposal D04B - XAFS1 6594, FAPERJ and CNPq.

Desenvolvimento de um dispositivo para determinação de constantes elásticas cristalográficas por medidas de difração síncrotron

Martinez, L. G.[1], Orlando, M. T. D.[2], Corrêa, H. P. S.[3], J.L.Passamai Jr[2], and Rossi, J. L.[1]

[1] Instituto de Pesquisas Energéticas e Nucleares - São Paulo SP Brazil
[2] Universidade Federal do Espírito Santo - Vitória ES Brazil
[3] Universidade Federal do Mato Grosso do Sul - Campo Grande MS Brazil

Os reatores nucleares PWR utilizam como combustível o dióxido de urânio - UO_2 - na forma de pastilhas sinterizadas acondicionadas em um tubo metálico conhecido como encamisamento ou cladding. O material empregado na confecção do cladding tem extremos requisitos tanto do ponto de vista nuclear como mecânico. Na maioria dos reatores em operação estes tubos são confeccionados em ligas de zircônio, especialmente as conhecidas como zircaloy. Um dos requisitos deste material nesta aplicação é sua elevada resistência à corrosão. No ambiente dos reatores PWR onde são empregados estão submetidos a altas pressões e temperaturas em ambiente aquoso e extremas condições de irradiação. Uma das possíveis falhas desta aplicação é a corrosão induzida por tensão. Assim, a determinação de tensões residuais decorrentes do processo de fabricação destes tubos é um parâmetro importante que deve ser controlado no projeto e fabricação de um elemento combustível nuclear. Uma nova liga de zircônio com adição de Nb, conhecida como Zirlo, vem sendo estudada por apresentar melhores propriedades de resistência à corrosão. Entretanto não há muita informação na literatura científica a respeito de propriedades deste material. Para a determinação de tensões residuais por difração de raios X é necessário conhecer as constantes elásticas de raios X que, dependendo da isotropia do material, podem ser diferentes para as diversas direções cristalográficas do cristal. Para isto foi projetado e construído um dispositivo para aplicação de tensões mecânicas às amostras durante as medidas de deformações elásticas através do método de $\sin^2\psi$. Foram medidas as deformações elásticas versus carga uniaxial aplicada para amostras de zircaloy e zirlo. Para a calibração do método foram medidos também materiais cujas constantes elásticas são bem conhecidas, como o ouro. As medidas foram realizadas na estação D12A - XRD1 do LNLS. Os resultados preliminares mostram que o dispositivo proposto é adequado para este tipo de experimento, porém necessitando ainda de aperfeiçoamento.

Acknowledgements: Os autores agradecem ao LNLS pelas facilidades experimentais e ao Dr. L. V. Ramanathan pela disponibilização dos materiais.

Poly(methyl methacrylate)- Clay nanocomposites prepared by in situ intercalative polymerization the effect of the acrylic acid

Silva, A.A.[1]

Universidade Federal do Rio de Janeiro - Rio de Janeiro RJ Brazil

Poly(methyl methacrylate) montmorillonite (MMT) nanocomposites were prepared by the swelling of organophylic montmorillonite with the monomer and therefore polymerized in situ via soap free. For inserting carboxylics groups in long chain of PMMA were prepared nanocomposite funcionalized with acrylic acid. The acrylic acid introduction confer greater interfacial interaction between inorganic portion (clay) and the organic one (polymer). The stonger adhesion between the clay and polymeric matrix, promoved by inserted carboxylics groups, contributed for the higher intercalation degree in the lamelas of the polymer chains. The thermal decomposition temperature (Td) of the nanocomposites funcionalized increase because of strong interfacial interaction between clay and polymer. The presence of clay increased the molar mass and decreased the polydispersity of polymers due, probably, to the reduction of transfer of chain reactions between the lamellas. The nanostructure of PMMA-clay nanocomposites samples were analyzed by Small angle X-ray scattering (SAXS). The SAXS patterns of PMMA-clay nanocomposites exhibit for all samples a single peak with a maximum located at 0.18 angstrons. This peak is attributed to tactoides that were not broken during polymerization Thus, part of the chains of PMMA able to penetrate into lamella and promote of intercalation. For nanocomposites prepared with largest OMMT content, an additional scattering at low q-range reveals the formation of clay-rich aggregates dispersed in the PMMA matrix. The average distance between clay nanoparticles can be estimated, resulting in value around 35 angstrons. This behavior is related to the better dispersion of lamellas and it is consistent greater interfacial interaction between inorganic portion (clay) and the organic one (polymer), due introduction of AA.

Acknowledgements: CNPQ

Structural and optical properties of Tb^{3+} and Er^{3+} doped BaY_2F_8

de Mello, A.C.S.[1], Baldochi, S. L.[2], and Valerio, M.E.G.[1]

[1] Universidade Federal de Sergipe - São Cristóvão SE Brazil
[2] Instituto de Pesquisas Energéticas e Nucleares - São Paulo SP Brazil

In this work Barium Yttrium Fluoride (BaY_2F_8-BaYF) doped with different concentrations of ions Tb^{3+} and Er^{3+} were characterized, aiming the application in radiation detection devices that use the scintillating properties. Two types of samples were produced in the CLA-IPEN-SP, polycrystalline samples, obtained via solid state reaction of BaF_2 and YF_3 under HF atmosphere, and single crystals, obtained via the floating zone melting method also in a HF atmosphere. The samples were characterized using the following experimental techniques: X-ray powder diffraction (DRX), radioluminescence (RL), optical absorption, dispersive X-ray absorption spectroscopy (DXAS) and extended X-ray absorption fine-structure spectroscopy (EXAFS). The X-ray diffraction pattern showed the presence of the phase BaY2F8 and a small amount of the phase $Ba_4Y_3F_{17}$ in the polycrystalline pure and Tb^{3+} doped samples. The other samples showed only the desired BaY_2F_8 phase. The radioluminescence measurements of the doped BaYF, when irradiated with X-rays, showed emission peaks in energies that are characteristics of the 4f-4f transitions of rare earths. The RL of the samples with 2 mol % and 3 mol % of Tb^{3+} showed quite intense peaks with a maximum emission peak at 545 nm. All samples showed a phosphorescent decay time of the order of seconds. Single crystals of BaYF doped with 2 mol % of Er^{3+}, in addition to one of the highest phosphorescence time, presents a quite strong RL in the green region of the spectra. The radiation damage was evaluated by the optical absorption techniques and the results showed that the formation of the absorption bands can be connected to colors centers generated by radiation in the matrix. Measurements of DXAS, done at the LNLS DXAS beamline, revealed that there is no change in the absorption edge of the dopant during irradiation.

Acknowledgements: This work was supported by CNEN

Crystalline and amorphous mixed basic carbonates as a source of nanometric: $Ce_{1-x}La_xO_{2-y}$ and $Ce_{1-x}Cu_xO_{2-z}$: PXRD and XAS characterization

E. E. Sileo[1] and Jobbagy, M.[2]

[1] Universidad de Buenos Aires - Buenos Aires DF Argentina
[2] Universidad de Buenos Aires - Buenos Aires Argentina

Ceria based oxides play a key role in materials science due to their relevance in diverse fields as solid oxide fuel cells or heterogeneous catalysis. In the latter case, rare earth doped ceria revealed noticeable properties. In particular Cu(II) and La(III) doped ceria are very active in the oxidation process of methane, carbon monoxide and soot. Crystalline and amorphous basic carbonate precursors may render ceria based oxides when exposed to dierent thermal treatments. In particular, metastable phases with tuned stoichiometry and high surface area can be obtained.We have synthesized several series of CeO_2 doped with Cu(II) and La(III) and we have explored the influence of the different thermal treatments in the thermal transformation to the nanocrystalline $Ce_{1-x}La_xO_{2-y}$ and $Ce_{1-x}Cu_xO_{2-z}$ oxides.

Acknowledgements: This work was supported by proposta LNLS (D04B-XAFS1- 6672/07) and Programacion UBACYT 2007

Experimentos XANES in situ em Catalisadores Ni/MCM-41

Brandão, S. T.[1], Oliveira, O.B.[1], Mundim, M.S. P.[2], and da Silva, G. J.[3]

[1] Universidade Federal da Bahia - Salvador BA Brazil
[2] Universidade de Brasília - Brasilia DF Brazil
[3] Universidade de Brasília - Brasília DF Brazil

A viabilidade econômica de processos catalíticos que permitam a obtenção de combustíveis menos poluentes, como a síntese de Fischer-Tropsch (FT), depende de rotas mais eficientes para a obtenção do gás de síntese (CO e H_2) que é utilizado como matéria-prima. A oxidação parcial do Metano (OPM) é uma das rotas alternativas para a obtenção do gás de síntese a partir do gás natural. Apresenta vantagens pelo fato de ser exotérmica, além de produzir gás de síntese numa proporção 2:1, que é a mais adequada no processo de FT. Neste trabalho foi investigado o efeito da adição de Paládio e Cério nas espécies de Níquel e, por conseguinte, nas propriedades catalíticas dos sistemas Ni/MCM-41 na (OPM). Os resultados de TPSR indicaram que a adsorção de Metano é mais favorecida nos sistemas contendo Paládio que se apresentaram como catalisadores mais ativos, propiciando a conversão de Metano em temperaturas mais baixas. Os perfis de TPR-CH_4 revelaram que ocorre redução de diferentes tipos de sítios com a elevação da temperatura. Os perfis TPR-H_2 ratificaram esta observação, e correlacionando-se estes dados com os de XPS, propõe-se a existência de espécies de NiO na superfície bem como NiSiO_3 e NiSiO_4. Isto indica uma forte interação metal-suporte. Análise de XANES in situ realizadas no LNLS permitiram acompanhar a cinética de redução das espécies de Níquel, que na forma de Ni metálico constituem sítios ativos destes catalisadores. Durante a ativação com H_2, dos sistemas contendo somente NiO, verificou-se a formação de Ni metálico a partir de 420 graus, e após duas horas de ativação quase todo o NiO foi reduzido a Ni. A adição de Paládio e Cério retardou a cinética de redução do NiO a Níquel metálico, e nestes casos supõe-se a presença de NiO residual nos catalisadores no final da ativação. Apesar disso, não houve comprometimento da atividade catalíca, no caso do Pd, ou da resistência as desativações por coqueamento, no caso do Ce. A XANES não indicou picos que estariam relacionados espécies NiSiO_3 e NiSiO_2, provavelmente por estarem em pequena concentração em relação ao NiO e Ni. Durante a reação de OPM in situ monitorada pela XANES,observou-se a re-oxidação dos sítios de Ni a NiO.

Acknowledgements: Agradecemos ao LNLS, FINEP - Rede Nacional de H_2, CNPq e Petrobrás pelo suporte fornecido.

Análise de catalisador comercial HTS por difração de raios X *in situ* na reação de deslocamento água-gás

Braga, A. H.[1], Rodella, C. B.[1], Olivira Junior N.G.O.[1], and Zanchet, D.[1]

Laboratório Nacional de Luz Síncrotron - Campinas SP Brazil

A reação de deslocamento água-gás (CO e vapor de água produzindo CO_2 e H_2) é de grande importância industrial na produção de hidrogênio, síntese de amônia e na remoção de CO, um gás potencialmente tóxico. Este trabalho avaliou o processo de ativação de um catalisador industrial HTS (*high temperature shift*), fornecido pela Oxiteno S. A. Ind e Com., composto por Fe_2O_3, CuO e Cr_2O_3, na reação de deslocamento água-gás, utilizando a técnica de difração de raios X (DRX) *in situ*. Estes experimentos foram realizados na linha de luz XRD2, do LNLS, com um forno acoplado a um sistema de alimentação de gás (na taxa de temperatura de $10^oC\ min^{-1}$ de 25^oC a 125^oC, e de $2^oC\ min^{-1}$, de 125^oC a 500^oC; fluxo de CO/He de 20 mL min^{-1} e de H_2O/He de 38 mL min^{-1}). A ativação do catalisador está relacionada principalmente à redução do Fe_2O_3 (hematita) a Fe_3O_4 (magnetita), e à redução de Cu^{2+} a Cu metálico. Porém, não é possível visualizar a presença de fases isoladas de Cr_2O_3 e do CuO na amostra. Assim, os óxidos puros também foram estudados por DRX para melhor compreender as modificações estruturais no ambiente de reação. Os resultados obtidos mostraram que a transição Fe_2O_3 para Fe_3O_4 no catalisador HTS ocorre na faixa de temperatura de 260^oC a 370^oC, formando cristais de magnetita de tamanho médio de 30 nm. Quanto ao Fe_2O_3 puro, a transição hematita-magnetita ocorre em temperaturas ligeiramente maiores (por volta de 320^oC a 410^oC), obtendo-se um tamanho final médio de 90 nm. Já o CuO, se reduz a cobre metálico, no intervalo de 160^oC a 200^oC, oxidando CO a CO_2 e produzindo H_2 nestas temperaturas; acima de 200^oC, ocorre acentuada sinterização (um efeito térmico que causa desativação do catalisador); o Cr_2O_3 não sofreu alterações nas condições testadas, como esperado. Esses resultados são coerentes com os dados da literatura, e sugerem que o óxido de cromo tem um importante papel, evitando a sinterização do óxido de ferro; já o óxido de cobre é ativo na conversão dos reagentes, mas sofre forte sinterização em altas temperaturas.

Acknowledgements: Os autores agradecem F.R. Zambello e S.B. Betim pelo suporte nos experimentos e a toda a equipe do LNLS pela infra-estrutura e apoio, à Oxiteno pelas amostras. A.H.B agradece a bolsa PIBIC-CNPq concedida.

Study of RF Magnetron sputtering TiOx and TiOxNy films

Albertin, K.F.[1] and I. Pereyra[1]

Universidade de São Paulo - São Paulo - São Paulo SP Brazil

Titanium oxide is very interesting material for different research areas. Titanium oxide has high refractive index (¿ 2,0), which is interesting for photovoltaic devices, where these films are utilized as antireflection coatings. The rutile phase of titanium dioxide presents a uniaxial refractive index and is birrefringent, thus interesting for optical applications. An important property is the high dielectric constant value (40), very interesting for MOS devices applications. TiO2 films present two important phases, Anatase and Rutile. The last one being the thermally stable phase and presenting the higher dielectric constant, approximately 80, Anatase is a thermally unstable phase with lower dielectric constant transforming in Rutile phase at temperatures over 600 oC. Titanium dioxide has high dielectric constant values, however it has a low band offset with respect to silicon (1.2 eV) and consequently when utilized as insulating layer in MOS devices a high leakage current density results. The addition of nitrogen producing TiOxNy alloys lead to improved properties for some of the mentioned applications. TSome works report that TiO2 ozone (O3) and N2O annealing treatment minimize the interface chemical reactions besides reducing the leakage current by several orders of magnitude. In this work RF Magnetron sputtering TiOx dielectric layers, utilizing different O2 partial pressures (15,20,25,30,35 and 40 percent), and TiOxNy films, utilizing different N2 partial pressures (5,10,15,20,25 and 30 percent) are produced and their physical, electrical, dielectric and optical properties are studied. The TiOx and TiOxNy obtained films were annealed at 550, 750 and 1000oC in N2 environment for 2 hours and the structural and electrical properties were studied through RBS, FTIR, optical absorption in the near IR-visible-UV range, Ti and O K-edges Xanes measurements and Raman scattering experiments.

Acknowledgements: The authors are grateful to the Brazilian agencies FAPESP and CNPq for financial support. To the Brazilian Synchrotron Light Laboratory (LNLS) for XANES O-K (SGM beam line) and Ti-K (XAS beam line) measurements.

The structural dynamics of FDU-1 ordered mesoporous silica calcination process

Mariano-Neto, F.[1], Silva, L.C.C.[1], Martins, T. S.[1], Matos, J. R.[1], and Fantini, M. C. A.[1]

Universidade de São Paulo - São Paulo - São Paulo SP Brazil

The aim of this work was to analyze the calcination process of cubic ordered mesoporous silica, FDU-1 type, synthesized with the tribock copolymer Vorasurf, at a highly acidic medium (HCl 4 mol.L^{-1}) and TEOS as silica source. The calcination process was performed using a heating rate of $2^oC.\ min^{-1}$ in the SAXS2 beamline, with a wavelength of 0.1608 nm and the oven under vacuum (10^{-3}torr), from room temperature up to 540^oC. The sample was kept at this temperature for 6 hours. Then, the oven was set on off and the temperature decreased naturally to room temperature. The SAXS data were collected every minute and averaged for a period of 15 minutes. The as-synthesized sample presents three diffraction peaks, which were followed in position and area for each temperature. As the calcination process proceeded, up to five peaks were visualized. Variations on lattice parameter, as well as on peak intensities were recorded. The polymer decomposition, wall densification and structure shrinkage were followed. The present results were compared to the calcination process of a bi-dimensional hexagonal ordered mesoporous silica, SBA-15 type, previously studied. The in-situ SAXS analysis of the calcination process under vacuum revealed a smaller shrinkage effect compared to the usual procedure in nitrogen and air.

Acknowledgements: Thanks are due to CNPq and FAPESP for supporting this research.

Parte VIII

Métodos e Instrumentação

Prototipagem rápida de microchips em vidro para separações eletroforéticas

Segato, T. P.[1], Coltro, W. K. T.[1], Mazo L H[1], and Carrilho, E.[1]

Universidade de São Paulo - São Carlos - São Carlos SP Brazil

Dispositivos miniaturizados para eletroforese tornaram-se uma poderosa ferramenta para separações analíticas. Estes microdispositivos têm muitas vantagens sobre a instrumentação convencional para eletroforese capilar (CE), incluindo reduzido consumo de amostra e tampão, menor tempo de análise e separações mais eficientes. Estes microchips têm sido fabricados em uma ampla variedade de materiais, e usando tanto fotolitografia convencional como métodos mais recentes de microfabricação. Nas tecnologias convencionais de microfabricação, a selagem dos canais de vidro é comumente realizada por processos térmicos a temperaturas acima de 600 ^{0}C. Estes processos exigem utilização de salas limpas, além de serem laboriosos, demorados, e muitas vezes irreprodutíveis. Logo, os microchips selados termicamente são inviáveis economicamente para serem usados como dispositivos descartáveis. O presente trabalho teve como objetivo mostrar uma metodologia barata, rápida e eficaz para selagem de microcanais de vidro, obtidos por fotolitografia e corrosão química em via úmida, contra substrato de vidro contendo película de PDMS de aproximadamente 50 μm de espessura. A magnitude do fluxo eletrosmótico (EOF) foi avaliada em uma faixa ampla de pH (2 a 12). Tal como esperado, foi observado um EOF catódico para todos os valores de pH. Para pH 7, o valor de EOF para dez medições consecutivas foi de 3,6 x 10^{-4} cm^2 V^{-1} s^{-1}. A magnitude e a estabilidade do EOF gerados no dispositivo de vidro/PDMS estão de acordo com os relatados na literatura para dispositivos de vidro ou quartzo. A eficiência para a separação de fluoresceína (FL) e isotiocianato de fluoresceína (FITC) obtida com o dispositivo proposto foi de cerca de 40000 pratos/m para ambos, e não foi observada ocorrência de cauda nos picos. A separação de uma mistura de cátions (Li^+, Na^+ e K^+) também foi monitorada nestes microchips (com alta resolução e eficiência) usando detecção oscilométrica. Estas características mostram que o dispositivo de vidro/PDMS tem um perfil eletroforético dominado principalmente pela superfície de vidro, onde a sílica da superfície interna do canal é responsável pela geração de fluxo eletrosmótico estável.

Acknowledgements: CAPES e LNLS.

Current Status of the Wavelenght Dispersive System of the XRF Beamline

Pérez, C. A.[1] and H. J. Sánchez[2]

[1] Laboratório Nacional de Luz Síncrotron - Campinas SP Brazil
[2] Universidad Nacional de Cordoba - Córdoba Cba Argentina

This work presents the status of the wavelenght dispersive system that is being currently commissioned in the XRF beamline of the LNLS.

XRF using energy-dispersive setups is a well-known technique. It has several advantages and the range of applications is increased everyday. In addition, many other techniques are derived from conventional XRF, for instance total-reflection analysis, micro-analysis, etc.

A different approach for detecting characteristic radiation is proposed by the so-called wavelenght dispersive systems. With this setup, fluorescent radiation is filtered by a perfect crystal and, via Bragsslaw, selected energies are detected by a proportional detector. In this configuration, the energy resolution is improved several orders of magnitudes at the cost of a longer measuring time.

A wavelenght dispersive system is currently mounted and in commissioning in the XRF beamline of the LNLS. At present the system has been located in a tentative place of the beamline and the first alignements have been carried out. In this stage a Si (111) crystal is being used and several samples are under study for the characterization of the equipment. After several manipulations we reached an energy resolution of 60 eV, which is a third of a typical solid state detector but one order of magnitude worse than the resolution expected for a system like this one.

More work will be carried out in order to obtain the normal parameters for this kinf of apparatus and in order to mount the system in a fixed place of the beamline. In this way, in a near future this equipment will be available for external users.

Acknowledgements: This work has been partially supported by the LNLS

Characterization of standard reference materials for powder diffraction

Martinez, L. G.[1], Orlando, M. T. D.[2], Corrêa, H. P. S.[3], Rocha, C. J.[1], Paiva-Santos,C.O.[4], and Ferreira, F. F.[5]

[1] Instituto de Pesquisas Energéticas e Nucleares - São Paulo SP Brazil
[2] Universidade Federal do Espírito Santo - Vitória ES Brazil
[3] Universidade Federal do Mato Grosso do Sul - Campo Grande MS Brazil
[4] Universidade Estadual Paulista - Araraquara - Araraquara SP Brazil
[5] Laboratório Nacional de Luz Síncrotron - Campinas SP Brazil

The calibration and alignment of powder diffraction equipments, both neutron and x-rays diffractometers, is generally performed by means of measurement of standard samples. These samples must have very well defined cell parameters and high stability. In experiments using synchrotron radiation or neutrons it is also necessary a precise determination of the energy (or wavelength) of the radiation beam, which can be made using a standard sample. For the determination of crystallite sizes and microstrains it is usual to determine the instrumental parameters, both in conventional laboratory and synchrotron diffractometers. In this case, besides having the crystal structure and cell parameters very well defined, it is imperative that the standard sample presents high crystallite size and low (or none) microstrains, in order to obtain diffraction peaks broadening due only to instrumental factors. For this purpose normally are used the NIST Standard Reference Materials for Powder Diffraction like Al_2O_3, Si, LaB_6 etc. In order to attend the demand of XRD community for altenative souce of standards, we are developing a set of materials that attempt to the requirements to be used in conventional laboratories and also in synchrotron and neutrons diffractometers as powder diffraction standards. We are working in the production of standard samples of Al_2O_3, Y_2O_3, among others. In this work are presented some preliminary results of these standard samples, measured in conventional equipment and synchrotron (D10B-XPD and D12A-XRD1 -LNLS), both in high- and low-resolution configurations. The experimental data were analyzed by Rietveld refinement and fundamental parameters method in order to determine crystallite size and microstrain, and are compared to the NIST LaB_6 standard. The results show that the samples fulfill the requirements to be used as powder diffraction standards.

Acknowledgements: Work supported by Brazilian Agency CNPq (proj. 480337/2007-1).

Implementation of confocal setup in the LNLS using polycapillary optics.

R.D. Pérez[1], H. J. Sánchez[2], Pérez, C. A.[3], and Rubio, M.[1]

[1] Centro de Excelencia de Productos y Procesos de Córdoba - Cordoba Argentina
[2] Universidad Nacional de Cordoba - Córdoba Cba Argentina
[3] Laboratório Nacional de Luz Síncrotron - Campinas SP Brazil

The confocal setup consists of x-ray lenses in the excitation as well as in the detection channel. In this configuration, a micro volume defined by the overlap of the foci of both x-ray lenses is analyzed. Scanning this micro volume through the sample, 1-3 dimensional studies can be performed. For intermediate thin homogeneous layers a scanning in the normal direction to the surface sample provides information of its thickness and composition. For multilayer samples it also provides the order of each layer in the stratified structure. For the confocal setup, we used a glass monocapillary in the excitation channel and a monolithic half polycapillary in the detection channel. The experiment was carried out at the D09B beamline of the LNLS using white beam. In the present work, application of the confocal μXRF in biological samples and multilayer samples are described. Also preliminary results of confocal μXRD are shown.

Acknowledgements: The authors would like to thank the financial support from the Brazilian Synchrotron Light Source (Under proposal LNLS D09B-XRF-5744/06 and D09B-XRF-6512/07); CONICET and FaMAF from Argentina. We are also grateful to the whole CEPROCOR and synchrotron team for perfect running conditions.

Experimental study of the elliptical polarization in monochromatic synchrotron X-ray beams

Droppa Jr., R.[1] and Morelhão, S.L.[2]

[1] Laboratório Nacional de Luz Síncrotron - Campinas SP Brazil
[2] Universidade de São Paulo - São Paulo - São Paulo SP Brazil

In the last years, the XRD1 beamline of the LNLS has been intensively used to perform X-ray phase measurements via interference of simultaneously diffracted waves (SDW), commonly known as multiple beam diffraction experiments [1, 2]. In such measurements, enhanced phase sensitivity of the SDW interference profiles are obtained by using a specific diffraction geometry in which the linear detector is placed at nearly 90 degrees from the incident beam direction. Hence, the X-ray photon energy is tuned to provide Bragg angles of 45 degrees in single crystal samples. Combining this diffraction geometry with the degree-of-freedom for rotating the incidence plane around the incident beam direction has led to a very interesting situation where the diffracted beam is parallel to the oscillation direction of the incident electric wavefield; remember that an accelerated charge does not irradiate along the acceleration direction (classical electrodynamics). Theoretically, for a 100% linearly polarized radiation (π-polarization) and at the exact $\pi/2$ diffraction geometry with the incidence plane at the horizontal position, the diffracted intensity should be zero in which has been called polarization-forbidden or polarization-suppressed reflections. Recently, during optimization procedures of the primary beam optics, i.e. adjustment of focusing mirror curvature, sagittal focus, apertures of the white beam and scattering slit-screen sets, it was noted a split of the Bragg peak as the sample diffraction plane approaches to the horizontal position, i. e. the storage-ring plane [3], contrarily to the expected very weak Bragg peak. In this work, by using a perfect Si (111) single crystal in the polarimeter-like diffractometer [4] of the XRD1, we carried out a detailed and systematic study of the above mentioned Bragg-peak split effect. The results clearly show a direct correlation between the intensities on each side of the split peak and elliptically polarized components below and above the photon beam. Therefore, the observed effect provides a simple tool for characterizing the amount of elliptical polarization in the synchrotron radiation.

References: [1]. S.L. Morelhão and S. Kycia, Phys. Rev. Lett., 2002, 89, 015501; [2]. S.L. Morelhão, L.H. Avanci and S. Kycia, Nucl. Intrum. Meth. B, 2005, 238, 175; [3]. R. O. Freitas, R. Droppa Jr., and S. L. Morelhão, LNLS 2005 Activity Report, 2005; [4]. S.L. Morelhão, J. Synchrotron Radiat. 2003, 10, 236.

Acknowledgements: This work was supported by ABTLuS.

Medição de tensões residuais em filmes finos por difração de raios X com ângulo de incidência rasante

Gómez, A. G.[1], Recco, A.A.C.[2], and Martinez, L. G.[3]

[1] Universidade de São Paulo - São Paulo - São Paulo SP Brazil
[2] Universidade de São Paulo - São Paulo - Sao Paulo SP Brazil
[3] Instituto de Pesquisas Energéticas e Nucleares - São Paulo SP Brazil

O desenvolvimento de tensões residuais em filmes depositados por técnicas de Deposição Física de Vapor é fortemente influenciado pelos parâmetros utilizados durante a deposição. Em este trabalho filmes de TiN foram depositados sobre substratos de aço AISI D2 numa câmara *Triodo Magnetron Sputtering* desbalanceado. Os parâmetros: temperatura, fluxo de gás e pressão foram mantidos constantes durante a deposição, e foram idênticos em todas as deposições. Três filmes foram depositados com valores de *bias* constante de -40V, -100V e -150V durante a deposição, outro filme foi depositado sem aplicação de *bias*. Em outros dois filmes o valor de *bias* foi variado durante a deposição, no primeiro o *bias* foi incrementado de -20 a -200V em diferentes passos e variando o *bias* cada 45 minutos. No outro filme o *bias* foi diminuído de -200 a -20V utilizando os mesmos intervalos de tempo. O valor de tensão residual foi medido utilizando difração de raios X com ângulo de incidência rasante com a finalidade de diminuir a influência dos picos do substrato. Para os filmes depositados com *bias* constante foi utilizado um único ângulo de incidência. Nos filmes onde o *bias* foi variado durante a deposição, diferentes ângulos de incidência foram utilizados com a finalidade de estudar o efeito da variação do *bias* nas tensões residuais. Os resultados mostraram que nos filmes depositados com *bias* constante, a tensão residual aumenta com o aumento do *bias* (negativo), de acordo com os resultados encontrados na literatura. O filme depositado com *bias* crescente não mostrou diferenças significativas no valor de *bias*, enquanto que o filme depositado com *bias* decrescente mostrou gradientes de tensão residual através da espessura do filme.

Acknowledgements: Ao Laboratório Nacional de Luz Síncrotron (LNLS). E ao Laboratório de Cristalografia do Instituto de Física da Universidade de São Paulo.

Future developments of the X-ray powder diffraction (D10B-XPD) beamline

Ferreira, F. F.[1] and Granado, E.[2]

[1] Laboratório Nacional de Luz Síncrotron - Campinas SP Brazil
[2] Universidade Estadual de Campinas - Campinas SP Brazil

The X-ray powder diffraction (D10B - XPD) beamline of the LNLS has been operating for external users since March 2004 [1]. Improvements on this beamline are being continuously made in order to optimize its performance, reliability, automation, ease of operation, as well as to expand the sample environment possibilities. A first prototype of the multi-detector/analyzer system was designed and tested and demonstrated a good performance. Some improvements have to be made in order to guarantee the total reproducibility of movements and consistency of signals detected by the scintillator counters. Ongoing work has been carried out and it is expected this system will be fully commissioned and available for users in the first semester of 2009. A recently acquired bender for the mounting of the sagittal crystal of the monochromator will be installed and commissioned during the first two months of 2009. The great reproducibility of motors repositioning and an expected improvement of the photon flux due to a better horizontal focusing of the X-rays beam are some of the advantages of this system.

References

[1] F.F. Ferreira, E. Granado, W. Carvalho Jr., S.W. Kycia, D. Bruno, and R. Droppa Jr., J. Synchr. Rad. 46-53, 13 (2006).

Acknowledgements: Thanks are due to the LNLS technical staff which has been contributing to the progress of the beamline and to FINEP for partial financial support.

New superconducting wiggler beamline (SCW)

Meyer, B.C.[1], Granado, E.[2], Neueschwander, R. T.[1], and Rodrigues, F[1]

[1] Laboratório Nacional de Luz Síncrotron - Campinas SP Brazil
[2] Universidade Estadual de Campinas - Campinas SP Brazil

A new superconducting wiggler (SCW) manufactured by Budker Institute of Nuclear Physics in Russia will be the third insertion device at LNLS and is scheduled for installation in summer 2009 at LNLS storage ring. The SCW above all increases the flux at higher photon energies in comparison with already installed insertion devices and thus allows experiments with hard x-ray synchrotron light between 15 keV and 30 keV for the first time at LNLS. A detailed study of various optical concepts for the central beamline guarantees an optimal choice achieving smallest focused beam, highest possible flux and energy resolution, beam stability and simple handling. We compare two optic designs of the beamline: (i) cylindrical collimating mirror, flat double crystal monochromator and toroidal focusing mirror as it is realized with the MX2 beamline and, (ii) cylindrical focusing mirror(s) and double crystal monochromator with second sagittal bent crystal. The study is based on simulations with the ray-tracing program SHADOW which was equipped with tools and improvements within this project. A critical issue is the total power (5 kW at 250 mA) and power density emitted by the SCW. Whereas 1 kW will be absorbed by the dipole and first mask all components in the white beam section of the beamline need to be designed to cope with the high heat load. A new photon shutter was designed which can permanently resist the entire beam (4 kW). The major part of power is caused by unusable lower energy photons. Annealed pyrolytic graphite filters remove the lower energy part of the power load and protect subsequent components. The study describe aspects with respect to the high heat load and considers the loss of flux and resolution caused by the high power load on the first mirror and crystal.

Acknowledgements: This work was supported by CnqQ. I specially thank my colleagues at mechanical project group of LNLS.

Scientific Opportunites with the New Superconducting Wiggler Beamline for Materials Science

Granado, E.[1]

Universidade Estadual de Campinas - Campinas SP Brazil

The new superconducting wiggler beamline of LNLS is presently being projected, and is expected to be available to external users in a couple of years. A multi-task central beamline is being sought, allowing for x-ray absorption and diffraction experiments in the energy range of 5-30 keV, with a flux enhancement of over 3 orders of magnitude at 20 keV with respect to bending magnet beamlines. Here, we will discuss some of the new scientific opportunities of current interest that will be available to the LNLS materials science users with this new powerful tool.

Acknowledgements:

Parte IX

Propriedades Estruturais, Eletrônicas e Magnéticas de Sólidos

New In-Situ Blends of Polyaniline and Polycardanol Characterized by SAXS/WAXS

Souza Jr, F. G.[1], Richa, P. R. F.[1], Cosme, T. A.[1], and Pinto, J.C.[1]

Universidade Federal do Rio de Janeiro - Rio de Janeiro RJ Brazil

Cardanol, a well known natural resource, was used to produce a conductive bio-resin in presence of formaldehyde, catalyzed by H_2SO_4. Before reticulation, polyaniline doped with H_2SO_4 (PAni. H_2SO_4) was blended with the resin. The blended material was cast into polypropylene cups and kept inside a desiccator under vacuum until complete water evaporation. The final in-situ polymer blend was solid and could not be dissolved in ordinary solvents, indicating that a reticulated material had been obtained. SAXS / WAXS studies were performed pointing to understand the morphology of prepared materials. Wide and small X-ray scattering (WAXS / SAXS) measurements were performed using the beam line of the Brazilian Synchrotron Light Laboratory (LNLS, Brazil - D11A -SAXS1 6597/07 and 7086/08; λ = 1.743 , d=1064mm), which yields a horizontally focused X-ray beam. All SAXS spectra were corrected for the parasitic scattering intensity produced by the collimating slits, for the non-constant sensitivity of the PSD, for the time varying intensity of the direct synchrotron beam and for differences in sample thickness. A new conductive material was presented, as obtained through in-situ blending of polycardanol and Polyaniline doped with H_2SO_4 . Polycardanol was produces in acidic conditions, in presence of H_2SO_4, in order to avoid dedoping of PAni.H_2SO_4. WAXS and SAXS results are very important once they are able to show that crystalline structure of PAni.$_2SO_4$ is destroyed during blending with polycardanol, meaning that polyaniline is dispersed homogeneously in the bio-matrix, which is a very good result from compression sensitivity point of view.

Acknowledgements: The authors thank CNPq, CAPES and FAPERJ for the financial support and scholarships. The authors also thank LNLS for technical and financial support on WAXS/SAXS (LNLS, Brazil - D11A -SAXS1 6597/07 and 7086/08) experiments.

Electronic and structural evolution of pentacyanonitrosylmetallates during thermal decomposition

Soria,B.[1], Taylor, M.A.[2], and Ceolin M.[3]

[1] Universidad Nacional de La Plata - La PLata B.A. Argentina
[2] Universidad Nacional de La Plata - La Plata Bs.As Argentina
[3] Instituto de Investigaciones Fisicoquimicas Teoricas y Aplic - La Plata BA Argentina

Several studies including the crystallographic, thermal and vibrational properties of a series of hydrated and anhydrous alkaline and alkaline-earth pentacyanonitrosylferrate, $[Fe(CN)_5NO]^{2-}$, have been previously performed (1-3 and references therein). These studies provided interesting results specially regarding the vibrational and photo-behavior of the NO group. However their structural and electronic changes triggered during thermal degradation are not well known. Moreover, the electronic distribution of the orbitals formed by the ligands and the central metal is not well known. In view of the findings already mentioned about the nitroprusside anion and their salts and to obtain information in other pentacyanonitrosylmetallates, our main purpose was to extend the study to their alkaline and transitions metals salts focusing on the thermal evolution of the local and electronic structure observed from the metallic sites. In this work, we present a systematic and extensive investigation of the thermal decomposition of the different complexes with general formula $A_m[B(CN)_5NO]_n$ where A= K, Co, B= Fe, Cr, Mn, m=1,3 and n= 1,2 using EXAFS, XANES, XRD, DTA, TGA and FTIR.

Referências

1. Gonzalez, S.R. , Piro, O.E. and Aymonino, P.J. J.Chem.Phys. 81 (1984) 625.
2. Soria, D.B., Amalvy, J.I., Piro, O.E.; Castellano, E.E. and Aymonino, P.J. J.Chem. Crystallogr. 26 (1996) 328.
3. Soria, D. B.; Chacón Villalba, M.E.; Piro, O.E. Polyhedron. 21 (2002) 1767-1774.

Acknowledgements: This work was partially supported by UNLP and CONICET (Argentine) and LNLS, Brazil.

Kinetics of crystallization in $Cu_{1-x}TM_xO$ (TM=Fe or Ni) by X-ray Absorption and Diffraction

Meneses, C. T.[1], Duque J.G.S.[1], and Knobel, M.[2]

[1] Universidade Federal de Sergipe - São Cristóvão SE Brazil
[2] Universidade Estadual de Campinas - Campinas SP Brazil

In the last years, studies involving *in situ* X-ray diffraction (XRD) and X-ray absorption (XAS) measurements using synchrotron radiations have increased tremendously and proved to be milestone to study time resolved crystallization and structural changes in several materials small [1-3]. Certainly, the interest in these studies is fundamentally important in order to control exactly over the particle size and the various synthesis conditions. The good control of theses parameters is one of the main reason for that these materials can be used for futures applications, as for example, to optimize properties optics [4]. In the previous works, we emphasized a study about the evolution of the growth NiO nanoparticle as function of temperature and we compare with the theoretical results to complete formation of NiO using both techniques X-ray absorption near edge spectroscopy (XANES) and another by XRPD [5]. In this work we concentrate to study the kinetic growth of $Cu_{1-x}TM_xO$ (TM=Fe and Ni) through *in situ* using both techiques XRD and XAS. We have observed in the experiment the changes in the XRD patterns and X-ray absorption near edge (XANES) profile, which allows us to see the beginning of doped-CuO particle. The effects of different doping were also studied. These studies provide new insight in the production of materials by hydrothermal technique, which will can be useful for improving the particle size control. We have demonstrated that the doping rate can influence the formation of impurities phases.

References:

[1] P. Zolliker et al., *Phys. Rev. B*, **42**, 6332 (1990).

[2] R. E. Morris et al., *J. Sync. Rad.* **3**, 301 (1996).

[3] S. O. Svensson et al., *J. Sync. Rad.* **4**, 83 (1997).

[4] N. R. Jana et al., *Chem. Mater.* **16**, 3931 (2004).

[5] C. T. Meneses et al., *J. Electron Spect. Related Phen.* **156-158**, 176 (2007); C. T. Meneses et al., Activity Report LNLS (2006).

Acknowledgements: This work has been supported by the LNLS under proposal submitted to XPD and DXAS beamlines.

Modeling the atomic structure of an Amorphous $Se_{90}S_{10}$ Alloy Produced by Mechanical Alloying

Sanchez, D. F.[1], K. D. Machado[1], Maciel, G.A.[1], Jóvári, P.[2], Brunatto, S. F.[1], and Stolf, S. F.[3]

[1] Universidade Federal do Paraná - Curitiba PR Brazil
[2] - Berlin Germany
[3] Universidade Estadual de Maringá - Maringá PR Brazil

The interest in chalcogenide glasses (glasses formed by elements Se, S and Te), has grown in recent years due to their technological applications in electronic, optoelectronic, optical and memory switching devices. Due to the promising applications of Se-S alloys and the lack of a systematic investigation of their structures, we think that a more detailed structural study about these amorphous alloys should be carried on. Thus, here we have studied the formation of an amorphous $Se_{90}S_{10}$ by mechanical alloying and also its structural and vibrational properties by using synchrotron x-ray diffraction (XRD), extended x-ray absorption fine structure spectroscopy (EXAFS), Raman spectroscopy (RS) and reverse Monte Carlo simulations (RMC) of the total structure factor $S(K)$ obtained from synchrotron XRD measurements. Vibrational modes of the alloy were determined by using RS, and these results showed the presence of Se-S pairs in the alloy, although the average coordination number concerning this pair is small. From EXAFS data obtained at three temperatures, $T = 300$ K, 200 K and 30 K, and using a cumulant analysis, average interatomic distances, average coordination numbers, Einstein temperatures, Debye-Waller factors and anharmonicity, given by the third cumulant, were obtained. The results indicate that Se-S pairs are more disordered and distorted than Se-Se pairs due to the milling process. In order to model the structure of the alloy, RMC simulations using the XRD total structure factor $S(K)$ were made. Then, information such as average coordination numbers, average interatomic distances and bond-angle distribution functions were obtained, and structural parameters obtained from RMC simulations agree very well with those found from EXAFS, reinforcing the results extracted from both techniques.

Acknowledgements: We thank the Brazilian agencies CNPq and CAPES for financial support. This study was also partially supported by LNLS (proposal no 7093/08).

Estructura atómica, dinámica local, anharmonicidad y expansión térmica en nanoaleaciones FexCu100-x: determinación del potencial interatómico mediante EXAFS empleando teoría de perturbaciones estadístico-cuántica.

Lede, E. J.[1] and Socolovsky, L. M.[2]

[1] Universidad Nacional de La Plata - La Plata Bs.As Argentina
[2] Universidad de Buenos Aires - Buenos Aires CapFe Argentina

Las técnicas de aleamiento mecánico han mostrado ser eficaces en la síntesis de aleaciones binarias nanoestructuradas metaestables. Presenta gran interés el estudio de sistemas binarios en los cuales la solubilidad mutua de sus componente básicos es baja en el equilibrio termodinámico debido a su calor de formación positivo. En el presente trabajo se investigaron mediante EXAFS, nanoaleaciones (Fex Cu100-x, 14Los datos EXAFS obtenidos sobre un conjunto de 4 muestras con diferentes tenores de Fe, fueron tratados simultáneamente en ambos bordes de absorción y para todas las temperaturas (8, 20, 35, 55, 80, 110, 145, 195, 245, 300). Un tratamiento convencional previo de los datos, sugirió una estructura FCC con una gran distribución de sitios ligeramente diferentes tanto para el Fe como para el Cu, variando con la concentración local (CL) de Fe. Para contemplar este hecho, se consideraron las constantes de fuerza del potencial, como funciones de la CL, y se adicionó en la ecuación empleada en el ajuste una función densidad de probabilidad

[1] A.N. Kravtsova, G.E. Yalovega, A.V. Soldatov, W.S. Yan b, S.Q. Wei b a ResearchJournal of Alloys and Compounds xxx (2008) xxxxxx The

Acknowledgements: Los autores agradecen al LNLS

Zr and Ag L-edge XANES studies of Ag nanoparticles in nanoporous Zr-Si-O thin films

Andrini, L.[1], Wolosiuk, A.[2], Angelomé, P. C.[2], Soler-Illia, G.J.A.A.[2], and Requejo, F. G.[1]

[1] Universidad Nacional de La Plata - La Plata Bs.As Argentina
[2] Comisión Nacional de Energia Atómica - Buenos Aires B.A. Argentina

Mesoporous zirconia-silica (MZS) have been extensively investigated, for their high potential in catalysis, in particular for creating controlled nanometric cavities with regular spatial separation [1]. The well-known activity of silver for selective oxidation of hydrocarbons [2] becomes the Ag-MZS system as a promissory model catalyst because the introduction of silver in the pores of MZS oxides gives highly ordered active catalytic sites.

We studied the modifications in the MZS oxide after introduction of silver into their pores. According to the crystal-field information obtained from the Zr L2,3 and Ag L2,3-XANES spectra we obtained direct evidence of charge transference between Ag nanoparticles and Zr ions in the surface of MSZ.

The Zr and Ag L2,3 XANES measurements were carried out at D04A-SXS beamline at LNLS (Campinas, Brazil). The preparation of oxides and the films were already reported elsewhere [1, 3]. The Ag nanoparticles were introduced into the pores of the MZS by immersion in a $AgNO_3$-EtOH solution followed with a slow chemical reduction with HCHO [4]. The MZS thin films supported on FTO have a molar ratio Zr/(Zr+Si) = 10, 90, and were studied before and after the Ag incorporation.

We have quantitatively obtained the nature of changes at the $\Delta h_{3/2;5/2}$ holes in Ag nanoparticles in MZS. There is an increment in the number of holes with respect to the pure Ag. After introducing Ag in the pores of the MZS film, there is a decrement of the splitting due to crystal field interactions, consistently with the electronic transfer from Ag to Zr.

References

[1] G.J.A.A. Soler-Illia et al., J. Mater. Chem. 14, 1879 (2004).

[2] V.I. Bukhtiyarov et al., Phys. Rev. B 67, 235422 (2003); S. Piccinin et al., Phys. Rev. B 77, 075426 (2008).

[3] E.L. Crepaldi et al., Chem. Comm., 1582 (2001); G.J.A.A. Soler-Illia et al., Chem Rev. 102, 4093 (2002).

[4] M.C. Fuertes et al., submitted.

Acknowledgements:

A pre-edge analysis of Ti K-edge XANES spectra of photoluminescent PZT powder

de Figueiredo, A. T.[1], Mastelaro, V.R.[2], Varela, J.A.[1], and Longo, E.[1]

[1] Universidade Estadual Paulista - Araraquara - Araraquara SP Brazil
[2] Universidade de São Paulo - São Carlos - São Carlos SP Brazil

PL emission at room temperature is typical of structurally disordered perovskite-like compounds. The $Pb(Zr_{0.53}Ti_{0.47})O_3$ (PZT) is a solid solution of lead zirconate and lead titanate with perovskite structure. In this work, PZT with different structural order was studied by Ti K-edge XANES. The pre-edge feature was evaluated. The XANES spectrum for PZT fully ordered powder confirm that the local structure around titanium atoms is characteristic of the structurally ordered PZT, therefore, with only TiO_6 units. This PZT powder not displays PL emission at room temperature. However, the disordered PZT powder displays PL emission at room temperature. The pre-edge of Ti K-edge spectrum to this powder reveals that there is more than a single coordination mode for titanium. Based in this study, the coexistence of more than a coordination mode for titanium is essential to PZT display PL emission at room temperature.

Acknowledgements: The authors gratefully acknowledge the financial support of FAPESP/CEPID. The research was partially performed at LNLS-National Laboratory of Synchrotron Light, Brazil.

Study of the changes in Ti coordination in $CaTiO :_3 Sm$ by Ti K-edge XANES

R. Oliveira da Silva[1], de Figueiredo, A. T.[2], Mastelaro, V.R.[3], and Longo, E.[2]

[1] Universidade Federal de São Carlos - São Carlos SP Brazil
[2] Universidade Estadual Paulista - Araraquara - Araraquara SP Brazil
[3] Universidade de São Paulo - São Carlos - São Carlos SP Brazil

Although photoluminescence (PL) has already been well established, this property has only been recently identified in structurally disordered titanates. Only structurally disordered titanates display PL emission at room temperature. In this work, samples of $CaTiO :_3 Sm$ heat annealed at different temperatures under crystallization temperature (disordered samples) and $CaTiO :_3 Sm$ crystalline (ordered sample) were studied by Ti K-edge XANES spectroscopy. The pre-edge region of Ti K-edge XANES spectra show strong changes due to changes in Ti coordination. XANES spectra of the disordered samples are characteristic of mixture of fivefold titanium coordination, TiO_5, with pyramidal structure containing four oxygen atoms at the plane end one at the apex and sixfold coordinated titanium atoms, TiO_6, with octahedral structure. The PL studies reveal that only disordered samples display PL emission. Thus, it was concluded that structural disorder is essential to titanates to exhibit PL emission at room temperature.

Acknowledgements: The authors gratefully acknowledge the financial support of FAPESP/CEPID. The research was partially performed at LNLS-National Laboratory of Synchrotron Light, Brazil.

Study of 1s3p resonant inelastic x-ray scattering processes in transition metals

Stutz, G.[1] and Tirao G.[1]

Universidad Nacional de Cordoba - Cordoba Argentina

Synchrotron radiation sources along with newly developed analyzers based on backdiffracting crystals have made the study of second order x-ray interaction processes, such as the resonant inelastic scattering, with high resolution feasible. Inelastic x-ray scattering in the resonant regime (also called resonant x-ray Raman scattering) can be visualized as an x-ray absorption process followed by x-ray emission, with a virtual intermediate state and a final state composed of a core-hole in an upper atomic level and an excited electron above the Fermi level. The resonance condition is achieved tuning the energy of the incident photons close to an absorption edge. Resonant inelastic x-ray scattering spectroscopy (RIXS) can thus yields information similar to that obtained from x-ray absorption and emission spectroscopies, provided that high energy resolution (i.e. less than or equal to the natural linewidth of the corresponding x-ray transition) is achieved. In recent years, RIXS has become a powerful technique to investigate electronic excitations and electronic structure in condensed matter. In this work, results from first RIXS studies with high energy resolution made at LNLS are presented. Experiments were performed at the D12A-XRD1 beamline of the LNLS. The experimental setup consists basically of a sagitally focusing double-crystal monochromator and a spectrometer based on a spherically focusing crystal analyzer in backdiffraction geometry. High energy resolution along with high transmission of the analyzed beam, required for a modern RIXS experiment, are unique properties of backdiffracting analyzers such as that used in present study. The mentioned spectrometer was conceived to perform experiments with high energy- and momentum-resolution in several regimes of the inelastic x-ray scattering. Whereas 1s2p RIXS processes have been widely studied in transition metals, the investigation of 1s3p processes, which can provide much more rich information about the electronic structure, is scarce. First test measurements have shown the feasibility of performing RIXS experiments with high energy resolution at LNLS. In this work results obtained in Cr, Mn, Co, Cu and Zn are presented. Characteristic features of the resonant inelastic scattering, such as dispersion of the inelastic peak, peak narrowing and intensity increase close to the resonance condition, were investigated and compared with theoretical predictions. While the strong dependence of the intensity with the incident energy is fairly good described by the simple independent electron model, this can not accurately reproduce the observed energy-dependent linewidth and dispersion.

Acknowledgements:

IRON DOPING IN TIN DIOXIDE NANOPARTICLES

Barrero, C.A.[1]

Universidad de Antioquia - Medellin Antio Colombia

C.A. Barrero1 and K. Nomura2

1Grupo de Estado Sólido, Sede de Investigación Universitaria, Universidad de Antioquia A A 1226, Medellín, Colombia 2Dep. Applied Chemistry School of Engineering, University of Tokyo Hongo7-3-1, Bunkyoku, Tokyo 113-8656

Understanding the origin of the magnetic interactions in oxide diluted magnetic semiconductors, ODMS, is actually a subject of intensive research and it is greatly enhancing our basic knowledge of magnetism. Many theories have been put forward but this subject is still a matter of controversy. In this field, it is of primary importance to prepare, under estrictly controlled conditions, samples free of impurities and clustering of magnetic ions. In this presentation, we will show the results of a series of works carried out by our groups and show possible future directions of research in this field. We have prepared pure Fe doped SnO2 nanopowders by two procedures: (i) polymerized complex method under neutral [1] and acidic [2] solutions and annealed at different temperatures and (ii) by mechanochemical alloying with [3] and without thermal treatment. Samples were characterized by XRD, FTIR, SEM, EPR, magnetization, and 57Fe and 119Sn Mössbauer spectroscopies. For both methods, samples without impurities are obtained only under restricted experimental conditions. Our results suggest that we are dealing with samples which exhibit very complex ferromagnetism coming from different sources that include not only interaction between ferric ions, but also interaction between magnetic defects. The nature of the magnetic defects is discussed in the present work. The dominance of a given source of magnetism greatly depends upon synthesis conditions.

[1] K. Nomura, C.A. Barrero, J. Sakuma, and M. Takeda, Phys. Rev. B 75 (2007) 184411. [2] J. Sakuma, K. Nomura, C.A. Barrero, and M. Takeda, Thin Solid Films 515 (2007) 8653. [3] L.C. Sánchez, A.M. Calle, J.D. Arboleda, J. Osorio, K. Nomura, and C.A. Barrero. Microelectronics J. (2008) in press.

Acknowledgements: Asahi Glass Foundation. Matsumae International Foundation. T. Ohki and T. Ikeda, Kobelco Research Institute Inc., for help in measuring VSM, and to S. Iio, School of Engineering, The University of Tokyo for help in measuring some Mössbauer spectra. CODI- Universidad de Antioquia.

Fe-doping and strain effects on structural and magnetotransport properties in La2/3Ca1/3Mn1-yFeyO3 thin films

Arnache, O.[1], Girata, D[1], and Hoffmann, A[2]

[1] Universidad de Antioquia - Medellin Antio Colombia
[2] Argonne National Laboratory - Argonne IL United States of America

The influence of ^{57}Fe-doping and strain effects on the structural and magnetotransport properties of undoped and lightly doped ^{57}Fe (1 and 3% at Mn site) La2/3Ca1/3MnO3 thin films and bulk powder samples have been studied. Thin films were grown on (100)-SrTiO3 (STO) and (100)-LaAlO3 (LAO) single crystal substrates, via high O2 pressure (500 mTorr) using dc magnetron sputtering. Conversion electron Mössbauer (CEM) spectra measured at room temperature in the paramagnetic regime of the Fe-doped samples do not show significant differences in the isomeric shift for the case of the La2/3Ca1/3MnO3 films doped with 1 and 3% iron. The isomeric shift values correspond to the presence of Fe in the 3+ state with octahedral coordination, thus indicating that Fe is incorporated into the structure by substituting Mn. The absence of further states in the spectra indicates that Fe is not involved in forming other additional impurity phases. The x-ray θ-2θ scan showed that all thin films on LAO and STO have single phase and c-axis strong orientation along the growth direction and the Fe doping gives rise to a relaxation of the epitaxial strain. Finally, we have observed that the saturation magnetization, Curie temperature, metal-insulator transition, and magnetoresistance vary nonmonotonically with increased Fe concentration. This behavior can be understood in terms of competing influences from the strain relaxation, which enhances the tendency to order ferromagnetically, and the reduced double exchange, which is detrimental to the ferromagnetic order.

Acknowledgements: We acknowledge C. Barrero and K. Nomura for the CEMS measurements. This work was supported by the following: COLCIENCIAS Projects No. 1115-05-17603 and 1115-0517617, CENM Grant No. 043-2005, the Universidad de Antioquia Grant No. SIU-24-1-28 GES in Colombia, and the U.S. Department of Energy, Basic Energy Sciences under Contract No. DE-AC02-06CH11357

DIFRAÇÃO DE RAIOS-X USANDO RADIAÇÃO SÍNCROTRON NO CRISTAL ORGÂNICO DE MBANP SUBMETIDO A CAMPO ELETRICO

C. M. R. Remedios[1], dos Santos, A. O.[2], de Menezes, A. S.[2], and Cardoso, L.P.[2]

[1] Universidade Federal do Pará - Belém PA Brazil
[2] Universidade Estadual de Campinas - Campinas SP Brazil

As respostas não-lineares de cristais têm origens nas não-linearidades moleculares, mas a estrutura cristalina e as interações intermoleculares têm também uma importância crucial na determinação da natureza dos efeitos produzidos. As curvas de Rocking da difração de raios-X, quando obtidas sob geometria de alta resolução, representam uma ótima ferramenta para o estudo unidimensional das pequenas distorções na célula unitária associadas à aplicação de campos elétricos externos em cristais que apresentam efeitos não lineares. Devido a essa característica da técnica, decidimos usá-la no presente estudo da aplicação de campo elétrico em cristais orgânicos. Trabalhos anteriores de outros pesquisadores visando estudar efeitos não lineares no MBANP foram feitos na direção [010] (direção do eixo polar do cristal) para a aplicação de campo elétrico[1]. O efeito do campo elétrico externo foi monitorado através de curvas de Rocking da reflexão (0010). As deformações estruturais em função do campo elétrico aplicado na direção polar do cristal MBANP, apresentaram uma histerese com forma de asa de borboleta, sendo possível investigar as principais características desse tipo de histerese a partir de cálculos moleculares[2]. Como as moléculas são organizadas de diferentes modos no cristal, a rotação do anel de benzeno em função de campo elétrico apresentará orientações diferentes, que pode resultar em um efeito de memória. Neste trabalho nós estudamos a aplicação de campo elétrico no eixo polar de cristais de MBANP fazendo medidas de curvas de Rocking na reflexão 400. As medições deste trabalho foram executadas na estação XRD1 do LNLS. As deformações estruturais devido à aplicação do campo elétrico mostram um comportamento do tipo histerese a exemplo do que foi observado anteriormente para as deformações ao longo do eixo b do cristal.

Referências

1. (Avanci L. H. at. All Physical Review B, v. 61, n. 10 pg. 6507, ano: (2000)
2. Avanci L. H. at. All Crystal Growth Design, v. 4 n. 5, pg. 1079, ano: (2004)

Acknowledgements: Os Autores agradecem ao CNPQ, LNLS e ABTLUZ pelo auxilio finaceiro suporte técnico e instalações que viabilisaram este trabalho

Structural characterization of ZrO_2-CeO_2 nanotubes

Acuña, L. M.[1], Lamas, D. G.[1], and Fuentes, R. O.[1]

Consejo Nacional de Investigaciones Científicas y Técnicas - Buenos Aires Argentina

ZrO_2-CeO_2 substitutional solid solutions are extensively used as redox or oxygen storage promoters in three-way catalysts, which are applied in controlling the emissions of NOx, CO and hydrocarbons from automotive exhausts. Because zirconia-ceria solid solutions have better catalytic properties than pure ceria, it is worth considering whether these solid solutions might also have other properties that are desirable for applications in solid oxide fuel cells (SOFCs). In particular, the metastable forms of the tetragonal phase have been widely investigated since they are the most suitable for applications. One of the most notable characteristics of some zirconia-based solid solutions is the existence of three tetragonal forms, all belonging to the $P4_2/nmc$ space group. The stable tetragonal form is called the t-form. There is also a t'-form with a wider solubility, but unstable in comparison with the mixture of the t-form and cubic phase. Finally, the t''-form has an axial ratio c/a of unity, but with the oxygen atoms displaced along the c axis from their ideal sites of the cubic phase (8c sites of the Fm3m space group).

In this work, a detailed crystallographic study performed by X-ray diffraction (XPD 10B beamline of LNLS) was carried out on ZrO_2-50, 70 and 90%mol CeO_2 nanotubes. The lattice parameters were refined by Rietveld method. ZrO_2-50 and 70%mol CeO_2 nanotubes exhibit the metastable t'-form and t''-form, respectively. The cubic structure is observed in ZrO_2-90%mol CeO_2 nanotubes. The crystallite size was determined by Scherrer's formula. The nanotube walls were composed of nanoparticles with an average crystallite size ranging from 4.8 nm to 7.2 nm.

Acknowledgements: This work has been supported by the Brazilian Synchrotron Light Laboratory (LNLS) under proposal D10B XPD - 7083, Agencia Nacional de Promoción Científica y Tecnológica (Argentina, PICT No. 14268 and PICT No. 38309) and YPF foundation.

XAS study of nanostructured $SrTi_{1-x}Fe_xO_3$ compounds

da Silva, L. F.[1], Maia, L. J. Q.[1], M.I.B.Bernardi[1], and Mastelaro, V.R.[1]

Universidade de São Paulo - São Carlos - São Carlos SP Brazil

In the last decades compounds with perovskite structure and ABO_3 formula (A and B are cations while O is the oxygen anion) have been intensively studied due their interesting physical properties as for example, photoluminescence and ferroelectricity. More recently, perovskite nanostructured compounds have been found to be promising materials in current science and technology. In this context, the Fe-doped strontium titanate ($SrTi_{1-x}Fe_xO_3$) nanostructured compounds has been the object many studies because the substitution of Ti by Fe atom creates different types of defects in the structure which have a significative effect on the sensing properties of this system. The conventional way to prepare $SrTi_{1-x}Fe_xO_3$, compounds is based on the solid-state reaction between $SrCO_3$, TiO_2 and Fe_2O_3 at relatively high processing temperature ($\geq 1000^oC$). After the synthesis by this method, nanostructured materials have been obtained by milling. On the other hand, it is well know that chemical synthesis based on the polymeric precursor method allows a low temperature ($\leq 700^oC$) crystallization and provides a high degree of control on the composition and on the particle size from some nanometers to micrometric size. In this work, we will present the results concerning the short-range order study of nanostructured $SrTi_{1-x}Fe_xO_3$ particles (x=0.0 up to 1.0) by using the polymeric precursors method. The Ti and Fe K-edge X-ray absorption spectra were collected at the XAFS1 and XAFS2 LNLS beam lines in order to investigate the effect of the substitution of Ti by Fe atoms on the short range order as well as on the chemical state of titanium and iron.

Acknowledgements: This work was supported by FAPESP and CNPq

Difração Múltipla de raios-X em co-cristais de L-Asparagina e L-Alanina

Pinheiro, G. S.[1], Melo, F. E. A.[2], Freire, P. T. C.[2], C. M. R. Remedios[3], Menezas, A. S.[2], and dos Santos, A. O.[4]

[1] Universidade Federal do Ceará - FORTALEZA CE Brazil
[2] Universidade Federal do Ceará - Fortaleza CE Brazil
[3] Universidade Federal do Pará - Belém PA Brazil
[4] Universidade Estadual de Campinas - Campinas SP Brazil

Atualmente os cristais de aminoácidos têm despertado muito interesse de muitos grupos de pesquisa em Física devido a suas propriedades físicas que possibilitam grande aplicabilidade tecnológica como, por exemplo: geração de segundo harmônico na óptica não-linear. Neste trabalho estudamos as propriedades estruturais de cristais de aminoácidos de L-Asparagina monohidratada e L-Alanina dopadas com os metais Cu, Cr, Eu, e Ni por Difração Múltipla de raios-X. As medidas de difração de Raios-X com radiação Síncrotron foram realizadas na estação XRD1 do Laboratório Nacional de Luz Síncrotron (LNLS), Campinas-SP. O fenômeno de difração múltipla (difração de n-feixes) ocorre sempre que a Lei de Bragg estiver sendo satisfeita para mais de um conjunto de planos cristalográficos da rede cristalina da amostra que está sendo analisada. Com a fonte de luz Síncrontron, na estação XRD1, é possível fazer análises usando comprimentos de onda no intervalo de $\lambda = 1$ a 2 . Para cada amostra foram realizadas varreduras do tipo Renninger usando radiação com comprimentos de onda fora e na borda de absorção do íon dopante. Desta forma, foi possível estudar a presença dos dopantes na estrutura dos cristais estudados. Nossas medidas indicam a presença de metais de transição de forma intersticial na estrutura dos cristais de aminoácidos analisados. Um resultado muito interessante em nossas medidas é que para pequenas concentrações de dopante ocorre um aperfeiçoamento na qualidade cristalina da superfície dos cristais. Isto pode ser observado através de picos de difração múltipla do tipo Bragg Superfície (BSD), que permitem analisar as características superficiais dos cristais. Mudanças consideráveis foram observadas nos hábitos de crescimento dos cristais estudados. Isto constitui mais um indicio da incorporação dos dopantes na estrutura dos cristais estudados.

Acknowledgements: Os autores agradecem ao CNPq, CAPES e FUNCAP pelo apoio financeiro.

Short and long range order study of $Bi_{(4-x)}La_xTi_3O_{12}$ ferroelectric System

Santos, V. B.[1], Mastelaro, V.R.[1], Mir, M.[2], Neves P.P[2], Doriguetto, A.C.[2], and Mascarenhas, Y.P.[1]

[1] Universidade de São Paulo - São Carlos - São Carlos SP Brazil
[2] Universidade Federal de Alfenas - Alfenas MG Brazil

The La substituted $Bi_4Ti_3O_{12}$ (BIT) compound exhibited excellent ferroelectric properties and fatigue free behavior. Although the electrical properties of this system have been extensively studied, few works have been published concerning the long and short range order structure, mainly the effect caused by the substitution of bismuth by lanthanum ions. The purpose of this work is study the short and the long range order structure on the La substituted BIT compound, hereafter denoted as BLT system. The BLT samples were prepared by a solid state reaction method. Sintered ceramic samples were obtained after a heat treatment at temperatures ranging from 1323 to 1523 K. The XRD data was collected at room temperature and below and above the Curie temperature on the D10B XPD LNLS beam line. Each pattern was measured from 8.5 to 110 in 2theta with a step size of 0.005 degree. X ray absorption near edge structure (XANES) spectra at the titanium K edge and lanthanum and bismuth $L3$ edges were collected at room temperature on the D04B XAFS1 beam line at the LNLS storage ring using a transmission mode. Preliminary XRD analysis shows that the studied samples are characterized by diffraction peaks as in the BIT phase. However, some low intensity, additional peaks associated to impurity phases were detected in the XRD pattern of some samples. XANES spectra collect at the Ti K edge and Bi and La $L3$ edges shows that the local structure around these atoms are not significantly affected by the substitution of Bi by La atoms and only few changes are observed at the medium range order. Ab initio calculations of the XANES spectra using the FEFF software was used in order to interpret the variations observed on the XANES spectra obtained at the Ti K edge.

Acknowledgements: This work was supported by CNPq and FAPESP. This research was partially carried out at the Brazilian Synchrotron Light Laboratory (LNLS), Projects D04B XAFS1 7791 and XPD 7661 and 7155.

Caracterizacao de cristais de KDP dopados com L-arginina através de difracao múltipla de raios-X utilizando radiacao síncrotron

Freire, P. T. C.[1], Pinheiro, G. S.[2], Melo, F. E. A.[1], C. M. R. Remedios[3], Moreira, S. G. C.[3], and dos Santos, A. O.[4]

[1] Universidade Federal do Ceará - Fortaleza CE Brazil
[2] Universidade Federal do Ceará - FORTALEZA CE Brazil
[3] Universidade Federal do Pará - Belém PA Brazil
[4] Universidade Estadual de Campinas - Campinas SP Brazil

Cristais de potáassio dihidrogenio fosfato (KDP), apesar de já terem sido bastante estudados, ainda são objetos de estudos em muitas pesquisas científicas. Estes materiais possuem muitas propriedades físicas importantes, como por exemplo: a geracao de segundo harmonico em ótica não linear. A busca por aperfeicoar as propriedades físicas destes cristais assim como controlar o seu hábito e tamanho de crescimento faz com que alguns pesquisadores estudem estes materiais dopados com metais de transicao ou com aminoácidos. Neste trabalho, cristais de KDP dopados com o aminoácido L-arginina foram crescidos pela técnica da evaporacao lenta do solvente. A concentracao de dopantes na solucão de crescimento variou de 0,25 mol por cento a 1 mol por cento Mudancas significativas nos hábitos de crescimento dos cristais foram verificadas neste trabalho. Foram realizadas medidas de absorcao de infravermelho (espectroscopia FT-IR) que confirmaram a dopagem dos cristais de KDP com o aminoácido L-arginina nas amostras estudadas. Medidas de difracao múltipla de raios-X com radiacao síncrotron foram realizadas na estação XRD1 do Laboratório Nacional de Luz Síncrotron (LNLS), Campinas-SP. A reflexão primária utilizada nas medidas de difracao mútipla foi a 4 0 0 e o comprimento de onda foi de 1,9228 angstron. As medidas de policristais foram realizadas em um difratometro X-PERT MRD e os resultados foram analisados pelo método de Rietveld utilizando o programa GSAS. As medidas de difracao de raios-X de pó e de difracao múltipla de raios-X mostraram que os cristais dopados possuem a mesma estrutura cristalina do cristal de KDP puro. Não foram observadas mudancas significativas nos parametros de rede dos cristais dopados com relacao aos parametros dos cristais puros, apesar da verificacao de modificacoes nos espectros de infravermelho e no hábito de crescimento dos cristais.

Acknowledgements: Agradecemos ao LNLS e ás agencias: FUNCAP, FAPESPA e FAPESP.

ZrO_2-CeO_2 solid solutions synthesized by different chemical routes: crystal structure and local order

Acuña, L. M.[1], Zimicz, M. G.[1], Lamas, D. G.[1], Fuentes, R. O.[1], S.A. Larrondo[2], Fantini, M. C. A.[3], and Craievich AF[3]

[1] Consejo Nacional de Investigaciones Científicas y Técnicas - Buenos Aires Argentina
[2] Universidad de Buenos Aires - Buenos Aires CapFe Argentina
[3] Universidade de São Paulo - São Paulo - São Paulo SP Brazil

ZrO_2-CeO_2 substitutional solid solutions have found application as redox or oxygen storage promoters in three-way catalysts because of their high oxygen storage capacity (OSC). Also, due to their excellent catalytic properties for direct oxidation of hydrocarbons, these materials have been proposed as anodes in intermediate temperature solid oxide fuel cells (IT-SOFCs). In particular, the electrical and catalytic properties are close related to the crystal structure of the powders. In previous XRD studies at LNLS, we found a tetragonal-to-cubic transition as a function of composition and also a tetragonal-to-cubic phase transition as function of temperature in ZrO_2-50 and 65 mol% CeO_2 nanopowders. In both cases, the cation-oxygen bond was also studied by EXAFS, finding a correlation between the structural and local changes.

In this work, we studied the influence of the synthesis methods on the structure and local order of ZrO_2-50, 70 and 90 mol% CeO_2 nanopowders. Compositionally homogeneous nanopowders were synthesized by gel-combustion and citrate complexation methods. Measurements were carried out at the D10B-XPD and D04B-XAFS1 beamlines of the LNLS. We found that the crystallite size and morphology of the powders have been strongly influenced by the synthesis method. Lattice parameters were refined by Rietveld method and local order around Zr cations were studied.

Acknowledgements: This work has been supported by the Brazilian Synchrotron Light Laboratory (LNLS) under proposals D04B - XAFS1 - 4700 and 6706, Agencia Nacional de Promoción Científica y Tecnológica (Argentina, PICT No. 14268 and PICT No. 38309), CONICET (Argentina, PIP No. 6559), CNPq (Brazil, PROSUL Program) and CAPES-SECyT and CNPq-CONICET cooperation agreements between Brazil and Argentina. Special thanks to Fundación YPF.

Characterization of a new material based on polyaniline doped with [Cs][$In(dmit)_2$], (cesium) [bis(1,3-dithiole-2-thione-4,5-dithiolato)indium (III)] by X-Ray Photoelectron Spectroscopy

Picciani, P.H.S[1], Comerlato, N.M.[1], Soares, B.G.[1], and Souza Jr, F. G.[1]

Universidade Federal do Rio de Janeiro - Rio de Janeiro RJ Brazil

A novel conducting hybrid material based on polyaniline doped with a monoanion derived from [cesium][bis(1,3-dithiole-2-thione-4,5-dithiolato)indium(III)], ([Cs][$In(dmit)_2$]), were prepared. The X-ray photoelectron spectroscopies confirmed that the [Cs] [$In(dmit)_2$] acts as the doping agent for the emeraldine base (insulating form of the polyaniline). This new material presented lower electrical resistivity values than the starting materials, and also formed a flexible, self-supporting film with good homogeneity. The XPS analysis constitutes a powerful tool for characterizing the doping degree of conducting polyaniline. From the characteristic binding energies of the photoelectron, the elements involved can be identified and the peak intensity can be directly related to the atomic concentration in the sample surface. In addition, the various intrinsic redox states of PAni as well as the different neutral and positive nitrogen spectra can be quantified from the properly curve-fitted N 1s core-level spectrum. The spectrum of the EB sample displayed peaks with binding energies at 397.4 and 399.4 eV, which are related to the imine and amine groups, respectively. In addition, one can observe a small signal at around 402 eV, attributed to the positively charged nitrogens. A very interesting result was observed in the spectrum of EB/[Cs][$In(dmit)_2$] (1:1 wt.) blend. This pattern is very similar to that found in polyanilines doped with hydrochloric acid. Furthermore, the polyaniline doped with dmit presented higher amount of the charged nitrogens (56.8 percent) indicating higher doping degree than the sample doped with HCl (46.4 percent). The ability of [Cs][$In(dmit)_2$] complex in doping polyaniline was also evaluated by others spectroscopic techniques as fourier transform infrared (FTIR) spectroscopy and ultraviolet-visible spectroscopy. Reference: Paulo H.S. Picciani, Fernando G. Souza Jr., Nadia M. Comerlato, Bluma G. Soares. Synthetic Metals (2007) 157, 1074-1079.

Acknowledgements: The authors would like to thank Conselho Nacional de Desenvolvimento Cientifico e Tecnológico, Coordenação de Aperfeiçoamento de Nível de Ensino Superior (CAPES) and Fundação de Amparo à Pesquisa do Estado do Rio de Janeiro (FAPERJ) for the financial support. The authors also thank the Laboratório Nacional de Luz Síncrotron for the technical support on the XPS experiments (LNLS- D04ASXS-6246/07).

XANES Study of Si and Zr in Composite Hollow Spheres

Andrini, L.[1], Arnal, P. M.[2], and Requejo, F. G.[1]

[1] Universidad Nacional de La Plata - La Plata Bs.As Argentina
[2] Universidad Nacional de La Plata - La PLata B.A. Argentina

Zirconia is an extremely important material with wide-ranging applications including as a high-performance transformation-toughened structural engineering ceramic and as a solid electrolyte, and has also found application as a catalyst and catalyst support, especially when durability to chemical attack is required [1].

The Zr L2-L3 and Si K-edges XANES measurements were carried out at D04A-SXS beamline at LNLS. The preparation of nanocrystalline zirconia and hollows spheres (@ZrO_2) were already reported elsewhere [2].

In this work we report a XANES study of Zr and Si present in @ZrO_2 to obtain information about the electronic and local morphological structure of Zr and Si. These hollow spheres are made of nanometer-sized zirconia domains surrounded at least partially by a Si-containing material. A pore structure extends from the inner surface, which defines the inner macropore, to the external surface of the spheres, allowing mater diffusion across the shell [3].

According to white line (WL) intensity and the feature of the Si K-edge absorption spectra, the Si atoms in @ZrO_2 samples have similar neighborhood that Si in SiO_2 and they are not forming $ZrSiO_4$. The evaluation of the splitting at the WL of the Zr L2,3 XANES spectra of the samples indicates that, for low treatments temperatures (293 K), the local environment of Zr is similar to ZrO_2, and for temperatures higher than 973 K, the phase of Zr in @ZrO_2 samples is similar to $BaZrO_3$, where Zr is octahedrally coordinated.

References

1. A. V. Chadwick et al., Chem. Mater. 13, 1219 (2001).
2. P.M. Arnal et al., Chem. Mater. 18, 1068 (2006).
3. P.M. Arnal et al., Angewandte Chemie Internation Edition, 45 (2006).

Acknowledgements:

Microstructural Evaluation of Rapidly Solidified Ti-Si-B Alloys via High Resolution TEM

Candioto, K.C.G.[1], Nunes, C. A.[1], and Coelho, G. C.[1]

Escola de Engenharia de Lorena - Universidade de São Paulo - Lorena SP Brazil

Rapidly solidification refers to rapid cooling of liquid metals/alloys at rates higher than 104 K.s-1, which may produce: refinement of the grain size, extension of the solubility limits; formation of nanocrystals; production of metallic glasses. In general, the produced materials present high chemical homogeneity and fine microstructure. In this study, Ti-Si-B samples (80 mg) with near sphere shape were levitated, melted and quenched under argon in a splat-cooler apparatus, producing discs of approximately 20 mm diameter by 0.05 mm thickness. The disks were characterized via X-ray diffraction (XRD) at room temperature and High-Resolution Transmission Electron Microscopy (HRTEM). The XRD results of several compositions indicated the possible formation of amorphous/nanocrystalline microstructures. Thus, HRTEM was carried out in order to fully characterize the microstructures. Four of the alloys were fully amorphous and seven presented an amorphous matrix with dispersed nanocrystalline regions.

Acknowledgements: This work has been supported by the Brazilian Synchroton Light Laboratory (LNLS) under proposal TEM 7415, CNPq (Proc. 142242/2007-1) and FAPESP (proc. 01/09529-7)

Structural features on corrosion inhibiting properties of siloxane-PMMA hybrid coatings by SAXS and XPS

Sarmento, V.H.V[1], Hammer, P.[1], Pulcinelli, S.H.[1], and Santilli, C.V.[1]

Universidade Estadual Paulista - Araraquara - Araraquara SP Brazil

Siloxane-poly(methyl methacrylate), PMMA, hybrid films were deposited by dip-coating on different substrates from a sol prepared by acid hydrolysis and condensation of silicon alkoxides: tetraethoxysilane (TEOS) and 3-methacryloxy propyltrimethoxysilane (MPTS) and by initialization of the methyl methacrylate (MMA) polymerization with benzoyl peroxide (BPO). The structural features of the films with varying TEOS/MPTS ratio and MMA/MPTS ratio were analyzed by Small Angle X-ray Scattering (SAXS) and X-ray photoelectron Spectroscopy (XPS) and the results were correlated with corrosion protection efficiency in saline environment through electrochemical classic techniques. It was found that the hybrids with TEOS/MPTS and MMA/MPTS ratios of 2 exhibit a highly crosslinked structure. Structural data obtained after the corrosion tests evidence that the formation of efficient diffusion barrier is directly related to increasing cross-linking density of the hybrid network.

Acknowledgements: The authors gratefully acknowledge FAPESP and CNPQ for financial support and the LNLS for the use of the SAXS beamline and the support of the line staff

Estudo das transformações estruturais de compósitos de ferro nanoestruturados em materiais carbonosos porosos em função da temperatura utilizando a linha D10B-XPD

Miguel A. Schettino Jr.[1], Freitas, JCC[1], Morigaki, M. K.[1], E. Nunes[1], Cunha, A. G.[1], Passamani, E. C.[1], and Francisco G. Emmerich[1]

Universidade Federal do Espírito Santo - Vitória ES Brazil

Nanopartículas metálicas dispersas em matrizes de sustentação têm atraído o interesse da comunidade científica devido as suas propriedades físicas, peculiares da dimensionalidade reduzida, e seu grande potencial para aplicações tecnológicas. Especificamente, materiais carbonosos contendo compósitos de Fe nanopartículados podem ser utilizados como: a) agente de contraste magnético para imagem por ressonância magnética nuclear de tecidos biológicos, b) precursor para síntese de nanotubos de carbono, entre outras. Este trabalho trata da produção e caracterização de compósitos nanoestruturados de Fe a partir da mistura de 2,0 g de carvão ativado e 1, 2, 3, 4 e 5 mL de pentacarbonil ferro ($Fe(CO)_5$) utilizando dois procedimentos de preparação simples e de baixo custo: i) sob atmosfera de argônio e com temperatura controlada em 120 C (Série I) e ii) em atmosfera e temperatura ambiente (Série II). As amostras foram investigadas utilizando experimentos de difração de raios-X (DRX, com λ=1,746) *in situ* durante o aquecimento da amostra, sob atmosfera de N_2, utilizando a linha D10B-XPD do Laboratório Nacional de Luz Síncrontron (LNLS). Amostras pré-determinadas foram estudadas por espectroscopia Mössbauer (EM) com fonte radiativa de ^{57}Co:Rh pelo método de transmissão. Apesar dos resultados de DRX à temperatura ambiente evidenciarem reduzida cristalinidade para as amostras das Séries I e II, ficou evidente a presença das fases α-Fe_2O_3 e Fe_3O_4 nas amostras da Série II, enquanto que nas amostras da Série I predomina apenas a fase Fe_3O_4. Quando submetidas ao aquecimento térmico, até a temperatura de 550 C, os DRX indicam um progressivo estreitamento dos picos de difração, confirmando a presença das citadas fases. Entre as temperaturas de 550 e 900 C, os compósitos de Fe, das Séries I e II, iniciam um processo de transformação por redução levando à formação do α-Fe, FeC e ainda contribuindo para o processo de grafitização do carvão ativado. Os espectros de EM registrados à temperatura ambiente das Séries I e II mostraram um comportamento para ou superparamagnético das nanopartículas dos compósitos de Fe, com parâmetros hiperfinos δ (deslocamento isomérico) de 0,34-0,35 mm/s e QS (desdobramento quadrupolar) de 0,71-0,85 mm/s, respectivamente.

Acknowledgements: LNLS, CAPES, CNPq

TERMODINÂMICA DE FORMAÇÃO E ESTRUTURA DE MICELAS REVERSAS DE $(EO)_{13}$ $(PO)_{30}$ $(EO)_{13}$ EM P-XILENO

Gomes, D. S. B.[1], Teixeira, A. V.[1], Da Silva, L. H. M.[1], and Rocha, J.C.[1]

Universidade Federal de Viçosa - Viçosa MG Brazil

A macromolécula do copolímero tribloco utilizada neste trabalho (Pluronic L64 - $(EO)_{13}$ $(PO)_{30}$ $(EO)_{13}$) apresenta uma estrutura composta por duas regiões hidrofílicas: *Poli(Óxido de Etileno-PEO)* e outra hidrofóbica: *Poli(Óxido de Proprileno)-PPO* que, em solvente orgânico, formam micelas reversas acima de uma certa concentração (*Concentração Micelar Crítica-CMC*) e quando adicionada pequenas quantidades de água. A partir do diagrama de solubilidade da água no sistema binário L64+P-Xileno foi possível encontrar a CMC e com medidas de SLS*(Static Light Scattering)* , DLS*(Dynamic Light Scattering)* e SAXS *(Small-Angle X-Ray Scattering)* confirmar a formação desses agregados. Além de correlacionar com a variação entálpica do sistema por medidas de Microcalorimetria (*Isothermal Titration Calorimetry-ITC*).

Acknowledgements: Este trabalho foi financiado pelas agências: CAPES, CNPq e FAPEMIG. Ao Dr. Pedro Licínio Depto.de Física UFMG por gentilmente ceder o Laboratório de Espalhamento de Luz.

Thermal expansion of Ta_5Si_3 and Cr_5Si_3

Ribeiro, L.S.[1], Suzuki, P. A.[1], Renosto, S. T.[1], Nunes, C. A.[1], and Coelho, G. C.[1]

Escola de Engenharia de Lorena - Universidade de São Paulo - Lorena SP Brazil

The thermal expansion of metallic silicides has been investigated aiming possible applications to the high-temperature structural materials. Since these silicides crystallize in non-cubic structures, their coefficients of thermal expansion are usually anisotropic. The anisotropy is undesirable since it gives rise microcrackings. The thermal expansion of M_5Si_3-type compounds (M = metal) has been recently investigated. The silicide Ta_5Si_3 crystallizes in Cr_5B_3-type tetragonal structure known as T_2-phase while Cr_5Si_3 crystallizes in W_5Si_3-type tetragonal structure known as T_1-phase. The aim of this investigation was the determination of the thermal expansion coefficients and anisotropy for Cr_5Si_3 and Ta_5Si_3. The alloys of nominal compositions: $Cr_{62.5}Si_{37.5}$, $Cr_{62}Si_{38}$, $Ta_{62.5}Si_{37.5}$ and $Ta_{62}Si_{38}$ were prepared by arc-melting under argon atmosphere. The $Cr-Si$ alloys were sealed in quartz tube under argon and heat-treated at 1473 K for 24 h. The $Ta-Si$ alloys were heat-treated at 2173 K for 3 h under argon atmosphere. The high-resolution X-ray diffraction measurements at temperatures up to 873 K were performed at $LNLS-D10B-XPD$ beamline. The monochromatized energy of X-ray beam was set to 9.5 keV. The high-temperature measurements have been performed coupling $Arara\ I$ furnace to the $Huber$ diffractometer. The measurements were carried out in vacuum condition. The structural parameters were determined from Rietveld refinement method. The lattice parameters a and c as function of the temperature shown linear behavior for both Cr_5Si_3 and Ta_5Si_3. The thermal expansion coefficients and anisotropy for Cr_5Si_3 and Ta_5Si_3 were calculated through the variation of the lattice parameters.

Acknowledgements: This work has been partialy performed at LNLS-D10B-XPD beamline under Proposal n^o 6715/07. We wish to acknowledge Dr. Fabio F. Ferreira for his assistance in the measurements at XPD beamline. L. S. Ribeiro acknowledge CAPES for the financial support.

XANES of (Hg,Re)-1223 superconductor under pressure up to 6 GPa

Orlando, M. T. D.[1], J.L.Passamai Jr[1], Martinez, L. G.[2], E. J. Carvalho[3], Garcia, F.[3], and Corrêa, H. P. S.[4]

[1] Universidade Federal do Espírito Santo - Vitória ES Brazil
[2] Instituto de Pesquisas Energéticas e Nucleares - São Paulo SP Brazil
[3] Laboratório Nacional de Luz Síncrotron - Campinas SP Brazil
[4] Universidade Federal do Mato Grosso do Sul - Campo Grande MS Brazil

XANES under pressure were measured using a DAC pressure cell on rhenium edge (L_{III} - 10.535keV). The measurement were carried out at D06 - DXAS LNLS beamline. AC magnetic susceptibility of $Hg_{0.8}Re_{0.2}Ba_2Ca_2Cu_3O_{8.7+d}$ superconductors with different oxygen content (d=0.5, 0.1 and 0.15) presented different T_c behaviour as a pressure function up to 9 GPa. For the sample with optimum oxygen content (d=0.1) there exist an increment of T_c as a pressure function, which can not be explained, taken into account the charge pressure transfer term to be vanish. In this study the behaviour of XANES intensity under pressure up to 6 GPa was correlated with changes in T_c and Eg and T2g populations. Our preliminary conclusion is that the oxygen configuration in rhenium octhaedral is optimum for d=0.1, and it is correlated with the 180^0 for O-Cu-O bond angle in the superconductor layer. The octahedral confiruration of rhenium oxide for optimum oxygen content (D_h symmetry) is connected to the tetrahedral configuration of CuO_2 layers, which is associated to the superconductor properties. Our first conclusion is that there exist a correlation between the ReO_3 octhaedral symmetry for optimum oxygem content (D_h) and the tetrahedral symmetry shown in the CuO_2 layers.

Acknowledgements: We thanks to LNLS for help, experimental support, and data measurements.

RADIATION DAMAGE AND RADIATION INDUCED OXI - REDUCTION OF Eu IONS IN RARE EARTHS DOPED $SrAl_2O_4$

Montes, PJR[1] and Valerio, M.E.G.[1]

Universidade Federal de Sergipe - São Cristóvão SE Brazil

A new Sol-Gel methodology enables the production of nanopowders using lower calcination temperatures and shorter times, when compared to other ceramic routes like solid state reaction [1]. DXAS technique (Dispersive X-ray Absorption Spectroscopy) uses dispersive optics that allows acquiring measurements of a range of energies of an X-ray absorption spectrum simultaneously. Thereby other parameters can be incorporated in analysis like time, temperature, pressure, etc. The ionizing radiation can induce the reduction of Eu ions in $SrAl_2O_4$: Eu^{3+} [2]. Analysis of the reduction dynamics can give information of the radiation damage process in the samples and DXAS technique can be used to follow it. The aim of this work is to study DXAS as well as X-ray Excited Optical Luminescence (XEOL) of pure and rare earths doped $SrAl_2O_4$ produced via a new Sol-Gel Proteic methodology. Pure and rare earths doped $SrAl_2O_4$ were prepared via a sol-gel proteic methodology, using coconut water as the initial solvent. All samples were previously analyzed using X-ray powder diffraction (XRD) and the prepared materials presented single crystalline phase. The luminescence of the samples (XEOL spectra) due to the absorption of the X-rays was measured simultaneously with the DXAS spectra. X-ray absorption spectrum shows the typical absorption associated to the L3 europium edge of Eu ions. XEOL emission shows an intense peak around 515 nm followed by a weaker emission peaking at 624 nm. The first XEOL peak is due to the emission of Eu^{2+} while the second one is due to Eu^{3+} transitions. The area of the sample that was irradiated became dark indicating the production of irradiation damage that can be connected to the reduction process of Eu^{3+} to Eu^{2+}.

[1] M. A. Macedo, J. M. Sasaki, Processo de Fabricação de Pós Nanoparticulados, INPI 0203876-5.

[2] P. J. R. Montes, M. E. G. Valerio, G. de M. Azevedo. NIMB, doi:10.1016/j.nimb.2008.03.140.

Acknowledgements: Work supported by CNEN, CNPq, FINEP. DXAS and XEOL measurements were done at LNLS Brazilian Synchrotron Light Laboratory-MCT, under project number DXAS-7311/07

Alterações estruturais em $Fe[Co(CN)_6]$ sob altas pressões

Catafesta, J.[1], Zorzi, J. E.[2], Garcia, F.[3], Haines, J.[4], Pereira, A. S.[1], and Perottoni, C. A.[2]

[1] Universidade Federal do Rio Grande do Sul - Porto Alegre RS Brazil
[2] Universidade de Caxias do Sul - Caxias do Sul RS Brazil
[3] Laboratório Nacional de Luz Síncrotron - Campinas SP Brazil
[4] Université Montpellier II - Montpellier France

$Fe[Co(CN)_6]$, que possui uma estrutura similar à da perovskita, mas baseada em ligações metal cianeto metal, apresenta coeficiente de expansão térmico quase nulo. Diversos materiais com coeficiente de expansão térmico negativo (ou próximo de zero) amorfizam em altas pressões, mas a correlação entre os dois fenômenos ainda é objeto de discussão. Por isso, é fundamental investigar essa correlação em diferentes tipos de estrutura com essa característica. O comportamento em altas pressões do $Fe[Co(CN)_6]$ foi investigado por um conjunto de técnicas complementares de análise *in situ*: difração de raios X por dispersão em energia e dispersão angular (tubo de raios X convencional), absorção no infravermelho, espectroscopia Raman e espectroscopia de absorção de raios X (radiação Síncrotron). Acima de 10GPa este material apresenta padrões de difração de raios X característicos de fases amorfas. A fase amorfa formada em altas pressões é retida após o alívio da pressão. Amostras de $Fe[Co(CN)_6]$ recuperadas de 17 GPa apresentam uma coloração escura, com brilho metálico. O conjunto de resultados sugere que a amorfização induzida por altas pressões em $Fe[Co(CN)_6]$ é associada a um processo de decomposição, formando uma matriz de CN_x e, possivelmente, nanopartículas de Fe/Co.

Acknowledgements: Este trabalho foi parcialmente finaciado por PRONEX/MCT, CNPq, CAPES, FAPERGS e LNLS.

XAFS study of $Zn_{0.85}Co_{0.15}O$ powders prepared by ball milling

A.M. Mudarra Navarro[1], L.C.Damonte[1], and Rodríguez Torres, C. E.[1]

Universidad Nacional de La Plata - La Plata Bs.As Argentina

During the last decade, materials for spintronics or magnetoelectronics were studied widely because of their unique characteristics of using charge and/or spin of electrons simultaneously. Diluted magnetic semiconductors (DMS) are one of the most promising candidates, not only due to their broad applications fields, but also flexibility for spin injection and bandgap tunability, which is essential for spin lifetime. DMS materials are formed when conventional semiconductors are doped with transition-metal (TM) ions. In this work we present an EXAFS (Extended X-ray absorption Fine Structure) and XANES (X-ray Absorption Near Edge Spectroscopy) characterization of polycrystalline Co-doped ZnO oxide ($Zn_{0.85}Co_{0.15}O$). The samples were prepared by mechanical milling. The starting materials were commercial ZnO and CoO powders. The milling was performed in air at increasing times from 1 to 16h. X-ray absorption spectroscopy (XAS) measurements were taken at room temperature in transmission mode at the Co K-edge, using a Si (111) monochromator at the XAFS2 beamline of LNLS. We observed that oxygen coordination around Co decrease from 6 (that expected for the starting CoO phase) to 3.5 (likely Zn in ZnO structure). Co-Co coordination almost disappears after 16 h of milling and a contribution of a layer of Zn at 3.25 A appears. The distance Co-Zn and the coordination number are similar to those expected for Co substituting Zn in wurzite structure.

Acknowledgements: This work was supported by CONICET (PIP 6005) and Laboratorio Nacional de Luz Sincrotron (LNLS), Brazil.

Molecular Structure and Dynamics of Polyfluorene Derivative Films

Faria, G. C.[1], Plivelic, T.S.[2], Souza,A.A.[1], R. F. Cossiello[3], Atvars, T.D.Z.[3], Torriani, I.[2], and deAzevedo, ER[1]

[1] Universidade de São Paulo - São Carlos - São Carlos SP Brazil
[2] Laboratório Nacional de Luz Síncrotron - Campinas SP Brazil
[3] Universidade Estadual de Campinas - Campinas SP Brazil

Polyfluorenes are promising class of conjugated polymers due to high efficient eletro and photoluminescence, high charge mobility and thus great prospects for optoelectronic applications. These properties are close related to the polymer structure and mobility, making worthwhile to investigate details of the microstructure and optical properties. In this way, the report presents an investigation of the microstructure and dynamics of two polyfluorene based polymers, said Poly(9,9-dioctylfluorenyl-2,7-diyl) (Be329) and Poly[(9,9-dioctilfluorenil-2,7-diil)-co-1,4 phenilene-vinilene)] (Ge108), using Wide-Angle X-ray Diffraction (WAXD), Nuclear Magnetic Resonance (NMR), Dynamic Mechanical Thermal Analysis (DMTA) and Fluorescence Spectroscopy (PL). The WAXD measurements revealed that cast films prepared with Be329 are semi-crystalline and undergo a structural modification at around 430 K. In contrast, WAXD measurements revealed that Ge108 as cast films do not present crystallinity, but forms aggregated structures similar to a mesomorphic liquid crystal phase. Assuming a model for the aggregated structure, where the phenyl rings planes are stacked parallel to each other with an average distance of d1 $\sim$ 4.5 and laterally spaced by d2 $\sim$ 18, it was possible to associate these distances with specific peaks in the WAXD pattern. By doing so, the evolution of d1 and d2 as a function of temperature was probed, revealing that d1 remains mostly constant as a function of temperature until 380 K and then start increasing, reaching 5.5 at 420 K. d2 also present a trend change at 380 K, but in this case it first increases swiftly and than become more constant. DMTA data show that both polymers have a low temperature molecular relaxation at $\sim$ 330 K and a high temperature relaxation at 370 K. The microscopic nature of these relaxations was elucidated by solid-state NMR methods capable of detecting molecular dynamics of individual chemical groups. The results revealed that the low temperature relaxation is associated with motion in the side-chain, occurring with activation energies of $\sim$ 20 kJ/mol. It was also observed that the fraction of mobile side chains is higher in the Ge108 sample, pointing to the presence of rigid side-chains in Be329, probably in the crystalline phase.

Acknowledgements: The authors would like to thank FAPESP and CNPq.

ELECTRONIC PROPERTIES OF COORDINATION COMPOUNDS OF THE DMIT, DMIO AND DMT LIGANDS

Lopes, L. J. S.[1], Guerra, A. C. O.[2], Ferreira, G. B.[1], and Turci, C. C.[1]

[1] Universidade Federal do Rio de Janeiro - Rio de Janeiro RJ Brazil
[2] Centro Federal de Educação Tecnológica - Rio de Janeiro RJ Brazil

The sulphur heterocyclic systems are important coordination ligands because their electrical conduction, ferromagnetism and non-linear optic (NLO) [1] properties. The variety redox and polarizability of the sulphur atoms in the compounds are the main factors that contribute to those properties. Photoabsorption and Photoelectron spectra in the S 1s region of some organic derivates DMIT, DMIO and DMT ligands have been acquired for $[Ni(dmit)][NEt_4]_2$, $[Ni(dmio)][NEt_4]_2$, $[Ni(dmt)][NEt_4]_2$, $[Ni(dmio)]Cs_2$ and $[Ni(dmt)]Cs_2$ compounds. All compounds were synthesized following the literature [1−3]. TEY and XPS spectra have been acquired at Soft X-ray Spectroscopy (SXS) beamline, LNLS-Campinas (D04A-SXS-7730). The samples were introduced into the main chamber as a solid using a carbon sticky tape. The work pressure was kept at 2 x 10-8 mBar. The ionization potentials (IP) of these compounds have been determined and the electronic transitions have been studied. *Ab initio* calculations, associated with improved virtual orbital (IVO) method, carried out using the GSCF3 program, were considered to help us with the assignments. The geometric parameters were optimized with the GAMESS program.

[1]Svenstrup, N.; Becher, J. Synthesis. 1995, 215.
[2]Cassoux, P., et al., Coord. Chemistry Reviews, 185, 213, 1999.
[3]Steimecke, G., et al., E. Phosphorus and Sulfur, 12, 237, 1982.

Acknowledgements: LNLN, FAPERJ, CEFET/RJ.

Síntese, Caracterização e Fotoatividade de Fotossensibilizadores Derivados de Protoporfirina IX

Uchoa AF[1] and BAPTISTA, MS[2]

[1] Universidade de São Paulo - Ribeirão Preto - Ribeirão Preto SP Brazil
[2] Universidade de São Paulo - São Paulo - São Paulo SP Brazil

Processos que envolvem sensibilização são extremamente importantes para diversas áreas do conhecimento, incluindo a biologia, a química e a medicina. A aplicação de sensibilização em medicina tem se destacado, especialmente, em face de uma modalidade alternativa de tratamento de câncer denominada terapia fotodinâmica (TFD). Uma das linhas de pesquisas fundamentais para a evolução da terapia fotodinâmica é o desenvolvimento de novos fotossensibilizadores (Fs) com composição definida, que absorvam na janela terapêutica (600-800nm) e que apresentem maior eficiência na indução de apoptose. Os Fs que apresentam cargas positivas e que são relativamente lipofílicos, permeiam membranas e são atraídos pelo potencial negativo das mitocôndrias, que tem papel central no controle da vida e da morte celular. Neste trabalho foi realizado um estudo da influência dos grupos funcionais na atividade dos Fs, através da funcionalização da protoporfirina IX (Pp IX). Todos os compostos, foram caracterizados estruturalmente de forma inequívoca através do espectro eletrônico (UV-vis e fluorescência), vibracional no infravermelho, RMN de 1H e 13C (1D e 2D) e espectrometria de massa e enviados para determinação estrutural por cristalografia de Raio X no LNLS. A série de compostos obtidos permitiu um estudo da relação entre a estrutura química do Fs com a sua fotoatividade. As propriedades fotofísicas foram caracterizadas por espectro de absorção e de emissão, fotólise de relâmpago a laser, eficiência quântica de fluorescência e de geração de oxigênio singlete. Estas determinações indicaram que as propriedades fotofísicas dos Fs não foram consideravelmente alteradas no processo sintético. Foi determinada a formação de agregados em solução aquosa e o equilíbrio monômero agregado foi deslocado no sentido da formação do monômero na presença de micelas de CTAB e SDS e de soro fetal, também é sabido que o fator de agregação esta relacionado com fatores conformacionais e pode ser melhor interpretado uma vez determinado a conformação por cristalografia de raio x. Observou-se, que a contribuição para desagregação é mais eficiente quando a carga da micela é oposta à do Fs. Foi determinado o coeficiente de partição octanol/água (logPo/a) em função do pH e constatou-se que os compostos que têm carga líquida apresentam valores de logPo/a entre -1 e 1 na faixa de pH entre 3 e 10.

Acknowledgements: Capes/Fapesp

Caracterização estrutural de formas polimórficas de insumos farmacêuticos

Neves P.P[1], Doriguetto, A.C.[1], Mir, M.[1], Camps, I.[1], Pereira, S. V.[1], Martins, F. T.[1], and Ellena J.[2]

[1] Universidade Federal de Alfenas - Alfenas MG Brazil
[2] Universidade de São Paulo - São Carlos - São Carlos SP Brazil

O presente trabalho aborda o fenômeno do polimorfismo em sólidos farmacêuticos. Em ciências dos materiais, polimorfismo pode ser definido como a habilidade de uma mesma substância existir em duas ou mais formas cristalinas. De forma geral, as diferentes formas polimórficas de uma dada substância apresentam diferentes propriedades físicas e químicas, as quais podem causar variações nos parâmetros farmacocinéticos e mecânicos de ingredientes farmacêuticos produzidos na fomra sólida. Portanto, para explorar as vantagens que o polimorfismo pode oferecer e garantir a segurança terapeutica de um dado fármaco é fundamental que a sua estrutura cristalina seja perfeitamente caracterizada. Neste trabalho foram investigadas as características estruturais de amostras dos insumos farmacêuticos do fluconazol, mebendazol e nimesulida por meio das técnicas de difração de raios X por pó (DRXP) e análises térmicas. Os difratogramas de DRXP coletados com as facilidades da radiação síncrotron do LNLS apresentaram ótima qualidade. A alta resolução dos dados permitiu separar sobreposições das reflexões de Bragg dos diferentes polimorfos e extrair informações estruturais (indexação) das fases cristalinas dos fármacos estudados, especialmente para o fluconzol e mebendazol, que em geral, são constituídos por mistura de formas cristalinas. Difratogramas coletados em função da temperatura mostraram que a forma monohidratada do fluconazol converte-se na forma anidra entre 50 e 60^{o}C. As medidas térmicas confirmaram os resultados obtidos por meio das medidas de DRXP. Estamos trabalhando os dados de DRXP com objetivo de resolver a estrutura cristalina das formas cristalinas desconhecidas destes fármacos.

Acknowledgements: A FAPEMIG, FUNED, Núcleo de Controle de Qualidade da UNIFAL-MG e ao Laboratório Nacional de Luz Síncrotron.

Ordem química local em nanocristais de GaSb em função da temperatura

Campos, C. E. M.[1] and De Lima, J.C.[1]

Universidade Federal de Santa Catarina - Florianópolis SC Brazil

A liga $GaSb$ nanocristalina foi produzida via mecano-síntese (MS) no Laboratório de Síntese e Caracterização de Materiais ($LSCM$) no DF-UFSC. A estrutura atômica desta liga foi determinada através da difração de raios X (XRD) como sendo do tipo blenda de zinco ($ZB - GaSb$) e suas propriedades térmicas e ópticas foram investigadas através de calorimetria (DSC) e espectroscopia Raman (RS) [1]. As larguras de linha do padrão de difração e medidas de microscopia eletrônica de transmissão de alta resolução (HR-TEM) atestam o caráter nanométrico da amostra. A transição semicondutor-metal da liga com pressão foi verificada por absorção de raios X (XAS) e Raman [2]. As pressões de transição observadas foram 9 GPa, por ambas técnicas, ligeiramente superiores que aquelas reportadas para amostras bulk (7 GPa). Já os modos de compressibilidade ficaram entre valores de cristais *bulk* e amorfos [3-5]. O presente pôster pretende complementar o rol de informações disponíveis acerca de nanocristais de $GaSb$ produzidos por MS, apresentando medidas XAS com função da temperatura, desde 10 K até 300 K. Também é objetivo desta apresentação levantar discussões com demais participantes da reunião acerca das estratégias e programas disponíveis para realizar o tratamento de dados EXAFS. Os resultados apontam para um aumento da desordem química e também um ligeiro aumento nas distâncias interatômicas com o aumento da temperatura, exatamente como esperado.

Referências:

[1] Campos, C. E. M., Lima, J. C., Grandi, T. A., Schmitt, M. and Pizani, P. S., J. Phys.: Condens. Matter 18 (2006) 86138622.

[2] Campos, C. E. M., Lima, J. C., Grandi, T. A., Pizani, P. S., Itié, J. P., Polian, A., Chervin, J.C., Saitovich, E. B., J. Phys.: Condens. Matter 20 (2008) 275212.

[3] Al-Douri Y Pdf file in the web yaldouri@yahoo.com.

[4] Cohen M L 1985 Phys. Rev. B 32 7988.

[5] Lyapin A G, Brazhkin V V, Bayliss S C, Sapelkin A V, Itie J P, Polian A and Clark S M 1996 Phys. Rev. B 54 14242.

Acknowledgements: Os autores desse estudo agradecem ao LNLS (proposta XAS 5728/07), CNPq e a CAPES pelo apoio financeiro; e a Profa. Dra. Ruth Hinrichs (IF-UFRGS) pelas imagens HR-TEM.

Chemical enviroment of europium in low silica calcium aluminosilicate glasses

Sampaio, J. A.[1], Filadelpho, M. C.[1], Rohling, J.H.[2], Medina, A.N.[2], Baesso, M.L.[2], and Andrade, A. A.[1]

[1] Universidade Estadual Norte Fluminense - Campos dos Goytacazes RJ Brazil
[2] Universidade Estadual de Maringá - Maringá PR Brazil

Europium doped glasses belong to an important class of materials because they can be used in a variety of applications such as two-dimensional x-ray imaging sensors, high-density memory devices, blue emitting phosphors for plasma display panels, and x-ray storage. Since divalent Eu emission intensity is strongly dependent on the temperature, these materials can be used as sensor devices. While divalent europium doped materials can be used as luminescent source in the UV to blue-green, the trivalent ones found applications in the orange-red region. The advantage of using glasses in relation to crystals lies in their homogeneity and ease of fabrication into various shapes, such as flat boards, fibers, and rods. Among the lanthanides elements only Sm, Eu, Tm, and Yb are susceptible to exist in the divalent state, and the finding of such a state in oxide glasses is an exception. Usually, only Eu^{2+} can be added into the glass network without difficulty and in a higher fraction than Eu^{3+} ions. Depending on the composition and preparation method, the ratio Eu^{3+}/Eu^{2+} can vary from 30 to 100%, as for example in the case of some borate glasses. Whereas in fluorofosphate glasses 30% of Eu ions can be reduced to the Eu^{2+} state, in metaphosphate glasses the proportion is only 2%, and in ultraphosphate glasses there is no observation of such state. To the best of our knowledge there is investigation regarding Eu valence state ratio in low silica calcium aluminosilicate glasses. In order to fill out this lack of information, in this work we have investigated the chemical environment of Eu in calcium aluminate glasses as a function of the Eu_2O_3 using X-ray Absorption Near Edge Structure (XANES). The Eu L_{III}-edge (6977 eV) x-ray absorption spectra were acquired at LNLS on the D08B-XAFS2 station. The data was collected in the fluorescence mode by a 15 element LEGe array Canberra GL0055S detector. At least six scans were collected for each sample, which were averaged to increase the quality of the experimental data. The data were analyzed by IFEFFIT package. From XANES spectra we observed that both Eu^{2+} and Eu^{3+} were present in the samples. For the sample doped with 5.0 wt% of Eu_2O_3 the ratio of Eu^{2+} is 26% and for Eu^{3+} is 74%. Magnetization measurements provided similar results, i.e., 30 and 70% respectively.

Acknowledgements: This work has been supported by the Brazilian Synchrotron Light Laboratory (LNLS) under proposal D04B - XAFS1 6594, FAPERJ and CNPq.

Long-range ordering in $Pb_{1-0.5x}La_xTiO_3$ relaxor ferroelectric ceramics

Doriguetto, A.C.[1], Neves P.P[1], Mir, M.[1], Mastelaro, V.R.[2], Mascarenhas, Y.P.[2], and Landre, I. M. R.[1]

[1] Universidade Federal de Alfenas - Alfenas MG Brazil
[2] Universidade de São Paulo - São Carlos - São Carlos SP Brazil

The understanding of the structural origin of relaxor ferroelectrics has been doubtlessly a long-standing puzzle in the field of ferroelectricity. Recently, we have carried out for the first time [*Neves et al. J. Phys. Chem. B 2004, 108, 14840-14849*] combined X-ray absorption spectroscopy (XAS) and X-ray diffraction (XRD) experiments to probe the sort- and long-range order in lanthanum-modified $PbTiO_3$ ceramic materials ($Pb_{1-1.5x}La_xTiO_3$, or PLT) for x ranging from 0 to 30 atom % of La. XRD results show that tetragonal structure fitted well to all samples, except to the one with x = 0.30 for which XRD results highlighted a cubic unit cell. In another work [*Mastelaro et al. J. App. Phys. 2008 submitted*], we have studied the long and short-range order structure of the PLT and its dependence with the normal and relaxor behavior presented on PLT ceramics with x=0.20 (normal ferroelectric) and x=0.30 (relaxor ferroelectric) by in-situ XRD and XAS techniques above and below T_c and T_m respectively. The XRD results shows that although the x=0.30 sample is characterized from dielectric measurements as presenting a relaxor character, a structural phase transition from a cubic to a tetragonal symmetry was observed below T_m. This behavior has been interpreted as a spontaneous phase transition effect where material that is a relaxor undergoes a spontaneous phase transition into a normal ferroelectric material upon cooling. Motivated by the interest in improving the comprehension of this important issue, this work is proposed for studying the PLT intermediate composition with x = 0.26. The XRD patterns were collected on a Huber diffractometer (D10B - XPD). To study the behavior of the phases as a function of the temperature, some peaks were selected and measured varying the temperature with a step of 10 K around the transition temperature (280 K). In order to determine precisely the structure below and above T_c, Rietveld refinements were performed on the patterns collected at 400 and 40 K. The crystallographic phases are discussed and compared with the compositions studied previously and with the sort-range order probed by XAS.

Acknowledgements: This work has been supported by LNLS (under proposal D10B - XPD 5816), FAPESP and FAPEMIG.

EFFECT OF THE STATE OF METALS OXIDATION ON POLYSULFUR LIGANDS

Turci, C. C.[1], Guerra, A. C. O.[2], Comerlato, N.M.[1], Lopes, L. J. S.[1], and Ferreira, G. B.[1]

[1] Universidade Federal do Rio de Janeiro - Rio de Janeiro RJ Brazil
[2] Centro Federal de Educação Tecnológica - Rio de Janeiro RJ Brazil

The 1,3-dithiole-2-thione-4,5-dithiolate ligand represents one of the main polysulfur systems of this class. The discovery of these no usual electric properties for transition compounds of the nickel group was the main incentive for these studies [1]. In the search of the understanding and reproduction of these properties, several coordination compounds with different metals were prepared systematically. Our research group works intensively in the preparation of compounds with several representative elements of the groups 14, 15, 16 [2–4]. In this current work, we related effects of the substitution of different transition metals in some borders of the sulfur (1s and 2p) for Photoabsorption and Photoelectron spectra, which are present in these systems. The coordinated metals chosen were zinc, copper, nickel and cobalt. The compounds containing cobalt were synthesized in two different oxidation states, +2 and +3, while the others ino only one state of oxidation, +2. The evaluated compounds were $[Zn(dmit)_2][NEt_4]_2$, $[Cu(dmit)_2][NEt_4]_2$, $[Ni(dmit)_2][NEt_4]_2$, $[Co(dmit)_2][NEt_4]_2$, $[Co(dmit)_2][PPh_4]$, $[Co(dmit)_2]Cs_2$. TEY and XPS spectra have been acquired at Soft X-ray Spectroscopy (SXS) beamline, LNLS-Campinas (D04A - SXS 5725, D04A - SXS -7730). The samples were introduced into the main chamber as a solid using a carbon sticky tape. The work pressure was kept at 2×10^{-8}mBar. The ionization potentials (IP) of these compounds have been determined and the electronic transitions have been studied. Ab initio calculations associated with improved virtual orbital (IVO) method, carried out from the GSCF3 program, were used to help us in the assignments. The geometric parameters were optimized with the GAMESS program. References [1] Cassoux, P., et al., Coord. Chemistry Reviews, 185, 213, 1999. [2] Comerlato, N., et al., Inorg. Chimica Acta, 357, 1487, 2004. [3] Comerlato, N., et al., Inorg. Chemistry Comm., 9, 522, 2006. [4] Comerlato, N., et al., Organomet. Chemistry, 693, 2424, 2008.

Acknowledgements: This work was supported by D04A - SXS 5725, D04A - SXS -7730 and FAPERJ. We also thanked the experimental support of the staff of SXS, especially to researcher Flavio Vicentine.

Synthesis and Properties of Titanate nanotubes modified.

Viana, B. C.[1], Ferreira, O.P.[2], SOUZA FILHO, A. G.[1], and Alves. O. L.[2]

[1] Universidade Federal do Ceará - FORTALEZA CE Brazil
[2] Universidade Estadual de Campinas - Campinas SP Brazil

This work reports the structural, morphological and vibrational properties of titanate nanotubes and nanoribbons obtained from bidimensional (lamellar) structures through hydrothermal treatment of TiO_2 in aqueous $NaOH$ solutions. The physical properties of these as-synthesized and heat-treated nanostructures are discussed in comparison with their bulk ($Na_2Ti_3O_7$ and $Na_2Ti_6O_{13}$) counterparts. The results obtained from transmission electron microscopy, scanning electron microscopy, atomic emission spectroscopy, energy dispersive X-ray spectroscopy, X-ray diffraction, infrared and Raman spectroscopies allowed concluding that the layers of both as-synthesized titanates nanotubes and nanoribbons are isostructural to the $Na_2Ti_3O_7$ lamellar compound. In the titanate nanotubes the chemical bonds are deformed because of the curvature of walls while in the titanates nanoribbons the layers present structural disorder by size effects. The thermal behavior of titanate nanoribbons is similar to those reported in literature for titanate nanotubes, where structural and morphological changes with increases of temperature are observed and indicated that the nanoribbons, at high temperatures, change to bulk with a phase mixing of $Na_2Ti_3O_7$ and $Na_2Ti_6O_{13}$. This is similar to what happens with the bulk $Na_2Ti_3O_7$ when thermally treated. Thus, we conclude that the chemical composition of both the titanate nanotubes and the titanate nanoribbons is the same, $Na_{2-x}H_xTi_3O_7.nH_2O$ ($0 \leq x \leq 2$). Also, we suggest that Raman spectroscopy can be used for an easy and quick identification of both morphology and structure changes of the nanosized titanates. After, we modified titanate nanotubes by incorporation of transition metals. We studied and characterized these samples in comparison with pure titanate nanotubes. we observed that ion exchanged nanotubes showed that the absorption edge exhibited a dramatic red shift into the visible light range.

Acknowledgements: Financial support from the Brazilian funding agencies CNPq, CAPES, FUNCAP and FAPESP is gratefully acknowledged. The authors are indebted to Dr. Carlos A. P. Leite for assistance with the TEM images and to Prof. C. H. Collins (IQ-UNICAMP, Brazil) for English revision. Bartolomeu C. Viana thanks to the laboratório nacional de luz sincrotron (LNLS) for training and images in transmission electron microscope - high resolution. This is a contribution of Millennium Institute of Complex Materials (PADCT/MCT) and the Rede Nacional de Pesquisa em Nanotubos de Carbono CNPq/MCT.

ESTUDO DA ESTRUTURA LOCAL DO $Ba_{0,77}Ca_{0,23}TiO_3$:Nd^{3+} POR ESPECTROSCOPIA DE ABSORÇÃO RAIOS-X.

Moraes, A. P. A.[1], SOUZA FILHO, A. G.[2], Azevedo, G. de M.[3], Antonelli, E.[4], and MPeko, J.-C.[4]

[1] Universidade Federal do Ceará - Fortaleza CE Brazil
[2] Universidade Federal do Ceará - FORTALEZA CE Brazil
[3] Laboratório Nacional de Luz Síncrotron - Campinas SP Brazil
[4] Universidade de São Paulo - São Carlos - São Carlos SP Brazil

Neste trabalho estudamos a estrutura atômica local do $Ba_{0,77}Ca_{0,23}TiO_3$ puro e dopado com Nd^{3+} via Espectroscopia de Absorção de Raios-X nas bordas K do Titânio (Ti) e Cálcio (Ca). A região da pré-borda do espectro de absorção da borda K do Ti apresenta três bordas (A,B,C) bem definidas. A borda "A" corresponde a transição quadrupolar 1s-3d no átomo de Titânio. A borda "B" também possui a componente quadrupolar 1s-3d e uma componente dipolar para o estado p induzida pela hibridização dos estados 3d do Ti com os estados p dos oxigênios vizinhos ao Titânio. A intensidade do pico B depende fortemente da natureza da Perovskita. A borda "C" é devido aos vizinhos do átomo de Ti e tem um caráter dipolar. Na borda K do Cálcio (Ca) existe uma pré-borda similar à encontrada em metais de transições 3d. A borda "A" é normalmente atribuída à transições eletrônicas a partir dos estados 1s do Ca ligados aos orbitais moleculares 2p do oxigênio ou 3d do Ca e suas origens podem estar relacionadas ao rearranjo dos átomos de oxigênio vizinhos aos íons do Ca. A borda B, C e D são originadas principalmente das transições 1s-4p do Ca de acordo com a regra de seleção do momento de dipolo. Cálculos de primeiros princípios foram realizados usando uma super-célula (2x2x2) $Ba_{0,77}Ca_{0,23}TiO_3$ usando o formalismo LDA implementado no código CASTEP e base do tipo DZP. Os resultados teóricos são discutidos comparando com os resultados experimentais na tentativa de identificar as transições observadas em cada borda.Os resultados obtidos por EXAFS mostram que o íon Nd^{3+} ocupa o sítio A quando incorporado na estrutura do BCT23 puro.

Acknowledgements: Este trabalho foi financiado pelo CNPQ e LNLS.

Structural characterization of $La_{0.80}Sr_{0.30}Mn_{0.90}Cr_{0.10}O_3$

Cavalcante, I. P.[1], Corrêa, H. P. S.[1], Dorotéia F. Bozano ou D. F. Bozano[2], Orlando, M. T. D.[3], and Martinez, L. G.[4]

[1] Universidade Federal do Mato Grosso do Sul - Campo Grande MS Brazil
[2] Universidade Federal de Mato Grosso - Cuiabá MT Brazil
[3] Universidade Federal do Espírito Santo - Vitória ES Brazil
[4] Instituto de Pesquisas Energéticas e Nucleares - São Paulo SP Brazil

In recent years, the development of conductive ceramics has been intensified not only due to demands in several areas, especially for their application in Solid Oxide Fuel Cells (SOFCs). The development of low internal resistance SOFC allows the increase of energy conversion efficiency as well as cost reduction. Nowadays the research efforts are concentrated mainly in the search for materials compatible to high temperature (approx. 800°C) operation, aiming to the elimination or reduction of thermal stress and losses in physical-chemical properties due to reactions among component materials, with consequent loss of performance. The lanthanum manganite (electrode material) and the lanthanum chromite (interconnector material) are constituent parts of SOFCs. In the present work the lanthanum manganite and chromite are studied in a solid solution, obtained via solid state reaction, presenting the composition $La_{0.80}Sr_{0.30}Mn_{0.90}Cr_{0.10}O_3$. In its structural characterization, preliminary analyses performed with copper radiation in conventional diffractometer showed a non efficient contrast between Mn and Cr. By means of synchrotron light we could make use of anomalous scattering, by collecting data close to the absorption edge of Cr (5.9625 keV). The measurement at the energy of 5.9625 keV produced a better contrast between the scattering factors of Cr and Mn atoms. The measurements were carried out at D12A XRD1 LNLS beamline.

Acknowledgements: The authors thank the LNLS for the use of its facilities and for technical support.

Electronic structure, stability and surface tension of ZrO_2 nanoparticles

Casali, R.A.[1], Ponce, C.A.[1], and Caravaca, M.A.[1]

Universidad Nacional del Nordeste - Corrientes Argentina

Based on previous experience in the characterization of group IV-B oxides, in different phases, simulated with the DFT based SIESTA code, small clusters and nanoparticles of ZrO_2, are studied up to a maximum size of 2.4 nm. The particle total energy is minimized by allowing the full relaxation of atomic coordinates. Nanoparticles with tetragonal symmetry and with different shapes and surface terminations, are here studied. Density of electronic states are characterized and correlated with structural order/disorder of the nanoparticle. The relation between size of the crystalline core, surface tension is attempted to found as a function of the size and shape of the particle, and surface termination. In order to mimic real nanoparticles, the change on the electronic structure and atomic coordinates are also studied upon doping with an oxygen vacancy. The present results conduct to the determination of particle internal pressure, which is though to correlate with phase transitions under extreme conditions, like high pressures.

Acknowledgements: This work was supported by Facultad de Ciencias Exactas and Facultad de Ingenieria, SECYT-UNNE and CONICET (Argentina) and by the Laboratorio Nacional Luz Sincrotron (Campinas, Brasil)

ESTRUTURA MAGNETICA DO INTERMETALICO TbCo2B2C

R. M. Briones[1] and ElMassalami,M; El Massalami, M; Massalami, M[1]

Universidade Federal do Rio de Janeiro - Rio de Janeiro RJ Brazil

Estudamos a magnetização, calor especifico, magnetostriçao e difração de nêutrons do composto TbCo2B2C. O composto manifesta um comportamento paramagnético Curie-Weiss na faixa de temperatura 77 ¡ T ¡ 300 K. Os momentos do Tb ordena se em Tc = 6.3K, e sua sub rede experimenta uma transição de fase ferromagnética com o eixo de fácil magnetização apontando na direção (100). Resultados de magnetostriçao mostram uma distorção da estrutura cristalina tetragonal para uma ortorrômbica embaixo de seu Tc. O TbCo2B2C tem a mesma estrutura cristalina do TbNi2B2C, mas sua estrutura magnética é diferente apresentando este uma estrutura antiferromagnética com TN = 15K, onde o Ni comporta-se como diamagnético. O surgimento do estado ferromagnético na sub rede do Tb no TbCo2B2C, induze um campo efetivo atuando sob os Co que poderia polarizar o subsistema Co 3d, mais os resultados da magnetização e difração de nêutrons (com monocristais) não mostraram tal ordenamento do Co o que indicaria que o campo efetivo atuando sob os Co é menor que o seu campo critico.

Acknowledgements: Agradeço ao Capes, pela bolsa de doutorado

Ternary Ni-based boro-aluminides (Al-Ni-B): their synthesis, structure, and physical characterization.

M. M. Elhadi[1] and ElMassalami,M; El Massalami, M; Massalami, M[1]

Universidade Federal do Rio de Janeiro - Rio de Janeiro RJ Brazil

The Ni-Based aluminides are potential candidates for engineering application at elevated temperatures. As such application requires, in addition, reasonable malleability and good creep-resistance; these aluminides are often alloyed with boron in order to overcome these drawbacks. This triggered an active interest in the investigation of the ternary phase diagram of the Al-Ni-B system. Despite the scientific and technological interest. There is hardly any information on the physical properties of the stable ternary Al-Ni-B compounds. The aim of this project is to map out the magnetic, transport, and thermal properties of these ternary compounds and to evaluate the role played by the metalloid in shaping these properties. Using induction and arc-melt techniques, we synthesized all ternary compounds that are reported to be stable at the 1000C isothermal section. In addition, we synthesized and investigated the structural and thermal stability of Al3Ni2B, Al2Ni3B, AlNiB3, and Al3Ni5B composition. The magnetization and specific heats os all samples were measured down to 20 mK. Neither superconductivity nor (de) localized magnetism has been observed in any sample, rather the magnetizations is small, positive, and temperature-independent and low-temperature specific heat is the sum of a Debye and a Sommerefeld contribution. It is observed that while the Debye temperatures are the same for all compounds, their magnetization and Sommerefeld coefficients are found to correlate strongly with the content of the Ni in each unit formula. This correlation is indicative of the substantial contribution of the Ni 3d band to the density of state at the Fermi level. For the particular case of Al3Ni20B6 (Sommerefeld coeffecien = 48 mJ/mol K), this contribution is found to be significantly higher than expected for such a type of aluminides. Based on the measured physical properties, we discuss the possible configuration of the electronic structures of the studied samples.

Acknowledgements: This Work was Supported by CNPq and El Neelain university-Sudan

Insights on growth mechanism of Carbon Nanofibers: Catalyst particle studied by Transmission Electron Microscopy and additional techniques

Roa, D. B[1], S de Oliveira[1], Ferlauto, A. S.[1], Ladeira L.O.[1], Magalhaes-Paniago, R.[1], and Lacerda, R. G.[1]

Universidade Federal de Minas Gerais - Belo Horizonte MG Brazil

A detailed investigation of catalyst particle is necessary to study the growth mechanism of Carbon Nanofibers (CNFs) and Transmission Electron Microscopy (TEM) is fundamental to this knowledge. Some analytical techniques associated with TEM was being used: Bright and Dark Field Images; Selected Area Electron Diffraction (SAD); High Resolution Transmission Electron Microscopy (HRTEM). As additional techniques: Scanning Electron Microscopy (SEM); Mössbauer Spectroscopy; Energy Dispersive X-Ray Spectroscopy (EDS). Series of depositions optimizing the parameters of CNFs growth using Ni as catalyst are presented for further understanding. It was possible to characterize the crystalline structure of CNF as herringbone type. The particle deriving from a catalyst film of Fe is the focus on analysis by TEM. The particles studied have chemical formula Fe_3C and orthorhombic crystal system. They usually consist on a great monocrystal obeying a orientation that seems to have crystallographic relations with the fiber axis. There is an evidence that the graphitic sheet arises in particular facets exposed by the particle. The Mössbauer Spectroscopy ratify the structure founded and also shows a small amount of other Iron's phase, Austenite γ-Fe, whose particles probably can not be founded by TEM. The EDS shows the chemical composition in a few points its particle and some elements, Si and O, seem to involve it. The information obtained provides facts that suggest a possible growth mechanism.

Acknowledgements: This work was supported by CNPq, Capes, Fapemig, LNLS e Rede de Nanotubos.

Lattice distortions in oxygen deficient $SrMnO_y$ compounds.

Suescun, L.[1], Dabrowski B.[2], Faccio, R.[1], and Mombrú, A.W.[1]

[1] Universidad de la República - Montevideo Uruguay
[2] Northern Illinois University - DeKalb Illin United States of America

$SrMnO_3$ with perovskite structure is the end member of the $La_{1-x}Sr_xMnO_{3-d}$ series, interesting from various technical and fundamental points of view. Materials with 0.2<x<0.4 and d<0.1 find application as SOFC cathodes while materials with x=0.5 (and d=0) show the CO/OO state typical of colossal magnetorresistant materials. Oxygen deficient $SrMnO_y$ 2.8<y<3 with perovskite structure is difficult to prepare [1]. A 3-step process that includes preparation of highly oxygen deficient $SrMnO_y$ y∼0.4 in pure Ar at 1400 C, oxidation to $SrMnO_3$ in air at 500 C and posterior reduction in H_2 or Ar (or a mixture of both) or high vacuum at low temperatures 200-500 C is needed to achieve the desired phases [2]. The last two steps of the synthesis are performed in a thermo-balance to achieve exact control of oxygen content. Structural distortions from the cubic $SrMnO_3$ compound are expected when oxygen content is reduced due to the increase in the average charge and size of B-site Mn, with consequent decrease in Goldschmidt tolerance factor. Distortion increases with decreasing oxygen content until a point where oxygen vacancies achieve ordering and the structure suffers a dramatic change in symmetry and properties. In the disordered state, $SrMnO_y$ are semimetals with significant ionic conductivity, which both disappear after charge and orbital ordering associated with oxygen vacancy ordering [3] at y=2.714. Different oxygen vacancy ordered phases with y=2.5 ($Sr_4Mn_4O_{10}$), 2.6 ($Sr_5Mn_5O_{13}$) and 2.714 ($Sr_7Mn_7O_{19}$) [4] but no data is available regarding higher oxygen contents. We have performed high resoultion x-ray powder diffraction experiments on $SrMnO_y$ 2.5<y<3 samples at D10B-XPD and 11BM-B stations at LNLS and APS-Argonne, USA aiming to fully understand structural relations and phase transitions in the ($SrMnO_y$) system. In this report we will show that a miscibility gap is found between vacancy ordered y=2.714 and disordered y=2.85 phases and the evolution of lattice distortions from tetragonal P4/mbm (2.93<y<2.99) to cubic Pm3m (y=3) symmetry through a rhombohedral R-3c in a narrow y region (2.99<y<3), generated by oxygen vacancies. [1] Negas T., Roth S.J. JSSC 1 (1970) 409. [2] Chmaissem O. et al, PRB 67 (2003) 094431. [3] Suescun L. et al, JSSC 180 (2007) 1698. [4] Suescun L., Dabrowski B., Acta Cryst. B 64 (2008) 177.

Acknowledgements: LS is indebted to the LNLS and ABTLUS for support to perform experiments at LNLS. Use of APS was supported by US DOE, BES contract No DE-AC02-06CH11357 and NSF grant No DMR-0302617.

Analysis of Prostate Tissues using SRTXRF

Leitão,R.G[1], Canellas,C.G.L[1], Palumbo, A.J[1], Souza, P.A.V.R[1], Nasciutti, L.E[1], Anjos, M. J.[2], and Lopes, R.T.[1]

[1] Universidade Federal do Rio de Janeiro - Rio de Janeiro RJ Brazil
[2] Universidade do Estado do Rio de Janeiro - Rio de Janeiro RJ Brazil

Prostate cancer (PCa) is one of the main causes of illness and death all over the world. In Brazil, prostate cancer currently represents the second neoplasia more frequent in man, representing 21% of the total number of cases. Total Reflection X-Ray Fluorescence spectroscopy using synchrotron radiation (SRTXRF) was applied to fifty nine patients: 44 Benign Prostate Hyperplasia (BPH), 11 PCa and 4 normal tissues of human prostate, in order to investigate the differences in the elemental concentrations in these tissues. The measurements were carried out at the X-ray fluorescence beam line at Brazilian National Synchrotron Light Laboratory (LNLS), in Campinas, São Paulo using a quasi-monochromatic beam produced by a multilayer monochromator at 16 keV to sample excitation. Elemental concentrations of the elements P, S, Cl, K, Ca, Fe, Cu, Zn, Br and Rb were determined. Experimental results were shown as the mean and confidence interval. Differences between two sets of data were compared by Student's t test. All statistical tests with a p-value of less than 0.05 were considered statistically significant. Utilizing Students t-test analysis on the obtained results, it was possible to observe that certain elements present statistical differences : P, Cl and K (BPH x Normal); P, Cl, K, Fe, Zn and Rb (PCa x Normal); Ca, Zn and Rb (BPH x PCa). Zinc concentration in BPH is approximately twice higher than in PCa, showing that Zn can be investigated as a bioindicator of the Prostate Cancer development.

Acknowledgements: This work was developed partially at Brazilian National Synchrotron Light Laboratory (projects XRF 5959 and XRF 6736) and had the financial support of CNPq and CAPES.

Structural and Magnetic Characterization of $Cu_{1-x}TM_xO$ (MT = Co, Fe, Ni)

Duque J.G.S.[1], Meneses, C. T.[1], and Knobel, M.[2]

[1] Universidade Federal de Sergipe - São Cristóvão SE Brazil
[2] Universidade Estadual de Campinas - Campinas SP Brazil

Stoichiometric CuO is a Mott-Hubbard insulator with a gap of the charge-transfer type [1]. On the other hand, it has been reported [2] that oxygen vacancies can cause a narrowing of its band gap. From the point of view of high-T_C superconducting cuprates, the CuO can offer an easier scenario to understand the role of the copper in the appearing of the superconductivity in cuprates high-T_C. Recently, Zheng et al. [2] observed the T_N suppression of CuO doped with a non-magnetic Li^{1+} ion. It is well known that this kind of doping create one hole in the valence band because the charge difference between Cu^{2+} and Li^{1+} ions. Magnetic order was shifted to around 100 K at concentrations larger than 16%. This suppression is believed to be due the different electronic structure of the Li^{1+} ion related Cu^{2+}. To test the role of the electronic structure in the magnetic ordering of CuO we have used the co-precipitation method to synthesize polycrystalline TM-doped CuO samples (TM = Ni^{2+} and Fe3+). The magnetic and structural properties of $Cu_{1-x}TM_xO$ samples have been investigated as function of doping concentrations(x). Magnetization measurement as function of temperature show that T_{N2} is suppressed from 213 K (CuO) to 70 K in the Fe-doped sample with concentration around x = 0.06. Surprisingly, for Ni-doped samples, T_N seem to be unaffected by the T_M substitution. X-ray absorption analysis be presented for the systems in regions of the magnetic transitions T_N.

References:
[1] J. Zaanen et al, Phys. Rev. Letters 55, 418, 1985.
[2] X. G. Zheng et al, Phys. Review B 67, 094610, 2004.

Acknowledgements: This work was supported by FAPESP and CNPq

HRTEM and XAS study of V_2O_5 nanoparticles prepared through the hydrothermal method

Avansi, W.[1], Ribeiro, C.[2], Leite,E.R.[3], and Mastelaro, V.R.[1]

[1] Universidade de São Paulo - São Carlos - São Carlos SP Brazil
[2] Empresa Brasileira de Pesquisas Agropecuárias - São Carlos SP Brazil
[3] Universidade Federal de São Carlos - São Carlos SP Brazil

The ease with different ions can be intercalated into the layered structure of $V_2O_5nH_2O$ compound makes it a promising material for applications such as lithium batteries, gas sensors, catalysts and electrochromic devices [1]. The application of this compound is strongly related of the morphology, the amount of water in the layered structure (n) and the oxidation state of vanadium atom. The objective of this work is the study of the short-range order structure and crystal growth mechanism in this material synthesized through a hydrothermal process, as a function of different synthesis parameters. The samples were prepared through a hydrothermalthe treatment of 0.06M peroxovanadate solution prepared by the dissolution of V_2O_5 powder in distilled water followed by the addition of 30% of H_2O_2. Depending on the temperature (in 60 200^{o}C range) and time of treatment, $V_2O_5nH_2O$ nanoparticles with different crystalline structure, morphology and amount of water content were obtained. The oxidation state and the local structure of vanadium atoms were obtained by measuring the X-ray absorption spectra at the V K-edge at the D04B-XAFS1 and D08B-XAFS2 LNLS beam lines. To study the morphology and the mechanism of nanoparticles growth, a high-resolution transmission electron microscopy (HR-TEM) provided by LME-LNLS was used. From the analysis of the XANES spectra we observe only the presence of V^{4+} ions and it was observed that the distortion on the VO_5 units varies with the temperature of heat-treatment. The local symmetry around vanadium atoms is particularly different on $V_2O_5nH_2O$ samples presenting a ribbon morphology. The analysis of HRTEM images clearly shows that the morphology of nanoparticles depends mainly on the time and temperature of the hydrothermal treatment. Moreover, HR-TEM micrographs shows that the nanoparticles growths preferentially on the [010] direction. [1] C. Xiong, A. E. Aliev, B. Gnade, K. J. Balkus, ACS Nano 2 (2), 293 (2007).

Acknowledgements: The authors are grateful to FAPESP and CNPq for financial support.

Crystallographic Changes Accompanying the Verwey Transition in a Magnetite from Steatite

Silva, F. D. da[1], FABRIS, J. D.[2], COUCEIRO, P.R.C.[3], and Goulart, A.T.[2]

[1] Centro Universitário de Patos de Minas - Patos de Minas MG Brazil
[2] Universidade Federal de Minas Gerais - Belo Horizonte MG Brazil
[3] Universidade Federal do Amazonas - Manaus AM Brazil

Magnetite (ideal formula, Fe_3O_4); cubic, space group *Fd3m* is a ferrimagnetic iron oxide (saturation magnetization, 95.0 J T^{-1} kg^{-1}, at 298 K) with inverse spinel structure. The mineral undergoes the Verwey transition, characterized by electrical, magnetic and a first order crystallographic structural change, from cubic to monoclinic, at T_V = 120 K. Below T_V, the electrical resistivity of the oxide increases by two orders of magnitude. The still currently prevailing model, originally proposed by Verwey, considers that the high conductivity of magnetite at higher temperatures is due to the fast electron transfer between Fe^{2+} and Fe^{3+} ions in octahedrally coordinated sites. At T less than T_V, the Fe^{2+} and Fe^{3+} ions tend to be increasingly ordered, towards ceasing the electron transfer process. In the present work, the crystallographic structural analysis of a magnetite from a steatite rock sample, with 298 K X-ray diffratometry from synchrotron source, basing on their cell dimensions only, suggests two distinguishable cubic lattices. The averaged chemical formula for this magnetite, as it can be deduced from chemical and 298 K-Mössbauer data and from corresponding structural Rietveld refinement of synchrotron X-ray diffration data is $[Fe^{3+}]\{Fe^{3+}_{0.95}Fe^{2+}_{0.88}\ Cr^{3+}_{0.04}\ Al^{3+}_{0.04}\ Mg^{2+}_{0.05}\ Ni^{2+}_{0.02}\phi_{0.02}\}O_4$, where ϕ = cation vacancy . The crystallographic structure below T_V for this magnetite was similarly inferred from synchrotron X-ray diffraction data, collected with the sample at 15 K. They were identified two crystallographic phases: one of them preserves the higher temperature cubic (space group, *Fd3m*) lattice, for T higher than T_V, and, as reportedly expected for synthetic samples but as a novel structural datum for a natural magnetite, the other is monoclinic (space group *P2/c*).

Acknowledgements: Work supported by the Brazilian Synchrotron Light Laboratory (LNLS), under proposal D10B - XPD 568806, CNPq and FAPEMIG (Brazil).

Local structure study of multiferroic RMn_2O_5 with EXAFS

Fabbris, G. F. L.[1], Maciel, G.A.[2], Granado, E.[3], Massa, N. E.[4], souza, J. A.[5], Alonso, J.A.[6], Azevedo, G. de M.[7], and Lope-Martinez, M.J.[8]

[1] Laboratório Nacional de Luz Síncrotron - SP Brazil
[2] Universidade Federal do Paraná - Curitiba PR Brazil
[3] Universidade Estadual de Campinas - Campinas SP Brazil
[4] Universidad Nacional de La Plata - La PLata B.A. Argentina
[5] Universidade Federal do ABC - Santo André SP Brazil
[6] Consejo Superior de Investigaciones Científicas - Madrid Spain
[7] Laboratório Nacional de Luz Síncrotron - Campinas SP Brazil
[8] Consejo Superior de Investigaciones Cientificas - Madrid Spain

Multiferroics are materials that present at least two of the ferroic characteristics: ferromagnetism, ferroelectricity and ferroelasticity. They have attracted great interest in recent years due to the complex interplay between lattice degrees of freedom and magnetic ordering, which remains poorly understood.

Temperature-dependent EXAFS measurements were utilized to investigate the local structure of RMn_2O_5 (R = Bi, Pr, Gd). Measurements were performed in transmission mode at both Mn (K-edge) and R (L3-edges) at LNLS XAFS2 beamline , in the temperature range from 20K to 300K, which encompasses the temperature of multiferroic transition (40K for all of them). The data for RMn_2O_5 were analyzed using IFEFFIT and FEFF programs. Herein we will focus on $BiMn_2O_5$, but preliminary analysis results for the other members will also be shown.

For $BiMn_2O_5$, Mn K-Edge results reveal a very small temperature dependence of the Debye-Waller factor (DWF) and an Einstein temperature (ET) from Mn-O bonds of 675±22 K, suggesting that MnO polyhedra are rigid. Above 125 K, structural distortions in the first coordination shell are observed at the Bi L3 Egde, in qualitative agreement with recent results for $TbMn_2O_5$ by Tyson et al [1]. The quantitative analysis relates the origin of such distortions to two very distinct values of DWT and ET (294±7K and 462±28K) for Bi-O bonds on the first shell. Our analysis disagree with Tyson's which presented an increase on distance of some Bi-O, not observed in our data. Our EXAFS analysis and XRD analysis by Granado et al. [2] suggest low energy vibrational modes associated with rigid rotations of the Mn-O polyhedra are operative, which might explain the low temperature linear expansion coefficient verified. Distortions related to multiferroic transition could not be identified, showing that any local structure change is very small. Similar behavior is observed for other members (Gd and Pr) of RMn_2O_5

[1]Tyson et al., PRB 2007, 75, 174413. [2]Granado et al., PRB 2008, 77, 134101.

Acknowledgements: This work was supported by FAPESP and CNPq.

Evaluation of the amorphous to crystalline phase transition temperature in Ti-Si-B alloys by Synchrotron Radiation XRD.

Candioto, K.C.G.[1], Nunes, C. A.[1], and Suzuki, P. A.[1]

Escola de Engenharia de Lorena - Universidade de São Paulo - Lorena SP Brazil

Rapid solidification is the process in which liquid metals or alloys are cooled at rates higher than 10^4 K.s^{-1}. In this process, refinement of the grain size, extension of the solubility limits, formation of nanocrystals and production of metallic glasses can be attained. In general, high chemical homogeneity and fine microstructure are observed in these materials. In this study, discs of Ti-Si-B alloys (80 mg, 20 mm diameter and 50 μm thickness) were produced via the splat-cooling process. Alloys of sphere-like shape were magnetically levitated, melted and then quenched under argon. The disks were characterized by X-ray diffraction (XRD), Differential Thermal Analysis (DTA) and High-Resolution Transmission Electron Microscopy (HRTEM). The formation of either amorphous or nanocrystalline microstructures were observed in several alloys. The classical characterization techniques allow just to obtain the information of initial and final r microstructures of these materials, without information about the phases transformation pathway in the direction of thermodynamic equilibrium. In this work, the combination of high-intensity XRD source as Synchrotron Radiation (SR), temperature-controlled furnace and image plate allowed to determine in-situ transition from amorphous to the crystalline state. The transition temperature was found to be very close to the temperatures determined by Thermal analysis (DTA). The phases detected after crystallization were Ti_{ss} and Ti_6Si_2B.

Acknowledgements: This work was supported by CNPq and LNLS

Low resolution structure of synthetic melanin aggregates in aqueous solutions and organic solvents

Torriani, I.L.[1], Silva, J.C.[1], Autreto, P. A. S.[1], D. S. Galvao[1], Caldas, M. J.[2], and Graeff, C. F. O.[3]

[1] Universidade Estadual de Campinas - Campinas SP Brazil
[2] Universidade de São Paulo - São Paulo - Sao Paulo SP Brazil
[3] Universidade Estadual Paulista - Bauru - Bauru SP Brazil

In an effort to find out details of the melanin fundamental structural unit, a great amount of information has been gathered using several techniques. The local short range order of the melanin molecular clusters has been described as consisting of five to seven 5,6-indolequinone units, arranged in planes which are pi-stacked with a spacing of 0.34 nm. Typical cluster size is 1.5-2.0 nm in lateral dimensions and 1.0 nm, in height. Nonetheless, structural details and dimensions of the aggregates are still not clearly defined and experiments did not answer the key question concerning the identification of the fundamental melanin protomolecule. More recently, small angle scattering of X-rays (SAXS) and neutrons (SANS) were performed. Several authors used these techniques, which are well designed to study macromolecules in solution to find details of melanin-copper ions interaction as well as chemical bleaching effects. A diversity of aggregated structures were proposed for these nanoscaled particles based on size and apparent shape. In this presentation we report the results of SAXS experiments performed with melanin synthetized from L-dopa and L-tyrosine in organic solvents, which were reported to be very effective for thin film formation. Water-based synthetic melanin was also studied for comparison purposes, since molecular aggregation behavior is known to vary with the route used for the synthesis. Reliable data was obtained for the water-based and DMSO dispersions. Data analysis was performed by conventional IFT methods and the overall shape and dimensional parameters of the melanin particles were obtained. Using ab-initio calculations, a low resolution 3D model is proposed for the basic melanin particle in aqueous media and DMSO.

Acknowledgements: FAPESP, CNPq, LNLS

MORPHOLOGICAL AND STRUCTURAL PROPERTIES OF EXPANDED AUSTENITE

C. A. Figueroa[1], Basso, R. L. O.[2], and Pimentel, V. L.[3]

[1] Universidade de Caxias do Sul - Caxias do Sul RS Brazil
[2] Universidade Estadual de Campinas - Campinas SP Brazil
[3] Laboratório Nacional de Luz Síncrotron - Campinas SP Brazil

Among the different Fe-N phases, expanded austenite (commonly called S, gammaN, or m phase) has attracted strong interest in the last two decades. A large number of scientific and technical works were devoted to explain the nature of expanded austenite, without bringing a full understanding of its structure and formation.In this work, we introduce new experimental data and interpretations about the nature of the expanded austenite obtained by ion nitriding of AISI 316. By magnetic force microscopy (MFM), two different phases were distinguished. Moreover, sputtered neutral mass spectrometry (SNMS) indicates that the phase transition occurs just in the inflexion of the nitrogen depth profile. Figure 1 shows both analyzes on a sample nitrided for 2 hr at 380oC. Furthermore, x-ray photoelectron spectroscopy (XPS) and ultraviolet photoelectron spectroscopy (UPS) were employed in order to characterize the electronic structure of the expanded austenite at different nitrogen concentrations. The interaction of 2p electrons from N and 3d electrons from Fe depends on nitrogen content, i. e., the present Fe-N phase on the surface. In addition, X-ray diffraction (XRD) experiments were used for further analysis of the crystallographic structure. The obtained lattice parameters are in agreement with previous works. We propose that the phase transitions and the inflexion of the nitrogen profile at the same point are different nuances of the same phenomena. Because the transition point is 14 at

Acknowledgements: This work was supported by FAPESP and CNPq

Caracterização de sub-frações de asfaltenos usando SAXS

Navarro, L. C.[1], Seidl, P.R.[2], Tasic, L.[3], and W. Loh[3]

[1] Escola de Química da UFRJ - Rio de Janeiro RJ Brazil
[2] Universidade Federal do Rio de Janeiro - Rio de Janeiro RJ Brazil
[3] Universidade Estadual de Campinas - Campinas SP Brazil

A combinação de modelagem molecular com dados analíticos leva a geração de estruturas tridimensionais que refletem as moléculas que tenderiam a se associar entre si, e não as médias comumente empregadas. Utilizando um dímero formado por estruturas que tendem a se associar como modelo para um agregado, pode-se investigar a influência de diferentes fatores, como o tipo e posição de substituintes ou heteroátomos sobre a associação e simular suas propriedades sob diferentes condições. Tomando o aumento da distância entre os planos dos anéis aromáticos como um indicador da tendência à desagregação, pode-se verificar o comportamento do agregado sob diferentes condições. A técnica de espalhamento a baixo ângulo foi utilizada,em conjunção com outras técnicas, para caracterizar os agregados formados por diferentes tipos de asfaltenos. Com a técnica SAXS é possível obter a dimensão característica da unidade base, o numero base de unidades no cluster e a dimensão fractal do cluster de asfaltenos As amostras analisadas foram amostras solidas, resultantes do fracionamento de asfaltenos de diferentes óleos e resíduos de vácuo, com diferenças notáveis em aromaticidade, usando para o fracionamento misturas de diferentes solventes. Todas as amostras para a analise SAXS, foram solubilizadas em tolueno em concentrações de 0,2

Acknowledgements: Esta pesquisa foi realizada com o auxilio do CNPq e do LNLS. P.R. Seidl posui bolsa de pesquisa PRH-ANP/FINEP e L.C.N Quintero bolsa de doutorado CNPq.

The origin of multiferroicity at $DyMn_2O_5$

Azimonte, C.[1], Granado, E.[2], and Terashita, H[1]

[1] Laboratório Nacional de Luz Síncrotron - Campinas SP Brazil
[2] Universidade Estadual de Campinas - Campinas SP Brazil

Multiferroics are materials where the lattice degrees of freedom, magnetism and ferroelectric ordering are intimately coupled. Usually, interactions between ferroelectricity and magnetism are weak, but this magnetoelectric coupling can lead to colossal cross-coupling effects, inducing magnetic (electric) properties changes with application of electric (magnetic) field, which explain their potential applications in multiple state memory devices. Recent discovery of coexistence and giant coupling of antiferromagnetism and ferroelectricity in frustrated spin systems such as $R\mathrm{MnO_3}$ and $R\mathrm{Mn_2O_5}$ (R=Tb,Dy,Ho) were responsible for the renewed interest in this class of materials. A particularly interesting case is the $\mathrm{DyMn_2O_5}$ compound, since it presents a colossal magnetodielectric effect associated with an unusual commensurate-incommensurate magnetic transition. The $\mathrm{RMn_2O_5}$ ferroelectric manganites are isostructural insulators with orthorhombic structure ($Pbam$), constituted by $\mathrm{Mn^{4+}O_6}$ octahedra and $\mathrm{Mn^{3+}O_5}$ pyramids. Interestingly, such structure holds spatial inversion symmetry, which is inconsistent with the existence of a ferroelectric phase. This encourages us to believe that ferroelectricity is the consequence of minor displacements of Mn ions relative to the center of the coordination polyhedra. Nevertheless, up to now, neither neutron nor x-ray diffraction experiments could supply any evidence for such shifts. For the first time, the lack of centrosymmetry has been detected using high sensitive X-Ray resonant diffraction technique in multiferroic $\mathrm{DyMn_2O_5}$, showing direct evidences of symmetry lowering to the ferroeletric phase driven by off-centre structural distortions at the Mn sites. The temperature dependence of the effect is strongly correlated to the macroscopic polarization, demonstrating its nature. We argue that this new element specific technique will be of invaluable importance in understanding the electrical/structural coupling behavior of this complex crystallographic system.

Acknowledgements: This work was supported by FAPESP, ABTLuS

Parte X

Superfícies, Interfaces e Nanossistemas

Nanocrystalline diamond formation in porous silicon obtained by Chemical Vapor Deposition/Infiltration (CVD/CVI) process

Miranda, C.R.B.[1], Baldan, M.R.[1], Beloto, A.F.[2], and Ferreira, N.G.[1]

[1] Instituto Nacional de Pesquisas Espaciais - São José dos Campos SP Brazil
[2] Instituto Nacional de Pesquisas Espaciais - São José dos Campos SP Brazil

A new design of hot filament plant with some new features states for Chemical Vapor Deposition/Infiltration (CVD/CVI) to obtain nanocrystalline diamond (NCD) films on porous silicon (PS) substrate was investigated. The main characteristic for the new CVD/CVI plant is the possibility of forced flow with the presence of vortex just above the porous silicon substrate (PS). In this CVD/CVI process, an additional methane flow was used, above or underneath the PS substrate, to ensures the production of pertinent carbon growth species directly on PS and into its pores. PS substrates were obtained by anodization etching process of n - type silicon wafer in a hydrofluoric acid (HF) solution containing acetonitrile (CH_3CN). Depositions were performed using Ar 90 vol. % , H_2 9 vol. % and CH_4 1 vol. %. In order to compare the efficiency of this new operating states for CVD/CVI the additional methane concentration was varied between 0.5 and 1.0 vol. % above and underneath the PS substrate. Scanning Electron Microscopy (SEM) and Field Emission Gun (FEG) were used to investigate PS and NCD film morphology. SEM images of NCD showed faceted nanograins and uniform surface texture covering all the supports among the pores resulting in an apparent micro honeycomb structure. To characterize the deposited or infiltrated diamond film and the influence of additional source on growth mechanism, Raman spectra confirmed the existence of sp^2 - bonded carbon at the grain boundaries. The spectra showed a peak that may be deconvoluted in two components at 1332 cm^{-1} (diamond) and 1345 cm^{-1} (D band). Two shoulders at 1150 and 1490 cm^{-1} also were observed and were assigned to transpolyacetylene (TPA) segments at the grain boundaries of NCD surfaces. In addition, x-ray diffraction analyses of all films presented characteristic diamond diffraction peaks corresponding to <111>, <220> and <311>.

Acknowledgements: The authors would like to thank CNPq (Process 141221/2005-4) for the financial support. Special thanks to LME/LNLS, Campinas.

Surface anisotropy, exchange bias and particle size effects in magnetite nanoparticles: a Monte Carlo simulation study

J. Restrepo[1]

Universidad de Antioquia - Medellín Antio Colombia

In this study we address the role of surface anisotropy on the hysteretic properties of magnetite Fe_3O_4 nanoparticles, and the circumstances yielding exchange bias behavior. Our analysis involves temperature dependence and particle size effects. Different particle sizes ranging from 2 nm up to 7 nm were considered. Our theoretical framework is based on a three-dimensional classical Heisenberg model with nearest magnetic neighbor interactions involving tetrahedral (A) and octahedral (B) irons. Cubic magnetocrystalline anisotropy for core spins, single-ion site anisotropy for surface spins, and interaction with a uniform external magnetic field, were considered. The cubic inverse spinel crystalline structure of magnetite was simulated in realistic manner. Additionally, the sign and magnitude of the different superexchange integrals involved, namely J_{AA}, J_{AB} and J_{BB}, as well as the valence state of the different iron cations, were also taken into account. The computation of equilibrium averages was carried out in the framework of a single-spin movement Monte Carlo-Metropolis dynamics. Our results revealed the onset of low temperature exchange bias behavior at high enough values of the surface anisotropy constant (K_S) for particle sizes below 3 nm. Susceptibility data, computed separately for the core and the surface, suggest differences in the hard-soft magnetic character at the core-surface interface. Such differences are K_S-driven and depend on the system size. Such a hard-soft interplay, via the surface anisotropy, is the proposed mechanism for explaining the observed exchange bias phenomenology. The dependence of the switching and exchange bias fields with the surface anisotropy and temperature is finally discussed.

Acknowledgements: This work was supported by the COLCIENCIAS 1115-05-17603 project, COLCIENCIAS-CONICYT Colombia-Chile 2005-206, FONDECYT grant 1050066 and 7080111, Millenium Science Nucleus "Basic and applied magnetism P06-022F", Sostenibilidad projects of the GES and GICM groups, and project IN1247CE of the Microelectronic and Scientific Instrumentation Group (Universidad de Antioquia).

Structure and electronic properties of magnetite clusters: A first-principles study

J. Restrepo[1]

Universidad de Antioquia - Medellín Antio Colombia

In this study we present results of electronic structure calculations for magnetite clusters on the basis of the LSDA+U approximation. The cluster size ranged between 33 and 113 atoms corresponding to length scales between around 7 and 12 in diameter respectively. Calculations on bulk magnetite were also carried out for comparison purposes. Initial atomic configurations before relaxation were simulated by considering both the cubic $Fd\bar{3}m$ and the monoclinic $P2/c$ symmetry space groups of magnetite Fe_3O_4. The charge and the magnetization per atom were computed. Results reveal clearly an Fe:O charge transfer process with important differences relative to the bulk depending on the cluster size. In particular, the charge distribution of the cluster having cubic symmetry and containing 113 atoms reveals a well-defined periodic pattern of Fe-pairs consistent with a partial charge ordering scenario. Results evidence that the total ground-state energy is smaller in the $P2/c$ phase than in the $Fd\bar{3}m$ phase, indicating that the low temperature monoclinic phase is energetically more stable even in clusters. Clusters with monoclinic symmetry are also characterized by an insulating state whereas those with cubic symmetry exhibit a very small gap. Finally, radial and angular distribution functions were also computed for structural characterization. Here, results reveal strong modifications of the starting crystalline structures after relaxation.

Acknowledgements: This work was supported by the COLCIENCIAS project 1115-05-17603, FONDECYT grant 1050066 and 7080111, Millenium Science Nucleus "Basic and applied magnetism"P06-022F, Sostenibilidad projects of the Solid State and the Microelectronic and Scientific Instrumentation Groups of the Universidad de Antioquia and DAAD-Mexico binational collaboration projects. We also acknowledge the computer time provided by Universidad Politécnica de Valencia as well as CNS, Ipicyt, México.

CHITOSAN INFLUENCE ON THE PHOSPHOLIPID ORGANIZATION

Lionzo, M. I. Z.[1] and Silveira, N. P.[1]

Universidade Federal do Rio Grande do Sul - Porto Alegre RS Brazil

Phospholipids are amphiphilic molecules whose dispersion in organic and aqueous mixtures gives to well known mesophases, depending on its concentration and molecular shape. Among the structures formed by phospholipid self-assembly, we can find micellar, lamellar, hexagonal and cubic phases. The interaction of phospholipids with another molecules, like polyelectrolyte polymers, can occur through the polar regions of these molecules. This association can affects the self-assembly properties as well as the polymer arrangement in solution. Phosphatidylcholine (phospholipid) and chitosan (polyelectrolyte) were mixed in various water/ethyl acetate compositions and the suspensions were analysed by Light Scattering. The experiments made were Small Angle X-ray Scattering [LNLS - Campinas], Dynamic Light Scattering [Brookhaven Instruments BI-DNDCW - IQ/UFRGS] and Transmited Light [Turbiscan - IQ/UFRGS]. The SAXS results showed anisotropy induced by share caused by the sample injection which the persistence was improved by chitosan. Inside the lamellar (lyotropic) structure was found one periodic distance formed by the phospholipid alone (∼4,6 nm) and by phospholipid/chitosan (∼5,0 nm). Micellar structures were also observed by the incidence of a broad intensity on the q 0.1 to 0.2 nm^{-1} region. Using SAXS, it was possible to follow a structural transition from a tight structure to a relaxed one, during the analysis time, in the sample containing chitosan. This occurrence could be attended because of the stability of each phase conferred by chitosan. DLS results showed that the increase of aqueous phase leaded to an association of the small structures by degrees. The structures varied from reverse micelles [below 20 nm], followed by micellar aggregates [20 to 100 nm], to lamellar (microgels) [100 to 1000 nm]. Besides, the chitosan presence generates bigger but similar micelles [20 to 100 nm], aggregates [200 to 500 nm] and microgels [500 to 1000 nm]. The distribution of the relaxation times in function of time denoted a clear transition to bigger structures that was confirmed by the transmitted light [Turbiscan analysis], which demonstrates modifications occurring over the system as a function of time. The results put some light on the effects of CH at the PC organization in organic/aqueous media. It was allowed to investigate the changes on the particles size/structure evolution during the time, pointing out the CH capacity to aggregate the PC molecules in an arranged way.

Acknowledgements: CNPq, CAPES, Rede Nanocosmeticos

Nonaqueous Synthesis of Antimony Tin Oxide Nanocrystals

R. Oliveira da Silva[1], Conti T. G.[1], Stroppa, D. G.[2], Longo, E.[3], and Leite,E.R.[1]

[1] Universidade Federal de São Carlos - São Carlos SP Brazil
[2] Laboratório Nacional de Luz Síncrotron - Campinas SP Brazil
[3] Universidade Estadual Paulista - Araraquara - Araraquara SP Brazil

Efforts to produce SnO_2 : Sb (antimony tin oxide-ATO), a widely used TCO in optoelectronics, by soft chemical routes were expended, in order to obtain low temperature processing of the desired devices. Also, soft chemical routes are considered promising to fulfill most of the requirements such as high crystallinity, purity, yields and reproducibility from the molecular precursor to the final product and general applicability. This work outlines the preparation of crystalline ATO nanoparticles fully redispersable in a solvent, by a nonaqueous synthesis that consists in one pot reaction, initiated by the addition of the molecular precursors (Antimony chloride and Tin chloride) into benzyl alcohol, followed by solvothermal treatment at 200^oC for about 48h. ATO particles were collected by centrifugation, washed twice with THF and dried at room temperature. The entire product presented a well crystallized structure, revealed by XRD peak width, with small particle size in the range of 3-10nm confirmed by HRTEM. The synthesis product showed stability as a colloid by re-dispersion in a THF with a surfactant, that allow the deposition of thin films in the same way of previous study with SnO_2 : Sb films.

Acknowledgements: FAPESP/CEPID 98/14324-0, CNPq and Dow Chemicals are gratefully acknowledged, we also acknowledge Dr. Luciano L. A. Montoro for his valuable help in the HRTEM experiment and analysis at LME-LNLS.

Structural studies of biocompatible iron oxide nanoparticles for biological applications

Socolovsky, L. M.[1]

Universidad de Buenos Aires - Buenos Aires CapFe Argentina

Nanoparticles produced by chemical methods join several desirable characteristics for both basic science and technology, like controlled size, small size distribution, and regular shapes. They can be capped with a biocompatible material for applications in medical therapies. Some hurdles have to be overcome to transform these nanoparticles in a reliable material for such applications. Among them, agglomeration tendencies, stability, rejection, survivor in a hostile medium. To address these difficulties, knowledge of nanoparticles structure is fundamental. We will show examples of the use of Small Angle X-ray Scattering and High-Resolution Transmission Electron Microscopy for characterizing samples of iron oxide nanoparticles capped with different biocompatible materials.

Acknowledgements: This work is supported by CONICET (Argentina, financial support), and LNLS (SAXS line and LME, use of facilities).

Relation between structural properties and in vitro release of amphotericin B from delivery system based on soya phosphatidylcholine

Pestana. K.C.[1], FRANZINI, C.M.[2], Sarmento, V.H.V[2], Chiavacci, L.A.[2], and OLIVEIRA, A.G.[2]

[1] Universidade Estadual Paulista Julio de Mesquita Fillho - Assis SP Brazil
[2] Universidade Estadual Paulista - Araraquara - Araraquara SP Brazil

In this work structural features of delivery systems containing the pharmaceutical biocompatible components soya phosphatidylcholine (SPC) and Tween (Tw) as surfactant, captex (CP) as oil phase and aqueous buffer were studied. These systems were formulated with and without the drug Amphotericin B (AmB) and the microstructure was characterized by polarized light microscopy and small angle X ray scattering (SAXS) as well as the ability to release AmB. The experimental results show the formation of lamellae structural organizations. The lack of these structures with the AmB addition demonstrates its significant influence on the drug release profiles. Moreover, the in vitro release assay showed that the increase of the O/S ratio in the formulations inhibited the constant rate of AmB release exhibiting an exponential decay profile. These features can be used to control the AmB delivery from system.

Acknowledgements: The authors wish to thank FAPESP, CNPQ and CAPES for their financial support and LNLS by smallangle X ray scattering (SAXS) measurements

Interação entre átomos de ouro e cobre com superfícies Si (111): Um estudo combinado de GIXRF e DFT.

Batista, A. P. L.[1], Carvalho, H.W.P[2], Ramalho, TC[3], Gobbi, A. L.[4], and Pérez, C. A.[4]

[1] Universidade de São Paulo - São Paulo - São Paulo SP Brazil
[2] Universidade Estadual Paulista - Araraquara - Araraquara SP Brazil
[3] Universidade Federal de Lavras - Lavras MG Brazil
[4] Laboratório Nacional de Luz Síncrotron - Campinas SP Brazil

O crescimento de filmes finos metálicos sobre superfícies semicondutoras tem sido amplamente estudada. É sabido que a estrutura geométrica e eletrônica são fortemente responsáveis pelas interações entre os átomos das superfícies metálicas e os das superfícies do semicondutor. Com base nestes fatores e na grande importância desse entendimento para a física fundamental, buscou-se neste trabalho, através de um estudo experimental e teórico avaliar a interação dos metais cobre e ouro com a superfície Si(111). Filmes finos de Cu e Au foram, por sputtering, depositados sobre wafers de Si (111), largura de 1,5 cm. Em seguida foram tratados à 100, 300 e 700 C, por 1s. Logo após, estes filmes metálicos foram removidos (ficando apenas átomos de Cu e Au , interagindo com o semicondutor) e levados para o feixe de linha XRF (LNLS), onde medidas de Fluorescência de raios-X a Incidência Rasante (GIXRF) foram tomadas. A penetração dos átomos em questão, foi determinada comparando a curva experimental com a curva teórica obtida por um programa computacional existente na linha XRF; o software executa cálculos, simulando as curvas de fluorescência em função do ângulo de incidência. Foi possível constatar que o átomo de ouro se difundiu melhor que o átomo de cobre. A fim de explorar ainda mais estes resultados, partimos para o auxílio da química computacional. Para a realização dos cálculos empregou-se o programa Gaussian98. Foi estudado a interaçã o entre os átomos de Cu e Au com a superfície em questão. Para tanto se fez uso da Teoria do Funcional de Densidade (DFT), funcional B3LYP. Conjunto de bases LANL2DZ foram empregadas para os metais; 6-31G(d) para o H e SDD para o Si. Para simular o semicondutor empregou-se o cluster Si_4H_7, considerando sítios de interação específicos nele. As distâncias entre os metais e os sítios foram otimizadas, obtendo-se as energias de interação. Curvas de energia potencial *versus* as distâncias aos sitios foram plotadas e uma menor energia foi obtida para o Au, sugerindo que este interagia melhor com o Si e, portanto se difundia mais, ou seja, concordancia com os resultados experimentais.

Acknowledgements: LNLS CNPq DQI-UFLA

STUDY OF NANOSTRUCTURED ZnO THIN FILMS PREPARED BY SOL-GEL SPIN-COATING BY SYNCHROTRON TECHNIQUES

Bojorge, C. D.[1], Cánepa, H. R.[1], Casanova, J. R.[1], A.F. Craievich[2], Heredia, E.[1], and Kellermann, G.[3]

[1] Consejo Nacional de Investigaciones Científicas y Técnicas - Buenos Aires Argentina
[2] Universidade de São Paulo - São Paulo - São Paulo SP Brazil
[3] Laboratório Nacional de Luz Síncrotron - Campinas SP Brazil

ZnO based films have been actively studied because of their applications as solar cells, gas sensors, piezoelectric transducers, ultrasonic oscillators and for different optoelectronic applications. Besides their interesting optical, electrical and piezoelectrical properties, this material exhibits a high chemical and mechanical stability. ZnO presents novel properties and potential applications in optoelectronic fields because its non linear optical properties, excitonic emission at room temperature and quantum size effect.

In the present work we studied pure and Al-doped ZnO thin films prepared by the sol-gel spin coating technique by grazing incidence X-ray diffraction (GIXRD), grazing incidence small-angle X-ray scattering (GISAXS) and X-ray reflectivity (XRR) methods.

We also compare the present pore distribution results in ZnO films obtained by spin coating technique with those obtained previously by dip coating.

Acknowledgements: The authors acknowledge various funding supports provided by CNPq (Brazil), PROSUL(Brazil), LNLS (Brazil), CONICET (Argentina) and YPF Foundation (Argentina).

Effects of organophilic clay on nanostructure of epoxy networks

Zaioncz, S.[1], Soares, B.G.[1], and DAHMOUCHE, K[2]

[1] Universidade Federal do Rio de Janeiro - Rio de Janeiro RJ Brazil
[2] Centro Universitário da Zona Oeste - Rio de Janeiro RJ Brazil

Polymer/layered silicate nanocomposites show, generally, improvement in mechanical properties, barrier properties, thermal resistance and flame retardant properties at lower clay loading in contrast to traditional polymer composites, which has attracted much attention in many fields. The key objective in preparing polymer/clay nanocomposites is to achieve exfoliation or delamination of the aggregates into tactoids and then into single layers because the improvement in final properties of nanocomposites is highly dependent on the degree of clay dispersion. But the final morphology often results from a coexistence of exfoliated sheets, tactoids and micron-size agglomerates. Poly(methylmethacrylate) (PMMA) have been the thermoplastic modifiers most frequently studied for epoxy resin. Its well known that a complete miscibility of the polymer with the epoxy prepolymer before curing occurs, and that a phase separation is observed after curing. The morphology of the generated materials depends on the initial formulation and curing conditions. The aim of the present work is to synthesize nanocomposites of the epoxy resin modified with poly(methyl methacrylate) (PMMA) and organophilic montmorilonite 1 and 2.5 wt. percent of the epoxy resin and examine their effect on the nanostructure of the epoxy networks. Since the density of the clay is much higher than of phase epoxy we attribute the X-ray scattering to the electronic density contrast between the silicate of the clay and polymeric phase. On the SAXS pattern of the nanocomposites reveals a correlation peak located around qmax=1.9 nm-1. This peak indicates a superstructure with a characteristic length equal to d=2π/q = 32 angstron for both compositions. This characteristic length can be considered as the average distance between intercalated platelets dispersed in the epoxy matrix. This length is characteristic of the intercalated nanocomposite formation. This result shows the good dispersion of the organo clay in the epoxy matrix. Further investigations are needed to quantify the dispersion of the particles in the nanocomposites, considering the size and the number of the particles.

Acknowledgements: LNLS, CNPq, CAPES and FAPERJ.

Local structure of nanocrystalline ZrO_2-Sc_2O_3 powders

Abdala, P. M.[1], Lamas, D. G.[1], Fantini, M. C. A.[2], and Craievich AF[2]

[1] Consejo Nacional de Investigaciones Científicas y Técnicas - Buenos Aires Argentina
[2] Universidade de São Paulo - São Paulo - São Paulo SP Brazil

ZrO_2-Sc_2O_3 ceramics exhibit the highest ionic conductivity among ZrO_2-based materials and, therefore, can be used as solid electrolytes in intermediate-temperature solid-oxide fuel cells. The polymorphs reported in this system have monoclinic, tetragonal, cubic or rhombohedral symmetries. The tetragonal phase can exhibit three different forms: t, t' and t"[1]. In a previous work carried out at the LNLS, nanocrystalline ZrO_2 1 to 13 Sc_2O_3 synthesized by a nitrate-gel combustion route were characterized by means of X-ray powder diffraction (XPD). These studied showed that all the nanopowders were single-phased exhibiting metastable forms of the tetragonal phase or the cubic one. The average crystallite size of these samples was about 10 nm. In the present work, the local order of ZrO_2-Sc_2O_3 solid solutions with Sc_2O_3 contents up to 13 mol% was studied by EXAFS. This study was performed in the D04B-XAS1 beamline of the LNLS in Zr K edge. EXAFS data were fitted with experimental standard $BaZrO_3$ using WINXAS code. The analysis for the tetragonal phase assuming the crystallographic model (2 oxygen subshells around Zr atoms, with 4+4 coordination, and equal Debye-Waller factors) did not achieve reasonable goodness factors. For this reason, three alternative models were explored for tetragonal samples (according to XPD analysis): one model keeping fixed coordination of 4+4 and free different Debye-Waller factors; a second model using free coordination numbers and equal Debye-Waller factors and a third model with three subshells fixing the coordination numbers to 4+2+2 and equal Debye Waller factors for the first and the second subshells. The goodness factors of the two first models are comparables; the results obtained with the third model yielded slightly better goodness factors. Cubic samples were fitted considering one oxygen subshell around Zr atoms with free coordination number and Debye Waller factor, obtaining a coordination number of 6, which is probably due to the oxygen vacancies generated by the high dopant content. These samples were also adjusted with the proposed models for the tetragonal samples. The Zr-O bonding distances were obtained for each model as a function of the composition and compared with the distances from XRD data analysis.

1. M. Yashima et al., Solid State Ionics 86-88 (1996) 1131

Acknowledgements: This work has been supported by LNLS,the scientific collaboration agreements CNPq-CONICET and CAPES-SECyT ,CNPq, ANPCyT, CONICET (Argentina, PIP No. 6559) and CLAF.

Photocatalytic decomposition of H_2O_2 by silicon wafer doped with Au and Cu: theoretical and experimental study

Carvalho, H.W.P[1], Batista, A. P. L.[2], Ramalho, TC[3], Gobbi, A. L.[4], and Pérez, C. A.[4]

[1] Universidade Estadual Paulista - Araraquara - Araraquara SP Brazil
[2] Universidade de São Paulo - São Paulo - São Paulo SP Brazil
[3] Universidade Federal de Lavras - Lavras MG Brazil
[4] Laboratório Nacional de Luz Síncrotron - Campinas SP Brazil

In this work we studied the effects of doping with Au and Cu on silicon wafer. The photocatalyst materials were obtained trough of contaminant implantation in silicon. Single thin layers 10.0 nm of Cu and Au were growth above Si wafers by sputtering method, after that were submitted thermal treatment during 1 s, by speed heat oven in temperature of 700 ^{o}C (Si-Au-700 and Si-Cu-700), then the films were removed by etching solution. The same procedure was performed, although for no thermal treated wafer (Si-Au-RT and Si-Cu-RT), this were the references. DRX data shown formation SiO_2 in silicon contamined with Au at 2θ 27 [2,3]. While for silicon doped with Cu nothing occurred. For reference and contamined can watch a intense signal at 2θ whose correspond a Si(111), in no thermal treated wafer, just this signal were observed. In this way, the Au seems toward the formation of silicon oxide. The Uv-vis spectra indicated different comportment for all wafers. The visible gaps were for all materials were minor that for pure silicon, and the Si-Cu-700 presents a minor gap among materials, its value was about 0.50 eV. TXRF analysis allowed studied a depth profile so that noon destructive[5]. For Si-Au-RT and Si-Au-700 occurred diffusion at 7-9 nm and 47-55 nm, respectively. Already for Si-Cu-RT and Si-Cu-700, we observed diffusion at 2-4 and 35-41 nm. In this way, Au presents deeper than Cu. This fact, depth profile, could influence photocatalytic activity this material. The tests for H_2O_2 degradations indicated that the better material was Si-Au-700, followed by Si-Cu-700. The performance of Si-Au-700 was twice greater than Si-Cu-700, and five times for pure silicon wafer. The theoretical calculations at DFT level were carried out targeting to explain some experimental findings[5]. Thus, we simulated the interactions energy between silicon structure doped with Au and Cu and the H_2O_2 molecule. Results show that interaction energy is minor among materials doped with Au. Therefore this data is in a good agreement with our experimental results.

1 Nichela, D App Catal B, 2008, 82, 1118. 2 Le Pege, Y Acta Cryst B 1976, 32, 2456-2459. 3 Jones, P.G.; .Acta Cryst B 1979, 35, 1435-137. 4 Postava, K; App Surf Sc 2007, 254, 416419. 5 Klockenkamper, R. Spectroc Acta B 2002, 32(10), 1593-1599.

Acknowledgements:

Growth of Indium Tin Oxide Nanobelts with controlled In:Sn ratio by Carbothermal Reduction Process

Orlandi, M.O.[1], Leite,E.R.[2], and Longo, E.[3]

[1] Universidade Estadual Paulista - Ilha Solteira - Ilha Solteira SP Brazil
[2] Universidade Federal de São Carlos - São Carlos SP Brazil
[3] Universidade Estadual Paulista - Araraquara - Araraquara SP Brazil

One dimensional (1D) nanostructured materials has been widely investigated in the recent past years because of their interesting properties. Among them, tin oxide and doped tin oxide are interesting materials from technological point of view, and are several works reporting these nanostructures. In this work it is presented a simple route to produce Indium Tin Oxide (ITO) nanobelts with different In:Sn proportion. The nanostructured materials were obtained using the carbothermal reduction process with co-evaporation of the oxides. Such process consists in put two crucibles (one of tin oxide plus carbon and another with indium oxide plus carbon) side by side in the center of a tube furnace in which the temperature, evaporation time and atmosphere flux were carefully controlled. For the synthesis it was used the temperature of 1200 ^{o}C, 2 hour of evaporation and nitrogen atmosphere flux of 50 sccm. In order to control the In:Sn ratio in the synthesized material, for each synthesis the amount of carbon mixed with each oxide was changed. After all syntheses the obtained material had a wool like appearance and was characterized by X-ray diffraction (XRD), transmission electron microscopy (TEM) and scanning electron microscopy (SEM) equipped with energy dispersive X-ray spectroscopy (EDX). The XRD data showed that is possible to grow structures in the SnO or In_2O_3 phases depending of the oxide to carbon proportion in each crucibles. By SEM it was observed that the wool like material has rectangular section transversal (nanobelts), are flat and homogeneous width. The TEM analysis showed that the belts are single crystalline and the belts in the In_2O_3 phase grows always in the [100] direction, and the EDS results showed that the belts have different Sn:In ratio depending of the molar concentration of the initial mixture of oxide with carbon. This is an interesting result because the literature shows that both electrical e optical properties of ITO depend of the Sn:In ratio.

Acknowledgements: We would like to thank the LME-LNLS for the electron microscopy facilities. The Fapesp and CNPq agencies are acknowledged for the financial support.

SMALL-ANGLE X-RAY SCATTERING STUDIES IN POLYMER COLLOIDS

Peruzzo, P. J.[1], Anbinder, P. S.[1], Plivelic, T.S.[2], and Amalvy, J. I.[1]

[1] Universidad Nacional de La Plata - La PLata B.A. Argentina
[2] Lund University - Lund Sweden

A synthetic polymer colloid (latex) is defined as a dispersion of polymer particles in a fluid medium (like water). The particles are generally spherical, monodisperse with a size range of about 50 nm to 500 nm in diameter. Small-angle X-ray scattering is a tool which allows the study of the structure and the interaction of these polymer colloids. Previously, we have discussed SAXS results performed on latex in the dried state, as film or powder. In this work SAXS-investigations on two series of latex dispersions are discussed. The first series is composed of polystyrene latexes where the colloidal stability is enhanced via a steric stabilization mechanism by chemically grafting of reactive diblock copolymers, forming a core-shell morphology. The second series of latexes is composed of nanocomposite particles dispersed in aqueous medium and prepared from the $in-situ$ polymerization of methyl methacrylate in the presence of preformed nanosilica particles. SAXS measurements on samples were performed at the SAXS2 beam line at the LNLS (Campinas, Brazil) using a monochromatic beam of wavelength 1.608 and exposure time of 300 sec, and a sample detector distance of 728.32 mm. In the first case, since the excess electron density of polystyrene latex particles in water is very small, the scattering from the layer of the polymeric stabilizers dominates the measured intensity. In the silica/poly(methyl methacrylate) latexes dispersions, the curves are compared with those obtained with the same particles but in the dried state after water evaporation. As expected the curves obtained in the dispersion state exhibit more oscillations allowing a more detailed analysis of the morphology. Porod's plots have an asymptotic linear regime for all the samples indicating the presence of abrupt and well-defined interface. The results in all case are discussed using information from dynamic light scattering and transmission electron microscopy.

Acknowledgements: The authors would like to acknowledge Brazilian Synchrotron Light Laboratory (LNLS), Campinas, Brazil; CICPBA and ANPCYT are thanked by financial assistance. PSA is member of ANPCyT, PJP is member of CONICET and JIA is member of CIC. O.R. Pardini is thanked for technical assistance.

Estudio XAFS de la estructura de nanopartículas Pd_xAu_{1-x} encapsuladas en tioles

Giovanetti, L. J.[1], Ramallo-López, J. M.[1], Requejo, F. G.[1], Grumelli, D.[2], Salvarezza R C[2], and Shon, Y. S.[3]

[1] Universidad Nacional de La Plata - La Plata Bs.As Argentina
[2] Instituto de Investigaciones Fisicoquimicas Teoricas y Aplic - La Plata BA Argentina
[3] Western Kentucky University - Bowling Green KY United States of America

Las nanopartículas bimetálicas pueden presentan efectos anómalos si los comparamos con lo que sucede en la escala de los mismos compuestos másicos. Así, por ejemplo es posible encontrar una interacción más intima entre dos metales debido a la mayor superficie de contacto entre ellos, lo que puede resultar en propiedades electrónicas o magnéticas nuevas. Para poder entender estos efectos es necesario determinar de manera precisa la estructura de la nanopartícula y la interacción entre los dos metales. Este tipo de sistemas resulta ideal para ser estudiado por espectroscopias de absorción de rayos X ya que es posible realizar estudios independientes desde el punto de vista de cada uno de los metales que la componen. En este trabajo presentamos un estudio EXAFS y XANES en los bordes $L_{2,3}$ y K del Pd y $L_{2,3}$ del Au de nanopartículas Pd_xAu_{1-x} encapsuladas en tioles. Los resultados muestran que no se forma aleación y las NPs presentan una estructura del tipo core-shell, siendo el nucleo de Au metálico y la cáscara de Pd, el cual se encuentra fuertemente sulfurado. Estos resultados se complementan con estudios TEM y SAXS.

Acknowledgements: Este trabajo fue financiado por la ANPCyT (PICT 06-17492 y 25515), UNLP y CONICET (PIP 6075/05) de Argentina y el LNLS, Brasil

GISAXS study of CoMo nanoparticles on Si(111) used for catalytic synthesis of single wall carbon nanotubes.

Giovanetti, L. J.[1], Kellermann, G.[2], dos Santos Claro, P. C.[3], A.F. Craievich[4], and Requejo, F. G.[1]

[1] Universidad Nacional de La Plata - La Plata Bs.As Argentina
[2] Laboratório Nacional de Luz Síncrotron - Campinas SP Brazil
[3] Universidad Nacional de La Plata - La PLata B.A. Argentina
[4] Universidade de São Paulo - São Paulo - São Paulo SP Brazil

Grazing-Incidence Small-Angle X-ray Scattering (GISAXS) is a versatile tool for characterizing nanoscale density correlations and/or the shape of nanoscopic objects at surfaces, at buried interfaces, or in thin films. GISAXS combines features from Small-Angle X-ray Scattering (the mesoscopic length scale, incident beam definition by multiple slits, area detector) and diffuse X-ray Reflectivity (the scattering geometry and sample goniometer). Recently, the group of Daniel E. Resasco [1] has shown that it is possible to catalytically synthesize vertically (V) and horizontally (H) aligned single wall carbon nanotubes (SWNT) on a flat substrate [2]. Samples studied in this work were prepared by catalytic reaction of CO using CO-MOCAT catalytic process [3]. The samples are synthesized over a p-typeSi wafer, with a SiO_2O. In present work we present a GISAXS and AFM study of V-SWNT in the first preparation stage to investigate the size, shape and order of the CoMo nanoparticles supported on Si(111) used as catalyst for SWCN. According to our first GISAXS analysis, our results are consistent with the presence of pyramidal-like supported CoMo nanoparticles with squared symmetry. This surprising finding has to be deeper analyzed to explain the origin of this spontaneous order.

Referências

1. Samples were synthetized and provided by D.E. Resasco and Z. Li. from School of Chemical, Biological and Materials Engineering, University of Oklahoma.
2. Zhang, Liang; Tan, Yongqiang; Resasco, Daniel E. Chemical Physics Letters 422(1-3), 198-203 (2006).
3. http://www.ou.edu/engineering/nanotube/comocat.html

Acknowledgements: This work has been partially supported by the Brazilian Synchrotron Light Laboratory (LNLS) under proposal D10A - XRD2 5849 and ANPCYT-CONICET, Argentina (projects PICT 17492 and PIP 6075).

Study of silver nanoparticles inclusion in single and multilayered mesoporous oxide films using XRR and 2D-SAXS

Fuertes, M.C.[1], Marchena M. H.[1], Wolosiuk, A.[1], and Soler-Illia, G.J.A.A.[1]

Comisión Nacional de Energia Atómica - Buenos Aires B.A. Argentina

Mesoporous oxide frameworks are attractive template matrices for embedding metal nanoparticles (NP). Interesting electrical and optical properties due to metal confinement fuel this attractive research area. In particular, metallic NP included in mesoporous thin films (NP@MPTF) are interesting nanocomposite systems with forthcoming applications in catalysis, and photonic or optoelectronic devices. In order to take advantage of both components, a sound understanding of the nanocomposite systems is needed. Although several NP@MPTF systems have been reported in the literature, some issues such as the quantitative analysis of mesopore filling, control of the reduction kinetics and the possibility of selectively locating NP in a given region of space remain relatively unexplored. In this work, controlled chemical reduction of Ag in the pore arrays of silica and titania mesoporous films (2-10 nm pore diameter) was used to prepare Ag@MPTF nanocomposites with variable metallic contents. Mesoporous single or multilayer films were used as matrices. X Ray Reflectivity (XRR) were used as a tool to assess metal loading into the films. The increase of electronic density for samples submitted to increasing reduction times was attributed to an increase in silver loading. Pore filling assessment by XRR was in agreement with EDS measurements. In addition, control of reduction conditions permitted to selectively locate Ag NP within a given type of layer. This leads to the possibility of creating highly controlled NP arrays, precisely located in mesoporous multilayers or even in distinct layers of mesoporous photonic crystals. Titania layers in an 8-layered titania-silica structure can be selectively modified with Ag NP in a single step. The changes in the diffraction signals due to the formation of NP inside titania ordered mesopores were studied by 2D-SAXS. The enhanced chemical reactivity of titania films for silver reduction controls the spatial arrangement and determines the homogeneous 1D localization of the Ag NP in multilayered architectures. XRR and SAXS measurements were performed at the D10A-XRD2 and D11A-SAXS2 lines of Laboratório Nacional de Luz Síncrotron, Campinas, SP, Brazil.

Acknowledgements: Grupo coloides (GQ-CNEA), N. De Vicenzo, M.C. Marchi (CMA-UBA), H. Troiani (CAB), Guinter Kellerman (LNLS). Funding: CNEA, CONICET (PIP 5191, fellowship for M.C.F), CSIC, ANPCyT, LNLS (Campinas, XRD2 and SAXS2 lines).

Estudos XANES e EXAFS de catalisadores de gálio suportados em zeólita H-ZSM5

Faro Jr., A. C.[1], Eon J-G.[1], Rodrigues, V. O.[1], Silva, R. F.[1], and Nogueira, L.[1]

Universidade Federal do Rio de Janeiro - Rio de Janeiro RJ Brazil

Zeólitas H-ZSM5 foram impregnadas ao ponto úmido com teores de Ga variando entre 2 e 10% p/p, sendo submetidas a pré-tratamentos redutivos e oxidativos, sendo a análise por espectroscopia XAFS foi feita em todos os catalisadores. A partir da interpretação dos espectros XAFS utilizando um modelo que consiste em uma parte do gálio sob a forma de uma fase segregada de β-Ga_2O_3 e a outra parte como clusters dispersos nos canais zeolíticos, foi possível correlacionar os efeitos do teor de gálio impregnado na zeólita e os diferentes pré-tratamentos sofridos pelos catalisadores com as quantidades das duas fases, e, ainda, com o tipo de espécie dispersa presente.

Mostrou-se que o aumento da quantidade de gálio impregnada na amostra leva à formação preferencial da fase segregada de β-Ga_2O_3 no exterior dos cristais da zeólita H-ZSM5, além de favorecer à formação de clusters maiores dentro de seus canais. Estes clusters, conforme determinado pela simulação dos espectros EXAFS possuem, provavelmente, quatro centros de gálio, bloqueando os canais zeolíticos devido ao seu tamanho, fato este que explica a diminuição da área superficial determinada pelo método BET com o aumento do teor de gálio nos catalisadores. Já no caso dos catalisadores com menores teores de gálio os clusters formados possuem dois centros de gálio, que em condições reacionais (condições redutoras) geram as espécies ativas de gálio nas reações de desidrocicloaromatização.

Acknowledgements: Os autores agradecem ao PRONEX Funcionalização de Hidrocarbonetos pelo auxílio financeiro, ao LNLS (Campinas) pela aprovação do projeto e concessão de auxílio na realização dos experimentos e ao Dr. Yiu Lau Lam do CENPES/PETROBRÁS pelo fornecimento da amostra de HZSM-5. RFS agradece ao CNPq a concessão de bolsa de mestrado. VOR agardece à CAPES a concessão da bolsa de doutorado.

EXAFS characterization of PdIr/USY catalysts

Faro Jr., A. C.[1], Eon J-G.[1], Rodrigues, V. O.[1], and FRANÇA, M. C. K.[1]

Universidade Federal do Rio de Janeiro - Rio de Janeiro RJ Brazil

For many years the search for efficient catalysts for HDA (hydrodearomatization), capable of increasing diesel's cetane number, with lower costs has been conducted. Among these, the noble metal based catalysts have been widely studied, as they show high hydrogenation activity at moderate pressures. Among the noble metal based catalysts, studies in the literature indicate that iridium has a higher hydrogenolys metal than platine (commonly used in these catalysts) and it's presence in the catalyst can, in principle, lead to the opening of naftenic rings using metallic catalysis instead of acid catalysis. On the other hand, it is well known that iridium is very sensible to sulfur poisoning, what can make it's industrial usage impracticable . In this context it is interesting to investigate if the addition of Pd to iridium catalysts would increase it's sulfur tolerance.

The active metal phase in the USY supported catalysts are probably highly dispersed, which made us adopt a structural model consisting of small metal clusters, whose radius and morphology were determined from the mean coordination number in each of the shells considered. These mean number of neighbours were determined by the correlation break method for the neighbour oxygens in both catalysts and for the first two metallic coordination shells in the Ir/USY catalysts, and by spectra simulation in k and Q-space for the first metallic shell in the 50% PdIr/USY catalyst.

Mean coordination numbers obtained were 7.0 for Ir/USY Catalyst and 6.6 for 50% PdIr/USY, which are equivalent to cluster diameters of 9.4 (Ir_{43} cluster) and 8.4 ($PdIr_{(19-43)}$ cluster) , respectively. Calculated dispersions were about 80% It's interesting to note that the iridium percentage in the PdIr clusters were 70%.

Acknowledgements: The authors would like to thank LNLS for the project approval (proposal D04B-XAFS1/5830) and financial support for carrying through of the experiments and to CENPES - Petrobrás for financial support to the project.

EXAFS characterization of the local disorder in Y2O3 nanoparticles produced via a coconut water-assisted sol-gel method

Gomes, M.A.[1], Valerio, M.E.G.[1], and Macedo, Z.S.[1]

Universidade Federal de Sergipe - São Cristóvão SE Brazil

The aim of the present work is the production of rare-earth doped Y2O3 nanoparticles and the study of the correlation between synthesis procedures, structural characteristics and optical properties of this material. When associated with polymers and functional molecules, these nanoparticles are used as fluorescent probes in biological imaging systems. Yttria was prepared using a coconut water-based sol-gel method. During the production process, the pH of the start solution was adjusted by adding ammonia hydroxide. This adjustment controls the agglomeration degree and, consequently, the size of the particles. The crystallization of the material was investigated by powder X-ray diffraction technique performed in situ during the calcinations. It was observed a strong dependence between the pH of the sample and the temperature of crystallization of the cubic equilibrium phase Ia-3. For samples prepared at pH 9 the crystallization temperature was 350 C, which is much lower than the temperature 850 C necessary to crystallize the samples without pH control. The particle size of the samples produced at different pH values ranged from 50nm to 10nm. From the EXAFS measurements of these samples it was possible to determine that particles of 50 nm present the same local order than bulk Y2O3. For the samples with particles size of 10 nm, a more disordered crystal structure, accompanied by a blue shift in the optical absorption spectra, was observed.

Acknowledgements: CAPES, CNPq, FINEP, FAPITEC-SE, Cerâmica Sergipe s/a, UFS-PAIRD

Correlations between magnetic phases and structural properties in Co/Ru superlattices

Alayo, W.[1], V. P. Nascimento[2], Miguel Tafur[1], F. Pelegrini[3], Y.T.Xing[1], and Baggio-Saitovitch, E.[1]

[1] Centro Brasileiro de Pesquisas Físicas - Rio de Janeiro RJ Brazil
[2] Universidade Federal do Espírito Santo - Vitória ES Brazil
[3] Universidade Federal de Goiás - Goiânia GO Brazil

Co/Ru magnetic superllatices were grown by magnetron sputtering and studied by X-ray diffraction (XRD), ferromagnetic resonance (FMR) and X-ray magnetic circular dichroism (XMCD). The main and the secondary uniform peaks are observed in the FMR spectra of samples with the Co layer thickness larger than 20 and are associated with the Co/Ru interfaces and the bulk Co regions, respectively. The main mode becomes more intense than the secondary one for increasing Ru layer thickness, t_{Ru}. This is attributed to the roughness and/or atomic interdiffusion which lead to an increase of the volume of the Co/Ru interfacial regions and a decrease of the pure Co for increasing t_{Ru}. The XMCD measurements were performed at the $L_{2,3}$ absorption edges of Co using the facility of the SGM beam line at LNLS. They provide Co spin magnetic moments less than the bulk Co value, confirming the presence of a Co magnetic region with a lower effective magnetization attributed to the Co/Ru interfaces.

Acknowledgements: This work was supported by the Brazilian agencies CLAF-CNPq, FAPERJ and by LNLS. We ackowledge the LNLS staff for the assistance at the SGM beam line.

Induced Magnetism in the NiO/Cu/NiFe and NiO/Cr/NiFe trilayers systems

Miguel Tafur[1], Alayo, W.[1], Y.T.Xing[1], Nascimento, V. P.[2], and Baggio-Saitovitch, E.[1]

[1] Centro Brasileiro de Pesquisas Físicas - Rio de Janeiro RJ Brazil
[2] Universidade Federal do Espírito Santo - São Mateus ES Brazil

The long range interaction between the antiferromagnetic NiO(35nm) and ferromagnetic NiFe(3nm) layers across the nonmagnetic Cr and Cu spacers have been studied by magnetization measurements and X-ray magnetic circular dichroism (XMCD). The strength of exchange bias coupling decays exponentially with the spacer thickness and extends up to 2nm for Cu and 1.8nm for Cr. Moreover, the observation of Cr and Cu XMCD signals, whose intensity decreases rapidly when the spacer thickness, gives evidences of an induced spin polarization in the spacers, which play a large role in mediating the exchange coupling between NiO and NiFe.

Acknowledgements: This work has been supported by the Brazilian funding agencies CNPq (CT-Energ) and FAPERJ (Pronex-Cientista do Estado and Pensa Rio) and by the Brazilian Synchrotron Light Source (LNLS) under Proposal N° D08A-SGM 4298. We acknowledge the LNLS staff for their prompt assistance at the SGM beam line. Y. T. Xing acknowledges the FAPERJ and W. Alayo PCI/CBPF for fellowships.

Photoabsorption and desorption studies on poly(3-hexylthiophene) at the S K-edge

Araujo,G.S[1], Arantes, C.[1], Roman, L. S.[2], and Rocco, M.L.M.[1]

[1] Universidade Federal do Rio de Janeiro - Rio de Janeiro RJ Brazil
[2] Universidade Federal do Paraná - Curitiba PR Brazil

Poly(3-alkylthiophenes), especially the poly(3-hexylthiophene), have already demonstrated their potentiality for application in opto-electronic devices combining mechanical and semiconducting properties. Different techniques have been employed with the aim of obtaining a complete understanding of their properties. In this work we present ionic desorption studies from poly(3-hexylthiophene) (P3HT) thin films, obtained at the sulphur K-edge using the single-bunch mode. Photon stimulated ion desorption (PSID) spectra were measured at different photon energies, following the corresponding NEXAFS spectrum, which shows a sharp peak and two broad bands related to electronic transitions from the sulphur 1s electron to unoccupied molecular orbitals. The TOF-spectra contains six intense structures, labelled I - VI, which appear below and above the absorption edge. A weak feature appears around 300 ns (peak VII) only at the photon energy equal that of the first intense peak in the NEXAFS spectrum. By simulations, the desorption of the sulphur species S^+ and S^{2+} were expected to appear at about 300 ns and 288 ns, respectively. Later studies on poly(3-methylthiophene) exhibited however strong contribution of S^+ and S^{2+} desorptions at the sulphur 1s-edge and none outside, which were interpreted in terms of the ASID mechanism. One possible explanation for these different observations is that the sulphur atoms may be screened from being at the surface by the hexyl side-chains, as suggested by Ponjée et al. in their ion scattering studies. This surface molecular structure would suppress sulphur desorption. Also, the sample preparation methodology was different, which may introduce different arrangements at the surface, which by its turn alter the desorption probabilities. Desorption ion yield curves for the ions presented in the P3HT mass spectra were plotted. All curves resemble the TEY NEXAFS spectrum, suggesting that the XESD mechanism plays an important role in the ionic desorption of this polymeric film at the S K-edge. The introduction of carbon nanotubes to the polymeric film will be also discussed.

Acknowledgements: This work has been supported by the Brazilian Synchrotron Light Laboratory (LNLS) under proposal D04A - SXS 5789. G.S.A thanks CAPES and M.L.M.R. and L.S.R. thank CNPq for finantial support. The authors would also like to thank the LNLS staff.

Core-shell atomic structure formation in Pt-X (X = Co, Cu or Pd) nanoparticles

Bernardi, F.[1], Silva, D. O.[1], Ribeiro, D.C.A.[1], Alves, M.C.M.[1], A. Traverse[2], Dupont, J.[1], and Morais, J.[1]

[1] Universidade Federal do Rio Grande do Sul - Porto Alegre RS Brazil
[2] Université Paris-Sud - Orsay France

The study of nanoparticles atomic structure has attracted much interest in the last past years. The control of shape has been widely applied to various material systems in recent years, providing an important handle for changing nanomaterial properties. Much effort has been dedicated to the study of core-shell structure, as well surface segregation in bimetallic nanoparticles. Those bimetallic nanoparticles consisting of a core-shell structure are of special interest because they have revealed novel physical and chemical properties, different of those obtained from monometallic systems. In this work, we have studied the atomic structure of Pt-X (X = Co, Cu or Pd) bimetallic nanoparticles subjected to H_2 reduction and posterior sulfidation under H_2S atmosphere, both at 300 ^{0}C. The systems were studied by x-ray absorption spectroscopy (XAS), x-ray photoelectron spectroscopy (XPS) and transmission electron microscopy (TEM) techniques. The results show the formation of a core-shell structure in all nanoparticles with a Pt-rich core and an X (Co, Cu or Pd) enriched shell.

Acknowledgements: We gratefully acknowledge the support given by the CNPq, CAPES, LNLS (proposals SXS 7648, SXS 6577, XAFS1 6575) and the LNLS staff. F. B. thanks the CNPq for his PhD fellowship

Study of structural deformation and Mn segregation in CdMnTe quantum dots

Scudeller, L. A.[1], Malachias, A.[2], and Ferreira, S. O.[1]

[1] Universidade Federal de Viçosa - Viçosa MG Brazil
[2] Laboratório Nacional de Luz Síncrotron - Campinas SP Brazil

CdMnTe is a diluted magnetic semiconductor considered as a model for application in spintronics, since a lot of magneto-optic and transport effects can be explored by changing the Mn composition. However, this system has a limitation related to the formation of Mn clusters for high Mn concentration. In this work we will report results about the effect of Mn concentration on the structure of CdMnTe quantum dots and ultra-thin layers. The samples have been grown on Si(111) substrates by molecular beam epitaxy and hot wall epitaxy with Mn concentration up to 10%. They have been characterized by grazing incidence x-ray diffraction at the LNLS XRD-2 beam line. We will report results of the in-plane and out of plane lattice constants and mosaicity of the quantum dots as a function of nominal coverage and Mn concentration. Previous results for pure CdTe QDs show that they are completely relaxed even for very low coverage and the mosaicity increases with coverage.

Acknowledgements: This work was supported by CNPq, CAPES, FAPEMIG and LNLS.

Scintillation Properties and Dopant Location in Rare Earths Doped $Ca_{12}Al_{14}O_{33}$ via XAFS and XEOL

Valerio, M.E.G.[1] and Montes, PJR[1]

Universidade Federal de Sergipe - São Cristóvão SE Brazil

$Ca_{12}Al_{14}O_{33}$ doped with rare-earth ions exhibits long lasting phosphorescence and can also be used as a scintillator. The aim of this work is to study the dopant incorporation and the mechanism of scintillation in $Ca_{12}Al_{14}O_{33}$ doped with rare earths via DXAS as well as X-ray Excited Optical Luminescence (XEOL), combined with photoluminescence and the sintillation efficiency. One of the possible mechanisms leading to the emission of light under X-ray excitation is the reduction of Eu^{3+} to Eu^{2+} [2] DXAS technique (Dispersive X-ray Absorption Spectroscopy) uses dispersive optics that allows acquiring measurements of a range of energies of an X-ray absorption spectrum simultaneously. Analysis of the reduction dynamics can give information of the radiation damage process in the samples and DXAS technique can be used to follow it. Pure and rare earths doped $Ca_{12}Al_{14}O_{33}$ were prepared via a sol-gel proteic methodology, using coconut water as the initial solvent. All samples were previously analyzed using X-ray powder diffraction (XRD) and the prepared materials presented single crystalline phase. Photoluminescence spectra of $Ca_{12}Al_{14}O_{33}$: Eu^{3+} and $Ca_{12}Al_{14}O_{33}$: Eu^{2+}, Nd^{3+} show typical emissions of Eu ions. The X-ray indeuced luminescence of the samples (XEOL spectra) due to the absorption of the X-rays was measured simultaneously with the DXAS spectra and the conventional XANES/EXAFS measurements. X-ray absorption spectrum shows the typical absorption associated to the LIII edge of the Eu ions. XEOL emission of $Ca_{12}Al_{14}O_{33}$: Eu^{2+}, Nd^{3+} shows an intense peak around 450nm followed by emission peaking arround 615nm. The first XEOL peak is due to the emission of Eu^{2+} while the second one is due to Eu^{3+} transitions. DXAS spectra as a function of time of doped samples show that the position of absorption edge does not change indicating that reduction of Eu ions do not ocurr in doped $Ca_{12}Al_{14}O_{33}$ samples.

[1] M. A. Macedo, J. M. Sasaki, Processo de Fabricação de Pós Nanoparticulados, INPI 0203876-5. [2] P. J. R. Montes, M. E. G. Valerio, G. de M. Azevedo. NIMB, doi:10.1016/j.nimb.2008.03.140.

Acknowledgements: Work supported by CNPq, RENAMI, CAPES and CNEN. EXAFS, DXAS and XEOL measurements were done at LNLS Brazilian Synchrotron Light Laboratory- MCT, under project number DXAS 7311 and XAFS 7285

Characterization of Au nanparticles immobilized in alumina nanoporous membranes

da Costa, M. V.[1], Feil, A. F.[1], Migowski, P[1], Machado, G[1], Dupont, J.[1], AMARAL L.[1], and Teixeira, S.R.[1]

Universidade Federal do Rio Grande do Sul - Porto Alegre RS Brazil

Metal nanoparticles are attractive catalysts because their large surface area-to-volume ratio allows efficient use of expensive metals. Moreover, in some cases the electronic properties of nanoparticles are sufficiently different from those of the corresponding bulk metal to allow large enhancements in catalytic activities. Gold colloids, for example, demonstrate high catalytic activity even though bulk gold is typically an ineffective catalyst. Porous alumina membranes provide an alternative support for nanoparticle immobilization. Importantly, flow through nanometer-diameter membrane porous results in rapid convective mass transport of reactants to immobilized metal nanoparticles. The nanoporous membranes were prepared by anodization process with an 8.5 wt% phosphoric acid solution at 150 V and 5^{o}C. In this work we use an especially convenient method for modifying alumina membranes with metal nanoparticles; layer-by-layer absorption of polycations and citrate-stabilized gold colloids. In this work we present a structural characterization by using X-rays diffraction and TEM microscopy of gold nanoparticles immobilized in nanoporous alumina membranes.

Acknowledgements: This work was supported by CNPq, CAPES and FAPERGS.

Water splitting using Gold nanoparticles embedded in TiO_2 nanotubes

Feil, A. F.[1], da Costa, M. V.[1], Weibel, D. E. or Weibel, D.[1], Migowski, P[1], Machado, G[1], Dupont, J.[1], AMARAL L.[1], and Teixeira, S.R.[1]

Universidade Federal do Rio Grande do Sul - Porto Alegre RS Brazil

Photocatalytic reactions on the surface of titania films and particles have been attracting much attention because of their possible application in the conversion of solar energy in chemical energy. Despite photochemical water-splitting reaction was discovered more than 30 years ago an efficient method to split water into H_2 and O_2 remains to be developed. Photocatalysts with high surface-to-volume ratios and reactivity dependent on their size started to be used in the last decade to split water. In this sense, nanotubes and their interesting chemical-physics properties with high surface area are promising systems for solar energy related applications such as hydrogen production. TiO_2 nanotubes were prepared by anodization of Ti foil 98.5% purity with 20V for 2h in an electrolyte solution composed by ETG plus 10wt% H_2O and 0.5 wt% NH_4F. Au nanoparticles were prepared by $HAuCl_4$, the particle size was tuned to 12 nm. The photocatalytic activity of the titania nanotubes and Au nanoparticles into TiO_2 nanotubes was evaluated by measuring the H_2 production in a mixture of water/methanol by gas chromatography. The preliminary results showed important H_2 production on TiO_2 nanotubes (6.1%) and samples with Au nanoparticles the efficiency increased to 7.2%. Characterization of TiO_2 nanotubes containing Au nanoparticles were accessed by X-Ray diffraction and electron microscopy.

Acknowledgements: This work was supported by CAPES, CNPq and FAPERGS

Estudo da Dessorção Iônica Induzida por Fótons em Filmes de HMDSO Polimerizados por Plasma

Veiga, A.G.[1] and Rocco, M.L.M.[1]

Universidade Federal do Rio de Janeiro - Rio de Janeiro RJ Brazil

O Hexametildisiloxano (HMDSO) é um monômero da classe dos organossílicos amplamente descrito na literatura e largamente utilizado na produção de filmes polimerizados por plasma com aplicações no campo de recobrimentos ópticos e hidrofóbicos, barreiras gasosas, sensores químicos biocompatíveis, dispositivos eletrônicos, entre outros. O conhecimento dos efeitos físico-químicos do raio-x mole sobre estes materiais são de grande relevância para elucidação da sua estrutura e avaliação de desempenho tecnológico . Neste trabalho realizaram-se estudos de NEXAFS e dessorção iônica estimulada por fótons (PSID) em filmes de HMDSO suportados em Si 100. Os experimentos foram realizados no Laboratório Nacional de Luz Síncrotron (LNLS) operando no modo single bunch segundo a fotoexcitação da borda K do silício e usando o TOF-MS para análise dos íons. Na borda K do silício pôde-se observar a dessorção de pequenos e grandes fragmentos. As curvas de rendimento iônico parcial foram determinadas para os principais fragmentos em função da energia do fóton. Os resultados mostraram que o processo Auger normal tem papel fundamental para dessorção iônica do Si^{2+}, um aumento significativo no seu rendimento iônico foi observado na primeira ressonância. O ASID pode ser também o responsável pela dessorção de fragmentos atribuídos ao $CH_3{}^+$ e $C_3H_9Si^+$. Essas observações permitem propor uma estrutura de natureza polimérica (silício ligado a cadeias de hidrocarbonetos) para o filme de HMDSO. A produção de H^+ e outros fragmentos moleculares parecem ser induzidos por ambos os mecanismos XESD e AISD.

Acknowledgements: CNPq, LNLS (em especial D04-SXS 2330) e Fraunhofer Institute of Dresden, Alemanha.

Micellar Solutions and Microemulsions formed with Ionic Surfactants applied as Corrosion Inhibitors: Characterization by Small-Angle X-Ray Scattering

Wanderley Neto, A. O.[1], Gurgel, A.[2], Dantas, T.N.C.[1], Moura, E.F.[1], and Dantas Neto, A.A.[1]

[1] Universidade Federal do Rio Grande do Norte - Natal RN Brazil
[2] Universidade Federal de Viçosa - Viçosa MG Brazil

The problem of corrosion has always been considered in technological activities. Surfactants may be used as inhibitors of corrosion on metallic surfaces with advantages, because of their unique properties when in solution or as part of microemulsion formulations. In this work, we use small-angle X-ray scattering (SAXS) to characterize some self-assembled systems containing a series of ionic surfactants, with potential applications as carbon-steel corrosion inhibitors in ducts used in the petroleum industry. Fatty acids obtained from castor oil and soybean oil (ricinoleic acid and linoleic acid, respectively) have been used to synthesize the surfactants, which were submitted to subsequent epoxidation or amination reactions. The purpose is to examine the influence of such organic moieties in the surfactants molecules in the adsorption phenomena occurring at solid-liquid interfaces. The SAXS technique is useful to determine size and shape of the dispersed particles (micelles or microemulsion droplets), providing a better understanding of the interfacial activity of the systems. Three ionic surfactants, from the carboxylate family, synthesized via epoxidation or amination reactions, have been used to prepare a number of aqueous micellar solutions and oil-in-water microemulsions, according to previous phase behavior studies. A fourth ionic surfactant, which does not contain the amine or epoxy groups on its structure, was also used as reference. The effects of salinity (0.5 M and 1.0 M NaCl aqueous solutions) and temperature (30^oC and 60^oC) were also assessed. The microemulsions were prepared with kerosene (as oil phase) and butan-1-ol (as cosurfactant). The results confirm the formation of approximately spherical micelles and microemulsion droplets, showing varying degrees of interaction, typically with a repulsive nature. In particular, salinity and surfactant concentration have marked effects on the scattering curves, enhancing the intensities of peaks generated for the optically isotropic samples. These data are important when proposing the best formulation for corrosion inhibitors with the surfactants tested.

Acknowledgements: The authors are thankful to LNLS for allocation of SAXS beamtime (Project D11A - SAXS1 - 7021) and travel expenses. A.O.W.N. also acknowledges ANP/PRH-14 for a PhD studentship.

SRSAXS to study the limits of different concentration regimes in polysacharide aqueous solutions

Caracciolo, N.[1], Boeykens, S.[1], and Vázquez, C[2]

[1] Universidad de Buenos Aires - Buenos Aires Argentina
[2] Comisión Nacional de Energia Atómica - Buenos Aires B.A. Argentina

Polymers present almost three different behaviours depending on the concentration range: in dilute regime with sufficiently low concentration, molecules do not interact with others and are free to diffuse and rotate without collisions: the polymers macromolecules interact primarily with the solvent; in semi-dilute range, the concentration is high enough causing rotational motion restriction and entanglement interactions. Finally in concentrated regime gel, macromolecules interact each others very strongly. This research investigated the structural concentration changes of aqueous biopolymeric solutions in the neighborhoods of the limits of the concentration regimes. The idea was to determine the concentration limit value for each given polymer system. To achieve this task, Synchrotron Radiation Small Angle X ray Scattering was used successful. The scattering patterns in the small angle regime describe features that are observed in a log Intensity versus log plot. The power law decay in the intensity reflects the power law scaling features of the matrix. We used the slope of this curves as an indicator of the matrix structural changes. Three polymeric systems of similar molecular mass were studied: scleroglucan, xanthan and polyoxyethylene. They were selected as different types of polymers based on their structural characteristics: an helical polyanion, an helical neutral (but polar) polysaccharide macromolecule and a linear non polar (and synthetic) polymer, respectively. SRSAXS measurements were performed at SAXS line in the LNLS facility. Three different types of curves of intensity I(q) were found for scleroglucan according to different macromolecules concentrations. This allows us to identify concentration limits for each regime: concentration up to 0.1%, dilute regime; concentration between 0.15% and 0.55%, semidilute regime; concentration more than 0.6% concentrate regime. Similar results were found for xanthan. Polyoxyethylene presents in the all range of concentrations studied the same type of curves, assuming that it has no structural changes.

Acknowledgements: This work was supported by grants from the following projects: I041 and I750 Universidad de Buenos Aires, Argentina, and 4168 National Laboratory of Synchrotron Light, Campinas, Brasil.

Simultaneous XAFS and XRD Studies of Water Intercalation in Synthetic Ni-Fluorohectorite

Ribeiro, L.[1], Mundim, M. S. P.[2], Fossum J. O.[3], and da Silva, G. J.[2]

[1] Universidade Estadual de Goiás - Anápolis GO Brazil
[2] Universidade de Brasília - Brasília DF Brazil
[3] Norwegian University of Science and Technology - Trondheim Norway

Synthetic Ni-Fluorohectorite (Ni-Fht), a trioctahedral clay, has the idealized chemical formula per half unit cell $Ni_x - (Mg_{(3-X)}Li_{0,6})Si_4O_{10}F_2$. It has a rather large surface charge of 1.2e/unit cell, originating from the substitution of Li^+ with Mg^{2+} in the octahedral layer compared to other synthetic smectites as for example laptonite (0.4e/unit cell) or montmorillonite (0.6e/unit cell) [1]. This property contributes for a characteristic process of water diffusion and it has been studied by many techniques such as XRD, XAFS and NMR [2] in a separated way. The XRD technique informs us about the diffusion process due to platelets motions related to the peak position in the spectrum. From its side XAFS technique shows the water solvation process around the intercalated cation Ni^{2+}, its interaction with the clay platelet and also with other Ni atoms forming a brucite type like structure. In this work we did a simultaneously X-Ray diffraction (XRD) and absorption spectroscopy (EXAFS) experiment as a function of temperature and humidity. An x-ray wavelength before the absorption edge of the Ni was chosen to generate the 2D image plate XRD spectra. The control of the relative humidity was done by circulating humidified or dehumidified air through a special cell designed for this purpose. The simultaneity of both techniques permitted us to investigate the clay water layer regime (information given by XRD) and the Ni^{2+} environment (XAFS) at a given temperature and humidity: analysis procedures associated with each technique will be discussed and compared.

[1] - G. Lvoll, B. Sandnes, Y. Meheust, K.J. Maly, J.O. Fossum, G.J. da Silva, M.S.P. Mundim, R. Droppa Jr., and D.M. Fonseca. *Physica B*, **370**, 2005.

[2] Lars Ramstad Alme. Water transport in selected nanoporous media. Master thesis, Norwegian University of Science and Technology - NTNU, 2007.

Acknowledgements: Acknowledgements: This work has been supported by the Brazilian Synchrotron Light Laboratory (LNLS) under proposal D04B-XAFS1 number 7121/08 and by Norwegian University of Science and Technology - NTNU (Trondheim/NO).

Au-Pd bilayred films grown by dc magnetron sputtering: structural, morphological, and chemical characterization

Machado, A.C.[1], Silva, P.J.M.[1], Gobbi, A. L.[2], Fantini, M. C. A.[3], Gheno, S. M.[1], Paulin Filho, P.I.[1], and Nascente, P. A. P.[1]

[1] Universidade Federal de São Carlos - São Carlos SP Brazil
[2] Laboratório Nacional de Luz Síncrotron - Campinas SP Brazil
[3] Universidade de São Paulo - São Paulo - São Paulo SP Brazil

Pd-Au system presents interesting properties. Pd is an excellent catalyst for many reactions, whereas Au alone is considered a poor catalyst. However, adding Au, the activity and selectivity of Pd catalysts enhances. Pd and Au films, having a thickness of 10 nm, were deposited by dc sputtering on 100 nm thick layers of Au and Pd, respectively, which were grown on Si(100) substrates. The structure, morphology, and chemical composition of the films were analyzed by X-ray reflectometry (XRR), X-ray diffraction (XRD), atomic force microscopy (AFM), and X-ray photoelectron spectroscopy (XPS). The XRR and XRD results are summarized as follows: the layer thickness for the Pd film was measured to be 9.5 nm, the layer thickness for the Au film was 9.9 nm, the lattice parameters for the Pd film and thick Au layer were 0.39011 nm and 0.4073 nm, the lattice parameters for the Au film and thick Pd layer were 0.40754 nm and 0.38946 nm, the grain sizes were 8.0 nm and 23.3 nm for the Pd and Au films, respectively. The nominal and real thicknesses of the Pd and Au thin films differ less than 5 percent. The lattice parameters of the Pd films are always larger than the standard value, while Au films present an opposite trend, showing the interface constraint on the crystal structure of the films. Also, the crystalline grain size of the Au film is larger than the Pd film. The AFM images showed a flat surface for the Au film, while the Pd film presented a surface covered by small grains (particles). XPS results indicated that the Pd thin film is partially oxidized, while the Au thin film was metallic.

Acknowledgements: The authors would like to thank Mr. Antonio C. F. Silveira for his assistance in the XRD measurements. This work was supported by LNLS, FAPESP, CAPES, and CNPq.

Formação e Caracterização de Fases Micelares e Líquido-Cristalinas Constituídas por Óleos e Surfatantes Siliconados

Ferreira, M.S.[1], Westfahl Jr., H.[2], and W. Loh[1]

[1] Universidade Estadual de Campinas - Campinas SP Brazil
[2] Laboratório Nacional de Luz Síncrotron - Campinas SP Brazil

Microemulsões são soluções microestruturadas de óleo e água estabilizadas por um filme interfacial composto por surfatantes. Podem ser do tipo gotas de óleo-em-água (O/A) ou água-em-óleo (A/O), ou ainda sistemas em que se têm água e óleo de forma contínua entrelaçadas em redes dinâmicas que recebem o nome de microemulsões bicontínuas (L_3). As suas aplicações abrangem vários campos, desde sistemas de liberação de fármacos a sínteses de nanopartículas. Óleos e surfatantes de silicone têm recebido uma grande atenção por possuir características importantes como, por exemplo, a sua baixa energia coesiva, que neste caso dificulta a formação destes sistemas. O objetivo deste trabalho é verificar em quais condições se obtém a máxima incorporação de água no óleo de silicone através da construção de diagramas de fases ternários com dois diferentes surfatantes. A técnica de espalhamento de raios-X a baixos ângulos (SAXS) foi utilizada para obter informações de duas regiões do diagrama com características distintas. A primeira região é formada por sistemas isotrópicos em que a água encontra-se no interior do óleo, tanto na forma de gotas (microemulsões A/O) como na forma de canais (L_3). As curvas obtidas na região de microemulsões bicontínuas foram usadas para a aplicação do modelo de Teubner-Strey, em que pôde-se confirmar a estrutura e calcular parâmetros como distância entre os domínios, comprimento de correlação e outros. A segunda região é formada por fases líquido-cristalinas (sistemas anisotrópicos), tais como fases lamelares (L) e hexagonais (H). As curvas de espalhamento nestes casos foram utilizadas para a indexação dos picos de correlação e obtenção de informações como espessura da bicamada, distância entre os planos, entre outros. Uma importante informação obtida refere-se a influência da estrutura do surfatante no tipo de fases formadas. Neste trabalho, em que se pretende obter fases normais, o surfatante que possuía a maior parte hidrofóbica favoreceu a formação de microemulsões A/O, em concordância com o parâmetro crítico de empacotamento. Desta forma, constatou-se que é relevante a construção de diagramas de fases para compreender o comportamento dos constituintes no sistema, e que no caso estudado, os surfatantes siliconados empregados conseguiram formar microemulsões A/O com uma incorporação máxima de até 20% de água.

Acknowledgements: LNLS, FAPESP e CNPq

Influence of interface and confinement phenomena in silicon based systems photoluminescence.

M. Ribeiro[1] and I. Pereyra[1]

Universidade de São Paulo - São Paulo - São Paulo SP Brazil

Silicon rich silicon oxynitride films with different composition exhibiting intense photoluminescence (PL) have been produced by PECVD technique. Even though the PL result is promising for the production of light emitting devices the phenomena responsible for the PL is still not well understood. Some authors attribute it to confinement effects while others to interfacial phenomena [1, 2]. In order to study the influence of interfacial contribution in the luminescent emission two types of silicon multilayer stacks were produced: a-Si/SiOx and a-Si/SiNx multilayer stacks based on a sequential arrangement with controlled layer size of a-Si:H and dielectric high gap material composed of 18 interfaces. The Silicon rich silicon oxynitride films and the stack silicon based systems were analyzed in order to compare the influence of controlled interfacial systems with multinterfacial silicon nanostructured systems. Through the results was possible to analyze the phase separation and the interface contributions of each system. The photoluminescence analyses showed that the PL emission peak is tunable with the amorphous silicon layer thickness. All films were characterized by: Fourier transformed infrared (FTIR), XANES, photoluminescence (PL) and high-resolution transmission electron microscopy (HRTEM). The results indicate that the films present amorphous silicon clusters as deposited and after heat treatment occurs structural changes with better definition of the x-ray absorption edges and partial crystallization promoting PL peak shift revealing the influence of the phase separation and confinement effect.

References:

1- W.K.Tan, M.B.Yu, Q. Chen, J.D.Ye, G.Q. Lo and D.L. Kwong, Appl. Phys. Lett. 90 (2007) 221103. 2- M. Ribeiro, I. Pereyra, M.I. Alayo, Thin Solid Films 426 (2003) 200.

Acknowledgements: The authors acknowledge to Prof. Dr. Marcia Temperini from Chemistry Institute, at University of São Paulo, for the help in the characterization of the Raman and PL experiments. The authors are also grateful to Brazilian agencies CNPq and FAPESP for financial support and to Laboratório Nacional de Luz Sincrotron(LNLS) at Campinas, SP, Brazil for the XANES and TEM experiments. The electron microscopy work has been performed with the JEM-3010 ARP microscopy of the LME/LNLS, Campinas, SP, Brazil.

Influência dos efeitos de tamanho de cristalito e de textura na reação de oxidação eletroquímica de monóxido de carbono sobre platina não suportada

Ciapina, E. G.[1], Santos, S.F.[1], and Gonzalez, E. R.[1]

Universidade de São Paulo - São Carlos - São Carlos SP Brazil

A reação de oxidação eletroquímica do monóxido de carbono (CO) sobre platina (Pt) é uma das reações mais estudadas em eletrocatálise, visto a sua enorme importância dentro da pesquisa em Células a Combustível. Entretanto, considerando-se materiais nano-estruturados, muitos aspectos relacionados à reação ainda permanecem não esclarecidos, como os efeitos de tamanho de cristalito, defeitos superficiais e a presença de aglomerados. Desta forma, este trabalho descreve um estudo da reação de eletro-oxidação de CO em meio ácido sobre Pt não-suportada, tendo como objetivo de se obter informações a respeito da sensibilidade da reação em relação ao tamanho de cristalito e de outros fatores estruturais. A amostra de Pt não-suportada foi preparada por redução química do precursor (H_2PtCl_6) com ácido fórmico a 80 graus Celsius. O material preparado, assim como uma amostra de Pt não suportada comercial, foram caracterizados por Microscopia Eletrônica de Transmissão, Espectroscopia de Absorção de Raios-X (XAFS1/LNLS) e Difração de Raios-X (XPD/LNLS). Os resultados mostraram que, de forma geral, as amostras são constituídas por aglomerados (50-200 nm) de nanopartículas de Pt da ordem de 10 nm, apresentando números de coordenação de aproximadamente 9 átomos. Também foi observada contração na rede cristalina, indicada tanto pelos parâmetros de rede obtidos por meio do refinamento de Rietveld, quanto pelas distâncias Pt-Pt obtidas por EXAFS. A quantidade relativa de planos cristalinos foi obtida pelo coeficiente de textura e apontou diferenças significativas entre o material preparado e o material comercial. Os experimentos eletroquímicos, realizados em meio de $HClO_4$ 0,1 mol/L a temperatura ambiente ($\sim$ 26 graus Celsius) evidenciaram o complexo comportamento da reação de oxidação de CO em meio ácido sobre nanopartículas de Pt não suportadas, e indicam que as diferentes quantidades de planos expostos e diferenças no tamanho de cristalito devido ao método de preparação provavelmente são os responsáveis pelos distintos comportamentos eletroquímicos encontrados.

Acknowledgements: FAPESP, CNPq, CAPES e LNLS

Direct strain and elastic energy evaluation in rolled-up semiconductor tubes by x-ray micro-diffraction

Malachias, A.[1]

Laboratório Nacional de Luz Síncrotron - Campinas SP Brazil

Rolled-up nanotubes (RUNTs) made of semiconductor layers have been intensively highlighted as promising systems for both basic and applied research. These structures can be produced by heteroepitaxy of two or more pseudomorphically strained thin films grown on top of an etchant-sensitive (sacrificial) layer. Selective etching is then used to release the top layers that relax elastically by rolling up into a tube. The RUNT diameter from some nanometers to hundreds of microns can be precisely controlled by varying the strain gradient in the layered structure. Such property was successfully explored to produce devices such as waveguides and resonators. Particularly, the strain configuration of RUNTs is considerably changed by partially releasing the RUNT from the substrate. Such free-standing optically active RUNTs are used in devices like ring resonators to prevent leaking of the optical modes into the substrate. Therefore, the final strain state of a free-standing RUNT and the understanding of the parameters that govern it is of great interest.

In this work we depict schematically the use of x-ray micro-diffraction as a tool to locally probe strain status and elastic energy in rolled-up semiconductor tubes. Using the micro-focusing capabilities of the ESRF ID01 beamline we have been able to quantitatively evaluate the lattice parameter relaxation of rolled InGaAs/GaAs tubes along the radial and tangential directions. Detuning the sample angle with respect to the substrate specular condition allows for measurements of the coplanar diffraction of individual RUNTs. The peaks observed can be fitted by employing continuous elasticity theory and a simple x-ray model which provides the tangential-radial lattice parameter distribution.

We show that its also possible to evaluate local strain and elastic energy in multi-layers and layers with dislocations, leading to new insights about the elastic behavior of the nanometric layers in these special conditions. For multilayer and tubes with dislocaitons the lattice relaxation along the longitudinal tube direction plays an important role for the final configuration, giving rise to a partial overall 3D strain relaxation.

Acknowledgements: This work was supported by the MPI-FKF (Stuttgart) and ESRF (Grenoble).

Propriedades estruturais de nanopartículas de Ge encapsuladas em sílica

Gasperini, A. A.[1], Avendano, E.[2], Gobbi, A. L.[2], and Azevedo, G. de M.[2]

[1] Universidade Estadual de Campinas - Campinas SP Brazil
[2] Laboratório Nacional de Luz Síncrotron - Campinas SP Brazil

A origem da fotoluminescência (PL) a temperatura ambiente em nanocristais do grupo IV encapsulados em matrizes dielétricas ainda não é muito bem compreendida e diferentes mecanismos foram propostos para explicar este fenômeno. Uma vez que o arranjo geométrico dos átomos determina as propriedades ópticas e eletrônicas, uma descrição detalhada da estrutura no nível atômico e o conhecimento de sua dependência com as condições de síntese são fundamentais. No presente trabalho, nanopartículas de Ge encapsuladas em filmes finos de sílica foram preparados via *co-sputtering* de Ge e sílica com subseqüente tratamento térmico a temperaturas entre 800^{o}C e 1050^{o}C. Variações na concentração de Ge, duração e temperatura do tratamento térmico resultaram em filmes contendo nanopartículas amorfas ou com estrutura diamante com diâmetros que variam entre 2 e 6 nm, como podem ser vistas através de imagens de HRTEM e medidas de XRD e GISAXS típicas das amostras estudadas. Resultados de EXAFS mostraram uma redução na magnitude da transformada de Fourier do sinal para as três primeiras camadas de coordenação, relativas ao material *bulk*, que podem ser entendidas como uma maior desordem estrutural experimentada pelas nanopartículas. Análise de espectros de EXAFS como função da temperatura mostraram que as ligações Ge-Ge nas nanopartículas são menores e mais rígidas do que no material *bulk*, com preferência para desordem nos ângulos de ligação ao invéz de desordem nas distâncias interatômicas.

Acknowledgements: Os autores gostariam de agradecer ao CNPq, FAPESP e ao LNLS.

Applying the LOC concepts to improve an *"electronic tongue"* system

Dantas, C.A.R.[1], Almeida, A.L.J.[2], Piazzetta,O.M.H[2], Gobbi, A. L.[2], and Riul Jr, A.[3]

[1] Universidade Estadual Paulista - Presidente Prudente - Presidente Prudente SP Brazil
[2] Laboratório Nacional de Luz Síncrotron - Campinas SP Brazil
[3] Universidade Federal de São Carlos - Sorocaba - Sorocaba SP Brazil

The micromachining technology is paving the way for microfluidic systems as the behaviour of fluidics in such systems has been extensively investigated and exploited in lab-on-a-chip (LOC) devices. The LOC concept has allowed the genesis of potentially powerful applications that can be rapidly performed, having low cost and waste of reagents/samples. In this way, we have been supported by *Micro-Fabrication Laboratory (LMF) at Brazilian Synchrotron Light Laboratory* (LNLS, Campinas - SP) to start microchannels fabrication integrating an *"electronic tongue"*

system into a LOC device. Microchannels were built in *polydimetilsiloxane* (PDMS), which were further sealed onto gold interdigitated electrodes (IDEs) by O_2 plasma exposure technique. Although the difficulties appeared during the process, our first efforts were successful. Therefore, ongoing measurements with alternative methods and materials are being undertaken to get the final goal: an *"e-tongue-on-a-chip"*

.

Acknowledgements: This work has been supported by LMF/LNLS, FAPESP and IMMP/CNPq.

Surface properties influence on electrochemical behavior of boron doped diamond produced at different doping levels

Ferreira, N.G.[1], Azevedo, A.F.[1], Baldan, M.R.[1], and Matsushima, J.T.[2]

[1] Instituto Nacional de Pesquisas Espaciais - São José dos Campos SP Brazil
[2] Instituto Nacional de Pesquisas Espaciais - São José dos Campos SP Brazil

Microcrystalline chemical vapor deposition (CVD) boron-doped diamond (BDD) films have demonstrated to be a proper electrode due to its remarkable properties correlated to applications such as wastewater treatment, electroanalysis and electrosyntesis. Thus, the rigorous control of diamond growth parameters is determinant to produce the suitable electrode for the required application. A systematic study of deposition, characterization, and electrochemical sensitivity of BDD is reported taking into account four different doping levels with high accuracy of its growth parameters that define its surface properties. So, different sample sets were prepared by hot filament CVD technique using the standard mixture of H2/CH4 by controlling the boron addition during the film growth. Diamond quality, morphology and crystallinity were characterized by scanning electron microscopy, Raman spectroscopy and X-ray diffraction techniques while the changes in film surfaces were analyzed by contact angle, cyclic voltammetry and synchrotron X-ray photoelectron spectroscopy. Each sample set followed a rigorous procedure to analyze the influence of aqueous media in BDD surface for each boron doping. This control is very important because as the boron level increases the grain size decreases enhancing the the sp2 density at the film grain boundary. The BDD hydrophobicity, reversibility, work potential window characteristics, as a function of the doping level, were related with its physical properties and its chemical surface; mainly associated with its natural oxidation (as-prepared BDD) or with its changing behavior forced by the cathodic pre-tratment.

Acknowledgements: This work was supported by CNPq anda Fapesp.

Dinâmica do Crescimento de Nanofios Semicondutores Auto-Sustentados de InP

Th. Chiaramonte[1], Tizei, L. H. G.[2], Ugarte, D.[2], and Cotta, M.A.[1]

[1] Universidade Estadual de Campinas - Campinas SP Brazil
[2] Laboratório Nacional de Luz Síncrotron - Campinas SP Brazil

Neste trabalho, investigamos a evolução do crescimento de nanofios de InP auto-sustentados, crescidos sobre substrato de GaAs(100), através do sistema de epitaxia por feixe químico, localizado no IFGW/UNICAMP. A posterior caracterização estrutural dos nanofios, via microscopia eletrônica de varredura por emissão de campo (SEM) e de transmissão em alta resolução (HRTEM) e também por espectroscopia de raios-X dispersiva em energia (EDS), foi realizada no laboratório de microscopia eletrônica do LNLS. Sabe-se que a taxa de crescimento do nanofio (R) depende da supersaturação da NP metálica, ou seja, no nosso caso, depende da quantidade de In que chega na NP de Au e é posteriormente expulso por ela para formar a fase semicondutora sólida. A fim de estudarmos a dinâmica do crescimento dos nanofios, foram crescidas amostras com diferentes fluxos de índio à temperatura de 420^{o}C. A literatura reporta que, nestas condições, o crescimento deve ocorrer no método vapor-sólido-sólido (VSS) uma vez que estamos abaixo da temperatura de fusão da liga Au-In criada na NP. Em nossas amostras, a estatística do comprimento dos nanofios nos permitiu determinar R em função dos fluxos de In e constatar uma instabilidade no crescimento para um fluxo de 6 sccm; observamos que R aumenta cerca de 3 vezes, saindo da tendência de um padrão exponencial do crescimento. Para explicar este resultado devemos considerar a concentração de In na NP de Au, observando o diagrama de fase da composição Au e In, associada a uma análise da estrutura cristalina destas amostras, através de HRTEM e de EDS. Dos resultados, verificou-se que os nanofios apresentam estrutura InP hexagonal com orientação ao longo da direção [0001]; também constatou-se que o aparecimento de defeitos ao longo do fio está diretamente relacionado com o aumento do fluxo de In (algumas monocamadas com mudança da estrutura InP hexagonal para cúbica), ou seja, fios com maior fluxo apresentam maior quantidade de defeitos. A quantificação dos átomos de In e Au existentes na NP após o crescimento, coloca em dúvida o tipo de mecanismo de crescimento dominante deste processo, isto é, vapor-líquido-sólido (VLS) ou VSS. Para a temperatura de crescimento empregada, acreditamos que a concentração de aproximadamente 20% de In no volume da NP de ouro abaixa sua temperatura de fusão, sugerindo uma transição para o modo VLS.

Acknowledgements: Este trabalho recebe o apoio financeiro da FAPESP e do CNPq.

Nanodiamond grown on porous silicon using reticulated vitreous carbon as a solid carbon source

Miranda, C.R.B.[1], Azevedo, A.F.[1], Baldan, M.R.[1], Beloto, A.F.[2], and Ferreira, N.G.[1]

[1] Instituto Nacional de Pesquisas Espaciais - São José dos Campos SP Brazil
[2] Instituto Nacional de Pesquisas Espaciais - São José dos Campos SP Brazil

The nanocrystalline diamond (NCD) films, formed on porous silicon (PS) substrate, through the etching of solid carbon, produced at different graphitization index, was investigated. Reticulated vitreous carbon (RVC) produced at three different heat treatment temperatures of 1300, 1500 and 2000 C were used to compare its influence on the NCD growth in a hot filament reactor. In this chemical vapor infiltration/deposition process a piece of RVC was used, just below the PS substrate, as an additional solid source of hydrocarbon, that ensures the production of pertinent carbon growth species like CH3 directly on the PS and into its pores. Field Emission Gun-Scanning Electron Microscopy (FEG-SEM) images showed faceted nanograins with uniform surface texture covering all the pores resulting in an apparent micro honeycomb structure. Raman measurements showed the D and G bands, as well as the typical two shoulders at 1150 and 1490 cm-1 attributed to NCD. The crystalline structures of these films, analyzed by X-ray diffraction, showed a main diamond peak of (111) orientation with $2Theta = 43.9$ and peaks of (220) and (311) diamond reflection at $2Theta = 75.5$ and 91.4 respectively. From Sherrers formula the average size was evaluated from 5 to 20 nm.

Acknowledgements: This work was supported by CNPq and FAPESP

Caracterização de Fases Líquido-Cristalinas por SAXS

Campos, DDP[1] and Bertran, C. A.[1]

Universidade Estadual de Campinas - Campinas SP Brazil

Cristais líquidos formados por Renex (surfactantes nonilfeniletoxilados com diferentes tamanhos de cadeia etoxilada, Oxiteno-Brasil), ciclohexano e solução salina vem sendo empregados como moldes na síntese de partículas de fosfatos de cálcio com morfologia e tamanho controlados. A caracterização de cristais líquidos por SAXS é possível pois estas fases apresentam ordem à longas distâncias e o vetor espalhamento (q) relaciona-se com as distâncias interplanares (d) de acordo com a relação: q= n2π/d. Neste trabalho, foram caracterizadas três fases formadas por misturas ternárias de Renex, solução salina e ciclohexano. Foram utilizados Renex com 4, 6 e 10 cadeias etoxiladas. A fase preparada com Renex com 4 grupos etoxilados apresentou estrutura hexagonal (n=1,$3^{1/2}$,$4^{1/2}$,...), a fase preparada com Renex com 6 grupos etoxilados apresentou estrutura lamelar (n=1,2,3,...) e aquela contendo Renex com 10 grupos etoxilados correspondeu a uma mistura de fases, sendo que uma delas apresentou estrutura hexagonal e a outra não foi caracterizada. Estes resultados mostram que cristais líquidos preparados com surfactantes com diferentes tamanhos de cadeias etoxiladas podem determinar o controle da morfologia e do tamanho de cristais de biocerâmicas de fosfatos de cálcio.

Acknowledgements: CNPq e LNLS

An angle-scanned photoelectron diffraction study on the surface structure of Pd growth on Nb(100)

Lussani, F.C.[1], Pancotti A.[1], Landers R[1], Carazzolle M.F.[1], and de Siervo A.[1]

Universidade Estadual de Campinas - Campinas SP Brazil

Ferrromagnetic ordering in non-ferromagnetic transition metals induced by structural effects such as lattice expansion and stacking faults have been predicted by several theoretical studies [1,2]. Despite the theoretical predictions, an unambiguous experimental demonstration of the ferromagnetic order in the case of Pd nanostructures and Pd ultrathin films was not attained [3]. Nb(100) surface is a template which could drive a Pd ultrathin film to an stable ferromagnetic state, depending on the growth condition and film tickness. The structural determination of Pd ultrathin films on Nb(100) is an important case to determine the existence of a possible ferromagnetic phase in Pd atoms, clusters and ultrathin films. Only a few studies of Pd films on Nb(100) are present in the literature [4] and a detailed structural determination of this surface has not been reported.

In this work we present a photoelectron diffraction study of Pd growth on Nb(100) and it surface structure determination. Pd ultrathin films varying from sub-monolayer to a few layers were grown on Nb(100) surfaces in UHV conditions by using a well controlled e-beam evaporation method. Angle-scanned photoelectron diffraction patterns of Pd 3d and Nb 3d peaks were measured using conventional Al K_α and synchrotron radiation. Intermediate photon energy of $h\nu = 750$ eV was provided by the SGM beamline at the Brazilian Synchrotron Light Laboratory. The data analysis was performed by comparison of the experimental and simulated photoelectron diffraction patterns. The simulations were based on different structural models considering the multiple scattering diffraction theory approach.

References:

[1] A. Delin et al., Phys. Rev. Lett. 92, 057201 (2004).

[2] T. Shinohara et al., Phys. Rev. Lett. 91, 197201 (2003).

[3] Hong, S. C., Phys. Rev. B 75, 172402 (2007).

[4] K. Osuch et al., Phys. Rev. B 71, 165213 (2005).

Acknowledgements: We would like to thank LNLS staff for helping in the SGM beamline in special P. T. Fonseca. This work has been supported by FAPESP, CNPq and CAPES.

STM AND TEM INVESTIGATION OF REACTIVE EPITAXY: HFSIX

Leite, M. S.[1], G.A. Fiorentini[1], Pimentel, V. L.[1], Montoro, L. A.[1], Ramirez, A.J.[1], and Medeiros-Ribeiro, G.[1]

Laboratório Nacional de Luz Síncrotron - Campinas SP Brazil

Hafnium dioxide (HfO2) is the strongest candidate to replace the silicon dioxide (SiO2) as the gate insulator in the Metal Oxide Semiconductor Field Effect Transistors (MOSFETs), the "heart"of our current technology for micro and nano-electronic devices. Even though the hafnium dioxide present a good dielectric constant (high-k), a very important property for the nano-electronic industry, agreat effort is needed in the study of the interface between Hf and Si. Hafnium silicide (HfSix) islanding occurs spontaneously when small amounts of metallic hafnium (Hf) are deposited on a Si (001) surface and subsequently annealed at 750oC. Different coverages were investigated and scanning tunneling microscopy (STM) measurements were performed in order to verify distinct stages of island formation. High resolution STM analysis allow the determination of the flatness of the islands top face, which is parallel to the Si(001) surface and, moreover, the interatomic spacing, which characterize the hafnium disilicide (HfSi2) C49 phase when measuring the bigger islands. Electron diffraction was also performed on the islands and compared to simulated diffraction patterns, leading us to conclude that the zone axis, perpendicular to the substrate surface, is the [013] direction of the silicide and its exposed surface is the (061) plane, corroborating previous STM results about the structure. Moreover, scanning tunneling spectroscopy (STS) was carried out over islands of different sizes and demonstrated their metallic behavior, which can severely impact the performance of semiconductor devices.

Acknowledgements: Rede SPM Brasil - CNPq / Fapesp / Hewlett Packard

Eletrocatálise de oxidação de etanol em monocamadas mistas de Pt, Ru e Rh depositadas em nanopartículas de Au/C

Lima, F. H. B.[1], Profeti, D.[2], Ticianelli, E. A.[1], and Gonzalez, E. R.[1]

[1] Universidade de São Paulo - São Carlos - São Carlos SP Brazil
[2] Instituto de Quimica de Sao Carlos - São Carlos SP Brazil

A eletrooxidação de etanol foi estudada em eletrocatalisadores formados por monocamadas puras e mistas de Pt-M (M = Ru e/ou Rh) depositadas em nanopartículas compostas por Au, suportadas em carbono de alta área, em eletrólito ácido [1]. As propriedades eletrônicas da monocamada de Pt nos diferentes substratos foram determinadas por XANES in situ. As atividades eletrocatalíticas para a reação de oxidação de CO adsorvido (intermediário) e etanol e os produtos da reação foram correlacionados com os resultados de XANES e FTIR in situ. Os espectros de XANES indicaram uma maior reatividade (maior adsorção de espécies oxigenadas) da Pt depositada em Au/C em relação à Pt em Pt/C. Além disso, os resultados evidenciaram maior reatividade da Pt na monocamada pura de Pt em relação à da Pt nas monocamadas mistas com Ru e/ou Rh. Isto pode ser devido à interação eletrônica da Pt com os átomos de Ru e Rh e/ou em função do efeito de repulsão entre espécies oxigenadas na superfície da monocamada mista. Os espectros de FTIR evidenciaram a presença de CO adsorvido, como produto da adsorção dissociativa do etanol, durante o curso da reação, para todos os materiais eletrocatalisadores. Isso comprova os resultados de XANES, que mostram alta reatividade da monocamada de Pt. A monocamada mista de Pt-Ru mostrou maior atividade eletrocatalítica para a oxidação de CO adsorvido (stripping the CO). Neste caso, é possível que os átoms de Ru tenham como função o fornecimento de espécies oxigenadas como o OH para a oxidação de CO adsorvido (mecanismo bifuncional) e diminuir a força da ligação Pt-CO, em virtude da repulsão lateral entre as espécies Pt-CO e Ru-OH. Os resultados também mostraram que a desidrogenação do etanol na Pt, produzindo acetaldeído [2], é a via majoritária e que somente um pequeno percentual se oxida até ácido acético.

[1] LIMA F.H.B.; GONZALEZ E. A., Appl. Catalysis B: Environmental 79: 341346-, 2008 [2] IWASITA T.; PASTOR E., Electrochim. Acta 39: 531-537, 1994.

Acknowledgements: Fapesp e LNLS

Catalisadores de Co suportados aplicados nos processos de reforma a vapor e reforma autotérmica do etanol

Liberatori, J. W. de C.[1], Ribeiro, R.U.[1], Zanchet, D.[2], and Bueno, J.M.C.[1]

[1] Universidade Federal de São Carlos - São Carlos SP Brazil
[2] Laboratório Nacional de Luz Síncrotron - Campinas SP Brazil

Atualmente, vem crescendo o interesse por fontes alternativas de produção de combustíveis, estimulado principalmente pela conscientização mundial dos efeitos poluidores dos combustíveis derivados de petróleo. Assim, a aplicação de células a combustível movidas a hidrogênio (H_2) é uma alternativa de grande interesse para o transporte e geração de energia limpa [1]. Este H_2 pode ser obtido a partir do gás natural ou através de processos de reforma a vapor do etanol (RVE), que vem de fontes renováveis (biomassa). A produção de H_2 a partir do etanol envolve as tecnologias de reforma do etanol e autotérmica [2]. Em ambas são aplicados catalisadores de metais suportados. Nossos estudos com catalisadores de Co suportados e promovidos (Co/Al_2O_3, Co/La_2O_3-Al_2O_3, $Pt/Co/Al_2O_3$, $Pt/Co/La_2O_3$-Al_2O_3,) mostraram que estes catalisadores sofrem desativação devido a alta deposição de carbono quando aplicados na RVE. Os dados de termogravimetria para este processo mostraram que a deposição de carbono, a 500^{o}C e razão molar água:etanol de 3:1, segue a seqüência: $Pt/Co/La_2O_3$-Al_2O_3 > $Pt/Co/Al_2O_3$ > Co/La_2O_3-Al_2O_3 > Co/Al_2O_3. Estes estudos mostraram também que a adição de pequena quantidade de oxigênio, reação autotérmica com razão molar água:etanol:oxigênio de (3:1:0,5), resulta em catalisadores altamente estáveis durante todo o período de análise (30 horas). Os resultados de termogravimetria destes catalisadores, nas condições de reação: 500^{o}C e razão molar água:etanol:oxigênio (1,6:1:1,2), mostraram uma formação pequena de carbono: Co/Al_2O_3 > Co/La_2O_3-Al_2O_3 > $Pt/Co/Al_2O_3$ > $Pt/Co/La_2O_3$-Al_2O_3. A reação de reforma autotérmica do etanol também foi acompanhada por XANES *in situ* para o catalisador de $Pt/Co/La_2O_3$-Al_2O_3. Estes resultados mostraram que catalisadores de Co suportados são promissores para aplicação na produção de hidrogênio no processo de reforma autotérmica do etanol. Observou-se ainda, através da análise por XANES *in situ*, que a adição de Pt favorece a redução das espécies de Co_3O_4 para CoO no processo de redução dos catalisadores de Co, onde ficou claro por esta análise que a redução ocorre em etapas (Co_3O_4 -> CoO -> Co). Os catalisadores foram também caracterizados por medidas BET, DRX, TPR, TG, MEV e FTIR-CO. [1] A Fatsikostas, A. N., Kondarides, D. I., Verykios, X. E., *Catal. Today*, 75 (2002) 145. [2] Llorca, J., Homs, N., Sales, J., Piscina, P. L., *J. Catal.*, 209 (2002) 306.

Acknowledgements: CNPq e LNLS

III-V Semiconductor Nanowires VLS Growth: Does Arsenic Diffuse Through the Metal Nanoparticle Catalyst?

Tizei, L. H. G.[1], Th. Chiaramonte[2], Cotta, M.A.[2], and Ugarte, D.[1]

[1] Laboratório Nacional de Luz Síncrotron - Campinas SP Brazil
[2] Universidade Estadual de Campinas - Campinas SP Brazil

III-V semiconductor nanowires (In, Ga, As, P) are promising objects to the development of new technologies and devices. One method of growing nanowires is the VLS (Vapor-Liquid-Solid) using epitaxy techniques (CBE, Chemical Beam Epitaxy, MBE, Molecular Beam Epitaxy, etc.), in which the growth is catalyzed by a metallic nanoparticle. For III-V semiconductor nanowires it is known that the group III atoms diffuse through the metallic nanoparticles and are incorporated in the wire at the metal/semiconductor interface. However, there is no data that confirms the route of incorporation of the group V atoms at growth pressures and temperatures. To study this problem, we have grown by CBE two nanowires samples with the heterostructure (times between parenthesis) InP (15 minutes)/InAs (2 minutes)/InP (15 seconds) at two different temperatures (420 C and 450 C), using gold nanoparticles as catalyst. Nanowires structure has been analyzed by TEM (Transmission Electron Microscopy) and its chemical composition by EDS (Energy Dispersed X-Ray Spectroscopy). Nanowires show wurtzite hexagonal crystal structure. We studied in detail the chemical composition at the InP/Au interface region. The growth is finished by a InP segment. However, for the 450 C sample, the region close to the gold particle displays a narrow As rich layer (about 3 nm thick). This is surprising because As is not originated from the growth atmosphere. EDS line scans perpendicular to the nanowires show no radial dependence, indicating that As is not present only at the surface, ruling out surface diffusion from the InAs segment. We speculate that the As diffuses through the Au nanoparticle and that at 450 C there is metastable concentration of As that is stocked in the nanoparticle, even during InP growth. Bulk room temperature phase diagrams do not show any mixture of As and Au. Thus, as the nanowire is cooled As is expelled, growing a thin As rich region. This result shows that As (group V) diffuses through the gold nanoparticle

Acknowledgements: The authors acknowledge FAPESP, CNPq and ABTLuS for funding, the LME-LNLS for the electron microscopes used in this work and the LME-LNLS staff for technical support.

Síntese e caracterização de nanopartículas de Platina

Meira, D. M.[1], Ribeiro, R.U.[1], Prieto, P. J. S.[1], Zanchet, D.[2], and Bueno, J.M.C.[1]

[1] Universidade Federal de São Carlos - São Carlos SP Brazil
[2] Laboratório Nacional de Luz Síncrotron - Campinas SP Brazil

Nanopartículas metálicas são materiais promissores em diversas aplicações em função de suas propriedades ópticas, magnéticas e catalíticas [1]. Em síntese coloidal é possível controlar propriedades como tamanho e forma de nanopartículas (NPs), o que representa uma vantagem na sua utilização como catalisadores modelo. Neste contexto, a estrutura de superfície de cristalitos metálicos pode ser drasticamente modificada na escala de 1-5 nm em reações sensíveis à estrutura[1]. Reações que ocorrem em átomos do tipo corners e edges (presentes em NPs e ausentes em sítios de alta coordenação como Pt(100) e Pt(111)) podem ser significativamente diferentes em sítios do tipo terraço. A atividade para as reações de reforma do metano aumenta com o aumento da dispersão e, portanto depende do tamanho de NPs[2]. No presente trabalho, Pt-NPs com diferentes tamanhos e formas foram sintetizadas segundo métodos descritos na literatura [3,4]. NPs esféricas de ∼4 nm foram obtidas utilizando-se metanol e PVP, de acordo com os resultados de TEM. O etilenoglicol em meio básico (NaOH) proporcionou a formação de partículas esféricas com ∼1,8 nm. E a adição alternada de alíquotas de soluções tanto do precursor como do PVP em etilenoglicol resultou na formação de NPs de ∼9,6 nm e morfologias cúbicas e tetraédricas . A etapa de remoção do PVP é essencial para tornar os sítios ativos do catalisador acessíveis às moléculas de reagente em uma reação catalítica. Assim, medidas de DRIFTS *in situ* foram realizadas durante o tratamento térmico (sob atmosfera de O_2/N_2) das Pt-NPs (4 nm) suportadas em Al_2O_3 comercial e indicaram que a remoção do PVP ocorre em temperaturas próximas a 400^{o}C. Em trabalhos anteriores Pt-NPs suportadas em óxidos metálicos (Al_2O_3 e CeO_2-Al_2O_3) resultaram em catalisadores ativos e estáveis para a reação de reforma do metano [5]. Desta maneira, as Pt-NPs sintetizadas no presente trabalho podem ser utilizadas como catalisadores modelo para reações de reforma, entre outras reações sensíveis à estrutura, com enfoque no estudo da influência de tamanho e forma de NPs. [1] R.M. Rioux, H. Song, M. Grass, S. Habas, K. Niesz, J.D. Hoefelmeyer, P. Yang, G.A. Somorjai, Top. Catal. 39 (2006) 167. [2] J. Wei, E. Iglesia, J.Catal. 224 (2004) 370 e 225 (2004) 116. [3] T. Teranishi, M. Hosoe, T. Tanaka, M. Miyake, J. Phys. Chem. B, 103 (1999) 3827. [4] R.M. Rioux, H. Song, J.D. Hoefelmeyer, P.Yang, G.A. Somorjai, J. Phys. Chem. B 109 (2005) 2192. [5] P.J.S. Prieto, diss. metrado, 2007.

Acknowledgements: FAPESP (07/57723-3), CNPq e LNLS

Índice Remissivo

Álvares, A.C.M., 16

A. Traverse, 198
A.F. Craievich, 80, 183, 190
A.M. Mudarra Navarro, 145
Abdala, P. M., 65, 185
Abraham, J. A., 56
Abreu, M. F., 85
ACF Santos, 55
Acuña, L. M., 129, 134
Adan Hajduk, 71
Alayo, W., 195, 196
Albertin, K.F., 101
Allegretti, S. M., 64
Almeida, A.L.J., 213
Alnornoz, Ana, 71
Alonso, J.A., 166
Alves, A. C., 28, 40
Alves, B.S.C., 38
Alves, M.C.M., 198
Alves, S.V., 13
Alves. O. L., 154
Amalvy, J. I., 89, 188
AMARAL L., 201, 202
Anbinder, P. S., 89, 188
Andrade, A. A., 94, 151
Andricopulo, A. D., 46
Andrini, L., 122, 136
Angelomé, P. C., 122
Anjos, M. J., 62, 162
Antonelli, E., 155
Arantes, C., 197
Arantes, F.C., 67
Araujo,G.S, 197
Ari M., 90
Arisi, G. M., 67
Arnache, O., 127
Arnal, P. M., 136
Arni, R.K., 24
Arruda, M. A. Z., 43
Assis, J. T., 62
Attie, M.R.P., 58
Atvars, T.D.Z., 146
Atzingen, M. V., 27
Autreto, P. A. S., 168
Avansi, W., 164
Avendano, E., 212
Azevedo Jr., W. F., 20, 21
Azevedo, A.F., 214, 216
Azevedo, G. de M., 155, 166, 212
Azimonte, C., 171

Bacani, R., 91
Baesso, M.L., 94, 151
Baggio-Saitovitch, E., 195, 196
Balan, A., 25
Baldan, M.R., 175, 214, 216
Baldochi, S. L., 97
BALLIANO, T. L., 46
BAPTISTA, MS, 148
Barbosa, J.A.R.G., 10, 15–18, 25
Barbosa, L.R.S., 35
Barrero, C.A., 126
Barroso, R.C., 9
Basso, R. L. O., 169
Bastos, I.M.D., 15
Bataghin, F. A., 13
Batista, A. P. L., 182, 186
Batista, T, 80
Beloto, A.F., 175, 216
Benedetti C.E., 42
Benevides, R. G., 20, 21
Bentley, M.V.L.B., 84
Bernardi, F., 198
Bernini, R.B., 51
Bertran, C. A., 217
Beton, D., 23
Bezerra, E.H.S., 21

Bezerra, G.A., 21
Boechat-Roberty , H.M., 55
Boeykens, S., 71, 74, 205
Bojorge, C. D., 183
Bongiovanni, G.A., 61
Braga, A. H., 100
Brandão, S. T., 99
Brunatto, S. F., 120
Bueno, J.M.C., 221, 223

C. A. Figueroa, 169
C. Lage, 33
C. M. R. Remedios, 128, 131, 133
Cánepa, H. R., 183
Caldas, M. J., 168
Camargo, A.C.M., 81
Campos, C. E. M., 150
Campos, DDP, 217
Camps, I., 149
Candioto, K.C.G., 137, 167
Canellas,C.G.L, 162
Caracciolo, N., 205
Caravaca, M.A., 157
Carazzolle M.F., 218
Cardoso, L.P., 128
Cardoso, S.C., 68
Cardoso, S.L., 85
Carrilho, E., 105
Carvalho, H.W.P, 182, 186
Casali, R.A., 157
Casanova, J. R., 183
Castro, A. R. B., 5
Catafesta, J., 144
Cavada, B.S., 20, 21
Cavalcante, I. P., 156
Cavasso Filho, R. L., 52, 53
Ceolin M., 118
Cernadas, R. A., 42
Chiavacci, L.A., 64, 181
Ciapina, E. G., 210
Cintra, A. O., 24
Coelho, G. C., 137, 141
Coltro, W. K. T., 105
Comerlato, N.M., 135, 153
Conceição, A. L. C., 36
Conti T. G., 179
Corrêa, H. P. S., 70, 95, 107, 142, 156
Corrêa, N. C. R., 37
Correia, N., 58
Cosme, T. A., 117
COSTA, D. M.A, 37
Costa, J. J. G., 73
Cotta, M.A., 215, 222
COUCEIRO, P.R.C., 165
Coutinho, L. H., 51
Craievich AF, 12, 65, 134, 185
Cunha, A. G., 139
Cury, F.A., 19
Cury, P.M., 19, 34

D. S. Galvao, 168
da Costa, M. V., 201, 202
da Silva, G. J., 79, 99, 206
da Silva, L. F., 130
Da Silva, L. H. M., 140
Dabrowski B., 161
DAHMOUCHE, K, 93, 184
Dantas Neto, A.A., 204
Dantas, C.A.R., 213
Dantas, T.N.C., 204
de Figueiredo, A. T., 123, 124
de Jesus, V. L. B., 55
De Lima, J.C., 150
de Mello, A.C.S., 97
de Menezes, A. S., 128
de Paula-Pereira Jr., M. V., 33
de Siervo A., 218
de Souza Guerra, C, 9
de Souza, G.G.B., 51
deAzevedo, ER, 146
Delatorre, P., 20, 21
Della Védova, Carlos O., 52, 53
Discola, K. F., 11, 13
Doriguetto, A.C., 132, 149, 152
Dorotéia F. Bozano ou D. F. Bozano, 156
dos Santos Claro, P. C., 190
dos Santos, A. O., 128, 131, 133
dos Santos, D. R., 85
Dos Santos, J. H. Z., 69
Droppa Jr., R., 109
Dupont, J., 92, 198, 201, 202
Duque J.G.S., 119, 163

E. E. Sileo, 98
E. J. Carvalho, 142
E. Nunes, 139
Ellena J., 149
ElMassalami,M; El Massalami, M; Massalami, M, 158, 159
Eon J-G., 192, 193
Erben, Mauricio F., 52, 53
Espinoza Quiñones, F.R., 72
Esteves, G. F., 10, 18

F. Pelegrini, 195
Fábregas, I. O., 63
Fabbris, G. F. L., 166
FABRIS, J. D., 165
Faccio, R., 161

Fantini, M. C. A., 65, 84, 91, 102, 134, 185, 207
Farah, C.S., 22, 23, 29
FARIA, Celso Murilo Nálio Matias de, 19
Faria, G. C., 146
Faro Jr., A. C., 192, 193
Feil, A. F., 92, 201, 202
Ferlauto, A. S., 160
Fernández de Rapp, M. E., 63
Ferreira Júnior, J. R., 12
Ferreira, F. F., 107, 111
Ferreira, G. B., 54, 147, 153
Ferreira, M.S., 208
Ferreira, N.G., 175, 214, 216
Ferreira, O.P., 154
Ferreira, S. O., 199
Figueiredo, L. T. M., 38
Filadelpho, M. C., 94, 151
Fischer, H., 12
Fischer, P., 4
Flora, D., 54
Fontes, M. R. M., 14
Fossum J. O., 79, 206
FRANÇA, M. C. K., 193
Francisco G. Emmerich, 139
Franco, R. N., 69
FRANZINI, C.M., 181
Freire, P. T. C., 131, 133
Freitas, JCC, 139
Freitas, M. B., 75
Freitas, S. M., 10, 15–18
Fuentes, R. O., 129, 134
Fuertes, M.C., 191

G.A. Fiorentini, 219
G.OLIVA, 46
Gómez, A. G., 110
Garcia, F., 142, 144
Garcia-Cairasco, N., 67
Gasperini, A. A., 212
Gatts, C., 85
GENCAPO, P., 34
Genu, V, 13
Gerlach, R.F., 9
Geronés, Mariana, 52, 53
Gheno, S. M., 207
Giacomini, R. A., 85
Giles, C., 75
Giovanetti, L. J., 189, 190
Girata, D, 127
Giuseppe, P. O., 27
Gobbi, A. L., 182, 186, 207, 212, 213
Gomes, D. S. B., 140
Gomes, M.A., 194
Gomes, T. S., 51
Gonzalez, E. R., 210, 220
Goulart, A.T., 165
Graeff, C. F. O., 168
Granado, E., 111–113, 166, 171
Gremião, M. P. D., 64
Grumelli, D., 189
Guerra, A. C. O., 54, 147, 153
Guido R.V.C., 46
Guimarães, B.G., 13, 27
Gurgel, A., 204
Guzzo, C.R., 22, 23

H. J. Sánchez, 56, 106, 108
Haines, J., 144
Hammer, P., 138
Hattori, G.Y., 66
Henrique, T, 19
Heredia, E., 183
Hoffmann, A, 127
Hofmann, S., 3
Horta, B. B., 11

I. Pereyra, 101, 209
Itri, R., 35

J. Restrepo, 176, 177
J.L.Passamai Jr, 95, 142
Jóvári, P., 120
Jardim, P. M., 90
Jobbagy, M., 98

K. D. Machado, 120
Kalkreudt,W., 69
Kellermann, G., 183, 190
Kern, L. M., 69
Knobel, M., 119, 163
Kobarg, J., 44
Kopke Salinas, R., 22, 29

L.C.Damonte, 145
Lacerda, R. G., 160
Ladeira L.O., 160
Lamas, D. G., 63, 65, 91, 129, 134, 185
Landers R, 218
Landre, I. M. R., 152
Lanza, D.C.F, 44
Lede, E. J., 121
Leitão, A.C., 33
Leitão,R.G, 162
Leite, M. S., 219
Leite,E.R., 164, 179, 187
Lenz, G., 44
Liberatori, J. W. de C., 221
Lima, F. H. B., 220

LIMA, I., 62
Lima, V.D., 93
Lionzo, M. I. Z., 178
Longo, E., 123, 124, 179, 187
Lope-Martinez, M.J., 166
Lopes, L. J. S., 147, 153
Lopes, R.T., 62, 162
Lula, I., 81
Lussani, F.C., 218

M. M. Elhadi, 159
M. Ribeiro, 209
M.A. Rizzutto, 72
M.I.B.Bernardi, 130
M.S. Arruda, 57
Módenes, A. N., 72
Macedo, Z.S., 194
Machado, A.C., 207
MACHADO, D. S., 80
Machado, G, 92, 201, 202
Maciel, G.A., 120, 166
Magalhães, S.D., 68
Magalhaes-Paniago, R., 160
Maia, L. J. Q., 130
Malachias, A., 199, 211
MANIERO, A. M., 57
Maniglia, J.V, 34
Marchena M. H., 191
Marchi-Salvador, D. P., 14
Mardegan, J. R. L., 75
Mariano-Neto, F., 102
Marinho, R. R. T., 57, 58
Marinkovic, B. A., 90
Mario de Oliveira Neto, 12, 80
Martinez, L. G., 70, 95, 107, 110, 142, 156
Martins, A. M., 43
Martins, F. T., 149
Martins, T. S., 91, 102
Mascarenhas, Y.P., 132, 152
Massa, N. E., 166
Mastelaro, V.R., 123, 124, 130, 132, 152, 164
Matos, J. R., 91, 102
Matsushima, J.T., 214
Maury, A. M., 71, 74
Mazo L H, 105
Mazzaro I., 75
Medeiros-Ribeiro, G., 219
Medina, A.N., 94, 151
Meira, D. M., 223
Meirelles, G. V., 44
Melo, F. E. A., 131, 133
Melo, J.O., 40
Melo,CPS, 45
Meneses, C. T., 119, 163
Menezas, A. S., 131
Meyer, B.C., 112
Migowski, P, 92, 201, 202
Miguel A. Schettino Jr., 139
Miguel Tafur, 195, 196
Mir, M., 132, 149, 152
Miranda, C.R.B., 175, 216
Miranda, P. C. M. L., 85
Mocellin,A., 58
Mombrú, A.W., 161
Monteiro, G., 11
MONTENEGRO, E.C., 55
Montes, PJR, 143, 200
Montoro, L. A., 219
Moraes, A. P. A., 155
Morais, J., 198
Moreira, B.J., 84
Moreira, S., 9
Moreira, S. G. C., 133
Morelhão, S.L., 109
MORELLO, L.G., 47
Morigaki, M. K., 139
Motta, F. S. N., 15
Moura TR, 21
Moura, E.F., 204
MPeko, J.-C., 155
Mundim, M. S. P., 57, 206
Mundim, M.S. P., 58, 79, 99
Murakami, M. T., 24

Naganao, C.S., 20
Nagem, R. A. P., 37
Nakamatsu, E. H., 11
Nascente, P. A. P., 207
Nascimento, ALTO, 27
Nascimento, V. P., 196
Nasciutti, L.E, 162
Navarro, L. C., 170
Naves de Brito, A., 57, 58
Netto, L.E.S., 11, 13
Neueschwander, R. T., 112
Neumann, M. G., 80
Neves P.P, 132, 149, 152
Nietmann, H., 19
Nogueira, L., 192
Nunes, C. A., 137, 141, 167

OLIVEIRA, A.G., 181
Oliveira, J. F., 26
Oliveira, M.A., 13
Oliveira, O.B., 99
Oliveira, T.M., 21
Olivira Junior N.G.O., 100

Orlandi, M.O., 187
Orlando, M. T. D., 70, 95, 107, 142, 156

Pérez, C. A., 56, 61, 106, 108, 182, 186
Paier, C. R. K., 41
Paiva-Santos,C.O., 107
Palacio, S.M., 72
Palacios, O.M., 74
Palumbo, A.J, 162
Pancotti A., 218
Paschoal, R. C., 54
Passamani, E. C., 139
Paulin Filho, P.I., 207
Pegos, V.R., 25
Peralba, M.C.R., 69
Percebom, A. M., 82
Pereira, A. S., 144
Pereira, G.R., 75
Pereira, S. V., 149
Perottoni, C. A., 144
Peruzzo, P. J., 89, 188
Pestana. K.C., 181
Piazzetta,O.M.H, 213
Picciani, P.H.S, 135
Pilling, S., 55
Pimentel, V. L., 169, 219
Pinheiro, G. S., 131, 133
Pinto, J.C., 117
Pinto, N.G.V, 9
Plivelic, T.S., 146, 188
Polachini, G. M., 34
Polachini, G.M., 19
Poletti, M. E., 36, 73
Polikarpov, I., 12, 80
Ponce, C.A., 157
Prieto, P. J. S., 223
Profeti, D., 220
PRUDENTE, F. V., 57
Pulcinelli, S.H., 138

R. F. Cossiello, 146
R. M. Briones, 158
R. Oliveira da Silva, 124, 179
R.D. Pérez, 61, 108
Ramalho, TC, 182, 186
Ramallo-López, J. M., 189
Ramirez, A.J., 219
Recco, A.A.C., 110
Renosto, S. T., 141
Requejo, F. G., 122, 136, 189, 190
Ribeiro, C., 164
Ribeiro, D.C.A., 198
Ribeiro, L., 79, 206
Ribeiro, L.S., 141
Ribeiro, R.U., 221, 223
Richa, P. R. F., 117
Riul Jr, A., 213
Rizzo, F., 90
Roa, D. B, 160
Rocco, M.L.M., 197, 203
Rocha, B.A.M., 20, 21
Rocha, C. J., 107
Rocha, H. S., 75
Rocha, J.C., 140
Rodella, C. B., 100
Rodríguez Torres, C. E., 145
Rodrigues, F, 112
Rodrigues, MCA, 67
Rodrigues, V. O., 192, 193
Rodriguez Pirani, Lucas, 52, 53
Rohling, J.H., 94, 151
Roman, L. S., 197
Romano, Rosana M., 52, 53
Rossetti F., 67
Rossetti, F. C., 84
Rossi, J. L., 95
Rubatto Birri, P.N., 61
Rubio, M., 61, 108

S de Oliveira, 160
S.A. Larrondo, 134
Salas, C.E., 37
Salvador, G. H. M., 14
Salvador, M. J., 66, 67
Salvarezza R C, 189
Sampaio, A.H., 20, 21
Sampaio, J. A., 94, 151
Sanchez, D. F., 120
Santacruz-Perez, C., 25
Santana, J. M., 15, 16
Santiago, P.S., 35
Santilli, C.V., 138
Santos, C. R., 18
Santos, R.A.S., 81
Santos, S.F., 210
Santos, V. B., 132
Sarmento, V.H.V, 64, 138, 181
Sawazaki, D.T.A., 66
Schaberle, F. A., 17
Schmitt, C.C. ou Cavalheiro, C.C.S, 80
Scudeller, L. A., 199
Segato, T. P., 105
Seidl, P.R., 83, 170
Sforça, ML, 26
Shon, Y. S., 189
Sigaud, L., 55
Silva Jr, F. G., 72
Silva, A. J., 10, 16–18

Silva, A.A., 96
Silva, D. O., 198
Silva, F. D. da, 165
Silva, H. A., 16
Silva, J.C., 44, 168
Silva, L.C.C., 102
Silva, M.P., 73
Silva, P.J.M., 207
Silva, R. F., 192
Silva,C.G.A., 69
Silva,L.B., 51
Silva,M.C.O, 14
Silveira, N. P., 178
Sinisterra R. D., 81
Slovic, A.M., 16
Smetana, J. H. C., 28, 39
Soares, A. M., 14
Soares, B.G., 93, 135, 184
Soares, M., 33
Socolovsky, L. M., 121, 180
Soler-Illia, G.J.A.A., 122, 191
Soprano, S. A., 42
Soria,B., 118
Sousa, M. H., 79
SOUZA FILHO, A. G., 154, 155
Souza Jr, F. G., 117, 135
Souza, A. L. R., 64
Souza, D. P., 29
souza, J. A., 166
Souza, P.A.V.R, 162
Souza, T. A., 42
Souza,A.A., 146
Stolf, S. F., 120
Stroppa, D. G., 179
Stutz, G., 72, 125
Suescun, L., 161
Suzuki, P. A., 141, 167
Szymanski, N., 72

Tabak, M., 35
Tajara, E.H., 19, 34
Tasic, L., 43, 170
Taylor, M.A., 118
Teixeira, A. V., 140
Teixeira, E. C., 28
Teixeira, S.R., 92, 201, 202
Teles, R. C. L., 17, 18
Terashita, H, 171
Terra, W.R., 23
Terruggi, C.H.B., 64
Th. Chiaramonte, 215, 222
Ticianelli, E. A., 220
Tirao G., 72, 125
Tizei, L. H. G., 215, 222
Torriani, I., 44, 146
Torriani, I.L., 168
Turci, C. C., 54, 147, 153

Uchoa AF, 148
Ugarte, D., 215, 222

V. P. Nascimento, 195
Vázquez, C, 71, 74, 205
Valentinuzzi, M. C., 56
Valerio, M.E.G., 97, 143, 194, 200
Varela, J.A., 123
Vasconcellos, J.F., 40
Vaz, T. H., 40
Veiga, A.G., 203
Viana, B. C., 154
Vidotto, A, 34
Vidotto, A., 19
Vieira, C.C.O., 58
Vilela, S. S., 24
Vitorazi, L., 85

W. Loh, 82, 170, 208
W. Wolff, 55
Wanderley Neto, A. O., 204
Weibel, D. E. or Weibel, D., 92, 202
Westfahl Jr., H., 208
Wolosiuk, A., 122, 191

Y.T.Xing, 195, 196
Yunes, J. A., 40, 45

Zaioncz, S., 184
Zanchet, D., 100, 221, 223
Zanchin, N. I. T, 26–28, 38–41, 47
Zanelato, P., 19
Zeri, AC;, 26, 45
Zimicz, M. G., 134
Zorzi, J. E., 144
Zucchi, O. L. A. D, 66, 67, 73